AN INVESTIGATION OF THE CHEMOPREVENTIVE MECHANISMS OF MASLINIC ACID

By

YAP WEI HSUM

A thesis submitted to the Department of Biological Science,
Faculty of Science,
Universiti Tunku Abdul Rahman,
in partial fulfillment of the requirements for the degree of
Doctor of Philosophy in Science
August 2011

ABSTRACT

AN INVESTIGATION OF THE CHEMOPREVENTIVE MECHANISMS OF MASLINIC ACID

Yap Wei Hsum

Cancer is a global threat to public health, causing great morbidity and high mortality rates. The World Health Organization (WHO) predicts that one in every four person will die from cancer by the year 2030. Cancer related mortality has not improved for the past several decades despite immense efforts in anti-tumour drugs research. The discovery and testing of novel compounds that are more effective and safer as cancer chemopreventive agents are intensively required. Recently, researchers have shifted interest to natural anti-inflammatory agents in fruits and vegetables. Preliminary studies on selected Malaysian plants showed that maslinic acid, an active compound isolated from the tubers of *Coleus tuberosus*, has strong anti-tumour-promoting activity. To develop maslinic acid as a potential cancer chemopreventive agent, this study aims to evaluate its molecular mechanism in the pro-inflammatory pathway, anti-oxidant defence system and its molecular response at the proteomics level. In the first part of the study, maslinic acid was isolated from the tubers of *Coleus tuberosus* according to previous established methods. Using a short term *in vitro* EBV-EA activation assay, maslinic acid was shown to have strong anti-tumour-promoting activity (IC_{50} = 25 μM). Further analysis revealed that maslinic acid suppressed more than 50 % pro-inflammatory enzyme COX-2 expression at 100 μM. Likewise,

100 μM of maslinic acid reduced 60 % NF-κB activity and abolished AP-1 DNA binding, both which are known to mediate COX-2 expression. It is possible that the suppression of COX-2 by this natural triterpene might be achieved via the NF-κB and AP-1 signaling pathways. In addition, maslinic acid induces the Nrf2-ARE pathway. Maslinic acid significantly induced HO-1 and NQO1 expression in a concentration-dependent manner and achieved maximal expression at 100 μM after 6 h treatment. Maslinic acid-induced HO-1 and NQO1 expression might be resulted from enhanced ARE binding observed from 3-12 h. Nuclear Nrf2 protein accumulation was increased up to 172 % after 3 h treatment. Through siRNA silencing studies, the transcription factor Nrf2 was demonstrated to be essential for maslinic acid induction of these enzymes. At the proteomics level, seventeen differentially expressed proteins in response to 50 μM maslinic acid including those involved in DNA replication, microtubule dynamics, nucleo-cytoplasmic trafficking, cell signaling, energy metabolism and cytoskeletal organization were identified by MALDI TOF-TOF MS. Proteins which are implicated in the cell cycle such as stathmin, RanBP1, and EB1 were validated by Western blotting. Further studies showed that maslinic acid induces G1 cell cycle arrest and regulates levels of G1-associated cell cycle components, e.g. cyclin D1 and p21 expression. There may be several mechanisms that are responsible for the cancer chemopreventive activities of maslinic acid, including suppression of the NF-κB/AP-1/COX-2 pro-inflammatory pathway, activation of the Nrf2 anti-oxidant response system and modulation of molecular targets associated with cell growth and survival. Reinforcing knowledge on the mechanisms of

chemopreventive agents helps in pursuing cancer prevention research and develops maslinic acid as a potential cancer chemopreventive agent.

ACKNOWLEDGEMENT

First of all, I would like to express my gratitude to my supervisor, Dr. Lim Yang Mooi, for giving me the opportunity to have my PhD project supervised by her. I also want to thank her for her patience, time and guidance during the process of my project and in the preparation of this thesis.

I am also very grateful to my seniors Jia Jie, Chin Piow, Shin Leong and Ooiean for their experience and important information provided for my project. Furthermore, I would like to thank Dr. Khoo Kong Soo for his assistance in my manuscript and thesis writing.

Special thanks to my lab mates, Teck Yew, Sok Yee, Siew Ling, Su Yin, Pei Shing, Sue Bee, Wyi Sian, Wei Ling, and Lisa who have supported me during the project. Lastly, I would like to express my deepest appreciation to my parents for their never ending support and encouragement in enabling me to successfully complete my research project.

APPROVAL SHEET

This dissertation/thesis entitled "**AN INVESTIGATION OF THE CHEMOPREVENTIVE MECHANISMS OF MASLINIC ACID**" was prepared by YAP WEI HSUM and submitted as partial fulfillment of the requirements for the degree of Doctor of Philosophy in Science at Universiti Tunku Abdul Rahman.

Approved by:

_____
(Associate Professor Dr. Lim Yang Mooi)
Date:……..
Supervisor
Department of Pre-clinical Sciences
Faculty of Medicine and Health Sciences
Universiti Tunku Abdul Rahman

_____
(Associate Professor Dr. Khoo Kong Soo)
Date:……..
Co-supervisor
Department of Chemistry
Faculty of Science
Universiti Tunku Abdul Rahman

FACULTY OF SCIENCE
UNIVERSITI TUNKU ABDUL RAHMAN

Date: _____

SUBMISSION OF THESIS

It is hereby certified that **YAP WEI HSUM** (ID No: **08ADD08104**) has completed this thesis entitled "AN INVESTIGATION OF THE CHEMOPREVENTIVE MECHANISMS OF MASLINIC ACID" under the supervision of Dr. Lim Yang Mooi (Supervisor) from the Department of Pre-clinical Sciences, Faculty of Medicine and Health Sciences and Dr. Khoo Kong Soo (Co-Supervisor) from the Department of Chemistry, Faculty of Science.

I understand that University will upload softcopy of my thesis in pdf format into UTAR Institutional Repository, which may be made accessible to UTAR community and public.

Yours truly,

_____

(Yap Wei Hsum)

DECLARATION

I hereby declare that the dissertation is based on my original work except for quotations and citations which have been duly acknowledged. I also declare that it has not been previously or concurrently submitted for any other degree at UTAR or other institutions.

Name _____

Date _____

TABLE OF CONTENTS

LIST OF TABLES

LIST OF FIGURES

LIST OF ABBREVIATIONS

ATF	Activating transcription factor
AP-1	Activator protein-1
ARE	Anti-oxidant response element
bzip	Basic leucine zipper
COX	Cyclooxygenase
EBV	Epstein-Barr Virus
EGCG	Epigallocatechin-3-gallate
EMSA	Electrophoretic Mobility Shift Assay
ERK	Extracellular-signal regulated kinase
GCL	Glutamate cysteine ligase
GST	Glutathione S-transferase
HO-1	Heme oxygenase-1
HRP	Horse Radish Peroxidase
IPG	Immobilized pH gradient
IκB	Inhibitory kappa B protein
IL	Interleukin

IKK	IκB kinase
JNK	JUN amino-terminal kinase
Keap1	Kelch like associated protein 1
LMP1	Latent membrane protein 1
LPS	Lipopolysaccharide
MALDI-TOF-MS	Matrix associated laser desorption ionization-time of flight-mass spectrometry
MAPK	Mitogen activated protein kinase
MAF	Musculoaponeurotic fibrosarcoma
m/z	Mass to charge ratio
NQO1	NAD(P)H:quinone oxidoreductase-1
Nrf2	Nuclear factor E2-related protein 2
NF-κB	Nuclear factor-kappa B
NMR	Nuclear magnetic resonance
PERK	Protein kinase RNA-like Endoplasmic Reticulum Kinase
PKC	Protein kinase C
PMA	Phorbol 12-myristate 13-acetate
ROS	Reactive oxygen species

SDS	Sodium Dodecyl Sulfate
SnB	Sodium *n*-butyrate
SOD	Superoxide dismutase
TNF	Tumour necrosis factor
VDAC1	Voltage-dependent anion-selective channel protein 1
2-DE	Two dimensional gel electrophoresis

CHAPTER 1

INTRODUCTION

Based on a global cancer statistics (GLOBOCAN 2008), approximately 12.7 million people were diagnosed with cancer and 7.6 million people died of the disease in 2008 (Jemal *et al*., 2011). Poor cancer survival may be caused by late stage diagnosis and adoption of cancer-causing behaviour such as smoking. WHO indicates that a significant proportion of the global cancer burden could be prevented (Danaei *et al*., 2005). The National Institute of Health (NIH) of US defines cancer prevention as the reduction of the number of deaths from cancer through the reduction of cancer incidence and suggests that cancer may be prevented by avoiding known risk factors such as carcinogens and smoking or by chemoprevention to reverse pre-neoplastic changes (Bode and Dong, 2009).

Drugs that have been evaluated in chemoprevention trials on high risk individuals and approved by the U.S. FDA include COX-2 inhibitor celecoxib for colon cancer prevention, selective estrogen receptor modulators tamoxifen and raloxifene for breast cancer prevention, and 5α-reductase inhibitor finasteride for prostate cancer prevention (Bode and Dong, 2009). However, these drugs did not receive widespread application due to serious side effects. For example, tamoxifen was associated with an increased risk for blood clots

and endometrial cancer in postmenopausal women while finasteride treatment was believed to be associated with increased risk for developing high grade prostate tumours.

Meanwhile, research has shown that phytochemicals in vegetables and fruits have potential to reduce risk of a variety of chronic and inflammatory conditions including cancer (Surh, 2003). Large-scale anticancer drug discovery and screening programs promoted by the National Cancer Institute USA (NCI) have played important roles in the development of anti-cancer natural compounds. Several lead compounds such as genistein from soybeans, lycopene from tomatoes, curcumin from turmeric, sulforaphane from asparagus, indole-3-carbinol from broccoli, and resveratrol from grapes and peanuts are in preclinical or clinical trials for cancer chemoprevention. Resveratrol for example has chemopreventive and chemotherapeutic potential in all three stages of carcinogenesis (initiation, promotion, and progression) (Athar *et al*., 2007). Resveratrol is currently in phase I studies in colorectal cancer patients and in healthy subjects at high risk of developing melanoma (Nobili *et al*., 2009).

Coleus tuberosus, Benth, a small ground plant with starchy tubers is locally known as 'ubi kemili'. Preliminary study on the crude extract of *Coleus tuberosus* showed that it has strong anti-tumour properties. According to Lim, the active anti-tumour compound in *Coleus tuberosus* tubers is identified as maslinic acid (Lim, 2002). Maslinic acid is a pentacyclic triterpene with

potential antioxidant and anti-tumour properties (Montilla *et al*., 2003; Reyes *et al*., 2006). It has been shown to inhibit proliferation and induce apoptosis in some tumour cell lines through regulation of reactive oxygen species. Maslinic acid induces apoptosis in HT-29 human colon cancer cells by activating the mitochondrial apoptotic pathway (Reyes *et al*., 2008). Maslinic acid has also been shown to reduce pro-inflammatory cytokines production in murine macrophages (Martin *et al*., 2006) and regulate gene expression profile associated with inflammation in murine liver (Guillen *et al*., 2009).

Tumours may originate from sites of infection or chronic inflammation. Approximately 25 % of all cancers are associated with chronic infection and inflammation. Epidemiological and experimental findings showed that non-steroidal anti-inflammatory drugs (NSAIDs), which are COX inhibitors, protect against several types of tumours. NSAIDs are promising chemopreventive agents, however reports on their cardiovascular toxicity, gastrointestinal side effects, liver and renal adverse effects have shifted interest to natural anti-inflammatory agents (Capone *et al*., 2007). Numerous dietary and medicinal phytochemicals in particular genistein, gingerol, capsaicin, EGCG, resveratrol and curcumin have been reported to selectively inhibit the COX-2 expression (Cerella *et al*., 2010). These natural compounds affect COX-2 expression at the transcriptional level by inhibiting NF-κB and AP-1 activities (Chun and Surh, 2004).

Another strategy for preventing cancer is to modulate the levels of enzymes that promote the elimination of endogenous and environmental carcinogens. A wide array of anti-oxidant and detoxifying enzymes, such as NQO1, SOD, GST, HO-1, and GCL protect against oxidative and electrophilic stress. Under physiological conditions, these enzymes are expressed constitutively at relatively low levels but the expression levels can be enhanced in response to natural compounds such as coumarins, diterpenes, indoles, curcumin, sulforaphane, and isothiocyanates (Eggler *et al*., 2008). The effects of these natural phytochemicals are mediated in part through activation of the Nrf2 signaling pathway. A distinct set of Nrf2-regulated proteins maintains cellular-reducing equivalents and potentiate anti-oxidant capacity, thereby reinforcing defense against inflammation (Kundu and Surh, 2010).

Concomitant induction of the Nrf2 cytoprotective pathway and inhibition of the NF-κB/AP-1-COX2 inflammatory signaling is a crucial mechanism by which medicinal phytochemicals exhibit their cancer chemopreventive effect. The proteomics approach can be used to elucidate the underlying mechanisms of chemopreventive phytochemicals. Proteomic techniques facilitate the qualitative and quantitative measurement of a broad-spectrum of proteins (Pastwa *et al*., 2007). Information derived from 2-DE and MALDI-TOF-MS allow the assessment of differentially expressed proteomes of cancer cells in response to chemopreventive drug treatment (Liebold *et al*., 2006). This may be useful for the discovery of drug-specific biomarkers.

Given that maslinic acid has potential anti-tumour and anti-inflammatory properties, whether it is capable of inhibiting the pro-inflammatory pathway that mediates COX-2 expression, activating the anti-oxidant defense system and modulating novel molecular targets should be evaluated. In order to confirm these assumptions, this study aims to:

(a) Isolate and characterize maslinic acid from the chloroform extract of *Coleus tuberosus* tubers,

(b) Determine the suppressive effect of maslinic acid on pro-inflammatory targets NF-κB and AP-1 binding activities as well as COX-2 expression,

(c) Evaluate the effect of maslinic acid at inducing detoxifying and anti-oxidant enzymes through activation of the Nrf2-ARE pathway, and

(d) Study the molecular response of maslinic acid at the proteomics level

Taken together, this study clarifies the role of maslinic acid as a potential cancer chemopreventive agent targeting various cell signaling molecules.

CHAPTER 2

LITERATURE REVIEW

2.1 Chemoprevention: An essential approach to cancer control

Many factors contribute to the development of cancer, including heredity, exposure to carcinogens and infectious agents (Weinberg, 2007). At the molecular level, cancer is a disease caused by genes. Recent investigation on the cancer genome at the chromosomal and nucleotide level revealed extensive genetic change (Ledford, 2010). This involves mutations of genes responsible for DNA repair, tumour suppressor genes, and oncogenes. Mutation of these genes alters the proliferative capacity and sensitivity to normal growth control mechanism, as well as distortions which increases susceptibility to cancer development (Knowles and Selby, 2006).

The carcinogenic process as described by Berenblum and Shubik (Yuspa, 1994) indicates that there are at least three major stages involved, i.e. initiation, promotion, and progression. Initiation is a rapid and irreversible process which includes the initial uptake or exposure to carcinogens directly at the DNA level, causing genotoxic damage; tumour promotion is a relatively lengthy and reversible process, referring to clonal expansion of mutated pre-neoplastic or pre-malignant cell; and progression is the final stage of

neoplastic transformation, with tumour growth and acquisition of invasive and metastatic potential (Surh, 2003).

The latency period in the promotion stage of carcinogenesis underscores the requirement for acquisition and accumulation of multiple events during cancer development. The rationale of cancer chemoprevention is to prevent or suppress these events before a series of complex genetic changes takes place which results in invasive and metastatic malignancy. "Cancer chemoprevention" is a term coined by Sporn in 1976, which defines the usage of pharmacological agents to reverse, suppress or prevent either the initial phase of carcinogenesis or the progression of neoplastic cells to cancer (Sporn *et al*., 1976).

Cellular and molecular events affected or regulated by chemopreventive agents include modulation of phase I/II drug metabolizing enzymes, DNA repair, cell cycle progression, cell proliferation, differentiation and apoptosis, growth hormonal activity modulation, ligands for nuclear receptor, and modification of chromatin structure. Certain mechanisms are interconnected and partially overlap. Modulation of a given end-point may be the result of a specific mechanism or the consequences of other mechanisms upstream (Flora and Ferguson, 2005). Many studies have been carried out on elucidating the molecular mechanisms of chemopreventive agents. Some of the mechanisms of action are discussed henceforth.

2.1.1 Modulation of phase I and II enzymes

Metabolism of xenobiotics (exogenous chemical substances in the body) is generally divided into phase I and phase II metabolisms. Chemical carcinogen may be activated via phase I metabolism (activation of pro-carcinogens to highly reactive carcinogens) or detoxified by phase II metabolism (involves conjugation process which increases polarity of the compounds thereby facilitating elimination). The physiological balance of these drug metabolizing enzymes between competing activating and detoxifying reactions determines the sensitivity of an individual to carcinogens. Thus, modulation of phase I and phase II enzymes by phytochemicals can confer protection against carcinogen-induced cellular damage (Issa *et al*., 2006).

Activation of anti-oxidant response element (ARE), a promoter region found in several genes encoding for detoxifying enzymes like NQO1, HO-1, GCS and SOD, has been used to screen for potential enzyme inducers. Transcription factor Nrf2, member of the basic leucine zipper (bzip) NF-E2 family of transcription factors is known to bind and activate ARE. Nrf2 is bound in cytoplasm to Keap1, and following dissociation Nrf2 migrates into the nucleus and enhances gene transcription through binding to ARE. Destabilizing the Nrf2-Keap1 complex is a potential mechanism targeted by detoxifying enzymes inducers to activate cytoprotective enzymes expression (Yu and Kensler, 2005).

2.1.2 Anti-oxidant activity

Oxidative stress generated by ROS may result in dysfunctional cell growth, differentiation, and death, which often occurs together with DNA mutations and ultimately leads to cancer development. Phytochemicals with antioxidant activities may exert their effects by absorbing free electrons and radicals. Compounds with hydroxyl groups attached to aromatic rings create an electron-rich environment that traps the ROS, preventing them from reacting with nucleophilic centers of cellular proteins and DNA. Some phytochemicals induce pro-oxidant rather than antioxidant activity at higher concentrations, thereby causing DNA damage and cell death (Issa *et al*., 2006).

Antioxidants target free radicals, which maybe generated from normal oxygen metabolism or during inflammatory responses. ROS may contain odd numbers of electrons e.g. superoxide (O_2^-), hydroxyl (OH^-), hydroperoxyl (HOO^-), peroxyl (ROO^-), and alkoxyl free radicals (RO^-), or even number of electrons such as hydrogen peroxide (H_2O_2) and lipid hydroperoxide (ROOH). Redox-sensitive transcription factors like NF-κB and AP-1 may be targeted by antioxidants since their activation promotes transcription of genes involved in cell cycle progression and cell proliferation (Loo, 2003).

2.1.3 Anti-inflammation

Arachidonic acid (AA) metabolism is the link to inflammation. AA is catalyzed by COX, lipoxygenase (LOX) and cytochrome P450 into eicosanoids metabolites. The eicosanoids are lipid-signaling mediators that play a central role in physiological and pathophysiological conditions. They have been identified as active carcinogens or tumour promoters; increased expression levels have detrimental effects on cancer development (Hyde and Missailidis, 2009). Anti-inflammatory agents may target AA-dependent pathway or AA-independent pathway. COX, LOX, and phospholipase A2 are considered AA dependent while nitric oxide synthase (NOS), 5-LOX, activating peroxisome proliferator-activator receptor (PPAR), NSAID activated gene-1 (NAG-1) and NF-κB are classified as AA-independent (Hyde and Missailidis, 2009).

The major mechanism of anti-inflammatory synthetic drugs or natural compounds relies primarily on their ability to inhibit the cyclooxygenase activity of the COX enzymes. COX-2 is the inducible form of COX which has a role in inflammatory and proliferative reactions (Kundu and Surh, 2008). Pro-inflammatory mediators such as growth factors (epidermal growth factor, transforming growth factor-β, and vascular endothelial growth factors), cytokines (TNF-α and IL-6), oncogenes (p53), and other factors that induce COX expression as well as the products of the COX and LOX pathways like prostaglandins, thromboxanes, leukotrienes are also targeted by anti-inflammatory agents (Murakami and Ohigashi, 2007).

2.1.4 Modulation of cell signaling pathways

Cellular signaling is a complex signal communication network which controls basic biological activities of cells and coordinates cell actions. The growth of cancer cells depends on multiple pathways. Altered proteins resulting from the mutations or defects of genes influence the way cells communicate with each other. Soy isoflavones including genistein, daidzein, and glycitein as well as indole-3-carbinol (I3C) and its *in vivo* dimeric product 3,3-diindolylmethane (DIM) from cruciferous vegetables target the NF-κB, phosphoinositide 3-kinase (PI3K)/Akt, and MAPK pathways (Figure 2.1) (Sarkar and Li, 2004).

Cellular targets such as NF-κB, IκB, and IKK control cell proliferation, apoptosis, inflammation, stress response within the NF-κB pathway; phosphoinositide-dependent kinase (PDK) 1 and PDK2 activate the Akt pathway, which play critical roles in cell survival; MAPK pathways consist of a three-tiered kinase core in which a MAPK kinase kinase (MAP3K) activates a MAPK kinase (MAP2K) that activates a MAPK (ERK, JNK, p38), regulate cell growth and survival; other molecular targets like Notch receptors, p53 protein as well as androgen receptors are involved in their respective pathways in cell regulation. All of these molecular players are targeted by chemopreventive agents in cancer chemoprevention (Dorai and Aggarwal, 2004).

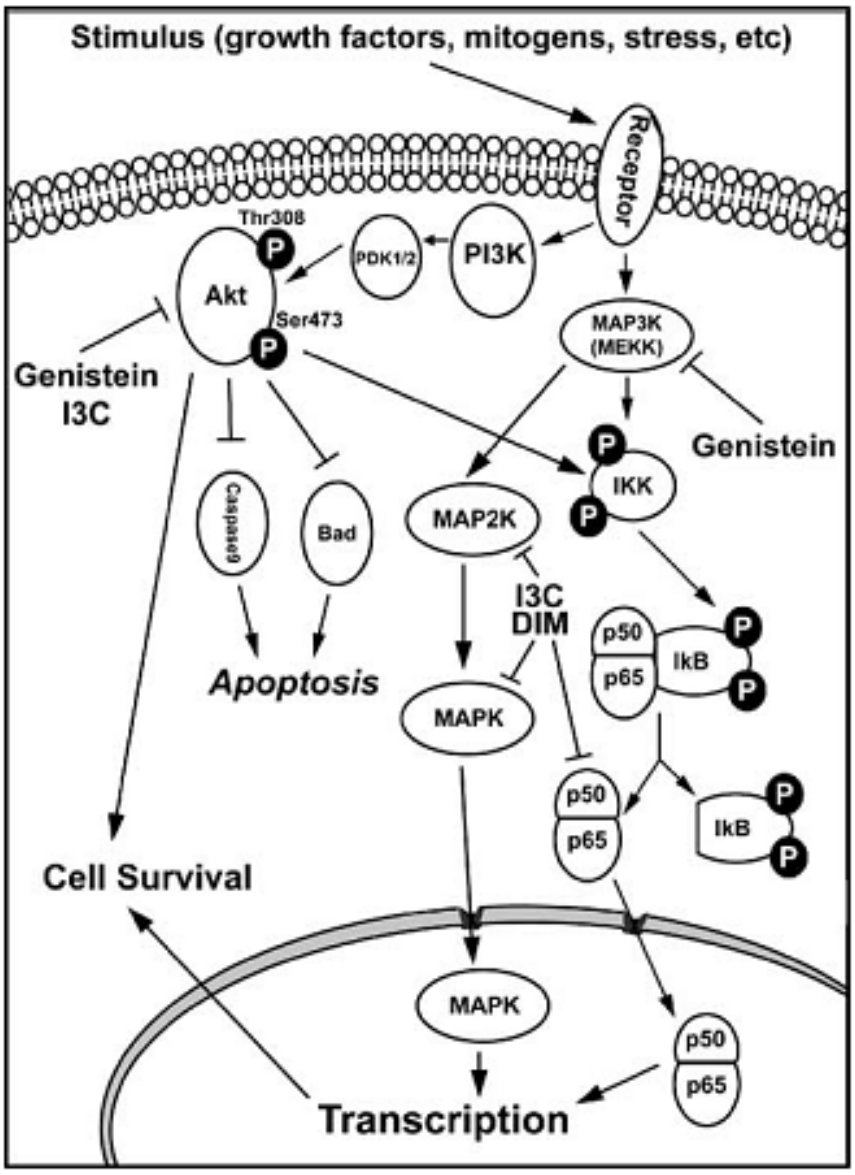

Adapted from Sarkar and Li, 2004

Figure 2.1: The effects of genistein, indole-3-carbinol (I3C), and 3, 3-diindolylmethane (DIM) in response to growth factors, mitogens, and stress. These chemopreventive phytochemicals may inhibit the kinase activity upstream of MAPK signaling or prevent nuclear translocation of the NF-κB transcription factor. They may also suppress the PI3K/Akt pathway which promotes cell survival and inhibits expression of pro-apoptotic proteins such as caspase-9 and Bad protein.

2.1.5 Induction of apoptosis and cell cycle arrest

Insensitivity to apoptosis induction and absence of normal cell cycle control mechanism promote uncontrolled cell proliferation. Many chemopreventive agents induce apoptosis through the mitochondria-mediated pathway. Stress signals elicited by these chemopreventive compounds regulate the trafficking of pro-apoptotic proteins (e.g. Bax and Bak) or anti-apoptotic proteins (e.g. Bcl-2 and Bcl-x), leading to the release of cytochrome c from the mitochondrial inner membrane, followed by formation of 'apoptosome' (formed by cytochrome c, apoptotic protease-activating factor 1 (APAF-1) and caspase-9). Caspase-9 further activates downstream effector caspases, such as caspase-3, -6 and -7, which degrade important intracellular proteins, leading to the morphological changes showing the phenotype of apoptotic cells. Meanwhile, disturbance of the balance among cyclins, cyclin-dependent kinases (CDKs) and CDK inhibitors (CDKIs) that governs the progression of the cell cycle by chemopreventive compounds can potentially inhibit proliferation of neoplastic cells (Figure 2.2) (Chen and Kong, 2005).

Some chemopreventive agents activate upstream kinases such as JNK or inhibit PI3K/Akt pathway to induce apoptosis; inhibiting NF-κB and AP-1 activation, thereby down-regulating anti-apoptotic and cell cycle regulating proteins; inducing caspase activation to execute cell death; down-regulating survivin and increasing p53 expression; eliciting cell-cycle arrest through the induction of CDKIs (p21 and p27) and the inhibition of CDK4, CDK2, cyclin D1 and cyclin E (Chen and Kong, 2005).

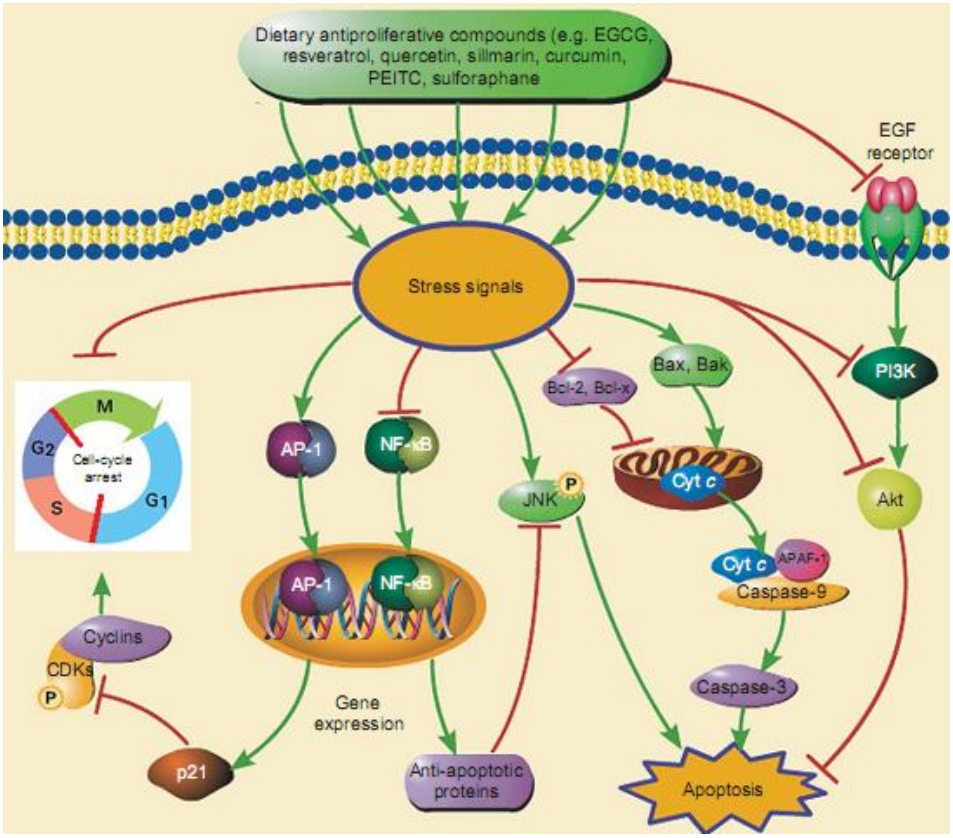

Adapted from Chen and Kong, 2005

Figure 2.2: Induction of apoptosis and cell-cycle arrest by natural chemopreventive agents. Stress signals relayed by chemopreventive compounds may trigger multiple pathways, including PI3K/Akt signaling, JNK signaling, NF-κB and AP-1 transcriptional activation as well as the release of Cyt c from mitochondria. This results in activation of cell death effectors such as caspase-3, inhibition of anti-apoptotic proteins and induction of CDK inhibitor proteins, which cause apoptosis and cell cycle arrest.

2.2 Phytochemicals: natural products from plants

The plant kingdom is a rich source of chemopreventive agents (Nobili *et al*., 2009; Russo, 2007). Phytochemicals are defined as secondary metabolites, or the non-nutritive components in plants, i.e. they are not essential for normal growth, development, or reproduction of the plant. Phytochemicals play a role in the adaptation of plants to ecological pressure. For example, several secondary metabolites function as poisons to ward off predators and pathogens, some act as coloured pigments and odoriferous substance to attract pollinators, while others serve as allelopathic chemicals which often harm or prevent other plants from becoming established in the vicinity of the plant (Cseke *et al*., 2006).

Secondary metabolites are generally classified into three categories based on their oxidation state. They are known as:

Terpenes are hydrocarbon based natural products that possess a unifying five carbon unit (isoprene) structure. Terpenes are known for their essential oils and use as fragrance while others have ecological and physiological functions like allelopathy and plant hormones. Examples of terpenes include lupeol, taxol, menthol, retinol, and caretenoids (Figure 2.3).

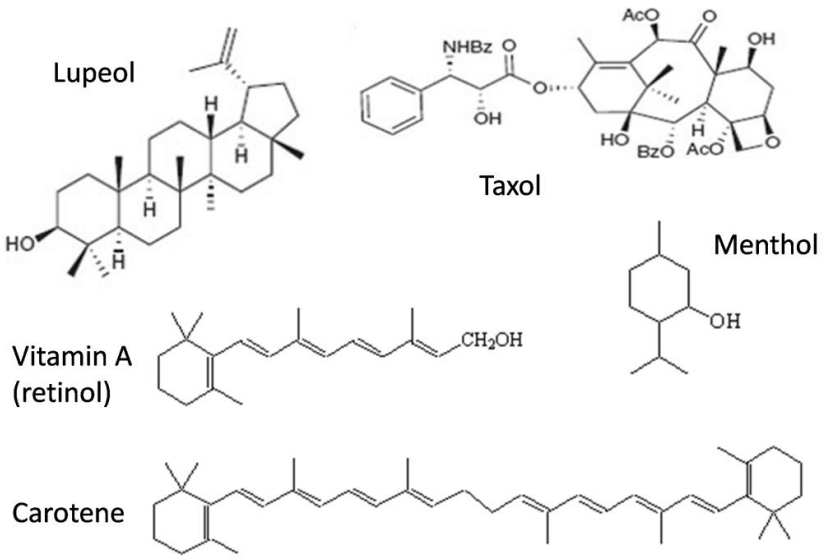

Figure 2.3: Structures of terpenic compounds

Aromatics are natural products with a carbocyclic or heterocyclic aromatic ring that generally contains one or more hydroxyl groups. Phenolic compounds have estrogenic functions (genistein) and antioxidant (quercetin, epigallocatechin gallate (EGCG), and resveratrol) activities (Figure 2.4).

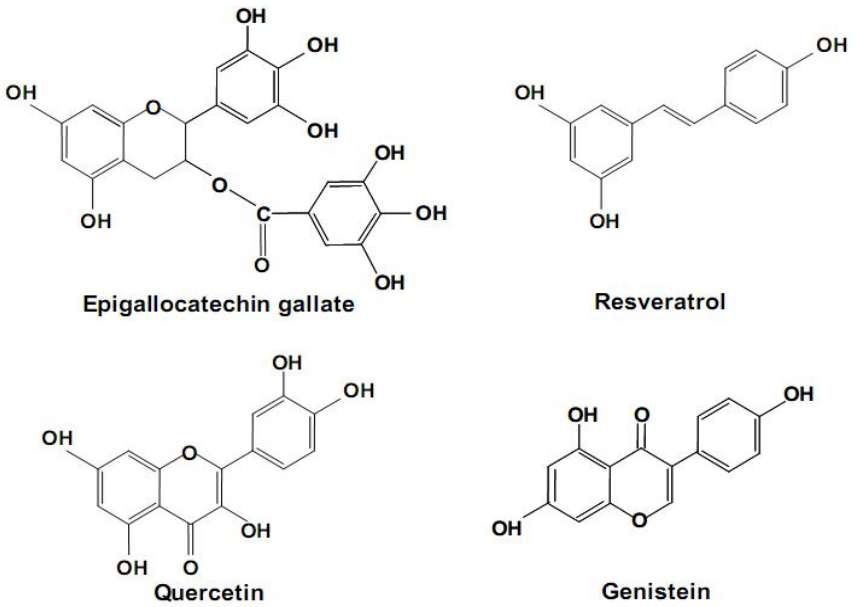

Figure 2.4: Structures of polyphenolic compounds

Amines and alkaloids are pharmacologically active and basic compounds derived from amino acids that contain one or more heterocyclic nitrogen atoms. Some of the well known alkaloids include vinblastine (anti-tumour alkaloid) and camptothecin (chemotherapy drugs) (Figure 2.5) (Cseke *et al*., 2006).

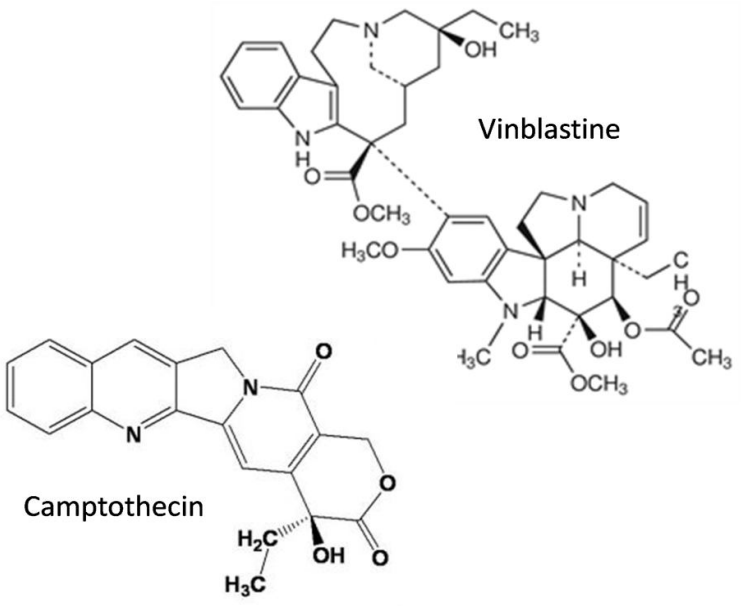

Figure 2.5: Structures of alkaloid compounds

2.2.1 *Coleus tuberosus*, Benth

Coleus tuberosus, known as 'ubi kemili' in the Malay language, is an herbaceous plant from the Lamiaceae family (Figure 2.6). The plant is found in the tropical and subtropical regions of India, Nepal, Burma, Sri Lanka, Thailand and Malaysia (Bajaj, 1994). In these countries, the tubers of *Coleus tuberosus* are eaten as vegetables and pickles while the leaves of other *Coleus* species are used as a spice.

(A)

(B)

Figure 2.6: *Coleus tuberosus* Benth from the Lamiaceae family. (A) Leaves and the (B) front and cut sections of *Coleus tuberosus* Benth tubers

Preparations from several *Coleus* species are used in Ayurvedic medicine in India (Bajaj, 1994). Secondary metabolites such as codeine, carvacrol, flavones, aromatic acids and tannins are found in *Coleus amboinicus*; diterpenoids such as forskolin, coleonols, coleons, barbatusin, cyclobutatusin, coleosol, coleol, coleonone, deoxycoleonol, 7-deacetylforskolin and 6-acetyl-7-deacetylforskolin are found in *Coleus forskohlii* (Joy *et al*., 2001). *Coleus tuberosus* has strong anti-tumour-promoting properties. One of the active anti-tumour promoting compounds has been identified as maslinic acid, a triterpene (Lim, 2002).

2.2.2 Triterpenoids

The C_{30} triterpenes have six isoprene units and are biosynthetically derived from squalene. They are colourless solids of high melting points found in plant resins, cork, and cutin. Over the past decade, a large group of cyclic triterpenoid-like substances which comprise more than 4000 different compounds such as free triterpenoids, triterpenic glycosides (saponins), phytosterols and their precursors have been identified (Cseke *et al*., 2006). Triterpenoids are studied for their anti-inflammatory, anti-oxidant, hepatoprotective, analgesic, antimicrobial, antimycotic, virostatic, immunomodulatory, and tonic effects (Dzubak *et al*., 2006).

Only a few triterpenoids are common in plants. These include the amyrins and ursolic and oleanolic acid, which are commonly found on the waxy coatings of

leaves and some fruits. Ursolic acid and oleanolic acid from the ursane and oleanane group of triterpenoids have been shown to act at various stages of tumour development, such as inducing tumour cell differentiation and apoptosis as well as inhibiting angiogenesis and invasion of tumour cells. They are effective inducers of metallothionein, a small cysteine rich protein acting like glutathione in the body defense against toxic stress, which may account for their ability to confer protection against chemically-induced liver injury (Liu, 2005).

2.2.3 Maslinic acid

Maslinic acid (2, 3-dihydroxyolean-12-en-28-oic acid) is a natural pentacyclic triterpene from the oleanane group. Low concentrations of maslinic acid are to be found in medicinal plants, such as *Centaurium erythraea* (Bellavita *et al*., 1974), *Olea europaea* (Mussini *et al*., 1975), *Elaeagnus oldahmi* (Tsuen-Ih *et al*., 1976), *Eugenia gustavioides* (Yazaki, 1977), *Aster yunnanensis* (Yu *et al*., 1995), and *Coleus tuberosus* (Lim, 2002). Maslinic acid has cytotoxic and anti-tumour activities (Kim *et al*., 2000). The anti-tumour effect of maslinic acid had been confirmed later by studies investigating its role in cell cycle arrest and apoptotic effects in colon cancer cells (Reyes *et al*., 2006). Maslinic acid induces apoptosis in HT29 human colon cancer cells via the mitochondrial pathway by inhibiting Bcl-2 expression, increasing the ratio of Bax, releasing cytochrome c from the mitochondria and activating caspase-9 followed by caspase-3 (Reyes *et al*., 2008). Maslinic acid also exerts immunosuppressive activities through reduction of pro-inflammatory

cytokines TNF-α and IL-1β production in LPS-stimulated murine macrophages (Martin *et al*., 2006) and regulates inflammatory gene expression profile in the mouse liver (Guillen *et al*., 2009). The molecular basis for the anti-inflammatory effect of maslinic acid entails further investigation.

2.3 Transcription factors NF-κB and AP-1

NF-κB and AP-1 are evolutionarily conserved transcription factors which act independently or coordinately to regulate gene expression involved in cell proliferation, differentiation, apoptosis, inflammation, angiogenesis, and tumour invasion (Kundu and Surh, 2005). Many of the activated pathways in tumourigenesis converge on NF-κB and AP-1 and elevated transcriptional activity of these transcription factors has been noted in various human malignancies (Nakshatri *et al*., 1997; Smirnov *et al*., 2001). They are therefore potential targets for cancer prevention (Aggarwal and Shishodia, 2006).

2.3.1 NF-κB signaling pathway

NF-κB is activated by signals that represent states of infection and stress, such as interleukin-1 (IL-1), tumour necrosis factor-α (TNF-α), dsRNA, lipopolysaccharide (LPS), sheer stress, and ROS. NF-κB refers to a general name that describe family members sharing an N-terminal reticuloendotheliosis (Rel) homology domain, which include p50 (also known as NF-κB1), p52 (also known as NF-κB2), p65 (also known as Rel A), c-Rel and Rel B. NF-κB dimers bind to κB sites in the promoters or enhancers of

target genes; the sequence on the κB site dictates the composition of the bound NF-κB dimer and also determines the co-activator requirements (Calzado *et al*., 2007).

NF-κB is regulated mainly through its localization (Figure 2.7). In resting cells, NF-κB proteins are kept in the cytoplasm associated with IκB proteins. These IκB proteins inhibit binding of NF-κB to its corresponding DNA sequence. Degradation of IκB is a tightly regulated event that is initiated upon specific phosphorylation by activated IKK. Following cell stimulation, IκB proteins undergoes rapid ubiquitin-mediated proteasomal degradation that results in the release of the bound, cytoplasmic NF-κB dimers. Cytoplasmic NF-κB then translocates to the nucleus and drives gene expression. NF-κB induces expression of growth factors and cytokines that are involved in stress response, inflammation, cell proliferation, cell cycle progression, metastasis and angiogenesis (Ghosh, 2007).

Aberrant NF-κB regulation has been observed in human hematopoietic and solid tumours. Chromosomal amplification, overexpression, and rearrangement of Rel/NF-κB components result in persistent NF-κB activation. Constitutive activation of upstream signaling kinases and mutations of inhibiting protein IkB were reported in several human cancer cell types (Ghosh and Hayden, 2008).

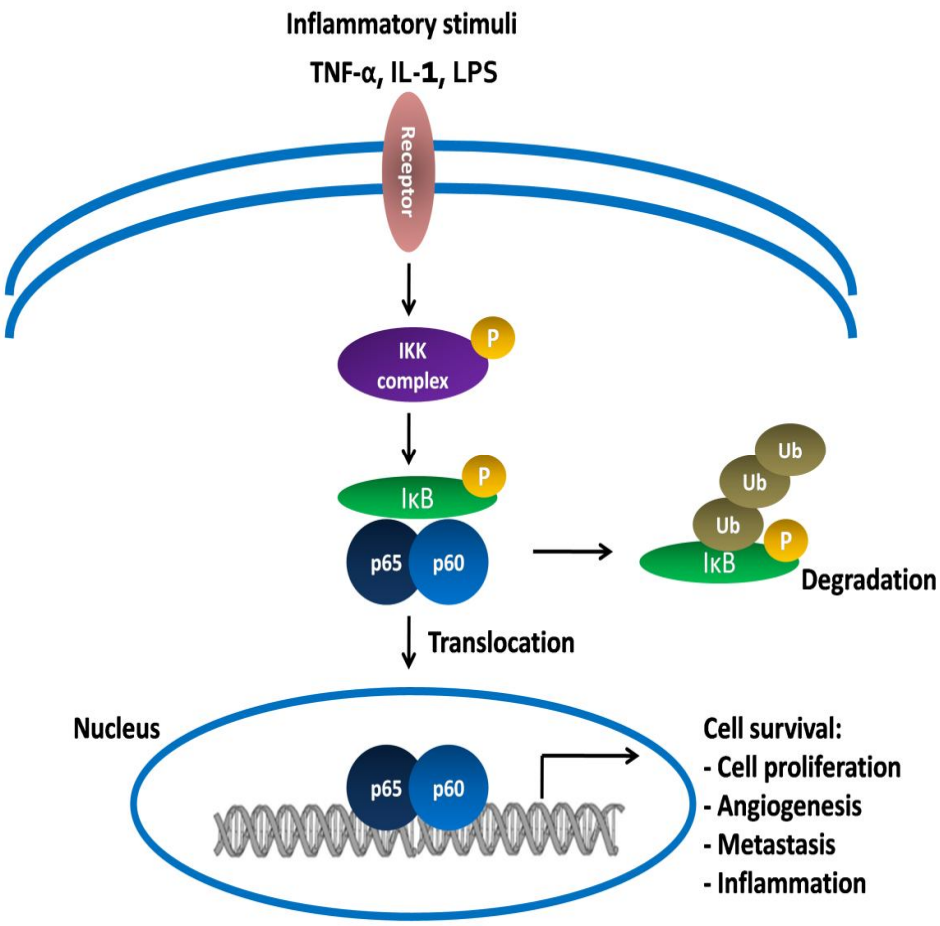

Figure 2.7: NF-κB activation pathway. In the NF-κB activation model, inflammatory stimuli induce activation of IKK complex. This results in the phosphorylation of IκB proteins and consequently their ubiquitin-mediated degradation. Released NF-κB dimers translocate into the nucleus and bind to the promoters or enhancers of target genes. NF-κB target genes are involved in cell proliferation, angiogenesis, metastasis, and inflammation (Ghosh and Hayden, 2008).

2.3.2 AP-1 signaling pathway

Extracellular stimuli such as growth factors, hormones, stress, cytokines, ROS and UV can induce AP-1 transcriptional activation. AP-1 is a dimeric transcription factor composed of members of the Jun, Fos, ATF and MAF protein families. There are many different combinations of AP-1 heterodimers and homodimers, and each specific combination regulates a particular set of genes. The basic leucine zipper (bzip) domain present in both Jun and Fos family proteins is required for AP-1 dimerization and DNA binding. AP-1 dimers bind with highest affinity to the TPA response element (TRE). Dimers also bind to unique elements such as the cAMP response element (CRE), serum response element (SRE), antioxidant response element (ARE), and MAF-recognition elements (MAREs). The choice of binding site may be tissue specific, affected by neighbouring sequences, or dependent upon interactions with other transcriptions factors or cofactors. AP-1 proteins can also interact with non-bzip proteins, including the p65 subunit of NF-κB, CREB binding protein (CBP)/p300, and retinoblastoma (Rb) (Matthews *et al*., 2007).

AP-1-regulated gene expression occurs through changes in *jun* and *fos* gene transcription and mRNA turnover, effects on Jun and Fos protein turnover, post-translational modifications of Jun and Fos proteins that modulate their transactivation potential, and interactions with other transcription factors that can either synergize or interfere with AP-1 activity. Some biological effects of AP-1 may be mediated by gene repression. These effects may be dependent on

the interactions of AP-1 proteins with transcriptional co-repressors and may also be affected by the nature of the AP-1 target site (Shaulian and Karin, 2002).

The predominant AP-1 activation signals travel through the MAPK cascade (Figure 2.8). Serum and growth factors induce AP-1 by activating the ERK, enhancing the transcriptional activity of Ternary complex factors (TCFs) that bind to *fos* promoters (Matthews *et al*., 2007). The induction of AP-1 by pro-inflammatory cytokines and genotoxic stress is mostly mediated by the JNK and p38 MAPK cascades. Once activated, JNKs are translocated to the nucleus, phosphorylate c-Jun and enhance its transcriptional activity (Vogt, 2002). The p38 and JNKs also phosphorylate and potentiate the activity of ATF2**,** which heterodimerizes with c-Jun to bind divergent AP-1 sites in the *c-jun* promoter. The contribution of p38 to AP-1 induction can be mediated by the direct phosphorylation and activation of ATF2 and TCF (Eferl and Wagner, 2003).

Constitutive expression of activated oncogenes, such as *RAS*, results in an elevation of AP-1 activity, mostly through persistent activation of ERK and JNK. AP-1 exert its effects by regulating genes involved in cell proliferation, differentiation, apoptosis, angiogenesis and tumour invasion. Overexpression of c-Fos results in osteosarcoma formation while c-Jun expression is important in the development of skin and liver tumours (Eferl and Wagner, 2003).

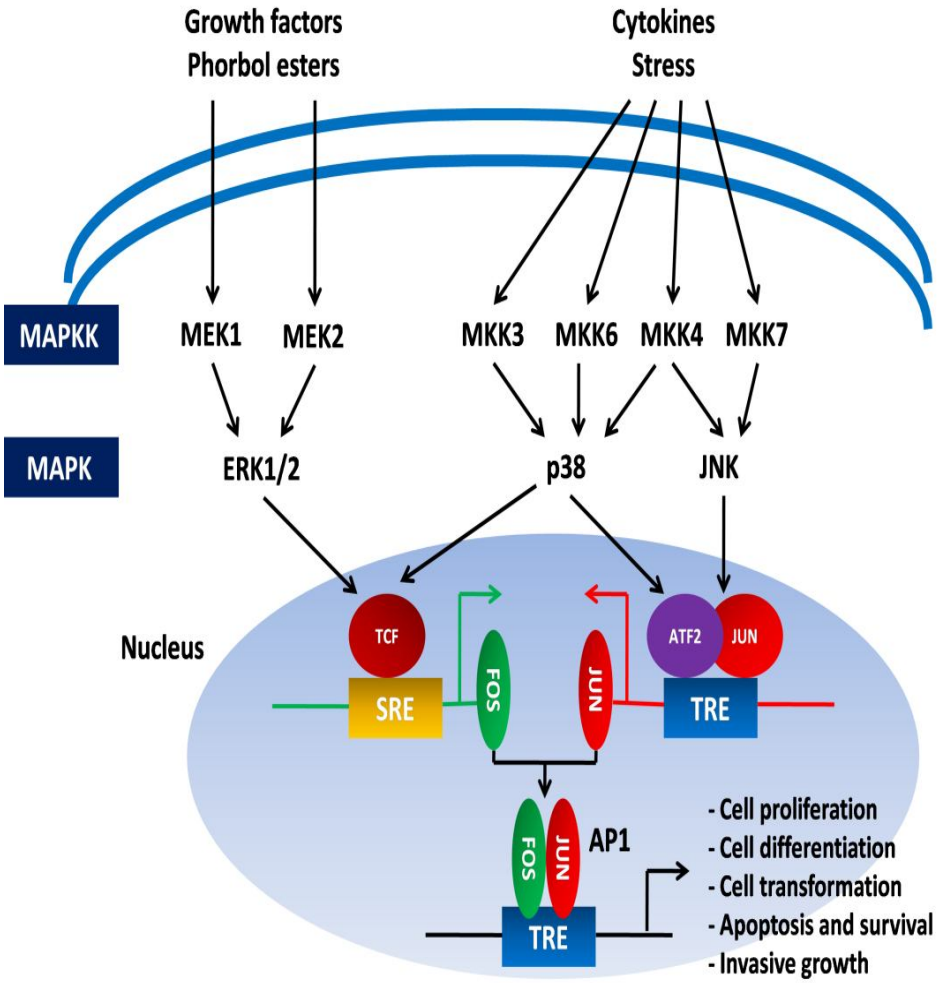

Figure 2.8: AP-1 activation pathway. AP-1 activity is stimulated by external signals (growth factors, phorbol esters, stress, and cytokines) to MAPKKs and MAPKs. MAPKs activate various transcription factors (TCF, ATF2 and JUN) that induce the transcription of *FOS* and *JUN* genes, thereby increasing the number of AP-1 complexes and activating AP-1 target genes. AP-1 target genes are involved in cell proliferation, differentiation, transformation, apoptosis and invasive growth (Eferl and Wagner, 2003).

2.4 Pro-inflammatory COX-2 enzyme

One of the target genes induced by NF-κB and AP-1 is the COX-2 enzyme. COX-2 is a pro-inflammatory immediate early response protein, which is chronically up-regulated in many pathological conditions. Strategies aimed at inhibiting COX-2 enzymatic activity have been applied for cancer treatment (Marks *et al*., 2000).

2.4.1 Mechanism of COX-2

In acting as a cyclooxygenase, prostaglandin (PG)H_2 synthase donates two oxygen molecules to arachidonic acid to form PGG_2, which is then converted to PGH_2 by its peroxidase activity. PGH_2 is an unstable endoperoxide which is converted by a number of cell-specific isomerases, leading to the formation of prostaglandins such as PGE_2, PGI_2, and PGF_{2a} (Figure 2.9).

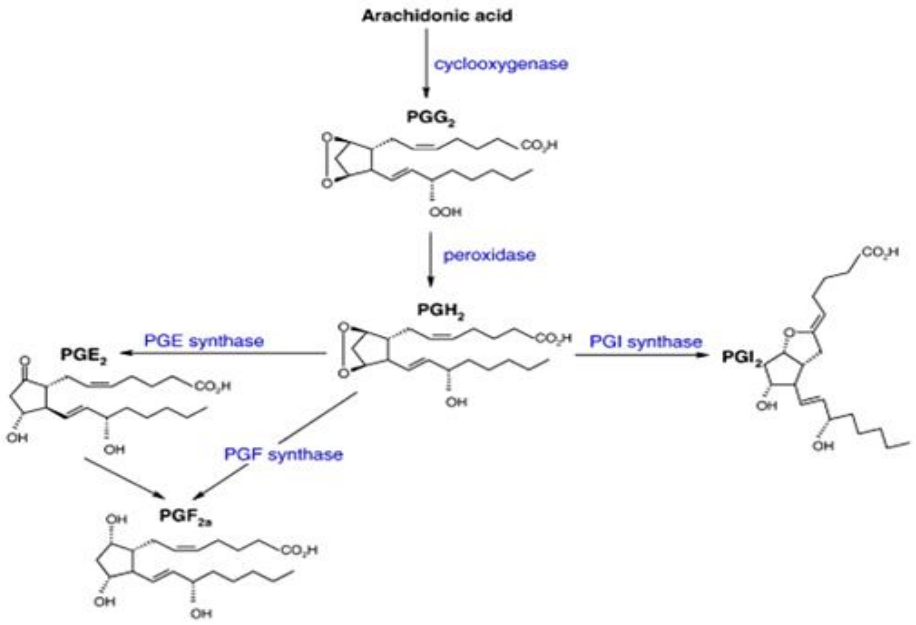

Figure 2.9: The COX pathway. The main arachidonic acid derivatives as catalyzed by COX and its isomerases (Hyde and Missailidis, 2009).

There are two COX enzymes, COX-1 and COX-2. Although both COX enzymes share similar catalytic activities, such as cyclooxygenase and peroxidase activities, they are regulated differentially. COX-1 is expressed at low levels in many tissues. This ensures a constant production of prostaglandins, which contributes to important physiological functions, such as platelet aggregation, renal water balance and gastric mucosal protection (Chun and Surh, 2004).

COX-2 is expressed in response to physical, chemical and biological stimuli (Murakami and Ohigashi, 2007). Upon stimulation, its expression is high and transient. This leads to a burst of prostaglandins production in a tightly regulated time-limited manner. Thus, depending on the COX isoform, the production of the same earlier precursor PGH_2 greatly differs in terms of the amount and timing of production (Cerella *et al.*, 2010). However, COX-2 expression may surpass normal physiological control and result in cancer formation. Constitutive COX-2 expression has been implicated in various types of malignancies. Transgenic mice that over-express COX-2 in mammary glands, skin or stomach are susceptible to develop malignancies, while COX-2 knockout mice are less prone to intestinal tumourigenesis, skin papillomagenesis, and mammary carcinogenesis (Kundu and Surh, 2008).

2.4.2 Prostaglandins and inflammation

Prostaglandins are produced in a wide range of human tissues and have a central role not only in inflammation but also in regulating other physiological processes, including blood clotting, wound healing, immune responses, bone metabolism, and nerve growth and development (Mead *et al*., 1986). Some pro-inflammatory prostaglandins such as PGE_2, $PGF_{2\alpha}$, and 15d-PGJ_2 have been reported to contribute to tumour development. Activation of PGE synthase leads to the formation of PGE_2. Elevated levels of PGE_2 have been observed in various types of human cancers. PGE_2 promotes cell proliferation and tumour associated-neovascularization while inhibiting apoptosis and immune response. Prostaglandins function through binding to G protein-coupled receptors, known as prostaglandin E (EP) receptors (EP1, EP2, EP3 and EP4). The EP receptors play significant roles in tumour growth and development (Kundu and Surh, 2008).

COX-2 may be targeted for cancer prevention and treatment. Selective COX-2 inhibitors have been able to reduce formation of tongue, esophageal, intestinal, breast, skin, lung, and urinary bladder tumours in experimental animals (Dannenberg and Subbaramaiah, 2003). However, recent findings in controlled clinical trials showed that selective COX-2 inhibitors are associated with increased cardiovascular risk. Nevertheless, incorporating genetic biomarker data may help to identify patients who are most likely to respond to COX-2 inhibitors (William *et al*., 2009).

2.5 Nrf2/ARE signaling pathway

Modulation of enzymes expression involved in both elimination/inactivation of carcinogens and in cellular antioxidant defense is another important chemoprevention strategy. Induction of cytoprotective gene expression normally occurs through the Nrf2-ARE signaling pathway (Lee and Johnson, 2004).

2.5.1 Nrf2/Keap1 regulation

Nrf2 is expressed in many tissues, particularly those associated with detoxification such as the liver and kidney and those that are exposed to the external environment, such as the skin, lung and gastrointestinal tract (Motohashi *et al*., 2002). Nrf2 belongs to a subset of bzip genes sharing a conserved structural domain designated as the "cap'n'collar" (CNC) domain and is highly conserved with the Drosophila transcription factor CNC (Mohler *et al*., 1995). The C terminal basic region, upstream of the leucine zipper region, is responsible for DNA binding, and the acidic region is required for transcriptional activation (Jaiswal, 2004).

In the absence of cellular stress, Nrf2 is bound within the cytosol by an inhibitory partner Keap1, which interacts with the actin cytoskeleton (Itoh *et al*., 1999). Analysis of the Keap1 amino acid sequence and domain structure-function shows that it has a BTB (broad complex, tramtrack, bric-a-brac)/POZ (poxvirus, zinc finger) domain and a Kelch domain (Dhakshinamoorthy and

Jaiswal, 2001), also known as the double-glycine repeat domain. The main function of Keap1 is an adaptor protein between Nrf2 and the Cullin3-based E3-ligase ubiquitinylation complex, leading to the ubiquitination of Nrf2 and subsequent degradation by the 26S proteasome (Cullinan *et al*., 2004).

Mechanisms that modify Keap1 and/or Nrf2 or disrupting the Nrf2:Keap1 interaction (Figure 2.10) will result in the up-regulation of cytoprotective gene expression (Lo *et al*., 2006). Nrf2/Keap1 complex may be disrupted by modification of cysteine residues within the Keap1 or the phosphorylation of Nrf2. Cysteine residues in the position of Cys151, Cys273, and Cys288 of Keap1 are active sites of modification (Huang *et al*., 2002). Several protein kinases, including Protein Kinase C (PKC), ERK, JNK, p38, and Protein kinase RNA-like Endoplasmic Reticulum Kinase (PERK), are known to phosphorylate Nrf2 and cause its release from Keap1.

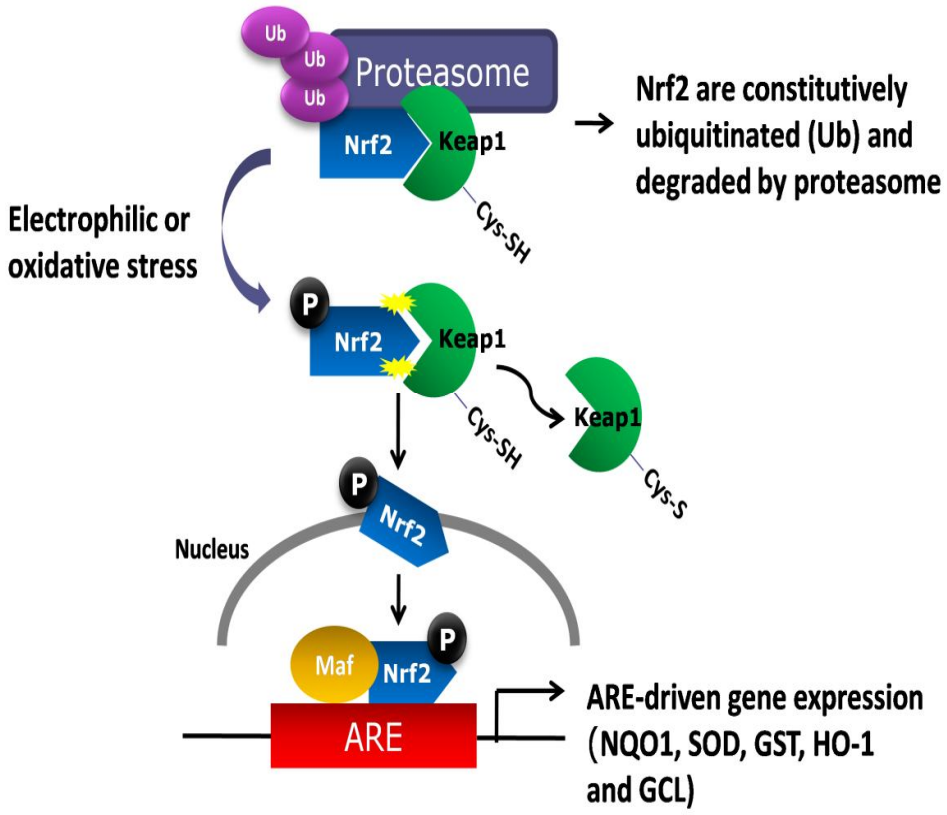

Figure 2.10: Mechanism of Nrf2-ARE signaling. Under normal physiologic conditions, Keap1 targets transcription factor Nrf2 for ubiquitination and proteasomal degradation. In the presence of oxidative stress, electrophiles or ROS react with the critical cysteine sulphydryl (Cys-SH) groups present in Keap1. Modified Keap1 no longer target Nrf2 for proteasomal degradation and results in Nrf2 stabilization and activation. Phosphorylation of Nrf2 by protein kinases might also facilitate dissociation of Nrf2 from Keap1. Stabilized Nrf2 then migrate into the nucleus and bind to its co-activator Maf protein (Maf) to transactivate ARE genes (Lee and Johnson, 2004).

2.5.2 Anti-oxidant response element (ARE)

ARE contains the *cis*-acting enhancer sequence that controls the basal and inducible expression of antioxidant genes in response to xenobiotics, antioxidants, heavy metals, and UV light (Rushmore *et al*., 1991; Copple *et al*., 2008). A nuclear localization sequence in the Nrf2 protein is known to facilitate its translocation from the cytoplasm to the nucleus (Jain *et al*., 2005). In the nucleus, Nrf2 protein dimerizes with small MAF proteins and bind to the ARE (Itoh *et al*., 1997). Nrf2 may also form heterodimers with other bzip transcription factors such as ATF4 prior to binding to the ARE (Nguyen *et al*., 2000). Nrf2 then stimulates transcription of downstream genes by recruiting transcriptional co-activators, particularly CBP through the Neh4 and Neh5 domains of the transcription factor (Zhu and Fahl, 2001). Different AREs have distinct sequence requirements. The sequence of a response element could manipulate the orientation of the activating transcriptional complex, thereby influencing interaction with required cofactors. In addition, the presence of a nucleotide in any given position of the ARE may determine whether Nrf2-Maf can bind in a stable manner. Some ARE sequences may represent suboptimal binding sites that prevent transcription from being dominated by Nrf2-Maf (Nioi *et al*., 2003).

2.5.3 Nrf2-inducible genes

Many genes encoding detoxifying, antioxidant, and glutathione-biosynthesis enzymes such as NQO1, SOD, GST, HO-1, GCL, aflatoxin B1 aldehyde reductase, microsomal epoxide hydrolase, ubiquitin/PKC-z-interacting protein

A170, peroxiredoxin 1, the heavy chain of ferritin, catalase, thioredoxin, carboxylesterase, aldehyde oxidase, aldehyde dehydrogenases, and 1-Cys peroxiredoxin are regulated by Nrf2 (Kobayashi and Yamamoto, 2006).

HO-1 is an anti-oxidant enzyme which converts heme to biologically active products, such as carbon monoxide (CO), biliverdin, which is quickly reduced to bilirubin and free iron which is sequestered by ferritin. The end-products of HO activity have protective effects; their formation are accompanied by heme removal which results in decreased oxidative stress, attenuation of inflammatory response, and a lower rate of apoptosis in numerous cell types (Kundu and Surh, 2010). HO-1 has important immunomodulatory and anti-inflammatory functions. Up-regulation of HO enzyme activity attenuated complement-dependent inflammation (Willis *et al.*, 1996). HO-1 knockout mouse develop chronic inflammatory disease and are highly vulnerable to endotoxins (Poss and Tonegawa, 1997).

NQO1 is a phase II detoxification enzyme which converts reactive quinones to hydroquinones by a double electron transfer mechanism. Induction of NQO1 in cells prevents one electron transfer-mediated generation of free radicals, thereby reducing the risk of DNA damage. NQO1 knockout mice are more susceptible to chemically-induced mouse skin carcinogenesis (Long *et al.*, 2000). Dietary administration of oltipraz, a potent inducer of NQO1 provides protection against carcinogen-induced aberrant crypt foci formation (Begleiter *et al.*, 2003). NQO1 expression decrease inflammatory response by down-

regulating cytokines expression such as TNF-α and IL-1β (Rushworth *et al*., 2008).

2.6 Proteomics in human cancer research

Recent publications on the cancer genomic analyses confirmed that there are common features in the associated pathways of solid tumours (Jones *et al*., 2008; Parsons *et al*., 2008). These genomic studies proved that cancer is a protein-pathway disease. Given that pharmacological interventions and diagnostic tests are directed at proteins rather than genes, a comprehensive study of the protein expression profile term 'proteomics' has great potential (Martin and Nelson, 2001).

Proteomics has rapidly expanded to include the discovery of novel biomarkers for early detection, diagnosis, and for the identification of novel drug targets (Pastwa *et al*., 2007). The goal of proteomics is to separate and elucidate the structure of all proteins, their function, expression profiles, and finally, the detection of protein-based cancer biomarkers that can be targeted for therapy.

2.6.1 Proteomics: A pharmacological approach to elucidate the chemopreventive properties of phytochemicals

Information derived from the differentially expressed proteomes of phytochemicals-treated cells may be potentially useful in the search for new drug targets. For example, treatment of lung cancer cells A549 with green tea

extracts induce up-regulation of several proteins that modulate actin remodeling and cell migration, including lamin A/C, annexin I and annexin II (Lu *et al*., 2009). Decrease or loss of annexin I expression in a number of cancers including breast, prostate, lymphoma, esophageal, and bladder cancers have been reported, indicating that annexin I may serve as a useful marker of cancer development and progression. Meanwhile, Hoelzl (2008) reported the alterations induced in human white blood cells by consumption of Brussels sprouts in a dietary intervention study with five participants. The study showed up-regulation of manganese superoxide dismutase (SOD) and down-regulation of heat shock 70 kDa (Hsp-70) protein (Hoelzl *et al*., 2008). Hsp-70 is involved in the regulation of apoptosis while SOD plays a key role in protection against reactive oxygen species mediated effects. Both proteins play a role in the malignant transformation of cells.

2.6.2 Two-dimensional polyacrylamide gel electrophoresis (2D-PAGE)

Two-dimensional polyacrylamide gel electrophoresis (2D-PAGE) has been widely used in comparing proteomes extracted from comparative samples. In 2D-PAGE, samples are fractionated according to their isoelectric point and molecular mass. After staining of the gel, spots that are more or less intense representing proteins up or down-regulated were excised from the gel and identified using mass spectrometry (Lopez, 2007).

The procedure of 2D-PAGE consists of a number of steps which include sample preparation, first dimension isoelectric focusing, second dimension dosium dodecyl sulfate (SDS)-PAGE, detection of protein spots, and image

analysis. Sample loads are often described as analytical or preparative. A typical analytical gel contains 50-150 µg sample, usually stained with silver or fluorescent staining methods while preparative gels are loaded with 1 mg total protein or more and usually stained with Coomassie Blue.

Samples of known protein concentrations were then applied to commercial IPG strips for first dimension isoelectric focusing. The complete voltage load during IEF is defined in volt-hour (Vhr). Best results were obtained with the shortest focusing phase at the highest possible voltage. Strips containing the focused proteins were then equilibrated in SDS buffer to transform the focused proteins into SDS-protein complex, and run on second dimension. The second dimension of 2D-PAGE separates proteins based on their molecular weights in polyacrylamide gels. Protein spots were then detected using a variety of staining methods such as Coomassie blue, silver and fluorescence staining. Silver staining is useful when searching for qualitative variations while Coomassie blue for the detection of quantitative variations.

2.6.3 Matrix-assisted laser desorption ionization – time of flight – mass spectrometry (MALDI-TOF-MS)

Following 2D-PAGE separation and gel staining, protein spots of interest were excised, digested with trypsin, and subjected to MS analysis. MALDI is a method which combines in-gel digests with a matrix before depositing onto a plate and insert into the mass spectrometer interface. A laser is used to volatilize the matrix, carrying the peptides into the gas phase for MS analysis. The instrument then selects and isolates the most intense peptide analyte. The

isolated ion then collides with inert gasses such as nitrogen or helium in a process referred to as collisional induced dissociation (CID). This process imparts energy to break bonds within the peptide, producing many fragment ions read out as MS/MS spectrum. TOF-MS refers to a mass analyzer configuration where ions are accelerated through a large electric field and then travel through a field-free flight tube, monitoring the time taken to reach a detector.

The MS/MS spectra are analyzed using computational algorithms for peptide identification. These algorithms calculate a score that evaluates the similarity between the observed MS/MS spectrum and a theoretical spectrum (e.g. Sequest) or uses a statistical approach to evaluate the probability of observing the MS/MS fragment ions (e.g. Mascot). The spectra were then analyzed to search for the peptide mass fingerprints and MS/MS data in the NCBInr database (Ahn *et al*., 2007).

CHAPTER 3

MATERIALS AND METHODS

3.1 Materials and cell culture

3.1.1 Chemicals

The chemicals, reagents, and antibodies used for this study are shown in Table 3.1

Table 3.1: List of chemicals, reagents, and antibodies

Supplier	Chemicals/reagents/antibodies
Sigma, USA	Roswell Park Memorial Institute (RPMI 1640)
	Minimum Essential Medium Eagle (MEM)
	Fetal bovine serum (FBS)
	Sodium bicarbonate
	Trypan blue
	Phorbol 12-myristate 13-acetate (PMA)
	Sodium *n*-butyrate (SnB)
	Bovine Serum Albumin- Fraction V
	Tween-20
	Protease inhibitor cocktail
	Genistein (≥ 90.0 % pure as determined by HPLC)
	Ursolic acid (≥ 90.0 % pure as determined by HPLC)
	Oleanolic acid (≥ 90.0 % pure as determined by HPLC)
	Boric acid (for molecular biology, ≥ 99 % HPLC)
	Glycerol (for electrophoresis, ≥ 99 %)

Table 3.1 (Cont)

Supplier	Chemicals/reagents/antibodies
Sigma, USA	Glycine (for electrophoresis, ≥ 99 %)
	Tris base (for molecular biology, ≥ 98 % HPLC)
	SDS (for molecular biology, ≥98.5% GC)
BioRad, Hercules, CA, USA	30% acrylamide and bis-acrylamide solution, 29:1
	DC protein quantification kit
	Kaleidoscope pre-stained Standards
GE Healthcare, USA	Urea (PlusOne reagents, 99.5 %)
	Thiourea (PlusOne reagents, 99.5 %)
	Dithiothreitol (DTT) (PlusOne reagents, 99 %)
	Iodoacetamide (IAA) (PlusOne reagents, 99 %)
	pH3-11NL immobilize pH gradient (IPG) buffer
Bio Basic Inc, Canada	3-[(3-Cholamidopropyl)dimethylammonio]-1-propanesulfonate (CHAPS)
	Ammonium persulphate (APS)
	N,N,N',N'-Tetramethylethylenediamine (TEMED)
Invitrogen, USA	Phosphate buffered saline (PBS)
	TrypLE™ Express
Calbiochem, Merck, Darmstadt, Germany	BAY 11-7085
	RanBP1 antibody
Cell Signaling Techonology, Beverly, MA	COX-2
	NQO1
	Stathmin
	EB1
	Cyclin D1
	p21
	beta actin
Pierce, Rockford	M-PER mammalian extraction reagent

Table 3.1 (Cont)

Supplier	Chemicals/reagents/antibodies
Santa Cruz Biotechnology, CA, USA	Nrf2 Keap1 Lamin B
Milipore, CA, USA	HO-1

Early antigen (EA)-positive sera from nasopharyngeal carcinoma patients were provided by Dr. Paul Lim Vey Hong from Tung Shin Hospital, Kuala Lumpur.

3.1.2 Cell culture

Two cell lines are used in this study: EBV genome carrying human lymphoblastoid Raji cells and the human hepatoma HepG2 cell line. Raji cells were purchased from Riken Cell Bank, Tsukuba, Japan while HepG2 cells were obtained from American Type Cell Culture, USA. The Raji cells were in suspension with rounded morphology; HepG2 cells are anchorage-dependent and have epithelium-like morphology. During the assays, cell viability of the culture was determined using Trypan blue dye exclusion method. Frozen cell stocks were stored in liquid nitrogen prior to use.

3.1.3 Medium preparation

Raji cells and HepG2 cells were maintained in RPMI-1640 medium and MEM, supplemented with 10 % of heat-inactivated fetal bovine serum (FBS). RPMI medium was prepared by dissolving 10.3 g of RPMI powder and 2.2 g of sodium bicarbonate in 1 L of double distilled water; MEM medium was prepared by dissolving 9.51 g of MEM powder and 2.31 g of sodium bicarbonate in 1 L of double distilled water. The pH of the medium was adjusted to 7.2 and filter sterilized using a 0.2 μm Milipore filter (Corning) into sterile bottles and kept at 4 ºC.

3.1.4 Maintenance of cell culture

Cells were maintained in 75 mL tissue culture flask incubated in a 5% CO_2 incubator (Nuaire CO_2 water-jacketed) kept at 37 ºC in a humidified atmosphere. The cells were observed regularly under the inverted microscope (Olympus, Japan) for any contamination and sub-cultured when it reached confluence.

In the process of subculturing HepG2 cells, medium was removed from the culture flask and the cells were washed with 4 mL PBS. One mL of trypsin-like enzyme without phenol red TrypLE™ Express was added. The cells in trypsin were left in 37 °C incubator in 5 % CO_2 for approximately 10 min, allowing cells to round up and detach from the wall of the flask. The cells were resuspended in 2 mL medium followed by repeated pipetting to break

cell clumps. The cells were spun at 1500 rpm for 5 min. The supernatant containing trypsin was removed. Cell pellet was resuspended in medium and seeded at a desired density for subsequent use.

3.2 Epstein-Barr Virus-Early Antigen (EBV-EA) Assay

Plant extracts were tested for their anti-tumour-promoting activity using a short term *in vitro* assay of Epstein–Barr virus-early antigen (EBV-EA) activation. The inhibition of EBV-EA activation was assayed using Raji cells (Ito et al., 1981). Raji cells (5×10^5 cells/mL) were incubated in 1 mL RPMI medium containing 3 mM SnB, 0.05 μM PMA, and 50 μg/mL plant extracts for 48 h. After 48 h of treatment, the cell suspension was centrifuged at 1000 rpm for 10 min, and the supernatant was removed. Smears of cell suspensions were fixed on Teflon slides. Cells were then stained with high-titer EBV-EA-positive sera from nasopharyngeal carcinoma patients followed by incubation with anti-human IgG (Fab specific) FITC conjugate. The indirect immunofluorescence technique was employed for detection (Murakami *et al*., 1995). In each assay, at least 200 cells were counted and the experiments were repeated thrice. The average extent of EA induction was determined and compared with that on positive control experiments in which the cells were treated with SnB and PMA only. The viability of treated Raji cells was assayed by the Trypan Blue staining method.

3.3 Isolation of maslinic acid

According to Lim (2002), the chloroform extract of *Coleus tuberosus* tubers has strong anti-tumour-promoting activity and the active compound has been identified as maslinic acid. Maslinic acid was thus isolated from this plant after which its cancer chemopreventive activity was investigated.

3.3.1 Plant materials and chemicals

Coleus tuberosus Benth was identified by Dr. Kamaruddin Mat Salleh from the Department of Botany, Universiti Kebangsaan Malaysia (UKM). Solvents used for isolation including n-hexane, chloroform, ethyl acetate, methanol, acetonitrile and ethanol were obtained from Merck, Darmstadt, Germany.

3.3.2 Preparation of plant crude extracts

A total of 40 kg *Coleus tuberosus* Benth tubers were collected from Banting, Selangor. The tubers were cut into small pieces (approximately 1-2 cm) and allowed to air dry in room temperature for 5 days. Air-dried and cut pieces of *Coleus tuberosus* tubers (5.24 kg) were macerated with 80 % ethanol at room temperature for a week. The ethanolic extract was then filtered and concentrated *in vacuo* at 45 ºC under 175 mbar using a rotary evaporator (Buchi, Rotavapor R-200). The extraction process was repeated thrice. The combined filtrate concentrated *in vacuo* yielded 180 g of crude ethanolic extract. The extract was then diluted with distilled water and partitioned with *n*-hexane, followed by chloroform. The partitioning of the crude ethanolic extract afforded 18 g of hexane fraction and 11 g of chloroform fraction.

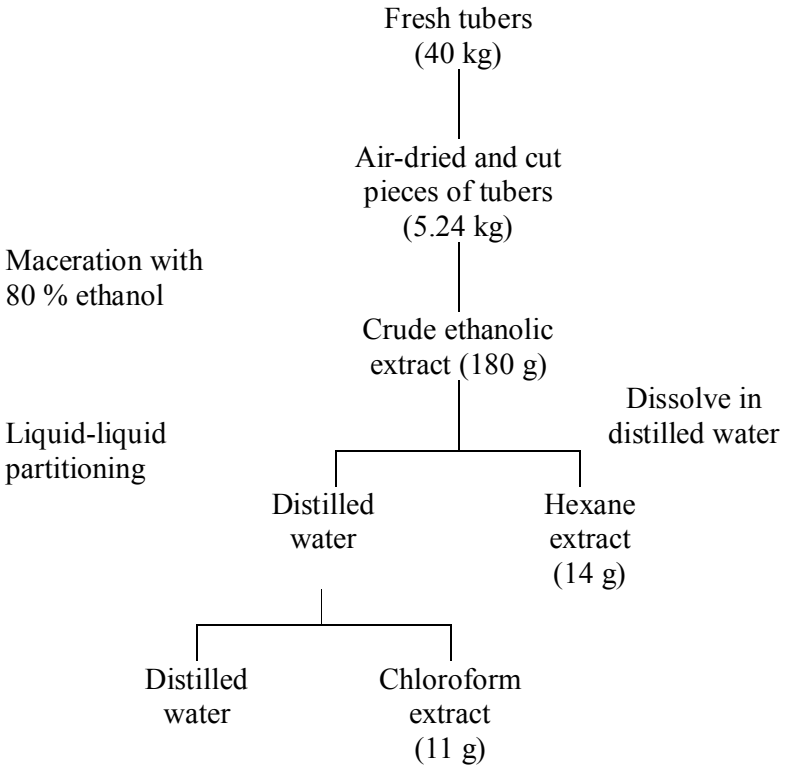

Figure 3.1: Preparation of *Coleus tuberosus* crude chloroform extract

3.3.3 Fractionation of chloroform crude extract

Lim (2002) found that the chloroform extract exhibited the strongest anti-tumour activity and therefore was selected for further fractionation. The chloroform fraction was mixed with silica gel 60 (9385) (Merck, Darmstadt, Germany) to make slurry. The remaining solvent was evaporated and the residue was pulverized using a spatula. The residue in powder form was transferred onto the top of a previously packed silica gel in a glass column (4 cm × 50 cm). The silica-packed column was first eluted with 100 % chloroform followed by a mixture of chloroform and ethyl acetate with increasing polarity (90:10, 80:20, 70:30, 60:40, 50:50, 40:60, 30:70, 20:80,

and 10:90), 100 % ethyl acetate, and a mixture of ethyl acetate and methanol with increasing polarity (90:10, 80:20, 70:30, 60:40, 50:50). The volume of each eluent was 200 mL. Eluates were collected in 30 mL glass vials. The collected fractions were guided by thin layer chromatography analysis (silica gel 60 F_{254}, 0.2 mm thickness, Merck, Darmstadt, Germany) to determine the pattern of compound separation. Fractions that showed similar patterns were combined and tested for their anti-tumour activities using a short term *in vitro* EBV-EA activation assay. The fraction with the strongest anti-tumour activity was subjected to a second round of silica-packed gravity column chromatography before they are purified by high performance liquid chromatography (HPLC).

3.3.4 Isolation and purification of active fractions

After silica gravity column chromatography fractionation, the active fractions were purified by HPLC separation (Shimadzu, Kyoto, Japan). In an analytical run, 20 μL of sample residue were dissolved in a mixture of 95 % ethyl acetate/ 5 % methanol (HPLC grade, Merck) before injected into the HPLC (Shimadzu, Kyoto, Japan) through a reverse phase column (Chromolith® RP-18, 4.6 mm × 100 mm, Merck, Darmstadt, Germany). The column was eluted with mixtures of acetonitrile and deionised water with decreasing polarity at 1 mL/min flow rate; the solvent system started from 100 % deionised water to 100 % acentonitrile from 0 to 15 min and hold at 100 % acentonitrile elution for another 5 min. Detection wavelengths were between 190 and 800 nm.

Upon obtaining the analytical HPLC profiles of active fractions, semi-preparative HPLC separation was performed to isolate the active pure compounds. A total of 200 µL samples were injected through a preparative reverse phase column (Chromolith® RP-18, 10 mm × 100 mm, Merck, Darmstadt, Germany), and was run for 8 min with gradient elution of deionised water: acetonitrile at 5 mL/min flow rate. The solvent system started from 100 % deionised water to 100 % acentonitrile at 0 to 5 min and hold at 100 % acentonitrile elution for another 3 min.The isolated compounds were then subjected to instrumental analysis for structural elucidation.

3.3.5 Instrumental analysis of isolated compounds

Isolated compounds were dissolved in deuterated methanol and sent for NMR analysis. The Proton (1H-NMR; 400 MHz) and Carbon (13C-NMR; 125 MHz) NMR spectra were determined using a JEOL JNM-LA400 spectrometer (JEOL, Tokyo, Japan) located at the Department of Chemistry in Universiti Malaya (UM). Approximately 10 mg of isolated compounds were analyzed by direct injection mass spectrometry (DIMS) analysis at the Chemistry department in Universiti Putra Malaysia (UPM). Mass spectrum was obtained in Electro ionization (EI) mode using a Shimadzu GCMS-QP5050A spectrometer (Shimadzu, Kyoto, Japan). Meanwhile, melting points and infrared spectra of the compounds were recorded using a Kofler hot stage microscope melting point apparatus and the Perkin-Elmer FT-IR model 1725X spectrometer, respectively.

3.4 NF-κB assay

3.4.1 Sample treatment

The effect of maslinic acid on the pro-inflammatory target NF-κB was investigated. We first determine the basal NF-κB activities and their levels induced in response to 0.05 μM PMA. The basal and PMA-induced NF-κB levels are not significantly different in Raji cells. Maslinic acid was thus tested for its inhibitory effect on NF-κB binding activity in non-induced Raji cells. For concentration-dependent studies, Raji cells (5×10^5 cells/mL) were plated in 24-well plates in the presence of 12.5, 25, 50, and 100 μM of maslinic acid for 8 h, and with 100 μM maslinic acid for 1, 2, 4, and 8 h in time course studies. After treatment, nuclear extracts of cells were prepared and analyzed for NF-κB activity. NF-κB inhibitor BAY 11-7085, ursolic acid and oleanolic acid were used as positive controls.

3.4.2 Cell fractionation

Nuclear extracts were prepared using the NE-PER Nuclear and Cytoplasmic Extraction Reagents (PIERCE, Rockford, USA). Cells harvested were incubated on ice in 100 μL cytoplasmic extraction reagent I (CER I) for 10 min. Cytoplasmic extraction reagent II (CER II) was then added to a final concentration of 0.5 % and the mixture was vortexed at 16,000 ×g for 10 min at 4 ºC. The supernatant was labeled as the “cytosolic extract”. The pellet was then extracted with 50 μL nuclear extraction buffer (NER) and protease inhibitors on ice for 30 min with occasional vortexing. Following

centrifugation at 16,000 ×g for 10 min at 4 ºC, the supernatant "nuclear extract" was collected. The concentration of protein extracts was determined using the DC protein quantification kit (Biorad, Hercules, California).

3.4.3 NoShift NF-κB Assay

NF-κB binding activity was determined using NoShift Transcription Factor Assay kit and NoShift NF-κB (p65) reagents (Calbiochem, Merck, Darmstadt, Germany). The NoShift Transcription Factor Assay kit contain components like Streptavidin plate, 4× NoShift Bind Buffer, 10× NoShift Wash buffer, NoShift antibody dilution buffer, poly (dI.dC), salmon sperm DNA, and tetramethylbenzidine (TMB) substrate. 1× NoShift Bind Buffer was prepared by combining 540 µL of ultrapure water and 180 µL 4× NoShift Bind Buffer while 1× NoShif Wash Buffer was prepared by combining 22.5 mL ultrapure water and 2.5 mL 10× NoShift Wash Buffer. Meanwhile, 1 N hydrochloric acid (HCl) was prepared by adding 83 µL concentrated HCl (12.1 N) to 917 µL sterile ultrapure water. NoShift NF-κB reagents (Calbiochem, Merck, Darmstadt, Germany) include NF-κB WT DNA (biotinylated, 10 pmol/µL), NF-κB Competitor DNA (50 pmol/µL), NF-κB Mutant DNA (50 pmol/µL), Anti-NFκB (p65), and goat anti-mouse IgG HRP conjugate.

The NoShift NF-κB binding reactions were carried out according to the manufacturer's instructions (Calbiochem, Merck Darmstadt, Germany). Briefly, 5 µL of nuclear extracts (10 µg) was mixed with 1 µL of biotinylated

double stranded NF-κB oligonucleotides (10 pmol/μL), 5 μL of 4× NoShift Bind Buffer, 1 μL of poly (dI.dC), 1 μL of salmon sperm DNA and top up with ultrapure water to a final volume of 20 μL. The reaction mixture was incubated on ice for 30 min. Then, 80 μL of 1× NoShift Bind Buffer was added to the 20 μL reaction mixture. The resulting 100 μL reaction mixture was subsequently transferred into wells of the Streptavidin-coated plate and incubated for 1 h at 37 ºC where the protein-DNA complex will be captured on the plate. After that, contents of the wells were removed and washed with 200 μL of 1× wash buffer 3 times for 5 min each. A 100 μL of primary antibodies (p65) were then added into the wells and incubated for another 1 h at 37 ºC. Next, the primary antibodies were removed and the wells were washed with washing buffer. This was followed by addition of 100 μL HRP-conjugated secondary antibody and incubated for 30 min at 37 ºC. After that, secondary antibodies were discarded and the wells were washed with 200 μL of 1× wash buffer 5 times for 5 min each. All washing steps were carried out with gentle agitation. After washing, chromogenic reactions were performed by adding TMB substrate to the sample wells and incubated for 10 min to develop colorimetric signal before stopping the reaction with 1 N HCI. The absorbance was then read at 450 nm with a microplate reader (Tecan, Switzerland).

In addition to the determination of NF-κB binding activity, control reactions including blank, non-specific and specific competition analysis were performed to determine the specificity of NF-κB binding.

3.5 AP-1 assay

3.5.1 Sample treatment

The basal AP-1 binding activity and their levels induced in response to 0.05 μM PMA were first determined. AP-1 binding activity was induced in response to both PMA and SnB, but not PMA alone in Raji cells (Section 4.4.1). The suppressive effect of maslinic acid on AP-1 binding activity was determined in PMA and SnB-induced Raji cells. For concentration-dependent studies, Raji cells (5×10^5 cells/mL) were plated in 24-well plates in the presence of 0.05 μM PMA, 3 mM SnB, and 12.5, 25, 50, and 100 μM maslinic acid for 4 h [AP-1 binding was most strongly induced after 4 h incubation with PMA and SnB (see Figure 4.17)] and with 100 μM of maslinic acid for 1, 2, 4, and 8 h in time course study. After treatment, nuclear extracts of cells were prepared and analyzed for AP-1 binding activity. Other pentacyclic triterpenes such as ursolic acid and oleanolic acid were used as positive controls.

3.5.2 Cell fractionation

Nuclear extracts were prepared using the NE-PER Nuclear and Cytoplasmic Extraction Reagents (PIERCE, Rockford). Cells were incubated on ice in 100 μL cytoplasmic extraction reagent I (CER I) for 10 min. Cytoplasmic extraction reagent II (CER II) was then added to a final concentration of 0.5 % and the mixture was vortexed at 16,000 ×g for 10 min at 4 ºC. The supernatant was labeled as the “cytosolic extract”. The pellet was then extracted with 50 μL nuclear extraction buffer (NER) and protease inhibitors on ice for 30 min

with occasional vortexing. Following centrifugation at 16,000 ×g for 10 min at 4 ºC, the supernatant "nuclear extract" was collected. The concentration of protein extracts was determined using the DC protein quantification kit (Biorad, Hercules, California).

3.5.3 LightShift Chemiluminescent EMSA Assay

The effect of maslinic acid on AP-1 binding activity in Raji cells was performed using the LightShift Chemiluminescent EMSA kit (PIERCE, Rockford). Biotin labeled AP-1 consensus DNA (5' CGCTTGATGA CTCAGCCGGAA 3') was obtained from Eurogentec AIT (Singapore). The LightShift Chemiluminescent EMSA kit contain two modules: the LightShift EMSA Optimization module which include components like 10× binding buffer, 1 µg/µL poly (dI–dC), 50 % glycerol, 1 % NP-40, 1 M KCl, 100 mM $MgCl_2$, and 5× loading buffer while the Chemiluminescent Nucleic Acid Detection Module contains blocking buffer, wash buffer, substrate equilibration buffer and chemiluminescent substrate.

The AP-1 binding reactions contained 10 µg nuclear protein extract, 1× binding buffer, 50 ng poly (dI–dC), 2.5 % glycerol, 0.05 % NP-40, 50 mM KCl, 5 mM $MgCl_2$, and 20 fM biotinylated AP-1 oligonucleotides. The binding reaction mixtures were top up with ultrapure water to 20 µL and were incubated on ice for 30 minutes. Then, 5 µL of 5× loading buffer was then added to the reaction mixture and 20 µL of the samples were loaded to a 5 % native polyacrylamide gel in 0.5× TBE (450 mM Tris, 450 mM boric acid, 10

mM EDTA) buffer. The gel was run at 100 V using Mini-Vertical unit SE-250 attaching with an EPS 301 power supply (GE Healthcare). The samples were electrophoresed until the bromophenol blue dye front has migrated approximately 2/3 to 3/4 down the length of the gel. The gel was then electroblotted onto a nylon membrane (PIERCE, Rockford) in a standard tank transfer apparatus for mini gels (Cleaver Scientific Ltd, USA). After that, transferred DNA was crosslinked to the membrane using a handheld UV lamp equipped with 254 nm lamp (UVItec, Cambridge, United Kingdom). The biotin-labeled DNA was detected using chemiluminescent substrate and the membrane was viewed using an Alpha Innotech gel imager (Alpha Innotech, Cell Biosciences, California). Competition reactions were conducted by adding 10-fold excess of specific and non-specific competitors (Eurogentec AIT, Singapore) to the reaction mix to establish specificity of binding.

3.6 COX-2 expression

3.6.1 Sample treatment

COX-2 expression and their levels induced in response to 0.05 μM PMA were first investigated. It was found that the basal and PMA-induced COX-2 levels were not significantly different (Section 4.5). For concentration-dependent studies, Raji cells (5×10^5 cells/mL) were plated in 24-well plates in the presence of 12.5, 25, 50, and 100 μM maslinic acid for 8 h and with 100 μM maslinic acid for 1, 2, 4, and 8 h in time course study. Ursolic acid and oleanolic acid were used as positive controls.

3.6.2 Preparation of cell lysates

In order to prepare whole-cell lysis extracts, cells were harvested, washed twice with ice-cold PBS and lysed using M-PER Mammalian Protein Extraction Reagent (PIERCE, Rockford) for 15 min at 4 ºC. After centrifugation at 12,000 ×*g* for 10 min at 4 ºC, the supernatant was collected. The protein concentration was determined using BioRad DC protein quantification assay.

3.6.3 SDS-PAGE and blotting

SDS-PAGE and Western blotting were done as previously described (Hsum *et al*., 2011). Ten µL of samples containing 50 µg of protein together with 10 µL of 2× sample loading buffer (130 mM Tris-Cl, 20 % glycerol, 4.6 % SDS, 0.02 % bromophenol blue, and 2 % DTT) were transferred into 1.5 mL eppendorf tubes and boiled for 5 min. Samples were cooled to room temperature and spun to bring down condensation prior to loading into the wells of a 12 % denaturing polyacrylamide gel. Five µL of Kaleidoscope pre-stained Standards (BioRad, Hercules, CA) was loaded to one end of the gel as the molecular weight marker. The gel was run with constant current of 20mA for about 1 h in the mini-vertical SE250 (GE Healthcare) unit with EPS 301 power supply (GE Healthcare). The gel was then carefully removed and electroblotted onto a 0.45 µm PVDF membrane (PIERCE, Rockford, USA) using standard tank transfer apparatus for mini gels (Cleaver Scientific Ltd, USA). A blotting 'sandwich' was assembled by stacking the sponge - filter papers - polyacrylamide gel - PVDF membrane - filter papers - sponge together in a

cassette which was then placed into the transfer tank and transfer for 1 h at 100 V. The PVDF membrane was pre-wet with MeOH and immersed in transfer buffer (25 mM Tris base, 192 mM glycine). Other materials like sponges and filter papers (Whatman) were also immersed in the transfer buffer before blotting.

3.6.4 Immunodetection

After transfer, the membrane was immersed in blocking buffer (3 % BSA in PBST buffer (0.05 % Tween-20 in PBS buffer)) for 1 h. The membrane was then incubated with COX-2 antibody at 1:1000 dilution ratio in 3 % BSA PBST buffer for another 1 h. After 1 h, primary antibody solutions were discarded and washed with PBST buffer 3 times for 10 min each, after which the membrane was incubated HRP-linked anti-rabbit secondary antibody at 1:10000 dilution in 3 % BSA PBST buffer for 45 min. The membrane was then washed again with PBST buffer 3 times for 10 min each. After the washing steps, the membrane was incubated with Immobilon HRP substrate (Millipore, Massachusetts) for about 5 min. Then, the moist membrane was wrapped in a plastic wrap and the labeled protein bands were visualized using a Alpha Innotech system gel imager (Alpha Innotech, Cell Biosciences, California). After that, the membrane was washed with PBST buffer and immersed into the stripping buffer (0.2 M glycine, 0.05 % Tween-20) for 15 min. The membrane was rinsed off with PBST buffer and the whole immunodetection process was repeated again for another antibody (rabbit β-actin antibody) for normalization.

3.7 Nrf2-ARE pathway studies

Apart from determining the pro-inflammatory NF-κB and AP-1 binding activities as well as COX-2 expression, maslinic acid was also tested for its effect on the Nrf2-ARE anti-oxidant defense pathway. The anti-oxidant enzyme HO-1 and detoxifying enzyme NQO1 expression, binding activity on the ARE, steady state levels of Nrf2 and Keap1 in the cytoplasm and nucleus as well as the requirement of Nrf2 for induction HO-1 and NQO1 expression were determined. The human HepG2 hepatoma cells which have been widely used in drug metabolism and chemoprevention studies were employed in this respect (Kassie *et al*., 2003; Jiang *et al*., 2003). The HepG2 cell line has a well-developed microsomal system and hepatic origin; this robust metabolic system is responsive to various environmental stimuli and stresses (Chen *et al*., 2004). In addition, there is a correlation between the regulation of phase II enzymes in HepG2 cells and primary human hepatocytes (Kassie *et al*., 2003; Westerink and Schoonen, 2007). Thus, HepG2 cells are used for studying regulation cytoprotective enzymes.

3.7.1 Sample treatment

HepG2 (1.5×10^5 cells/mL) cells were seeded in 60 mm dishes for 24 h and then treated with various concentrations of maslinic acid (12.5, 25, 50, and 100 μM) for 12 h in concentration-dependent studies and at 100 μM maslinic acid for 1, 3, 6, and 12 h in the time course study. The total mRNA and proteins of maslinic acid-treated cells were harvested to determine its effect on the anti-oxidant enzyme HO-1 and detoxifying enzyme NQO1 gene and

protein expression. In a separate set of experiment, the protein extracts of maslinic acid-treated cells were fractionated into cytoplasmic and nuclear fractions to determine its effect on the steady state levels of Nrf2 and Keap1 protein expression in the cytoplasm and nucleus. Meanwhile, the nuclear extracts of maslinic acid treated cells were also used for ARE binding study. Oleanolic acid, a known Nrf2 inducer (Liu *et al*., 2008; Reisman *et al*., 2009) was used as the positive control.

3.7.2 Cell fractionation

Cytoplasmic and nuclear extracts were prepared using the NE-PER Nuclear and Cytoplasmic Extraction Reagents (PIERCE, Rockford). Cells were incubated on ice in 100 µL cytoplasmic extraction reagent I (CER I) for 10 min. Cytoplasmic extraction reagent II (CER II) was then added to a final concentration of 0.5 % and the mixture was vortexed at 16,000 ×g for 10 min at 4 ºC. The supernatant was labeled as the "cytosolic extract". The pellet was then extracted with 50 µL nuclear extraction buffer (NER) and protease inhibitors on ice for 30 min with occasional vortexing. Following centrifugation at 16,000 ×g for 10 min at 4 ºC, the supernatant "nuclear extract" was collected. The concentration of protein extracts was determined using the DC protein quantification kit (Biorad, Hercules, California).

3.7.3 Transient transfection of short interfering RNA (siRNA)

A preliminary experiment was first carried out to determine the knockdown efficiency of Nrf2-siRNA. In the silencing studies, it is necessary to test at least three siRNAs targeting the same gene. A total of four predesigned siRNAs against human Nrf2 and one control scrambled siRNA were purchased from Qiagen, Germany. HepG2 cells seeded at a density of 1.25×10^5 cells/mL in a 6-well plate were either non-transfected, transfected with 25 nM siRNA-Nrf2 or scrambled-siRNA (Con-siRNA) using siPORT NeoFX transfection reagent (Applied Biosystem, USA). The siRNAs were introduced into the cells using the Fast Forward Transfection Protocol in which cell seeding and transfection were carried out on the same day. After 48 h, total mRNA and protein were extracted for real time RT-PCR and Western blotting analysis to determine the silencing efficiency.

Among the four tested Nrf2-siRNAs, siRNA-Nrf2-1 significantly reduced Nrf2 expression and was selected for further studies. After 48 h transfection with siRNA-Nrf2-1, medium containing the siRNA and transfection reagent were removed and replaced with fresh medium containing 100 μM maslinic acid. As some studies reported that HO-1 and NQO1 expression were most strongly induced after 4-8 h treatment (Hartsfield *et al*., 1998; Tanigawa *et al*., 2007), cells were incubated with maslinic acid for additional 8 h before total mRNA and proteins were extracted for real time RT-PCR and Western blotting analysis.

3.7.4 Real time reverse transcription-polymerase chain reaction (RT-PCR)

Total RNA was prepared using the RNeasy Mini kit (Qiagen, Germany). The RNeasy Mini kit contains RNeasy spin columns, Buffer RLT, Buffer RW1, Buffer RPE, and RNase free water. Briefly, cells were lysed in 350 µL lysis buffer RLT and homogenized. One volume of 70 % ethanol was then added to the lysates, creating conditions that promote selective binding of RNA to RNeasy membrane. The samples were then applied to the RNeasy Mini spin column and spun at 8000 ×g for 15 s. Total RNA were bound onto the column membrane during the centrifugation. The spin column was then washed using buffer RPE and RW1. RNA was eluted with 30 µL of RNase free water in sterile 1.5 mL collection tubes.

The primer pairs for HO-1, NQO-1, Nrf2, and beta actin are designed using online tool primer3 and checked with PREMIER Biosoft for stability of the primers. The primers were obtained from 1st Base (Singapore). The oligonucleotide primers forward, 5′- TTACTATGGGATGGGGTCCA-3′, and reverse, 5′- TCTCCCATTTTTCAGGCAAC-3′, were used to amplify human NQO1; the primers forward, 5′-TCCGATGGGTCCTTACACTC-3′, and reverse, 5′-TAAGGAAGCCAGCCAAGAGA-3′, were used to amplify human HO-1; the primers forward, 5′-CGGTATGCAACAGGACATTG-3′, reverse 5’-AGAGGATGCTGCTGAAGG AA-3’ were used to amplify Nrf2 gene, and the primers forward, 5′-CGACTTCGAGCAAGAGATGG-3′, and reverse, 5′-AGCACTGTGTTGGCGTACAG -3′, were used to amplify the human beta actin housekeeping gene.

RT-PCR was performed using the Quantifast SYBR Green RT-PCR kit (Qiagen, Germany). The kit contains 2× Quantifast SYBR Green RT-PCR Master Mix (HotStarTaq *Plus* DNA Polymerase, Quantifast SYBR Green RT-PCR Buffer, dNTP mix and ROX passive reference dye), Quantifast RT Mix (mixture of Omniscript and Sensicript Reverse Transcriptase), and RNase free water. The reaction mix was prepared according to Table 3.2. The samples were kept on ice while preparing for the reaction mix. Appropriate volumes of reaction mix were dispensed into PCR tubes after which template RNA (50 ng/reaction) was added to the individual PCR tubes containing the reaction mix. The real time cycler was programmed as recommended in the manual (QuantiFast™ SYBR® Green RT-PCR Handbook). Briefly, template RNA was reverse transcribed at 50 ºC for 10 min. After reverse transcription, the PCR step was started at 95 ºC for 5 min to activate HotStar Taq DNA Polymerase followed by 35 cycles of 2-step cycling, with denaturation at 95 ºC for 10 s and a combined annealing /extension step at 60 ºC for 30 s. Data was acquired during the combined annealing/extension step.

Table 3.2: Real time RT-PCR reaction mix setup

Components	Final Concentration	Volume/reaction
2 × QuantiFast SYBR Green RT-PCR Master Mix	1 ×	12.5 µL
Forward primer (10 µM)	1 µM	2.5 µL
Reverse primer (10 µM)	1 µM	2.5 µL
QuantiFast RT Mix		0.25 µL
Template RNA (25 ng/µL)	50 ng	2.0 µL
RNase free water		5.25 µL
Total volume reaction		25.0 µL

Results obtained from real time RT-PCR will be quantified using the relative quantification method – Delta Delta Comparative Threshold (DDCT) (Livak and Schmittgen, 2001). This involves comparing the C_t values of the samples of interest with a control or calibrator such as a non-treated sample. The C_t values of both the calibrator and the samples of interest were then normalized to a housekeeping gene beta-actin. For the relative quantification procedure to be valid, the amplification efficiencies of the target and the reference genes must be approximately equal. The amplification efficiencies of each primer pairs have been validated (Appendix B).

3.7.5 Western blotting

Whole-cell lysates were prepared using M-PER Mammalian Protein Extraction Reagent (PIERCE, Rockford, USA). Cells were lysed for 15 min at 4 ºC. After centrifugation at 12,000 ×*g* for 10 min at 4 ºC, the supernatant was collected. The protein concentration was determined using BioRad DC protein quantification assay.

Briefly, 10 µL of samples containing 50 µg of protein together with 10 µL of 2× sample loading buffer (130 mM Tris-Cl, 20 % glycerol, 4.6 % SDS, 0.02 % bromophenol blue, and 2 % DTT) were transferred into 1.5 mL eppendorf tubes and boiled for 5 min. Samples were cooled to room temperature and spun to bring down condensation prior to loading into the wells of a 12 % denaturing polyacrylamide gel. Five µL of Kaleidoscope pre-stained Standards

(BioRad, Hercules, CA) was loaded into one end of the gel as the molecular weight marker. The gel was electrophoresed with constant current of 20mA for about 1 h in the mini-vertical SE250 (GE Healthcare) unit with EPS 301 power supply. Gel was then carefully removed and electroblotted onto a 0.45 μm PVDF membrane (PIERCE, Rockford, USA) using standard tank transfer apparatus for mini gels (Cleaver Scientific Ltd, USA). A blotting 'sandwich' was assembled by stacking sponge - filter papers - polyacrylamide gel - PVDF membrane - filter papers - sponge together in a cassette which was placed into the transfer tank and transfer for 1 h at 100 V. The PVDF membrane was pre-wet with MeOH and immersed in transfer buffer (25 mM Tris base, 192 mM glycine) until ready to use. Other materials like sponges and filter papers (Whatman) were also soaked in transfer buffer before blotting.

After transfer, the membrane was immersed in blocking buffer (3 % BSA in PBST buffer (0.05 % Tween-20 in PBS buffer)) and blocked for 1 h. The membrane was incubated with respective primary antibodies, namely HO-1 (1:1000), NQO1 (1:1000), Nrf2 (1:200), Keap1 (1:200) beta-actin (1:1000) and lamin b (1:200), at their corresponding dilution ratios in 3 % BSA PBST buffer for another 1 h. After 1 h, primary antibody solutions were discarded and washed with PBST buffer 3 times for 10 min each, after which the membrane was incubated HRP-linked secondary antibody at 1:10000 dilution in 3 % BSA PBST buffer for 45 min. The membrane was then washed again with PBST buffer 3 times for 10 min each. After the washing steps, the membrane was incubated with Immobilon HRP substrate (Millipore, Massachusetts) for about 5 min. Then, the moist membrane was wrapped in a

plastic wrap and the labeled protein bands were visualized using a Alpha Innotech system gel imager (Alpha Innotech, Cell Biosciences, California).

3.7.6 LightShift Chemiluminescent EMSA Assay

The effects of maslinic acid on the ARE binding activity in HepG2 cells were performed using the LightShift Chemiluminescent EMSA kit (PIERCE, Rockford). The biotin-labeled ARE probe (5' TTTTCTGCTGAGTCAAGGG TCCG 3') was obtained from Eurogentec AIT (Singapore).

The Nrf2 binding reactions contained 10 µg nuclear protein extract, 50 ng poly (dI–dC), 75 mM KCl, 0.3 % NP-40, 7.5 % glycerol, 2.5 mM DTT, and 20 fM biotinylated Nrf2-ARE oligonucleotides. The binding reaction mixtures were top up with ultrapure water to 20 µL and were incubated on ice for 30 minutes. Then, 5 µL of 5× loading buffer was then added to the reaction mixture and 20 µL of the samples were loaded onto a 5 % native polyacrylamide gel in 0.5× TBE (450 mM Tris, 450 mM boric acid, 10 mM EDTA) buffer. The gel was run at 100 V using Mini-Vertical unit SE-250 attaching with an EPS 301 power supply (GE Healthcare). The samples were electrophoresed until the bromophenol blue dye front has migrated approximately 2/3 to 3/4 down the length of the gel. The gel was then electroblotted onto a nylon membrane (PIERCE, Rockford, USA) in a standard tank transfer apparatus for mini gels (Cleaver Scientific Ltd, USA). After that, transferred DNA were crosslinked on the membrane using a handheld UV lamp equipped with 254 nm lamp (UVItec, Cambridge, United Kingdom). The biotin-labeled DNA was detected

using chemiluminescent substrate and the membrane was viewed using an Alpha Innotech gel imager (Alpha Innotech, Cell Biosciences, California). Competition reactions were conducted by adding 10-fold excess of specific and non-specific competitors (Eurogentec AIT, Singapore) to the reaction mix to establish specificity of binding.

3.8 Proteomics study

3.8.1 Sample treatment

The molecular response of maslinic acid in Raji cells was investigated using 2-DE approach. Raji cells (5×10^5 cells/mL) were plated in 24-well plates along with 50 μM of maslinic acid for 4, 8, 16, and 24 h. Total cell lysates were prepared as described in Section 3.8.2 for 2D-PAGE and Section 3.8.7 for Western blotting.

3.8.2 Total protein extraction for 2D-PAGE

Total cell lysates were extracted using urea/thiourea lysis buffer (7 M urea, 2 M thiourea, 4 % CHAPS, 40 mM DTT, 0.5 % pH 3-11 NL IPG buffer, protease inhibitor mix). The cell lysate was centrifuged at 14,000 ×*g* for 10 min at 4 °C. After centrifugation, pre-chilled acetone was added to the supernatant to remove contaminants. The samples were then incubated for 2 h at –20 °C, after which they were centrifuged at 13,000 ×*g* for 10 min at 4 °C, and the supernatant was removed. The resulting protein pellets were dissolved in a rehydration buffer (7 M urea, 2 M thiourea, 4 % CHAPS, 0.5 % pH3-11

NL IPG buffer, 20 mM DTT, 0.02 % bromophenol blue). Biorad RCDC Protein Assay reagents (Biorad, Hercules, California) were used to determine the protein concentration. The protein samples were then stored at –80 °C.

3.8.3 2D-PAGE conditions

Protein separation was carried out as described previously (Wang *et al*., 2009), with minor modifications. Hundred and fifty µg of proteins were loaded to the non-linear pH 3-11 IPG strips (13 cm; GE Healthcare) which were used for SDS-PAGE gels for silver staining while 1 mg of proteins were loaded to the IPG strips which were eventually used for SDS-PAGE gels for Coomassie staining. The IPG strips were rehydrated with protein samples for 12 h at room temperature. After rehydration, proteins on the strips were focused at 20,000 Vh at 20 °C using a Ettan^{TM} IPGphore system (GE Healthcare). After focusing, the strips were reduced using 1 % DTT and alkylated with 2 % iodoacetamide (GE Healthcare) in equilibration buffer (6 M urea, 50 mM Tris.Cl, 30 % glycerol, 2 % SDS, 0.02 % bromophenol blue) for 15 min at room temperature with gentle agitation. For the second dimension of electrophoresis, the equilibrated strips were loaded on 12.5 % polyacrylamide gels and then covered with 0.5 % agarose to fix the strip. Electrophoresis was carried out at 20 mA for 2.5 h.

3.8.4 Image analysis and spot selection

ProteoSilver^{TM} Plus Silver Stain kit (Sigma, USA) was used for silver staining and colloidal blue staining kit (Invitrogen Life Technologies) for Coomassie-blue staining of SDS-PAGE gels. Gels were scanned to produce the proteome maps of the control Raji cells and maslinic acid-treated Raji cells. Silver-stained gels (in triplicates) of untreated Raji cells and maslinic acid-treated cells were compared using Image-Master 2D Platium 7 software (GE Healthcare). Protein spots with $\geq$ 2-fold changes and $p < 0.05$ were selected for in-gel digestion.

3.8.5 In-gel digestion

Selected protein spots were excised from Colloidal Blue-stained gels. These spots were destained for 10 min, thrice, with 25 mM ammonium bicarbonate. The destained gel spots were washed thrice with 10 % acetic acid/50 % methanol for 1 h each time and then washed twice with deionized water for 30 min each time. The gels pieces were immersed in 100 % ACN until they turned opaque and were dried in a vacuum centrifuge. The dried gel particles were rehydrated with 10 ng/nL trypsin in 50 mM ammonium bicarbonate (pH 8.0) and were incubated at 37 °C for 4 h. The digests were dried by vacuum centrifugation for about 15 min and subjected to MALDI TOF-TOF MS analysis.

3.8.6 Database searching and protein identification

The digested peptide samples were analyzed by MALDI TOF-TOF MS using a 4800 Proteomics Analyzer (TOF/TOF) (Applied Biosystems, USA). The instrument was operated in a positive ion reflection mode of 20 kV accelerating voltage. Combined MS-MS/MS searches were conducted with Data Processing Software GPS Explorer^{TM} software v 3.6 (Applied Biosystems). The spectra were processed and analyzed with the MASCOT v 2.1 software (Matrix Science Ltd, London, UK) to search for the peptide mass fingerprints and MS/MS data in the NCBInr database using the parent ion mass. The error tolerance was 100 ppm and the MS/MS fragment mass tolerance was 0.2 Da. Carbamidomethylation of cysteine (fixed modification) and methionine oxidation (variable modification) were taken into consideration. A protein score greater than 82 was considered to be significant ($p < 0.05$).

3.8.7 Western blotting

Whole-cell lysates were prepared using M-PER Mammalian Protein Extraction Reagent (PIERCE, Rockford, USA). Cells were lysed for 15 min at 4 ºC. After centrifugation at 12,000 ×*g* for 10 min at 4 ºC, the supernatant was collected. The protein concentration was determined using BioRad DC protein quantification assay.

Briefly, 10 μL of samples containing 50 μg of protein together with 10 μL of 2× sample loading buffer (130 mM Tris-Cl, 20 % glycerol, 4.6 % SDS, 0.02 % bromophenol blue, and 2 % DTT) were transferred into 1.5 mL eppendorf tubes and boiled for 5 min. Samples were cooled to room temperature and spun to bring down condensation prior to loading into the wells of a 12 % denaturing polyacrylamide gel. Five μL of Kaleidoscope pre-stained Standards (BioRad, Hercules, CA) was loaded into one end of the gel as the molecular weight marker. The gel was run with constant current of 20mA for about 1 h in the mini-vertical SE250 (GE Healthcare) unit with EPS 301 power supply. Gel was then carefully removed and electroblotted onto a 0.45 μm PVDF membrane (PIERCE, Rockford, USA) using standard tank transfer apparatus for mini gels (Cleaver Scientific Ltd, USA). A blotting 'sandwich' was assembled by stacking sponge - filter papers - polyacrylamide gel - PVDF membrane - filter papers - sponge together in a cassette which was placed into the transfer tank and transfer for 1 h at 100 V. The PVDF membrane was pre-wet with MeOH and immersed in transfer buffer (25 mM Tris base, 192 mM glycine) until ready to use. Other materials like sponges and filter papers (Whatman) were also immersed in the transfer buffer before blotting.

After transfer, the membrane was immersed in blocking buffer (3 % BSA in PBST buffer (0.05 % Tween-20 in PBS buffer)) and blocked for 1 h. The membrane was incubated with respective primary antibodies, namely RanBP1 (1:1000), EB1 (1:500), stathmin (1:1000), cyclin D1 (1:1000), p21 (1:1000), amd beta-actin (1:1000), at their corresponding dilution ratios in 3 % BSA PBST buffer for another 1 h. The primary antibody solutions were then

discarded and washed with PBST buffer 3 times for 10 min each, after which the membrane was incubated HRP-linked secondary antibody at 1:10000 dilution in 3 % BSA PBST buffer for 45 min. The membrane was then washed again with PBST buffer 3 times for 10 min each. After the washing steps, the membrane was incubated with Immobilon HRP substrate (Millipore, Massachusetts) for about 5 min. Then, the moist membrane was wrapped in a plastic wrap and the labeled protein bands were visualized using a Alpha Innotech system gel imager (Alpha Innotech, Cell Biosciences, California).

3.8.8 Cell cycle analysis

Raji cells (5×10^5 cells/mL) were seeded in 24-well plates and incubated with 50 μM of maslinic acid for 4, 8, 16, and 24 h. The cells were then fixed in 70 % (v/v) ethanol and stored overnight at -20 °C. The ethanol-suspended cells were centrifuged for 5 min at 200 ×g. The ethanol was discarded. The cell pellet was rinsed with PBS and centrifuged. The supernatant was removed and the pellet was resuspended in 500 μL PBS together with 4 μL of propidium iodide (PI) staining solution (2.5 mg/mL) and 1 μL RNase (10 mg/mL). Cells in the PI-containing solution were incubated for 10 min at 37 °C after which they were analyzed by flow cytometry. The flow cytometer was equipped with a 488 nm laser and PI flow emission was detected on the FL2 channel. Ten thousand cells were recorded for each data point and the results analyzed on CellQuest® software. Boundary markers were manually positioned on the histogram plots to determine the percentage of cell population at different stages of the cell cycle.

CHAPTER 4

RESULTS

4.1 Characterization of maslinic acid and tormentic acid from *Coleus tuberosus,* Benth

4.1.1 Isolation and purification of ct6-1 and ct6-2

Based on previous methods, the chloroform extract was found to exhibit the strongest anti-tumour activity and therefore was selected for fractionation using silica gravity column chromatography (Lim, 2002). There were a total of 120 fractions collected from the fractionation of chloroform crude extract. The appropriate fractions guided by thin layer chromatography analysis were combined into 12 fractions (CT1-CT12). The combined fractions were subjected to a short term *in vitro* EBV-EA activation assay to determine their anti-tumour activities (Table 4.1). Fraction CT-6 having the strongest anti-tumour-promoting activity was selected for further isolation and purification.

Table 4.1: Anti-tumour activities of the combined fractions obtained after silica gravity column chromatography of chloroform crude extract

Sample	Cell viability (%)	Anti-tumour activity [Inhibition rate (%)]
CT1 (0.58 g)	84.30	59.27 ± 20.73
CT2 (0.41 g)	82.85	25.47 ± 15.27
CT3 (0.50 g)	88.60	69.27 ± 15.90
CT4 (0.14 g)	85.03	66.79 ± 16.82
CT5 (0.08 g)	61.35	82.04 ± 14.88
CT6 (0.55 g)	0.00	84.83 ± 15.49
CT7 (0.50 g)	0.00	77.16 ± 11.54
CT8 (0.42 g)	0.00	63.24 ± 18.33
CT9 (0.33 g)	2.87	58.78 ± 14.01
CT10 (0.56 g)	67.75	77.35 ± 16.74
CT11 (0.43 g)	66.60	75.01 ± 12.53
CT12 (0.54 g)	51.02	64.53 ± 10.96

The percentage cell viability was assayed using the Trypan Blue dye exclusion method. It was determined by dividing the number of viable cells to the total number of cells × 100 %.

Fraction CT6 was then subjected to column chromatography on silica gel, eluted with *n*-hexane and ethyl acetate solvent mixtures of increasing polarity to give 40 fractions. Using thin layer chromatography analysis, the appropriate fractions were combined into 5 sub-fractions (CT6-1 – CT6-5) and their anti-tumour activities determined. The anti-tumour activities of fractions CT6-1 to CT6-5 were shown in Table 4.2. Fractions CT6-2, CT6-3 and CT6-4 which have strong anti-tumour activities were selected for further purification. The isolation steps were shown in Figure 4.1.

Table 4.2: Anti-tumour activities of the combined fractions obtained after silica gravity column chromatography of fraction CT6

Sample	Cell viability (%)	Anti-tumour activity [Inhibition rate (%)]
CT6-1 (0.0682 g)	9.29	66.80 ± 3.10
CT6-2 (0.0893 g)	7.32	86.23 ± 2.90
CT6-3 (0.2044 g)	1.79	77.34 ± 4.10
CT6-4 (0.165 g)	56.19	77.34 ± 8.54
CT6-5 (0.009 g)	68.71	52.79 ± 8.54

The percentage cell viability was assayed using the Trypan Blue dye exclusion method. It was determined by dividing the number of viable cells to the total number of cells × 100 %.

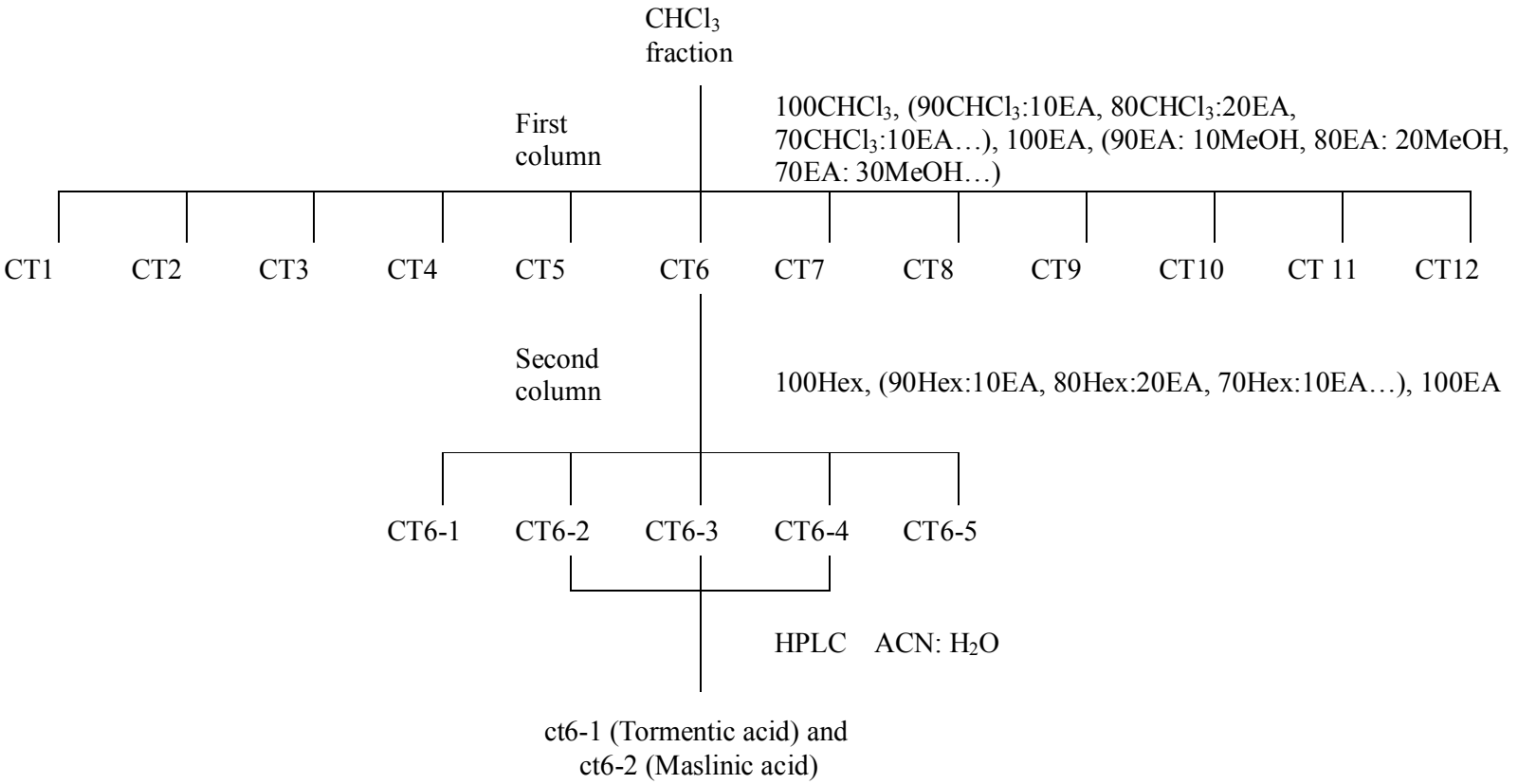

Figure 4.1: Isolation scheme of the compounds ct6-1 (tormentic acid) and ct6-2 (maslinic acid)

Fractions CT6-2, CT6-3 and CT6-4 which have strong anti-tumour-promoting activities were analyzed using analytical HPLC (Shimadzu, Kyoto, Japan) to identify the number of compounds present and their purity.

(A) CT6-2

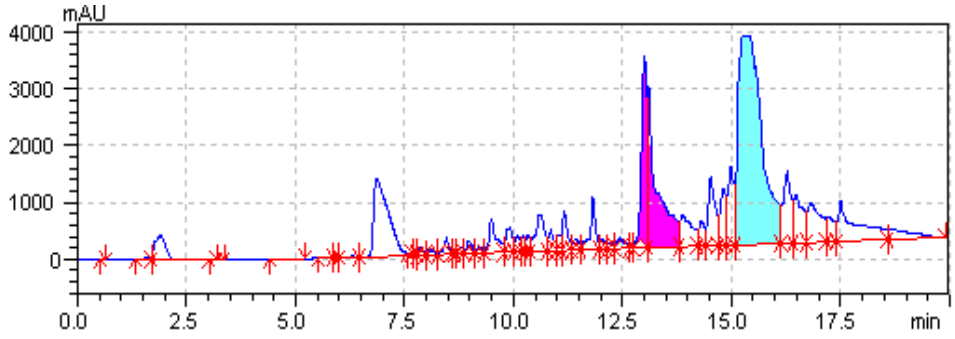

(B) CT6-3

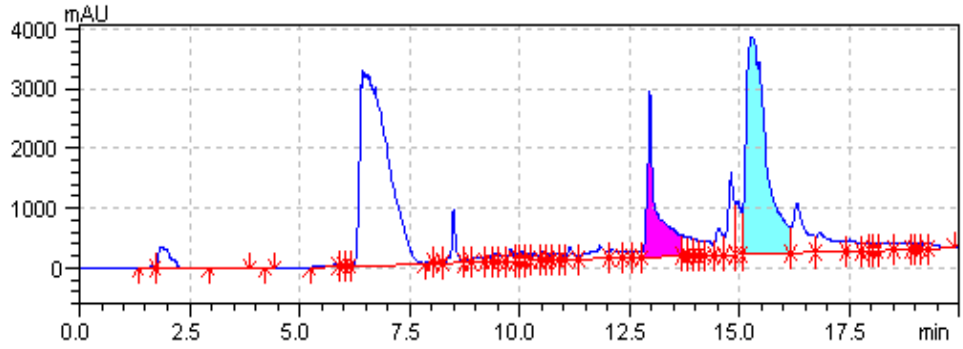

(C) CT6-4

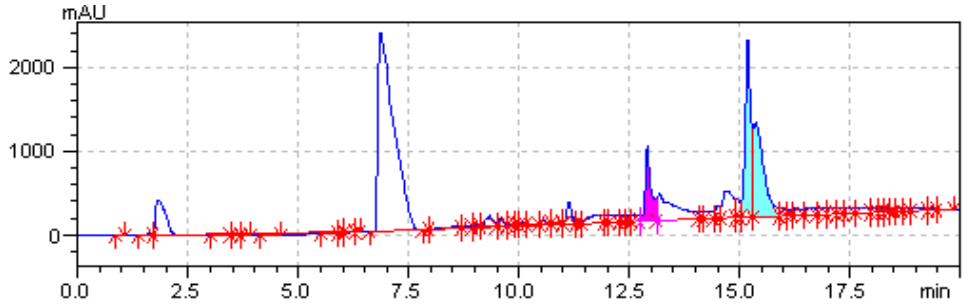

Figure 4.2: Analytical HPLC profiles of fractions CT6-2, CT6-3, and CT6-4. Two major compounds (red coloured and blue coloured) were identified in these sub-fractions. The broad peak at 7th min is the ethyl acetate solvent peak.

As shown in Figure 4.2, two major compounds were identified with the retention times of 13 min and 15.5 min, respectively. These compounds were purified using preparative HPLC method. The two compounds (ct6-1 and ct6-2) isolated are 95 and 90 % pure as determined by analytical HPLC (Figure 4.3).

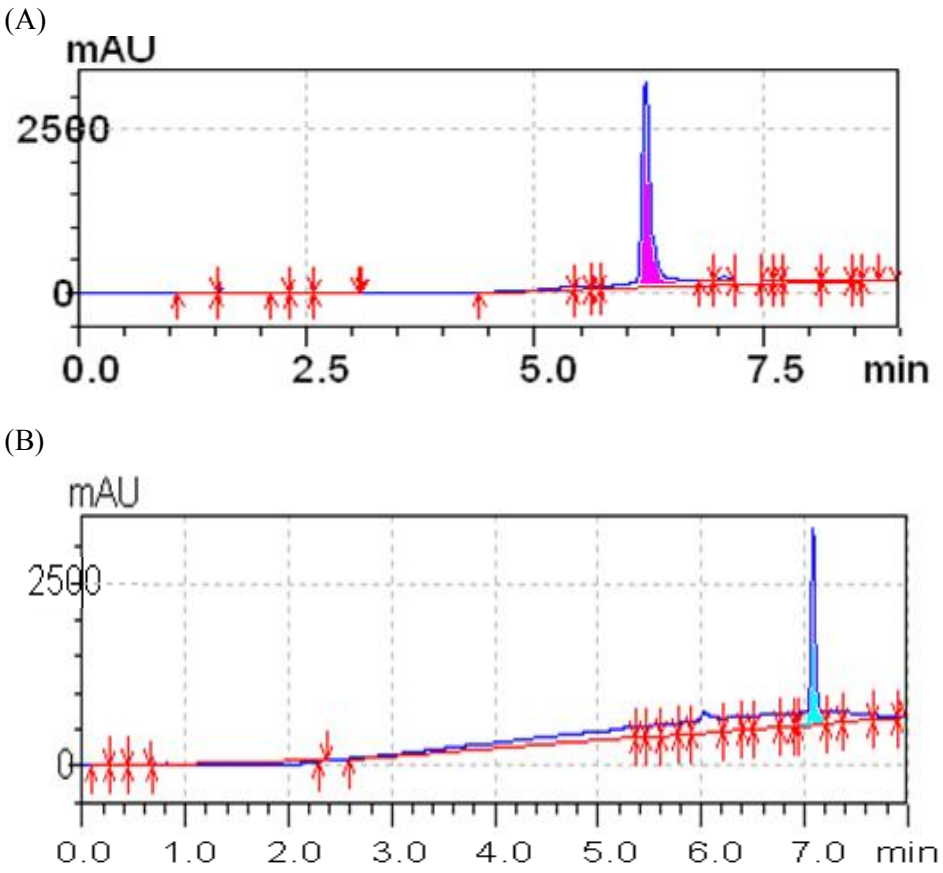

Figure 4.3: Analytical HPLC profiles of isolated compounds (A) ct6-1 and (B) ct6-2. The compound ct6-1 and ct6-2 are of 95 and 90 % pure as determined from the HPLC peak area.

Isolated compounds were then subjected to instrumental analysis for structural elucidation and their anti-tumour activities were determined by the EBV-EA assay.

4.1.2 Structural elucidation of ct6-2 (maslinic acid)

A total of 40 mg of ct6-2 was isolated in the form of white amorphous solid. The melting point is 260-262 ºC. Examination of the IR spectrum (Figure 4.4) indicated the presence of carboxylic acid carbonyl C=O (1700 cm^{-1}) and hydroxyl -OH (3448 cm^{-1}) functional groups. Other absorption bands were detected at 2945 (CH), 1458, 1387, 1304, 1273, 1208, 1184, 1030, and 826. The mass spectrum of ct6-2 (Figure 4.5) has a molecular ion peak at *m/z* 472 (M^+) corresponding to the molecular formula $C_{30}H_{48}O_4$. The base peak appeared at *m/z* 248. Other molecular ion peaks were observed at *m/z* 454 (M^+ - H_2O), 426 (M^+ - HCO_2H), 408 (426 – H_2O), 203 (248 - COOH), 133, 119, 105, 95, 81, 69 and 56 (Alam *et al*., 1996; Lim, 2002).

Assignments of the carbon and proton chemical shifts were made by comparison of the spectral data with the chemical shift values (Table 4.3 and 4.4) of the targeted compound maslinic acid (Lim, 2002; Yamagishi *et al*., 1988; Kojima and Ogura, 1986). The ^1H NMR spectrum of ct6-2 (Figure 4.6) displayed an olefinic proton at δ 5.24 (t) assigned to H-12 and a methine proton at δ 2.85 (dd) assigned to H-18. The seven methyl singlets are located on quaternary carbons that resonate at δ 1.01 (C-23), δ 0.81 (C-24), δ 0.80 (C-25), δ 1.00 (C-26), δ 1.16 (C-27), δ 0.90 (C-29) and δ 0.93 (C-30). These data strongly suggest the presence of an olean-12-en skeleton. Comparison of the proton and carbon chemical shifts at C-2 and C-3 to the corresponding carbons and protons in the targeted compound maslinic acid (Kojima and Ogura, 1986; Yamagishi *et al*., 1988; Lim, 2002) suggested the presence of two hydroxyl

groups at C-2 and C-3, respectively. The broad peak at the absorption of 3448 cm^{-1} in the IR spectrum also indicated the presence of hydroxyl groups.

Evidence for confirming the skeleton of the molecule was provided by ^{13}C NMR spectrum (Figure 4.7). The two methine protons at δ 3.60 and 2.90 ppm are coupled to the two hydroxylated carbons resonating at δ 69.5 (C-2) and 84 (C-3). Meanwhile, presence of two olefinic carbon signals at δ 145.3 (C-13) and 123.3 (C-12) again suggest that it is an olean-12-ene found in pentacyclic triterpenes. The carboxylic acid carbonyl signal resonating at δ 182.1 was assigned to quaternary carbon 17, which is supported by the presence of the carboxylic acid carbonyl at the absorption of 1700 cm^{-1} in the IR spectrum.

Orientation of the two hydroxyl groups at C2 and 3 was then determined by comparing to the spectral data reported by Kojima and Ogura (1989). It was clear that the structure has an α-oriented hydroxyl and β-oriented hydroxyl group at carbon 2 and 3, respectively. The resonance of two methane protons at δ 3.60 and δ 2.90 were found to be similar to the δ values of the corresponding carbon (δ 3.68 at C-2 and δ 2.99 at C-3) of 2α,3β-$(OH)_2$, which are presented in Table 4.5. Furthermore, the distance ($\Delta\delta_{2-3}$) between the chemical shifts of H-2 and H-3 is 0.7 ppm, which is accepted in positioning the hydroxyl groups in 2α,3β-$(OH)_2$ (Kojima and Ogura, 1989). Hence, ct6-2 was characterized as 2α, 3β-dihydroxyolean-12-en-28-oic acid (maslinic acid) (Figure 4.8).

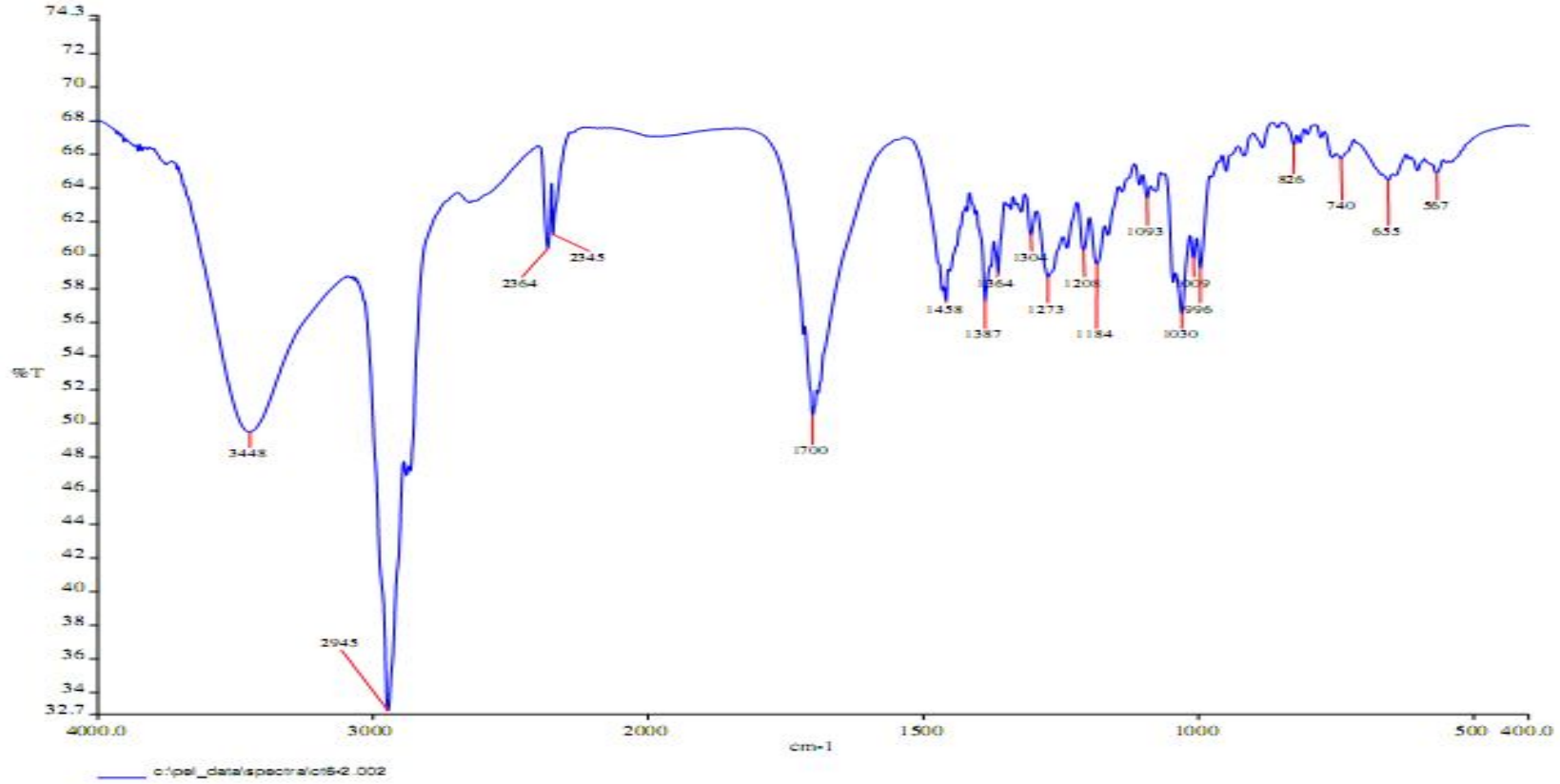

Figure 4.4: Infrared spectrum of ct6-2

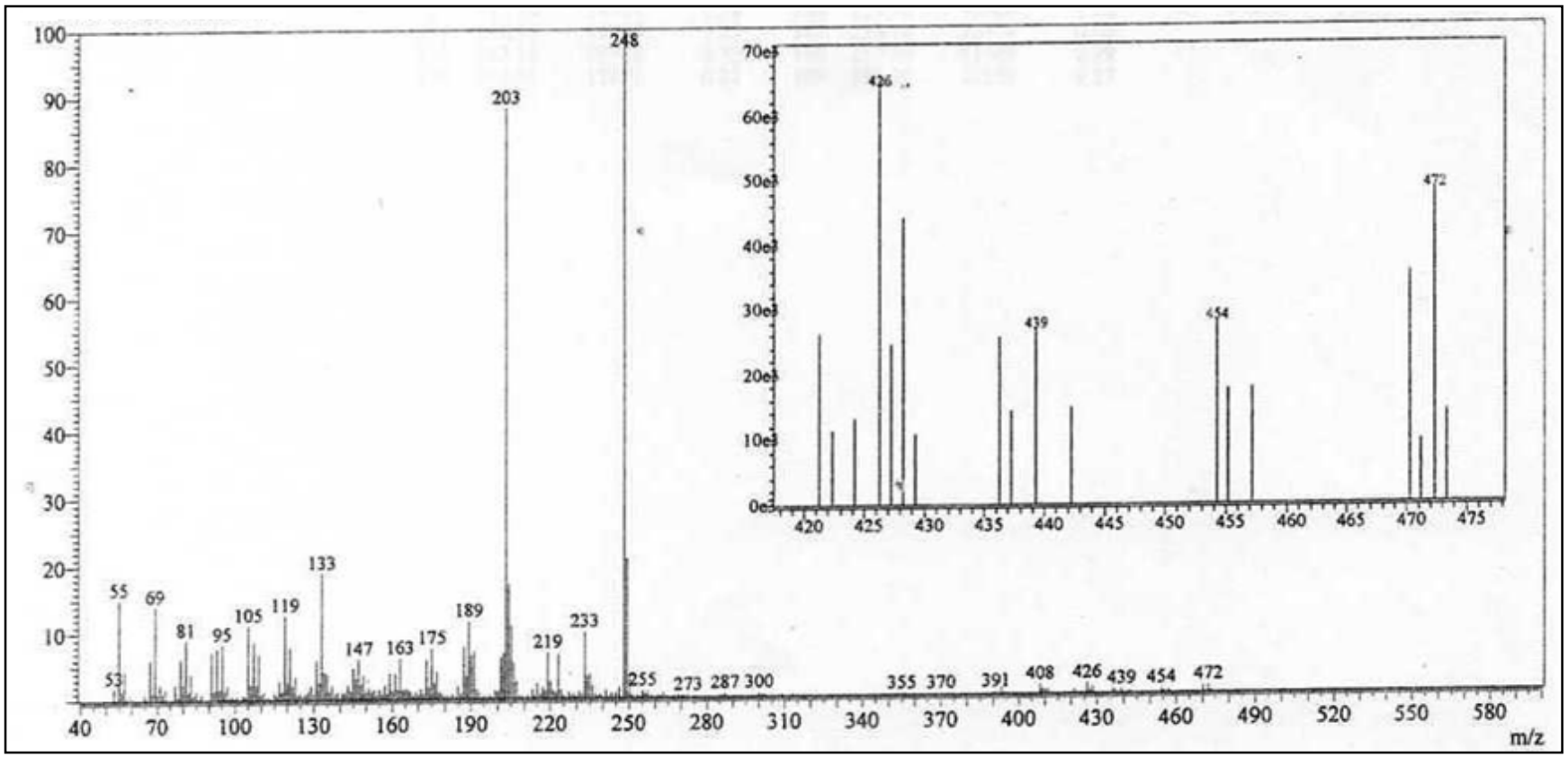

Figure 4.5: Mass spectrum of ct6-2

Table 4.3: ^{13}C NMR chemical shifts of ct6-2 and maslinic acid

Carbon Position	ct6-2	Maslinic acid (Lim, 2002)	Maslinic acid (Kojima and Ogura, 1986)
1	47.6	47.6	46.4
2	69.5	69.2	68.8
3	84.5	84.2	83.8
4	40.6	40.2	39.1
5	56.7	56.3	55.3
6	19.6	19.3	18.3
7	33.8	34.6	32.6
8	40.5	40.2	39.1
9	48.8	48.4	47.5
10	39.3	38.9	38.3
11	24.6	23.8	23.5
12	123.3	123.1	122.0
13	145.3	144.9	143.6
14	43.0	42.6	41.7
15	28.8	26.4	27.6
16	24.0	24.3	23.1
17	47.9	47.3	46.6
18	42.7	42.3	41.3
19	47.2	46.8	45.8
20	31.6	31.4	30.7
21	34.9	33.5	33.8
22	33.6	33.5	32.3
23	29.3	29.1	28.6
24	17.7	17.3	16.8
25	17.5	17.3	16.8
26	17.1	17.0	16.8
27	26.4	26.4	26.0
28	182.1	181.6	178.0
29	33.9	33.5	33.1
30	24.0	23.9	23.5

Table 4.4: ^{1}H NMR chemical shifts of ct6-2 and maslinic acid

Position	ct6-2	Maslinic acid (Lim, 2002)	Maslinic acid (Yamagishi *et al*., 1988)
1	-	-	-
2	3.60 (m)	3.60 (m)	3.62 (m)
3	2.90 (d)	2.90 (d)	2.90 (d)
4	-	-	-
5	-	-	-
6	-	-	-
7	-	-	-
8	-	-	-
9	-	-	-
10	-	-	-
11	-	-	-
12	5.24 (t)	5.24 (t)	5.25 (t)
13	-	-	-
14	-	-	-
15	-	-	-
16	-	-	-
17	-	-	-
18	2.85 (dd)	2.84 (dd)	2.85 (dd)
19	-	-	-
20	-	-	-
21	-	-	-
22	-	-	-
23	1.01 (s)	0.97 (s)	1.01 (s)
24	0.81 (s)	0.78 (s)	0.82 (s)
25	0.80 (s)	0.78 (s)	0.81 (s)
26	1.00 (s)	0.94 (s)	1.00 (s)
27	1.16 (s)	1.14 (s)	1.16 (s)
28	-	-	-
29	0.90 (s)	0.90 (s)	0.91 (s)
30	0.93 (s)	0.91 (s)	0.94 (s)

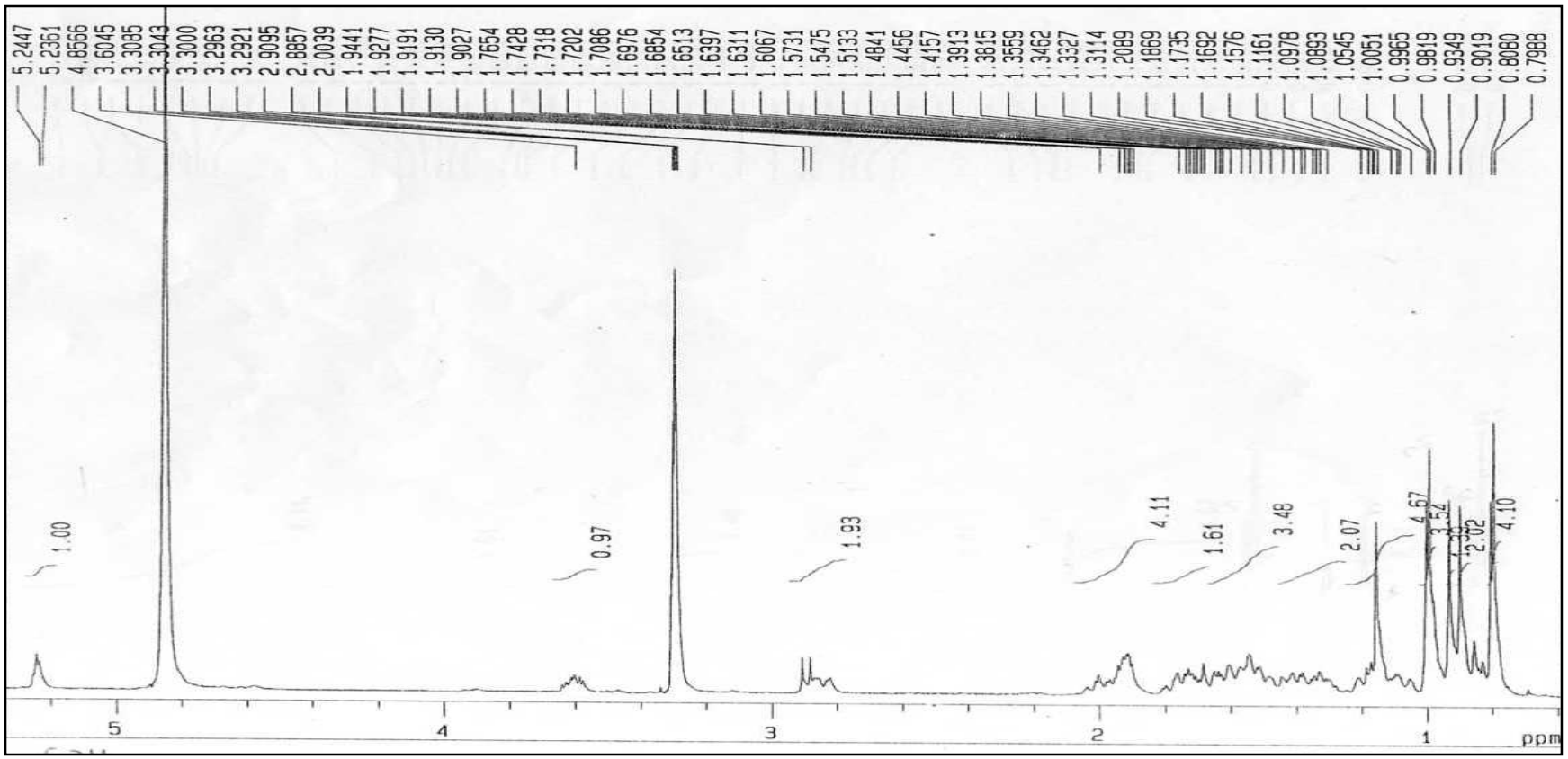

Figure 4.6: Proton NMR of ct6-2

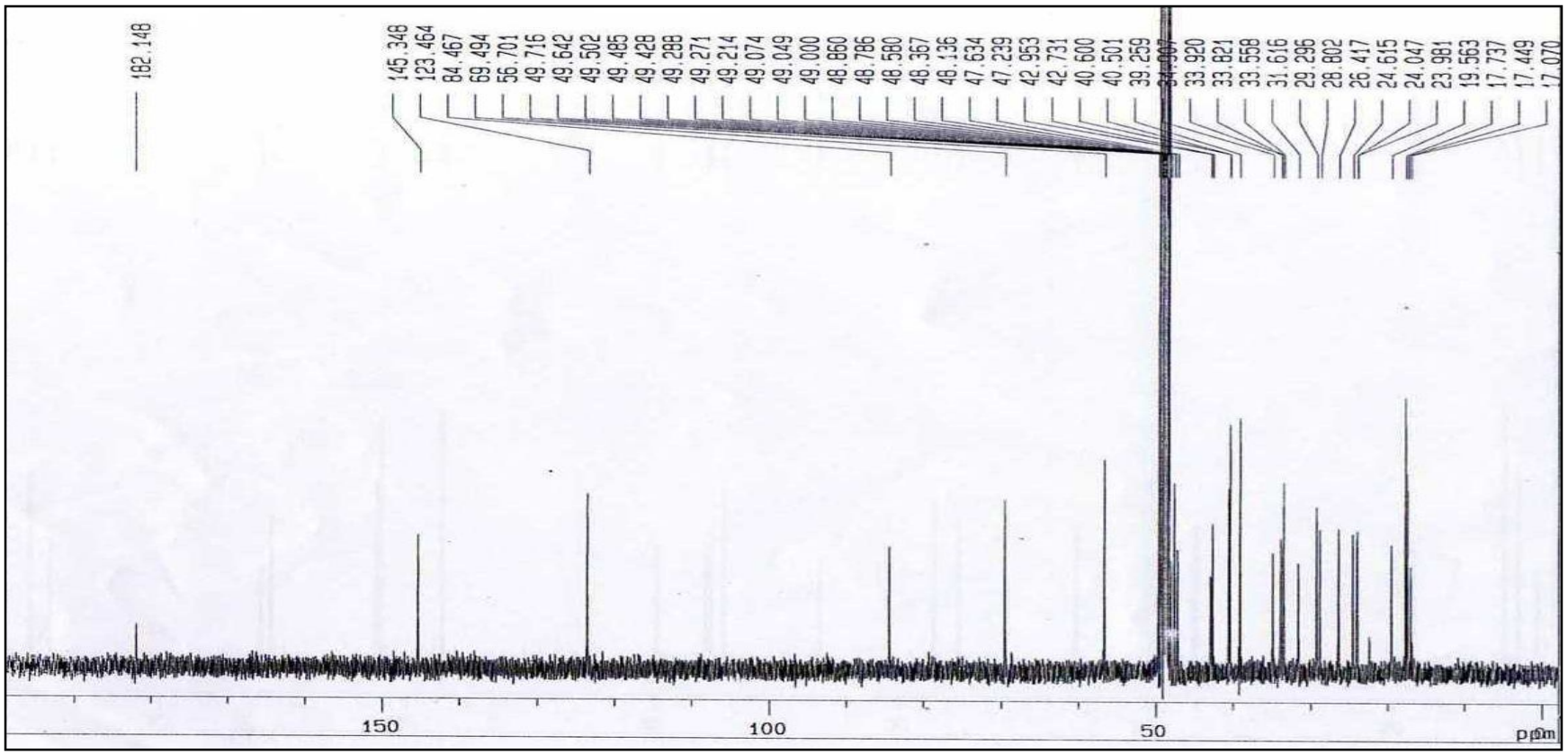

Figure 4.7: Carbon NMR of ct6-2

Table 4.5: ^{1}H-NMR signals of methyl-2, 3-dihydroxy urs-12-en-28-oates and their diacetates

Assignments	2β,3α-$(OH)_2$	2β,3α-$(OAc)_2$	2β,3β-$(OH)_2$	2β,3β-$(OAc)_2$	2α,3β-$(OH)_2$	2α,3β-$(OAc)_2$	2α,3α-$(OH)_2$	2α,3α-$(OAc)_2$
2-H	3.75 ddd (17, 10, 2)	4.95 ddd (13, 6, 5)	4.08 ddd (4, 4, 3)	5.31 ddd (4, 4, 3)	**3.68 ddd** (11, 10, 4.5)	5.10 ddd (11, 10.5, 4.5)	4.00 ddd (12, 4.5, 3)	5.23 ddd (12, 4.5, 3)
3-H	3.63 d 10	5.03 d 6.5	3.20 d 4	4.61 d 4	**2.99 d** 10	4.75 d 10.5	3.43 d 3	4.96 d 3
12-H	5.27 t 3.5	5.25 t 3.5	5.25 t 3.5	5.24 t 3.5	5.24 t 3.5	5.23 t 3.5	5.25 t 3.5	5.25 t 3.5
18-H	2.23 d 11	2.23 d 11	2.22 d 11	2.22 d 11	2.22 d 11	2.23 d 11	2.23 d 11	2.24 d 11
23-H_3	0.90 s	1.00 s	1.00 s	0.89 s	1.02 s	0.89 s	1.02 s	0.87 s
24-H_3	1.00 s	0.91 s	0.99 s	1.04	0.81 s	0.90 s	0.86 s	0.98 s
25-H_3	1.09 s	1.14 s	1.23 s	1.19	0.98 s	1.06 s	0.97 s	1.03 s
26-H_3	0.73 s	0.75 s	0.75 s	0.76	0.73 s	0.74 s	0.73 s	0.74 s
27-H_3	1.07 s	1.10 s	1.06 s	1.06	1.07 s	1.06 s	1.08 s	1.11 s
29-H_3	0.85 d 6	0.85 d 6	0.84 d 6	0.85 d 6	0.85 d 6	0.84 d 6	0.85 d 6	0.85 d 6
30-H_3	0.93 d 6	0.94 d 6	0.93 d 6	0.94 d 6	0.93 d 6	0.94 d 6	0.94 d 6	0.94 d 6
Ome	3.69 s	3.60 s	3.59 s	3.60	3.59 s	3.60 s	3.60 s	3.60 s
Oac		2.01 s 2.06 s		2.02 2.04		1.97 s 2.05 s		1.95 s 2.11 s

(Cited from Journal of Phytochemistry by Kojima and Ogura, 1989)

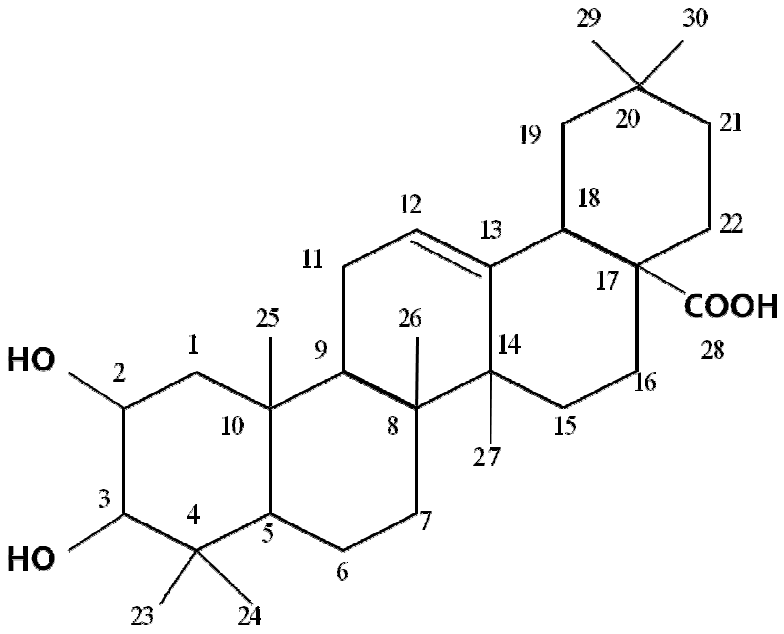

Figure 4.8: Molecular structure of maslinic acid

4.1.3 Structural elucidation of ct6-1 (tormentic acid)

Another compound ct6-1 (50 mg) was isolated along with maslinic acid. The melting point of ct6-1 is 270-272 ºC. The IR spectrum (Figure 4.9) indicated the presence of carboxylic acid carbonyl C=O (1701 cm^{-1}) and hydroxyl -OH (3451 cm^{-1}) functional groups. Mass spectrum (Figure 4.10) data analysis exhibited important ions associated with amyrins (Degaldo *et al*., 1989). The molecular ion peak observed at *m/z* 488 corresponded to the molecular formula $C_{30}H_{48}O_5$. The base peak which appeared at m/z 146 ($[C11H14]^+$) is a characteristic peak of a tertiary hydroxyl function present at C-19 in the urs-12-ene skeleton (Ojinnaka *et al*., 1980). Other important peaks were noted at m/z 470 $[M-H_2O]^+$, 442 $[M-HCOOH]^+$, 424 $[M-HCOOH-H_2O]^+$, 246, 218 and 201 (Ngounou *et al*., 1988; Yamagishi *et al*., 1988). The data is comparable to tormentic acid which had similar molecular ion peak and base peak (Jin *et al*., 2004).

Assignments of the carbon and proton chemical shifts were made by comparison of the spectral data with the chemical shift values (Table 4.6 and 4.7) of tormentic acid (Yamagishi *et al*., 1988; Taniguchi *et al*., 2002; Lim, 2002; Saimaru *et al*., 2007). The ^{1}H-NMR (Figure 4.11) showed resonances of six singlet methyl groups at δ 0.78 (C-25), δ 0.87 (C-24), δ 0.99 (C-26), δ 0.99 (C-23), δ 1.19 (C-29), and δ 1.28 (C-27), a doublet methyl group at δ 0.93 (C-30) and an olefinic proton at δ 5.29 (H-12). This data indicated that ct6-1 has an urs-12-ene skeleton. Meanwhile, the methyl singlet observed at δ 2.55 (H-18) is indicative of a substituent group on the tertiary carbon atom of C-19.

Two methine protons at δ 3.92 (ddd, H-2) and δ 3.30 (d, H-3) on the other hand were suggestive of a 2, 3-dihydroxy structure.

Strong evidence for the ursane-type skeleton of ct6-1 was provided by the ^{13}C NMR spectrum (Figure 4.12). A pair of olefinic carbons at δ 129.4 (C-12) and 140.1 (C-13) are compatible with the existence of the olefinic proton at δ 5.29 (C-12). These data suggest that compound ct6-1 belonged to the urs-12-ene pentacyclic triterpenes. The two methine protons at δ 3.92 and 3.30 ppm are coupled to carbon resonating at δ 67.2 (C-2) and 80.1 (C-3). The carboxylic acid carbonyl signal resonating at δ 182.9 was assigned to C-17. Comparison of the carbon chemical shifts at C-2, C-3, and C-19 to the corresponding carbons in tormentic acid suggested the presence of hydroxyl groups at these carbons (Taniguchi *et al*., 2002; Saimaru *et al*., 2007).

Orientation of the three hydroxyl groups was determined by comparison to the spectral data. The location and α-disposition of the tertiary hydroxyl group at C-19 were established by the observed paramagnetic-induced shifts of the Me-29 (δ 1.19) and Me-27 (δ 1.28) signals, which were of the order reported for geminal and vicinal de-shieldings in similar structural environments (Pereda-Miranda and Gascbn-Figueroa, 1988; Delgado *et al.*, 1989). The resonance of two methine protons at δ 3.92 and δ 3.30 were found to be similar to the δ values of the corresponding carbons (δ 4.09 at C-2α and δ 3.37 at C-3β) reported in Taniguchi *et al* (2002). Hence, ct6-1 was characterized as 2α, 3β, 19α-trihydroxyurs-12-en-28-oic acid (tormentic acid) (Figure 4.13).

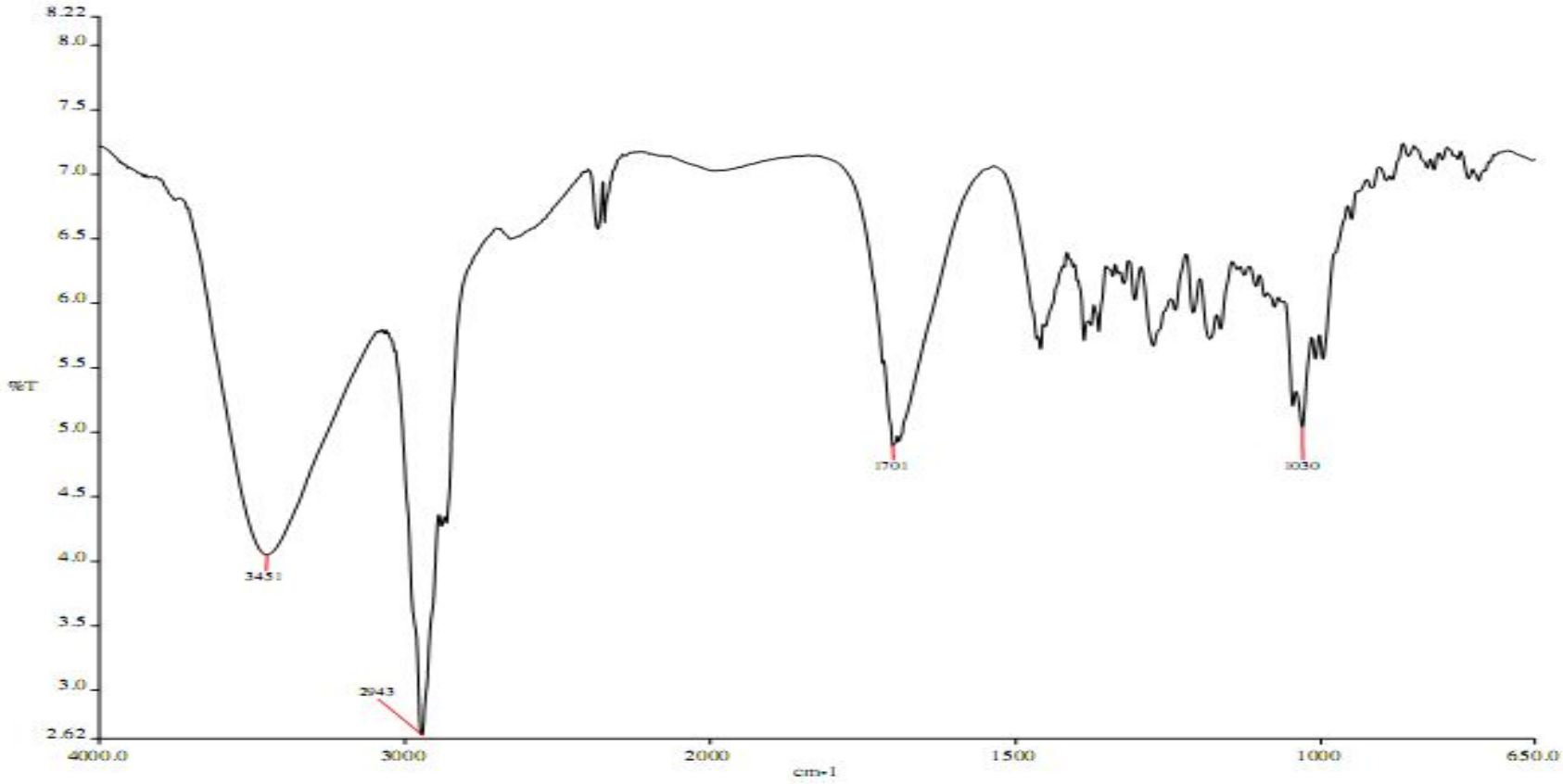

Figure 4.9: IR spectrum of ct6-1

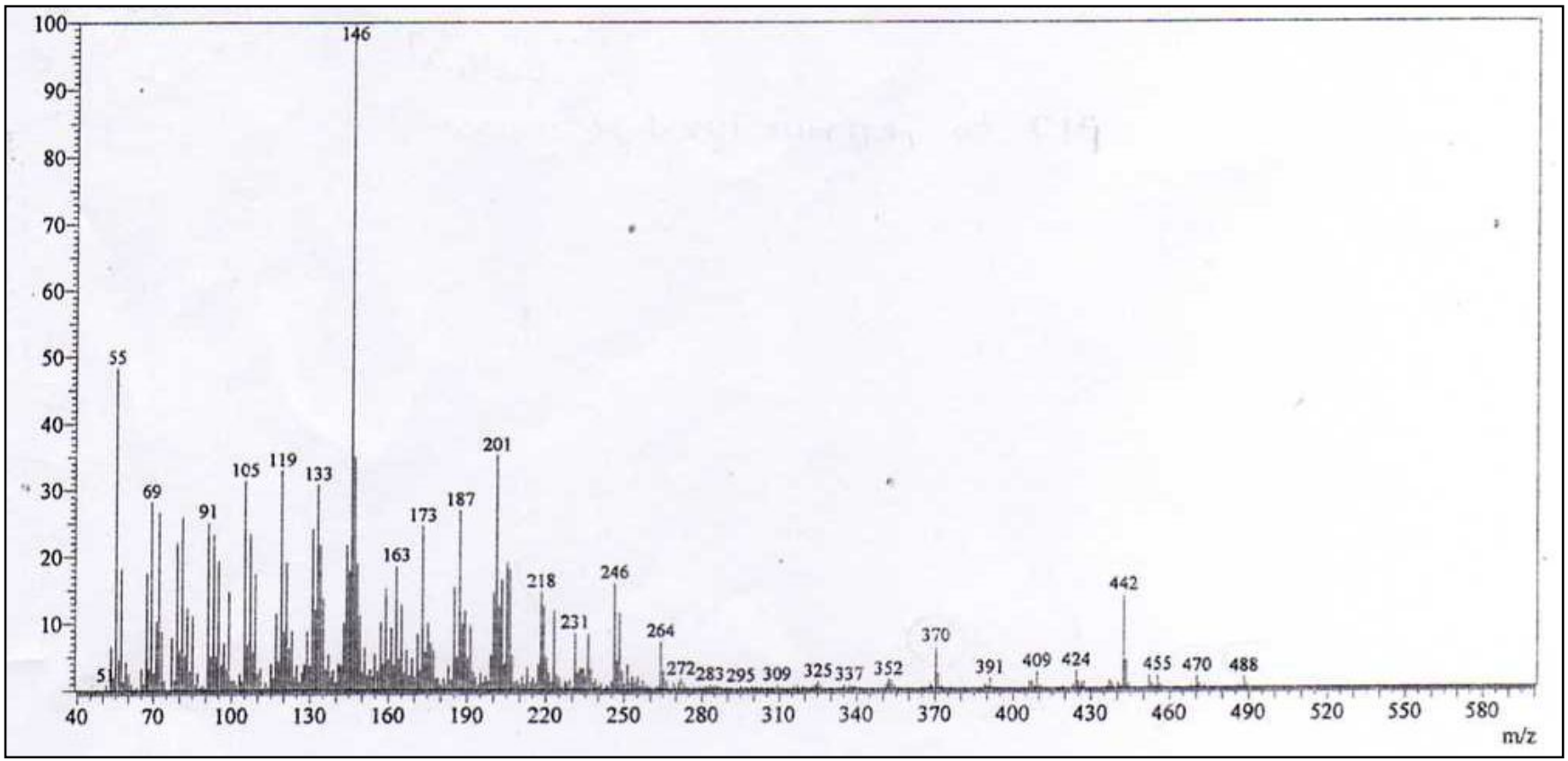

Figure 4.10: Mass spectrum of ct6-1

Table 4.6: ^{13}C NMR chemical shifts of ct6-1 and tormentic acid

Position	ct6-1	Tormentic acid (Taniguchi *et al*., 2002)	Tormentic acid (Saimaru *et al*., 2007)
1	48.4	48.0	47.9
2	67.2	68.6	68.5
3	80.1	83.9	83.8
4	39.5	39.9	39.8
5	55.1	56.0	55.9
6	19.3	19.0	18.9
7	34.1	33.5	33.5
8	41.3	40.5	40.3
9	48.2	47.9	47.8
10	39.3	38.5	38.4
11	24.7	24.1	24.1
12	129.4	128.0	127.7
13	140.1	140.0	140.1
14	42.5	42.2	42.1
15	29.6	29.3	29.3
16	26.6	26.4	26.4
17	48.3	48.3	48.3
18	55.1	54.6	54.6
19	73.6	72.7	72.7
20	42.7	42.4	42.4
21	27.1	27.1	27.1
22	39.0	38.5	38.5
23	29.2	29.3	29.3
24	17.7	17.7	17.6
25	16.9	16.9	16.8
26	17.6	17.2	17.3
27	24.9	24.7	24.7
28	182.9	180.6	181.2
29	27.3	27.1	27.0
30	16.6	16.9	16.7

Table 4.7: ^{1}H NMR chemical shifts of ct6-1 and tormentic acid

Position	ct6-1	Tormentic acid (Taniguchi *et al*., 2002)	Tormentic acid (Yamagishi *et al*., 1988)
1	-	-	-
2	3.92 (ddd)	4.09 (ddd)	3.62 (ddd)
3	3.30 (d)	3.37 (d)	2.91 (d)
4	-	-	-
5	-	-	-
6	-	-	-
7	-	-	-
8	-	-	-
9	-	-	-
10	-	-	-
11	-	-	-
12	5.29 (t)	5.58 (t)	5.28 (t)
13	-	-	-
14	-	-	-
15	-	-	-
16	-	-	-
17	-	-	-
18	2.55 (s)	3.04 (s)	2.50 (s)
19	-	-	-
20	-	-	-
21	-	-	-
22	-	-	-
23	0.99 (s)	1.26 (s)	1.02 (s)
24	0.87 (s)	1.07 (s)	0.81 (s)
25	0.78 (s)	1.00 (s)	0.80 (s)
26	0.99 (s)	1.10 (s)	1.00 (s)
27	1.28 (s)	1.70 (s)	1.25 (s)
28	-	-	-
29	1.19 (s)	1.42 (s)	1.19 (s)
30	0.93 (d)	1.11 (d)	0.95 (d)

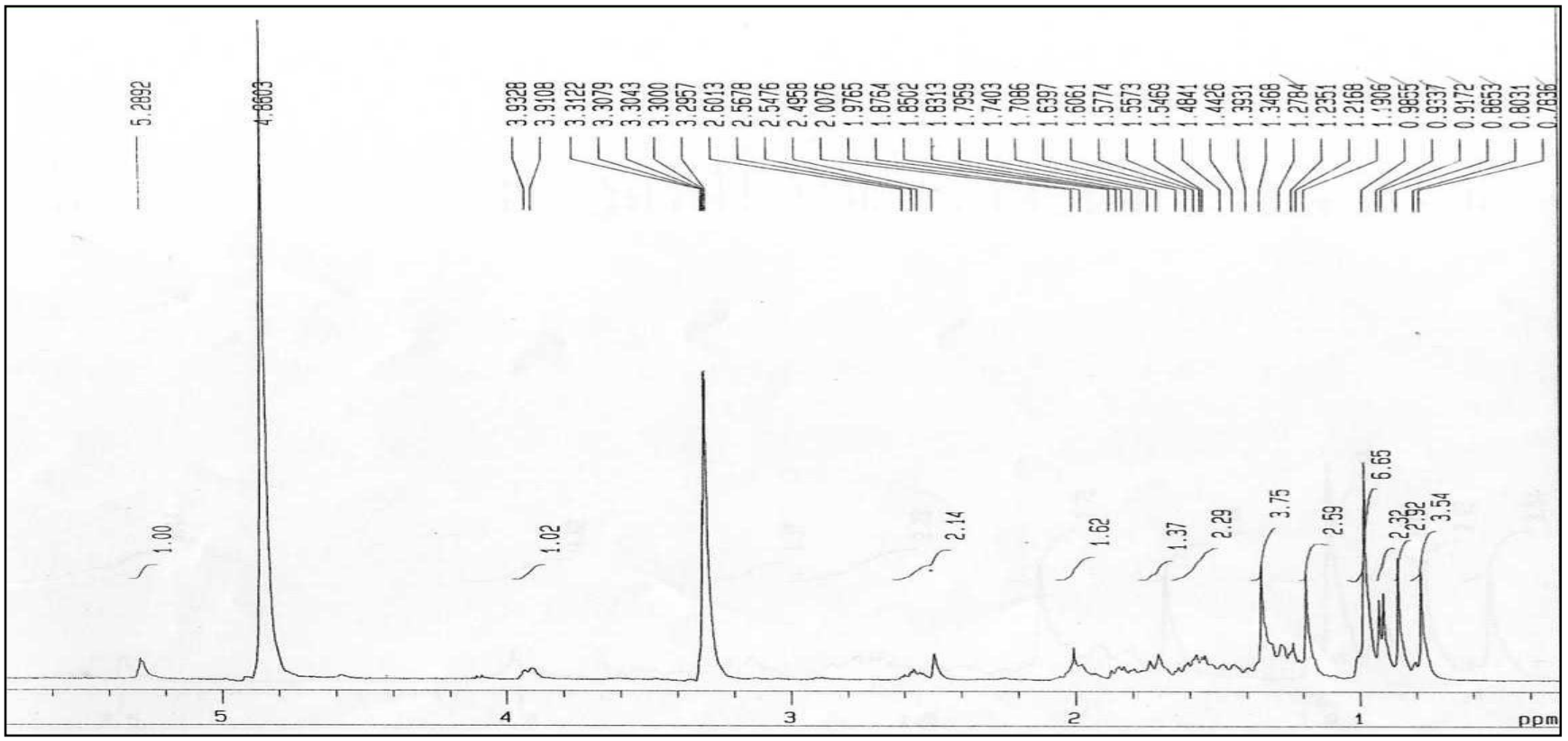

Figure 4.11: Proton NMR of ct6-1

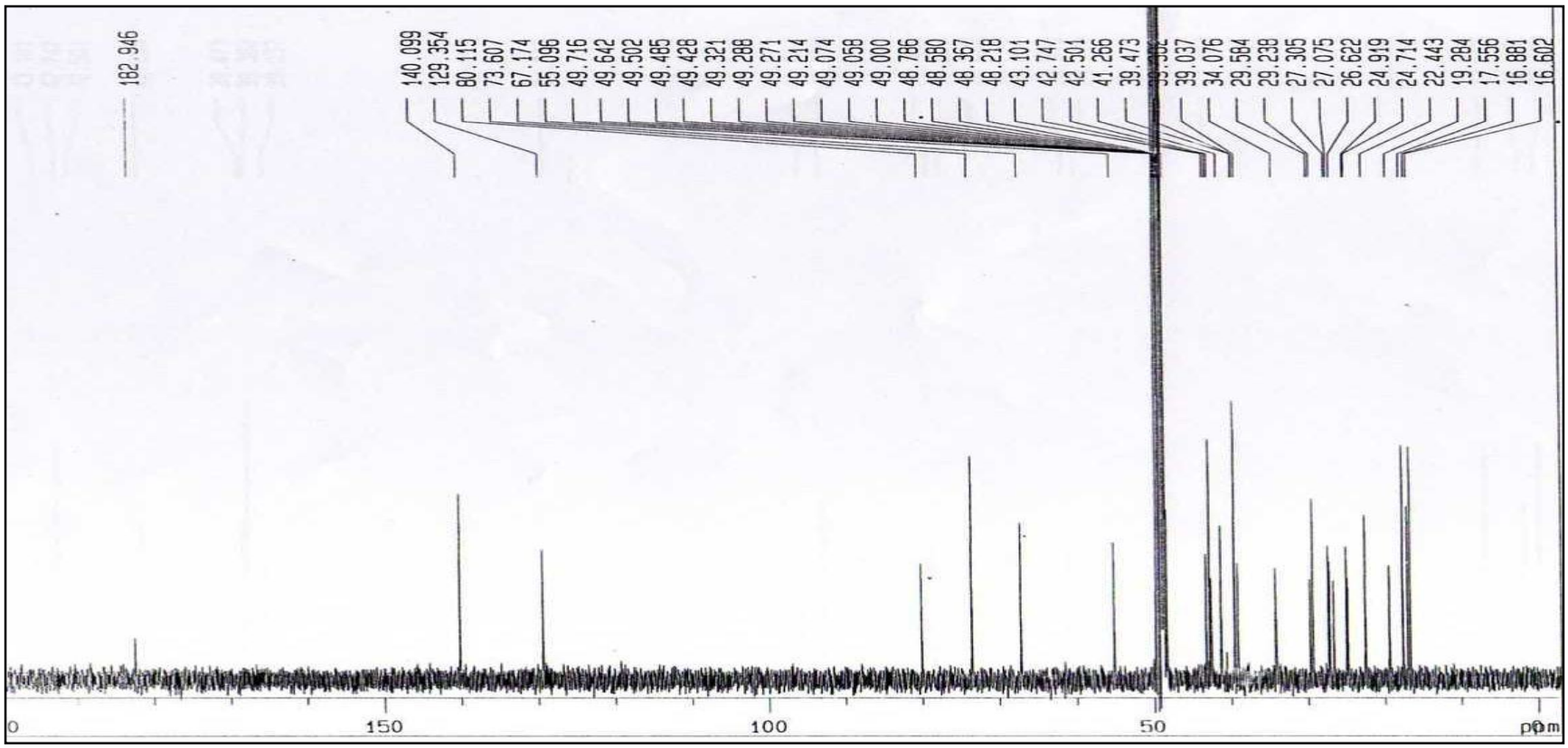

Figure 4.12: Carbon NMR of ct6-1

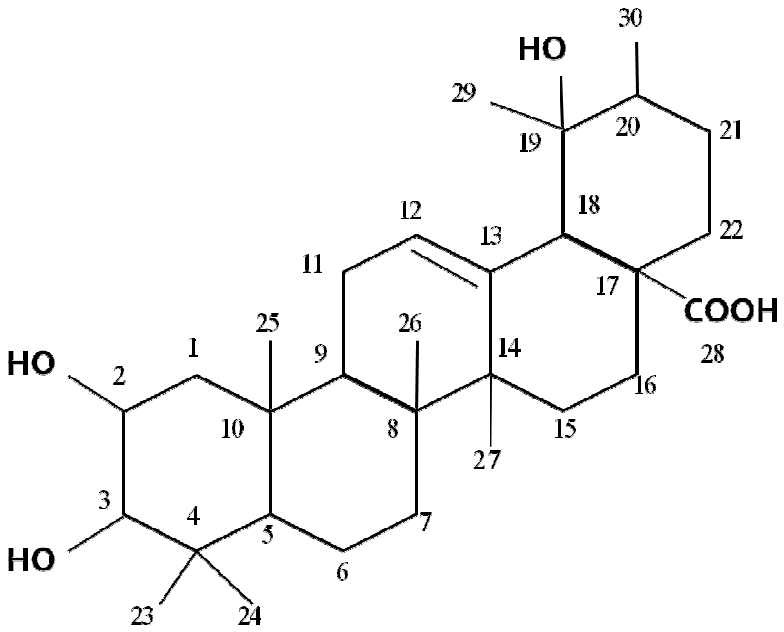

Figure 4.13: Molecular structure of tormentic acid

4.2 EBV-EA inhibition of maslinic acid and tormentic acid

Tormentic acid and maslinic acid isolated from the chloroform fraction of *Coleus tuberosus* were tested for their anti-tumour-promoting activity using the short term *in vitro* EBV-EA activation assay. The inhibitory effects of tormentic acid and maslinic acid were benchmarked against genistein and oleanolic acid. The inhibitory effects of each compound are presented in Table 4.8. Maslinic acid has stronger (IC_{50}=25 μM) anti-tumour activity compared to oleanolic acid (35 μM) but weaker than genistein (20 μM). Maslinic acid, oleanolic acid and genistein have strong anti-tumour promoting activity, with more than 70 % inhibitory effect at 100 μM (Figure 4.14). All three compounds inhibit Raji cell growth and the cytotoxic effect is concentration-dependent. In comparison, tormentic acid exhibit the lowest IC_{50} value (90 μM) but did not affect Raji cell viability.

Table 4.8: The 50 % inhibitory concentration (IC_{50}) of EBV-EA activation by maslinic acid, tormentic acid, oleanolic acid, and genistein

Compounds	IC_{50} (μM)
Maslinic acid	25
Tormentic acid	90
Oleanolic acid	35
Genistein	20

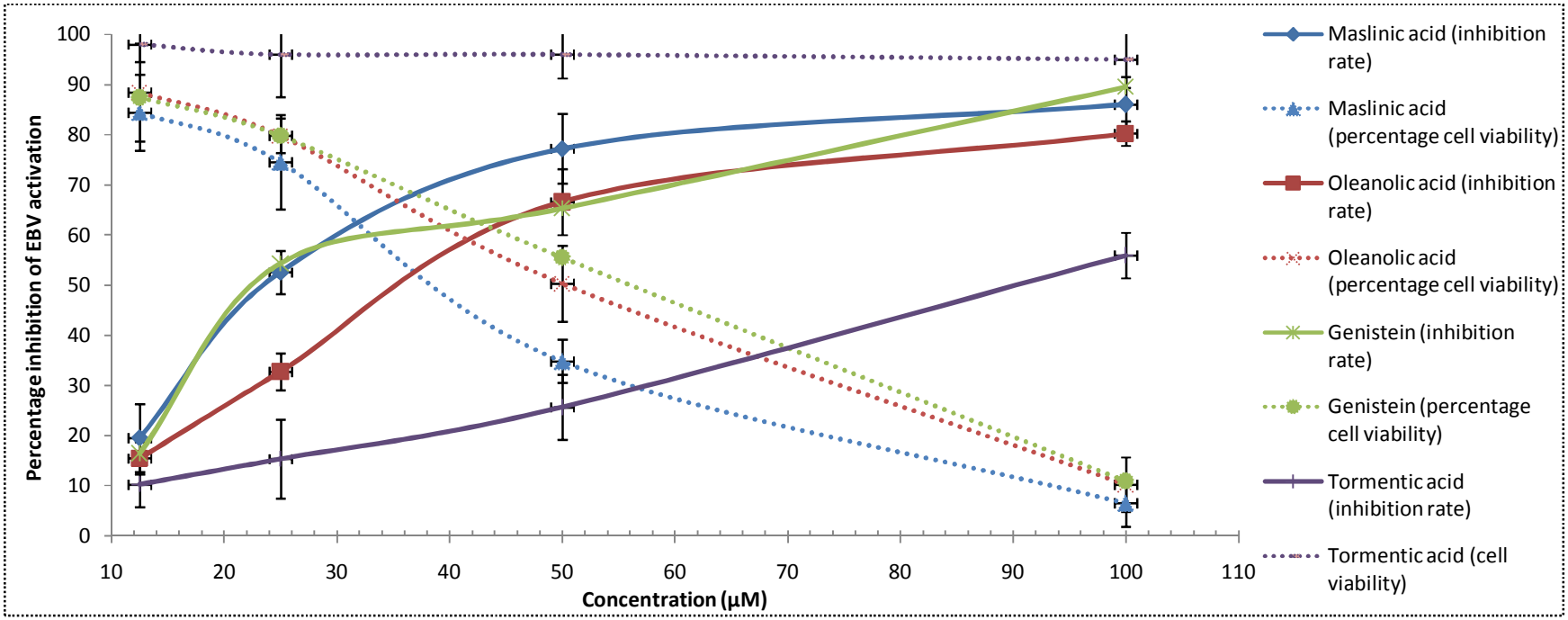

Figure 4.14: Inhibition of EBV-EA activation by maslinic acid, tormentic acid, oleanolic acid, and genistein. Raji cells (5×10^5 cells/mL) were incubated with 3 mM SnB, 0.05 μM PMA, and indicated concentrations of compounds for 48 h. After 48 h, smear of cell suspensions were fixed on Teflon slides and stained with high-titer EBV-EA-positive sera from nasopharyngeal carcinoma patients. In each assay, at least 200 cells were counted and the experiments were repeated thrice. The average extent of EA induction was determined and compared with positive control experiments in which the cells were treated with SnB and PMA only. The viability of treated Raji cells was assayed by the Trypan Blue staining method.

4.3 Inhibitory effects of maslinic acid on NF-κB (p65) binding activity in Raji cells

4.3.1 Determination of basal NF-κB activity in Raji cells

One of the major mechanisms that causes transcriptional activation of NF-κB is the DNA binding activity. The basal NF-κB binding activity in Raji cells was first determined. As shown in Figure 4.15, untreated Raji cells have strong NF-κB binding activity as compared to PMA-induced cells, showing that it has constitutive nuclear NF-κB activity. Raji cells (virus non-producer type) is an EBV genome-carrying human lymphoblastoid cell line. The constitutive NF-κB activity in Raji cells may be the effect of EBV infection in human B lymphocytes, which results in expression of latent membrane protein-1 (LMP1), activation of NF-κB, increased cell proliferation and transformation of cells to lymphoblastoid cell lines (LCL) (He *et al*., 2000; Zou *et al*., 2007). LMP1 strongly activates IKK activity and induces IκBα degradation, leading to NF-κB activation and transcription (McFarland *et al*., 2000). This constitutive NF-κB activity is essential for the growth and survival of EBV-transformed lymphoblastoid cell lines (LCLs) and inhibition of NF-κB induces apoptosis in these cells.

Control reactions including blank (NF-κB probe only), non-specific competition analysis (reaction of NF-κB probe, nuclear extracts and non-specific competitor mutant DNA) and specific competition analysis (reaction of NF-κB probe, nuclear extracts and specific competitor DNA) were performed. The NF-κB binding activity in Raji cells is specific as the presence of non-specific competitor (mutant DNA) did not affect the NF-κB binding

activity in Raji cells. However, the binding activity was significantly reduced in the presence of specific competitor DNA (Figure 4.15).

The blank which was performed in the absence of protein extract has a low NF-κB activity (A_{450nm} = 0.05). Incubation of NF-κB probe together with Raji cell nuclear extracts resulted in a significant increase of NF-κB activity (A_{450nm} = 1.42). In order to establish the specificity of the NF-κB activity induced, 10 fold molar excess of non-specific and specific competitor DNA were added for each competition analysis. The 'mutant' DNA sequence is a scrambled, non-biotin labeled version of the binding sequence; it will not compete for protein binding with the NF-κB probe and therefore did not cause significant reduction in NF-κB activity (A_{450nm} = 1.37). The specific competitor DNA was a NF-κB probe without biotin labels. The specific competitor DNA competes for protein binding but cannot be captured on the Streptavidin plate due to absence of the biotin label, therefore reducing the amount of protein detected (A_{450nm} = 0.15). This was done to verify that the specific competitors compete for specific binding of NF-κB.

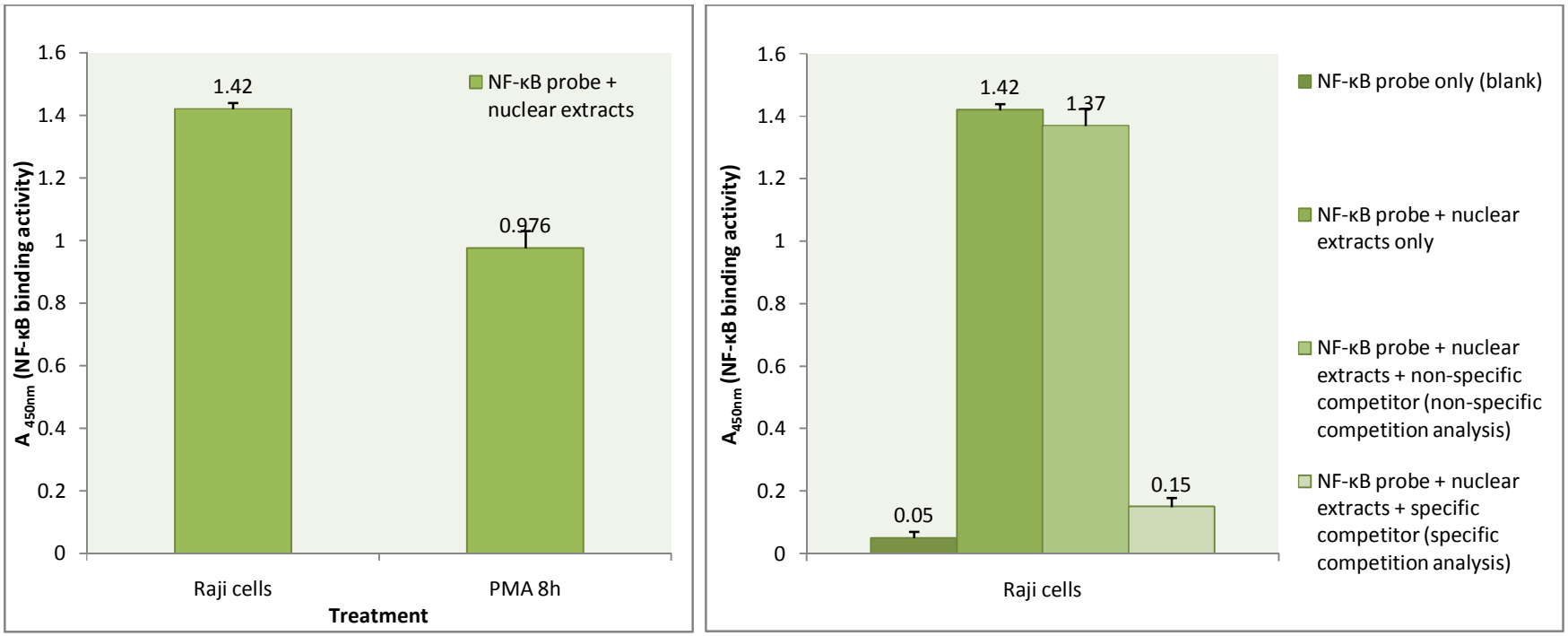

Figure 4.15: NF-κB (p65) DNA binding activity in Raji cells. Raji cells were either treated with vehicle (0.05 % ethanol) or induced with 0.05 μM PMA for 8 h. The nuclear extracts of non-induced and PMA-induced Raji cells were prepared and analyzed for NF-κB activity using the NoShift Transcription Factor Assay kit. Control reactions including blank (NF-κB probe only), non-specific competition analysis (inclusion of NF-κB probe, nuclear extracts and non-specific competitor mutant DNA) and specific competition analysis (inclusion of NF-κB probe, nuclear extracts and specific competitor DNA) were performed. Each data point represents the average mean ± S.D. of three independent experiments.

4.3.2 Concentration- and time-dependent inhibition of NF-κB activity

The inhibitory effect of maslinic acid on the constitutive NF-κB (p65) binding activity in Raji cells was evaluated. Other natural triterpenoids such as ursolic acid and oleanolic acid and standard NF-κB inhibitor BAY 11-7085 were also tested. Maslinic acid inhibited NF-κB (p65) binding activity in a concentration-dependent manner (Figure 4.16) and achieved more than 60 % inhibition at 100 μM. As shown in Figure 4.17, maslinic acid inhibited 65.5 % NF-κB (p65) activity after 4 h treatment and the inhibition effect reached 82.7 % after 8 h treatment. Ursolic acid and oleanolic acid also suppress NF-κB (p65) binding activity in a concentration-dependent manner. Ursolic acid inhibits 68.6 % NF-κB activity at 100 μM while oleanolic acid only inhibits 46.8 % activity at the same concentration (Figure 4.16). The stronger NF-κB inhibitor ursolic acid was further tested for its inhibitory effect in a time course study. Ursolic acid inhibited 61.4 % NF-κB activity after 4 h and achieved 77.8 % inhibition after 8 h. NF-κB inhibitor BAY 11-7085 on the other hand exhibit potent suppressive effect. BAY inhibits 41.3 % NF-κB activity in 2 h treatment and the inhibition effect achieved more than 75 % after 8 h treatment.

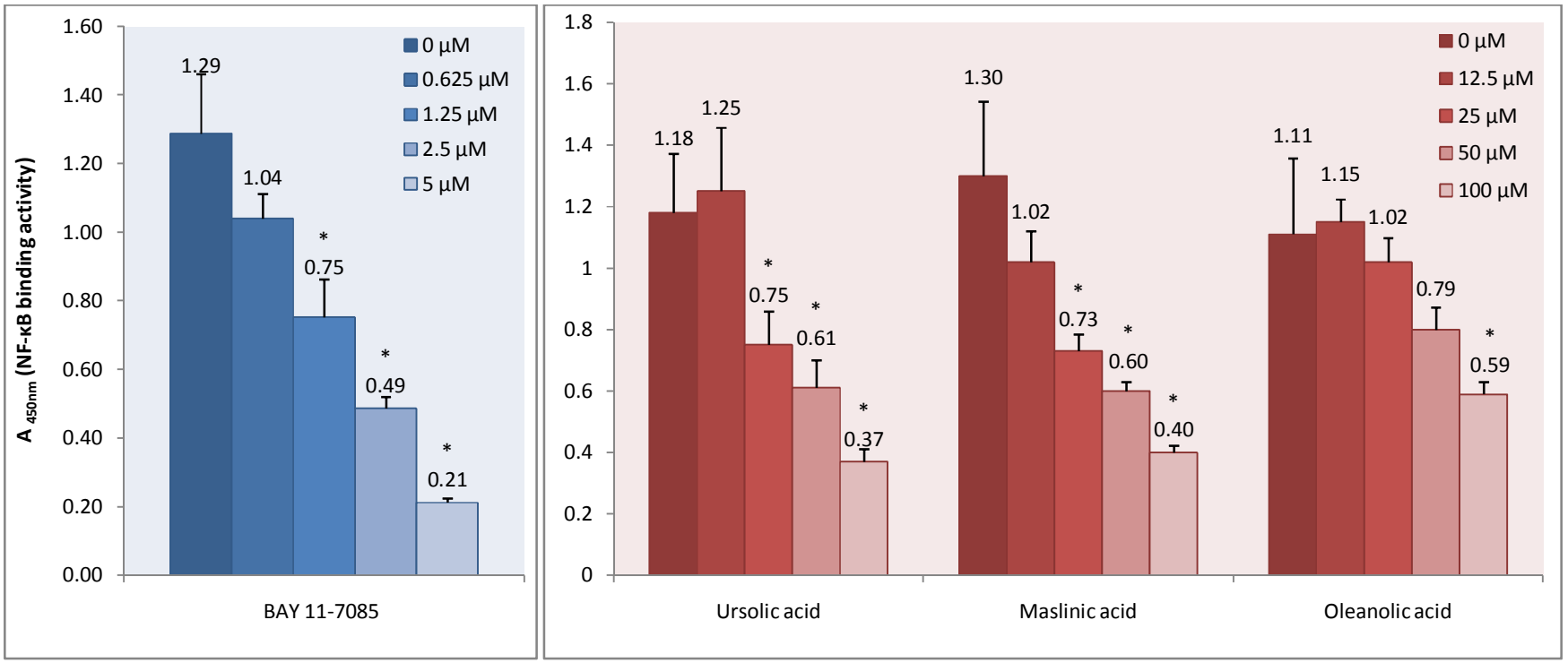

Figure 4.16: Concentration-dependent effects of NF-κB inhibitor BAY 11-7085, ursolic acid, maslinic acid, and oleanolic acid on NF-κB (p65) activity in Raji cells. Nuclear extracts were prepared after 8 h treatment and quantified for NF-κB activity using the NoShift Transcription Factor Assay kit and NoShift NF-κB (p65) reagents. Each data point represents the average mean ± S.D. of three independent experiments. Asterisk (*) represents $p<0.05$ compared to untreated control (0 μM).

The percentage change of NF-κB is calculated by dividing the absorbance of treated samples (e.g. 12.5, 25, 50, 100 μM) to that of the untreated (0 μM) sample × 100 %; percentage inhibition of NF-κB is obtained by the following equation: 100 % - (percentage change of NF-κB).

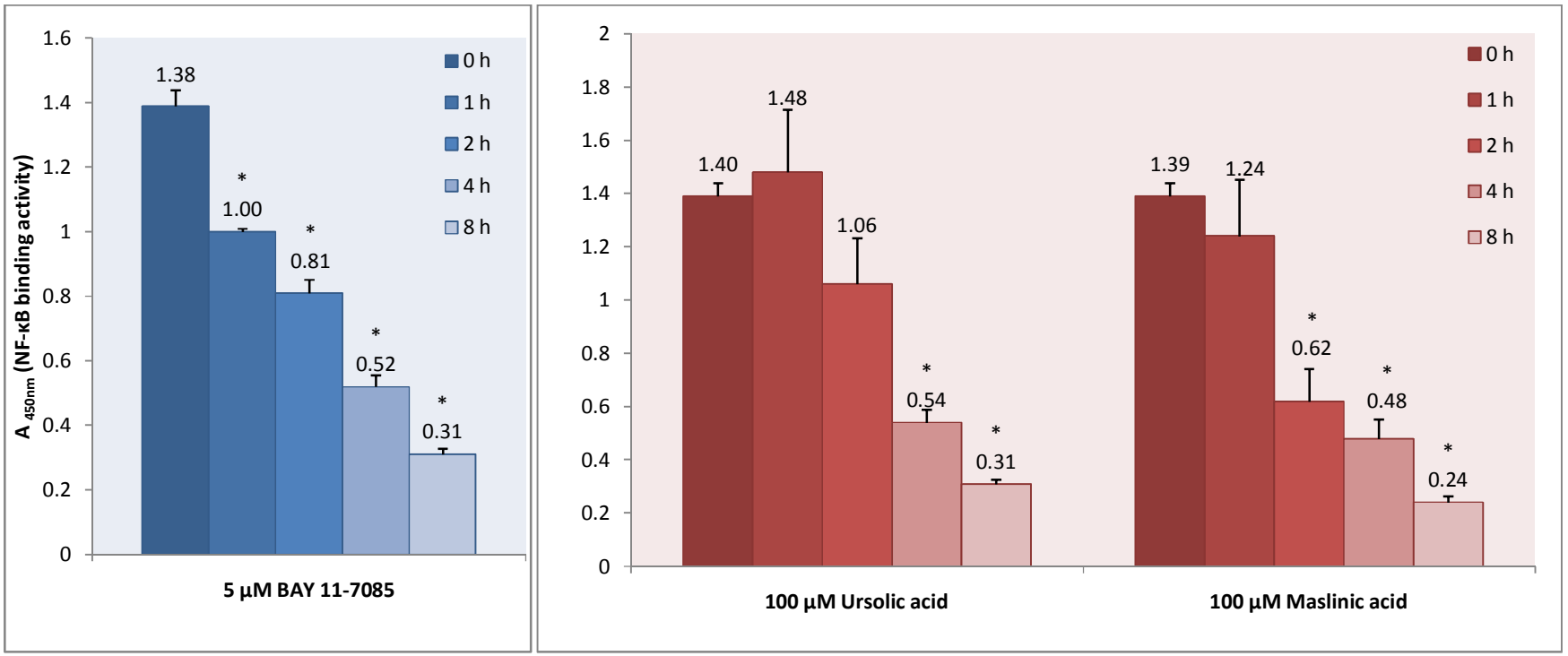

Figure 4.17: Time course inhibitory effects of NF-κB inhibitor BAY 11-7085, ursolic acid, and maslinic acid on NF-κB (p65) activity in Raji cells. Nuclear extracts were prepared after 1, 2, 4, and 8 h treatment and quantified for NF-κB activity using the NoShift Transcription Factor Assay kit and NoShift NF-κB (p65) reagents. Each data point represents the average mean ± S.D. of three independent experiments. Asterisk (*) represents $p<0.05$ compared to untreated control (0 h).

The percentage change of NF-κB is calculated by dividing the absorbance of treated samples (e.g. 1, 2, 4, 8h) to that of the untreated (0 h) sample × 100 %; percentage inhibition of NF-κB is obtained by the following equation: 100 % - (percentage change of NF-κB).

4.4 Inhibitory effects of maslinic acid on AP-1 binding activity in Raji cells

4.4.1 Determination of the basal AP-1 binding activity in Raji cells

The AP-1 binding activity in Raji cells was strongly induced by the combined treatment of both PMA and SnB (Figure 4.18). There was no binding observed in the first and second lanes which contain the AP-1 probe by itself and the AP-1 probe together with non-induced Raji cell nuclear extracts, respectively. A faint binding was detected in the third lane in which Raji cells were stimulated with PMA. The combined treatment of PMA together with SnB, however, induced a strong binding in the forth lane. Competition analysis was then carried out to determine the specificity of this binding induced. As seen in lane 5 and 6, AP-1 binding was not affected in the presence of non-specific competitor (unlabeled NF-κB) probe but was abolished in the presence of a specific competitor (unlabeled AP-1 probe). The unlabeled NF-κB probe, which does not affect the PMA and SnB-induced AP-1 binding, was used as the non-specific competitor. The unlabeled AP-1 probe has the same sequence as the AP-1 probe but lack biotin labels. It competes with the AP-1 probe for protein binding but cannot be detected, thus reducing the binding observed.

The induction of AP-1 binding by PMA and SnB, but not PMA alone might be due to the histone deacetylase inhibitor activity of SnB. Sodium *n*-butyrate is known to cause histone hyperacetylation and reversible inhibition of histone deacetylases, leading to acetylation of core histones H3 and H4 (Hebbes *et al*., 1988; Sealy and Chalkley, 1978). Histone hyperacetylation promotes transactivation of a specific gene, probably by relaxing specific segments of

DNA and histones, thereby facilitating the binding of transcription factors (Lee *et al*., 1993; Grunstein, 1997). In addition, induced AP-1 DNA binding activity might also be the outcome of EBV lytic cycle activation in Raji cells in response to EBV inducing agents such as PMA and SnB (Hong *et al.*, 2004). Entry into the viral lytic cycle is initiated by expression of the immediate-early EBV proteins BamHI Z Leftward reading Frame 1 (BZLF1) (Zalani *et al*., 1996). BZLF1, a bZIP protein with sequence homology to c-Jun and c-Fos, binds and transactivates promoters containing AP-1-like motifs (Urier *et al*., 1989; Farrell *et al.*, 1989).

Lane	1	2	3	4	5	6
AP-1 probe	+	+	+	+	+	+
Cell lysates	-	+	+	+	+	+
PMA	-	-	+	+	+	+
SnB	-	-	-	+	+	+
Unlabeled AP-1 probe	-	-	-	-	+	-
Unlabeled NF-κB probe	-	-	-	-	-	+

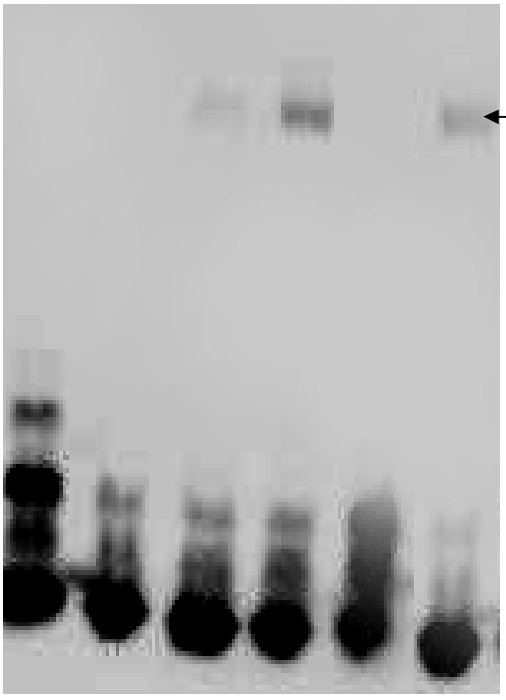

Figure 4.18: AP-1 DNA binding activity in Raji cells. The Raji cells were either treated with vehicle (0.05 % ethanol), induced with 0.05 μM PMA or combination of both 0.05 μM PMA and 3 mM SnB for 4 h. Ten fold molar excess of unlabeled AP-1 DNA and unlabeled NF-κB DNA were added in the competition reactions to establish the specificity of AP-1 binding.

4.4.2 Concentration- and time-dependent inhibition of AP-1 binding activity

The inhibitory effect of maslinic acid on the AP-1 binding activity was compared with those of ursolic acid and oleanolic acid. As shown in Figure 4.19, maslinic acid inhibited AP-1 binding activity in a concentration-dependent manner and completely abolished the induced binding at 100 μM. Maslinic acid-mediated inhibition of AP-1 binding started as early as 2 h and the inhibition continued until 8 h (Figure 4.20). Its inhibitory effect is comparable to ursolic acid which also suppressed AP-1 binding activity at similar concentrations. In contrast, oleanolic acid only partially inhibited the induced AP-1 binding activity at 100 μM after 8 h.

The AP-1 binding activity was transiently up-regulated upon incubation with PMA and SnB, with maximal induction at 4 h. A similar increase in AP-1 binding activity was also reported in SnB-treated HL-60 cells (Mollinedo *et al*., 1993). Apparently, AP-1 binding activity is regulated at the transcriptional and post-translational level (Eferl and Wagner, 2003). In response to transcriptional activation induced by PMA and SnB, the number of AP-1 complexes may increase, enhancing binding activity and subsequently activating AP-1 target genes. Post-translational events involving phosphorylation by various kinases regulate AP-1 transactivating potential, DNA-binding capacity and the stability of AP-1 components (Eferl and Wagner, 2003). Both transcriptional and posttranslational events might contribute to the sharp increase in AP-1 binding activity at 4 h.

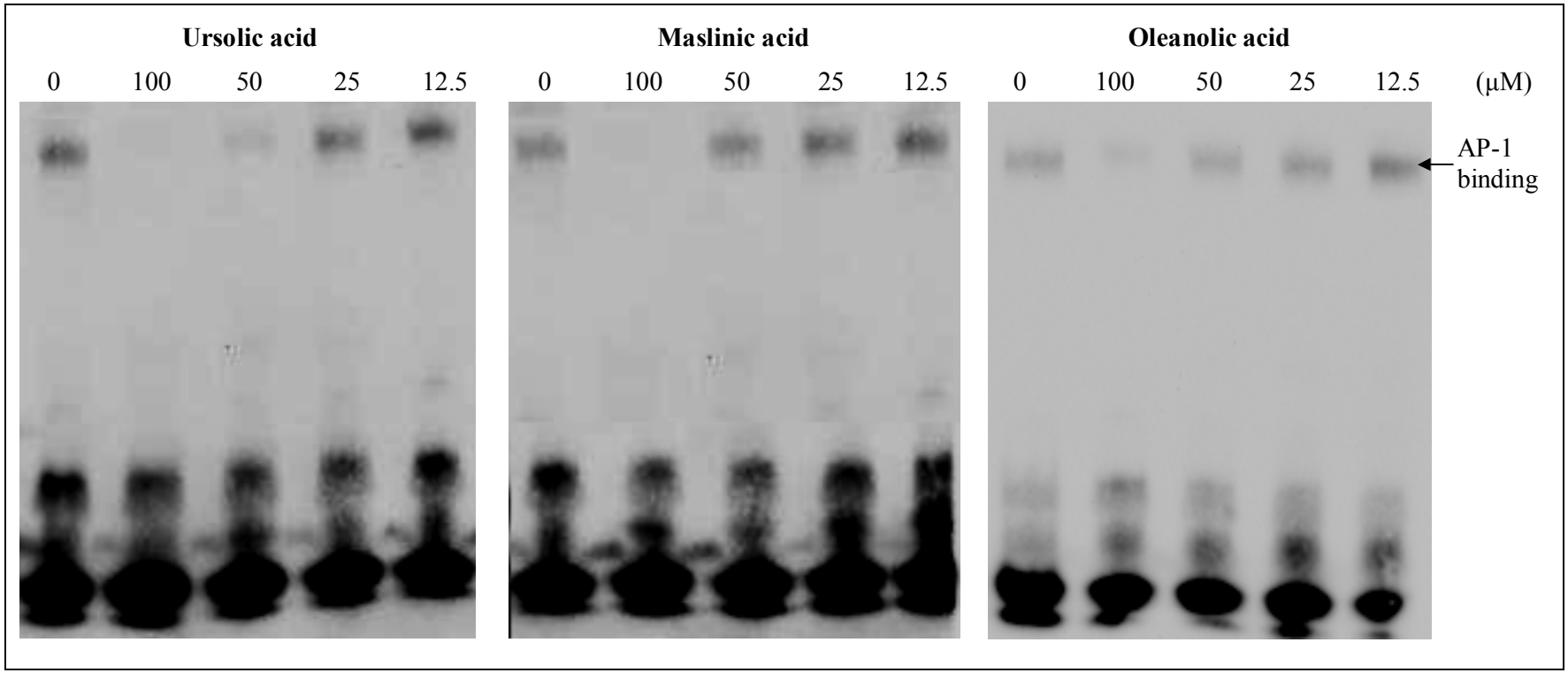

Figure 4.19: Concentration-dependent effects of maslinic acid, ursolic acid and oleanolic acid on PMA and SnB-induced AP-1 DNA binding activity in Raji cells. Raji cells were treated with 0.05 μM PMA, 3 mM SnB along with various concentrations (12.5, 25, 50, and 100 μM) of ursolic acid, maslinic acid and oleanolic acid for 4 h. The nuclear extracts were prepared and analyzed for AP-1 binding activity using the LightShift Chemiluminescent EMSA Assay. Data presented are representative of three independent experiments showing similar trends.

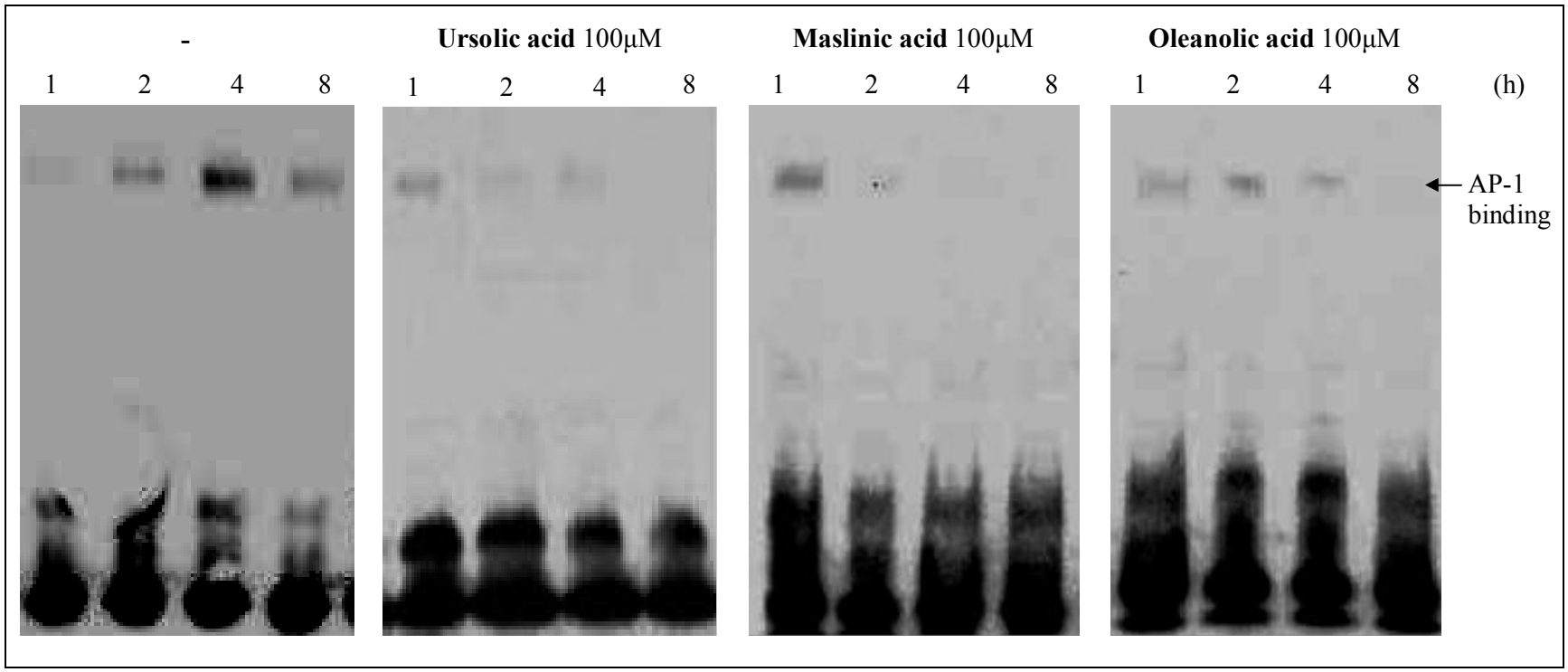

Figure 4.20: Time course inhibitory effects of ursolic acid, maslinic acid, and oleanolic acid on PMA and SnB-induced AP-1 DNA binding activity in Raji cells. Raji cells were treated with 0.05 μM PMA, 3 mM SnB along with 100 μM ursolic acid, maslinic acid and oleanolic acid for 1, 2, 4 and 8 h. The nuclear extracts were prepared and analyzed for AP-1 binding activity using LightShift Chemiluminescent EMSA Assay. Data presented are representative of three independent experiments showing similar trends.

4.5 Suppressive effects of maslinic acid on COX-2 expression

4.5.1 Determination of the basal COX-2 expression in Raji cells

The basal COX-2 expression in Raji cells and the expression induced in response to PMA treatment were first determined. Western blot analysis (Figure 4.21) showed that Raji cells express COX-2 and that the level of PMA-induced COX-2 expression increase by only 18 %. The fact that Raji cells express COX-2 protein agrees with studies which confirm that B lymphoma cells are capable of expressing COX-2 compared to primary B cells (Graf *et al*., 1999). Findings suggested that COX-2 protein expression is part of the process whereby B cells become malignant and that certain B cell malignancies require COX-2 for survival (Wun *et al*., 2004). In addition, COX-2 mRNA and protein expression levels in EBV-positive cells were significantly higher than the levels in EBV-negative cells (Kaul *et al*., 2006). This suggests the possible role of some EBV latent antigens (e.g. LMP1 and EBNAs) in transcriptional control of COX-2 (Murono *et al*., 2001). Up-regulation of COX-2 by EBV proteins during latency may result in the tumourigenic phenotype (Kaul *et al*., 2006).

4.5.2 Concentration- and time-dependent suppression of COX-2 expression

Maslinic acid suppressed COX-2 expression in a concentration-dependent manner and inhibited more than 50 % COX-2 at 100 μM (Figure 4.22). In the time course study, COX-2 expression was inhibited by 8, 22, 45, and 55 % after 1, 2, 4, and 8 h treatment (Figure 4.23). Oleanolic acid showed similar suppressive effect as maslinic acid, with 57 % inhibition at the highest

concentration tested (100 μM). In comparison, ursolic acid which inhibited 61 % COX-2 expression at 25 μM has the strongest suppressive effect among the three triterpenoids. COX-2 expression is almost undetectable after 4 and 8 h treatment with 100 μM ursolic acid.

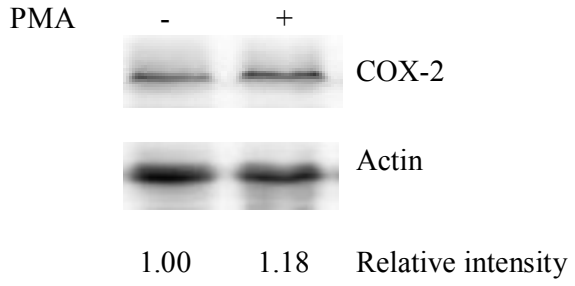

Figure 4.21: Basal and PMA-induced COX-2 expression in Raji cells. Cells were either treated with vehicle (ethanol) or 0.05 μM PMA for 8 h. Total cell lysates were analyzed for COX-2 expression by immunoblotting. COX-2 expressions were normalized to the corresponding beta-actin levels. The values shown represent the fold change relative to that of the non-induced Raji cells (-PMA). Each data represents average of three independent experiments.

The percentage change in protein expression is calculated by the following equation: (relative intensity of treated sample – 1.00) x 100 %

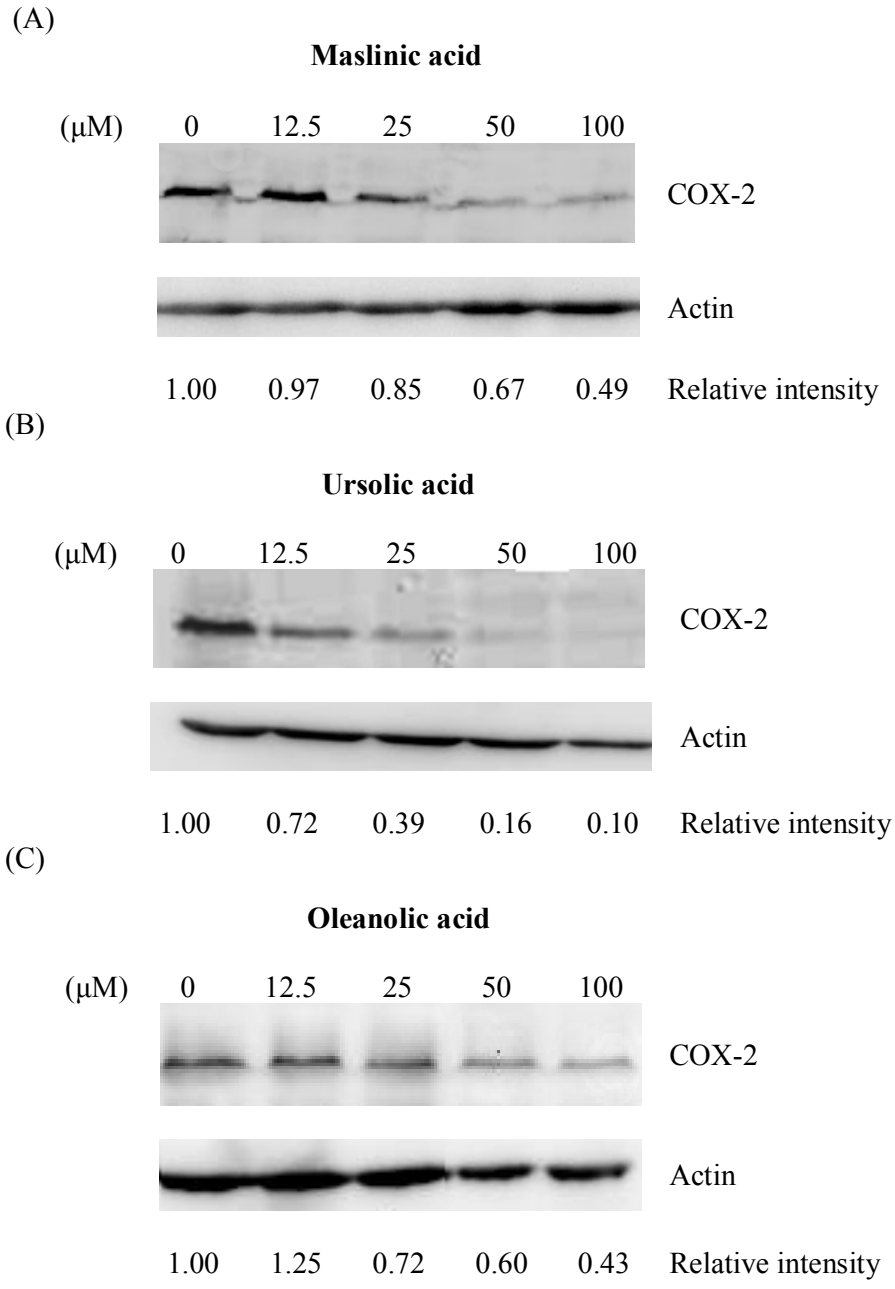

Figure 4.22: Concentration-dependent effects of (A) maslinic acid, (B) ursolic acid, and (C) oleanolic acid on COX-2 expression in Raji cells. Raji cells were treated with 12.5, 25, 50 and 100 μM of maslinic acid, oleanolic acid, and ursolic acid for 8 h. COX-2 expression were normalized to the corresponding beta-actin levels. The values shown represent fold change compared to that of the untreated cells (0 μM). Each data represents average of three independent experiments.

The percentage change in protein expression is calculated by the following equation: (relative intensity of treated sample – 1.00) x 100 %

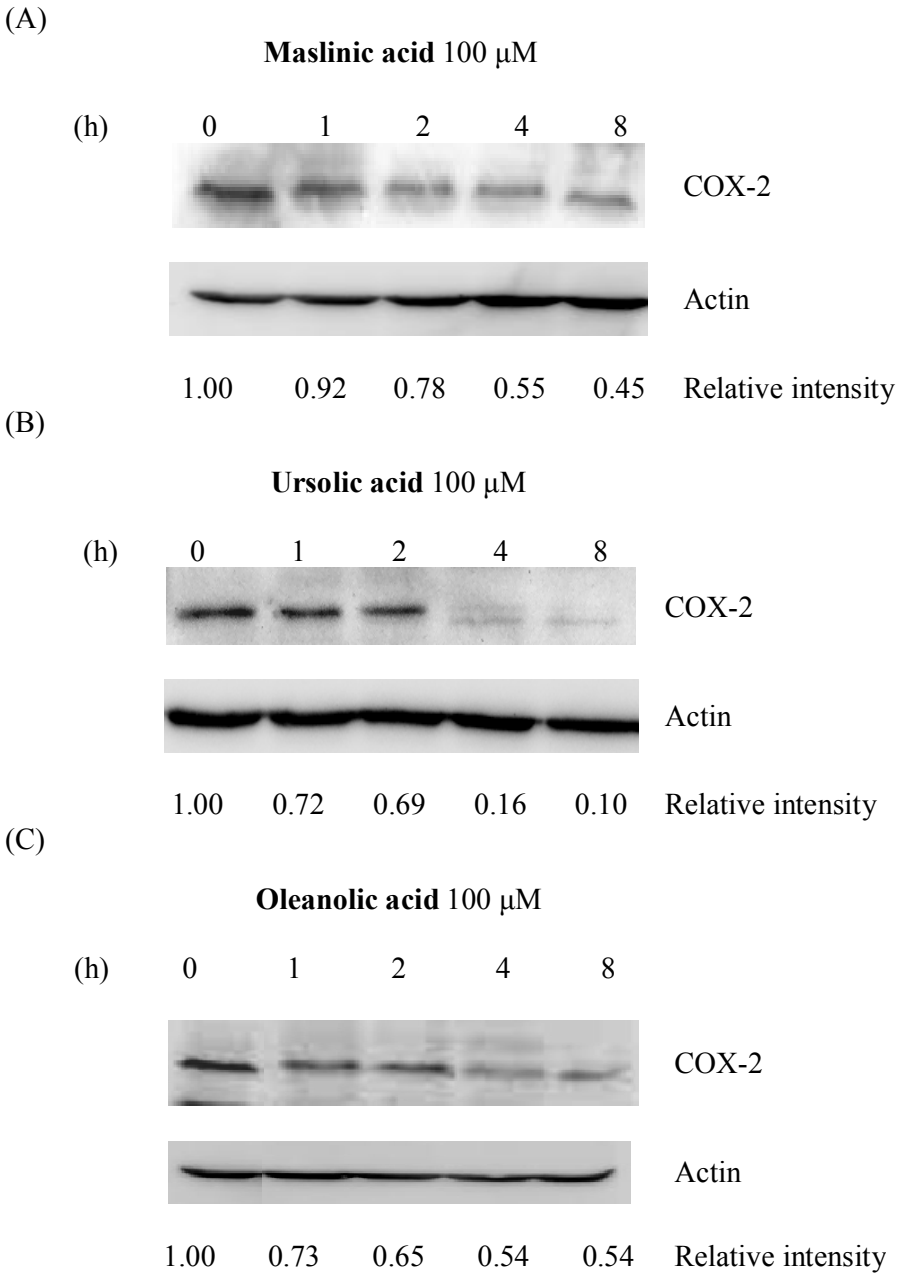

Figure 4.23: Time course inhibitory effects of (A) maslinic acid, (B) ursolic acid, and (C) oleanolic acid on COX-2 expression in Raji cells. The protein expression of COX-2 and β-actin were monitored after 1, 2, 4, and 8 h of treatment. COX-2 levels were normalized to the corresponding beta-actin levels. The values shown represent the fold change compared to untreated cells (0 h). Each data represents average of three independent experiments.

The percentage change in protein expression is calculated by the following equation: (relative intensity of treated sample – 1.00) x 100 %

4.6 Effects of maslinic acid on the Nrf2-ARE pathway in HepG2 cells

4.6.1 Induction of HO-1 gene and protein expression

Maslinic acid significantly enhanced HO-1 expression in a concentration-dependent manner and this expression reached a maximum response at 6 h treatment. As shown in Figure 4.24, HO-1 mRNA and protein expression were increased up to 2.5 fold and 92 % respectively, at the highest concentration tested (100 μM). HO-1 mRNA was up-regulated from 1.7 fold (1 h) to 3.3 fold after 6 h and remained induced at 2 fold expression after 12 h treatment (Figure 4.25). A similar effect of maslinic acid was observed at the protein level. Treatment with maslinic acid resulted in 46 % induction after 1 h, 48 % induction after 3 h, and 105 % induction after 6 h. Oleanolic acid also increased HO-1 expression in a concentration-dependent manner (Figure 4.26). Oleanolic acid induced HO-1 mRNA expression up to 2.64 fold at 100 μM. HO-1 mRNA was enhanced up to 2.9 fold at 6 h and the expression remained high at 2.67 fold after 12 h oleanolic acid treatment (Figure 4.27).

(A)

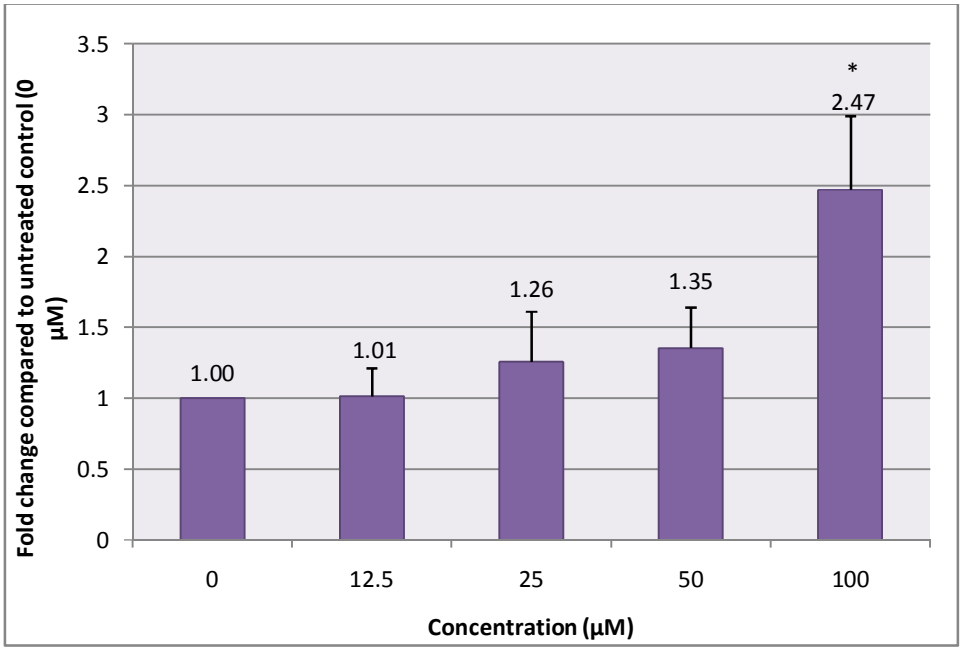

(B)

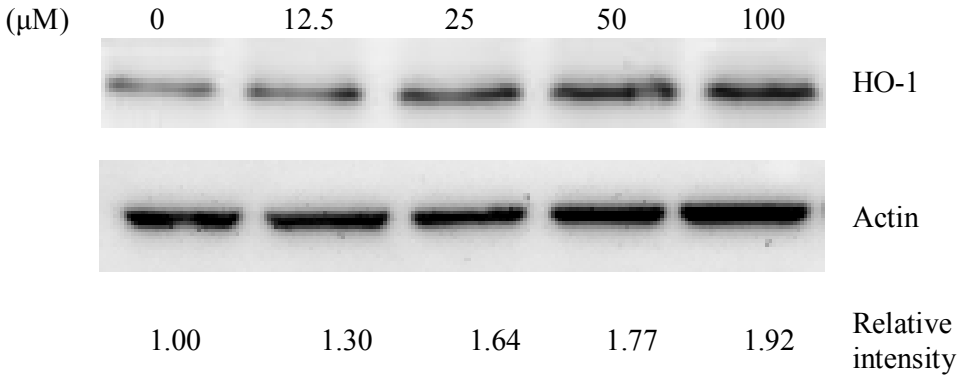

Figure 4.24: Concentration-dependent effects of maslinic acid on anti-oxidant enzyme HO-1 gene and protein expression. HepG2 cells were exposed to 12.5, 25, 50, and 100 µM of maslinic acid for 12 h and analyzed for HO-1 (A) mRNA expression by RT-PCR [Values represent mean ± SD of three separate experiments, each performed in triplicate. Asterisk (*) represents $p< 0.05$ when compared to the untreated control (0 µM)] and (B) protein expression by Western blotting [The HO-1 protein expression were normalized to beta actin followed by analysis of the relative intensity. The values shown are representative of fold change compared to untreated control (0 µM)].

(A)

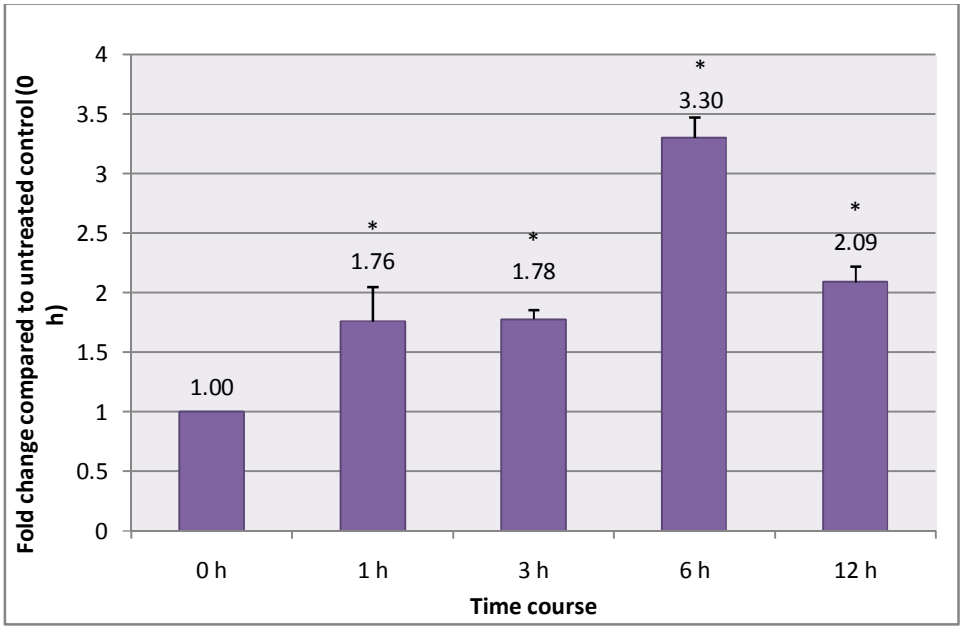

(B)

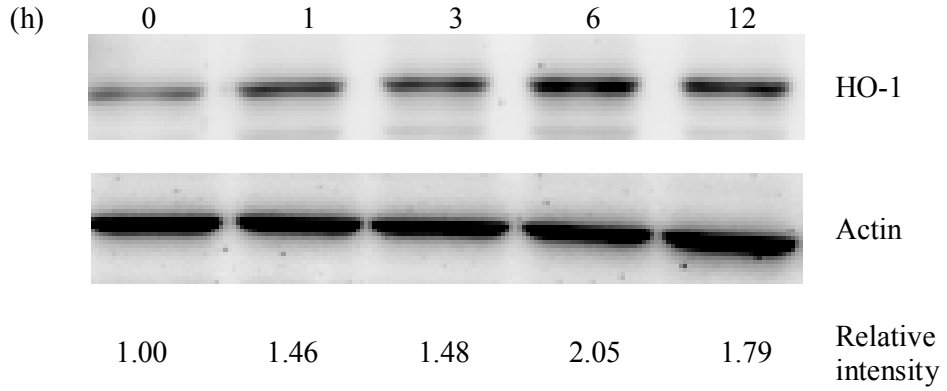

Figure 4.25: Time course effects of maslinic acid on anti-oxidant enzyme HO-1 gene and protein expression. HepG2 cells were exposed to 100 µM of maslinic acid for 1, 3, 6 and 12 h and analyzed for HO-1 (A) mRNA expression by RT-PCR [Values represent mean ± SD of three separate experiments, each performed in triplicate. Asterisk (*) represents $p< 0.05$ when compared to the untreated control (0 h)] and (B) protein expression by Western blotting [The HO-1 protein expression were normalized to beta actin followed by analysis of the relative intensity. The values shown are representative of fold change compared to untreated control (0 h)].

(A)

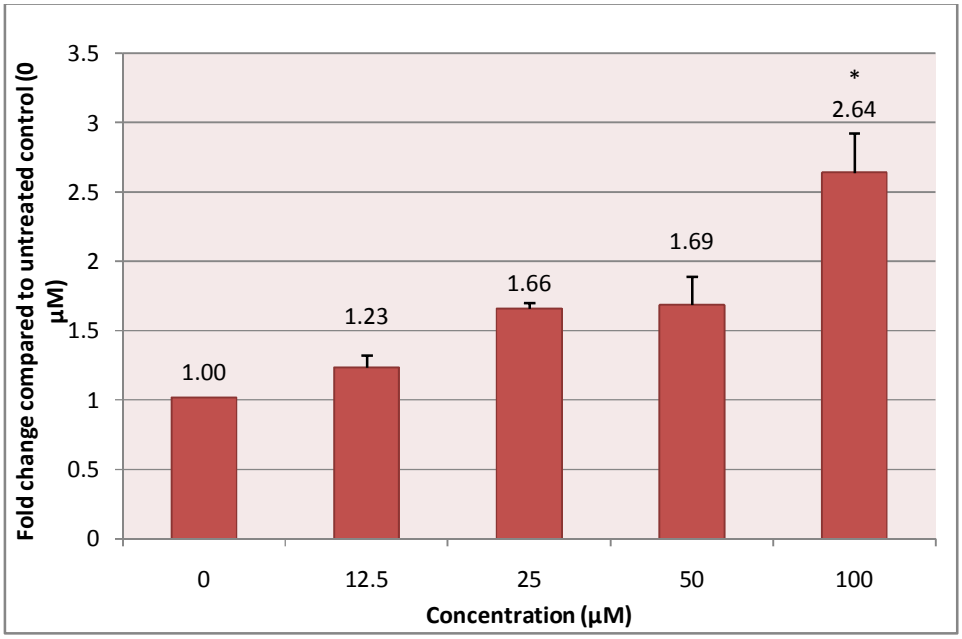

(B)

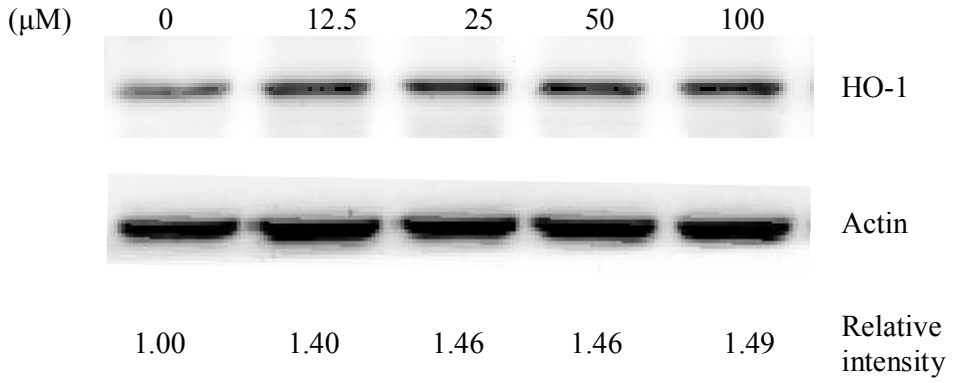

Figure 4.26: Concentration-dependent effects of oleanolic acid on anti-oxidant enzyme HO-1 gene and protein expression. HepG2 cells were exposed to 12.5, 25, 50, and 100 μM of oleanolic acid for 12 h and analyzed for HO-1 (A) mRNA expression by RT-PCR [Values represent mean ± SD of three separate experiments, each performed in triplicate. Asterisk (*) represents $p< 0.05$ when compared to the untreated control (0 μM)] and (B) protein expression by Western blotting [The HO-1 protein expression were normalized to beta actin followed by analysis of the relative intensity. The values shown are representative of fold change compared to untreated control (0 μM)].

(A)

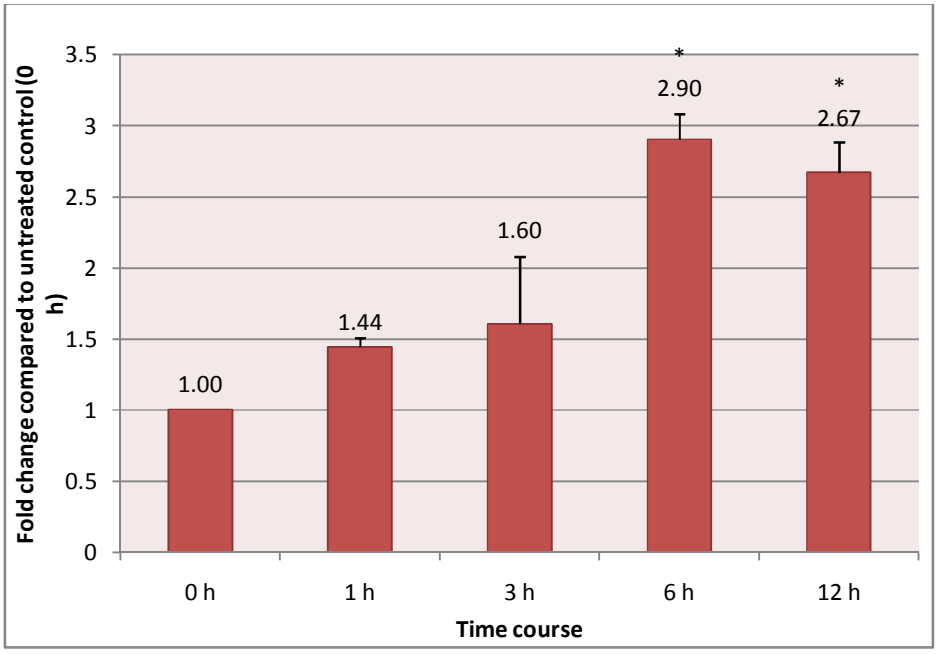

(B)

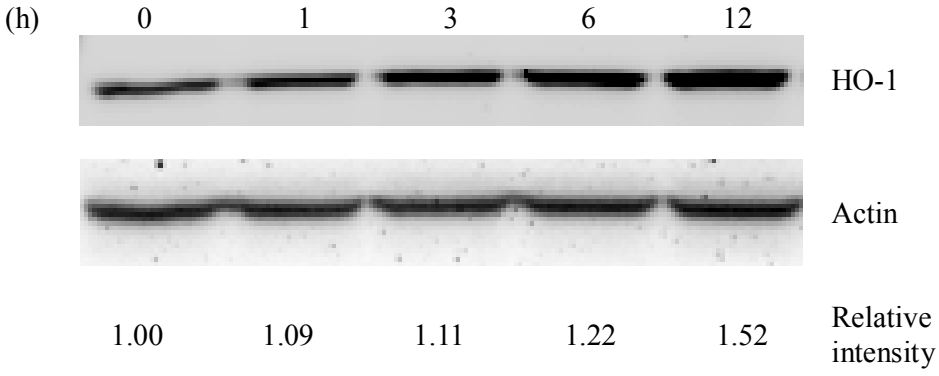

Figure 4.27: Time course effects of oleanolic acid on anti-oxidant enzyme HO-1 gene and protein expression. HepG2 cells were exposed to 100 µM of oleanolic acid for 1, 3, 6 and 12 h and analyzed for HO-1 (A) mRNA expression by RT-PCR [Values represent mean ± SD of three separate experiments, each performed in triplicate. Asterisk (*) represents $p< 0.05$ when compared to the untreated control (0 h)] and (B) protein expression by Western blotting [The HO-1 protein expression were normalized to beta actin followed by analysis of the relative intensity. The values shown are representative of fold change compared to untreated control (0 h)].

4.6.2 Induction of NQO1 gene and protein expression

Maslinic acid induced NQO1 expression in a concentration-dependent manner and the maximal expression was observed at 6 h. NQO1 gene expression levels were enhanced up to 1.60 and 1.58 fold when treated with 50 and 100 μM maslinic acid (Figure 4.28). The mRNA induction corresponded to the protein expression in which 85 and 78 % of NQO1 protein were induced upon treatment with 50 and 100 μM maslinic acid. The highest induction levels (4 fold mRNA and 85 % protein expression) were observed at 6 h after treatment in the time course study (Figure 4.29). By contrast, the effect of oleanolic acid was weaker (Figure 4.30). In time course study, the most abundant NQO1 gene and protein expression were 2.5 fold and 34 % (Figure 4.31) compared to the untreated control after 6 h of treatment.

(A)

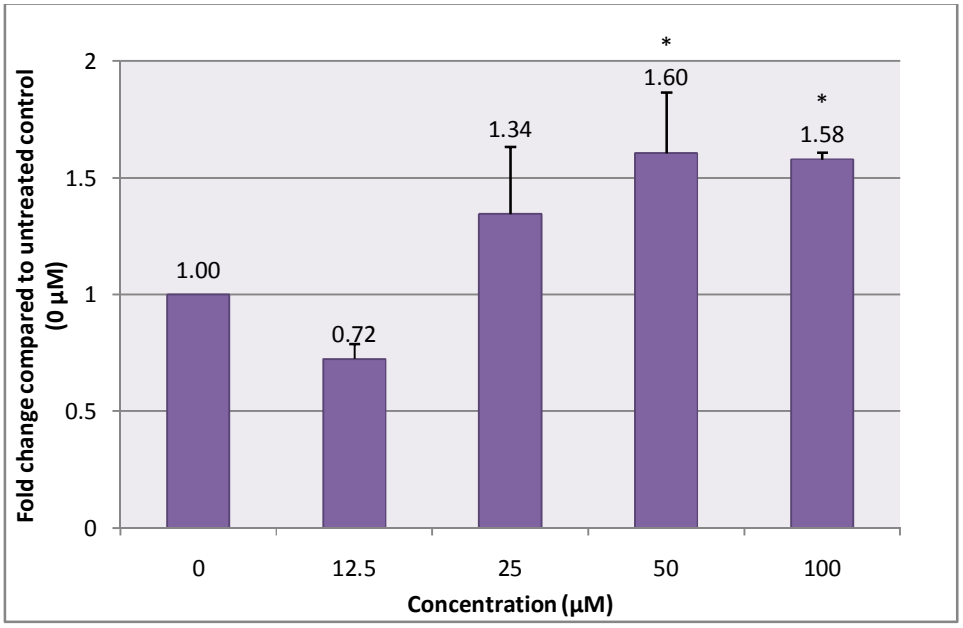

(B)

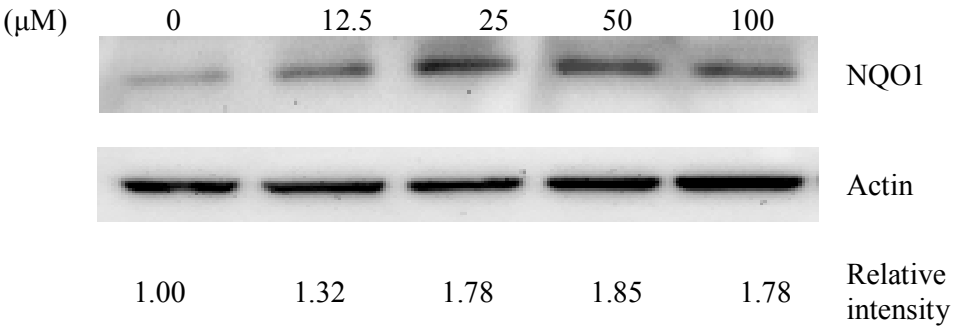

Figure 4.28: Concentration-dependent effects of maslinic acid on detoxifying enzyme NQO1 gene and protein expression. HepG2 cells were exposed to 12.5, 25, 50, and 100 µM of maslinic acid for 12 h and analyzed for NQO1 (A) mRNA expression by RT-PCR [Values represent mean ± SD of three separate experiments, each performed in triplicate. Asterisk (*) represents $p<$ 0.05 when compared to the untreated control (0 µM)] and (B) protein expression by Western blotting [The NQO1 protein expression were normalized to beta actin followed by analysis of the relative intensity. The values shown are representative of fold change compared to untreated control (0 µM)].

(A)

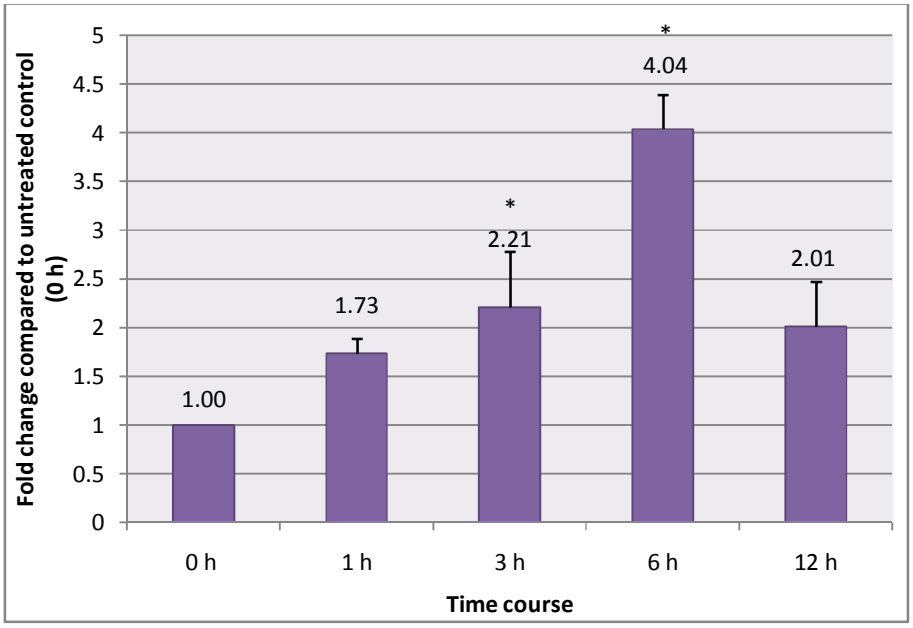

(B)

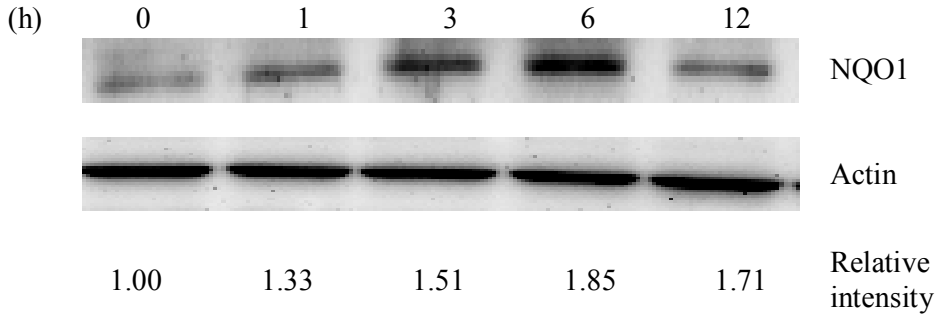

Figure 4.29: Time course effects of maslinic acid on detoxifying enzyme NQO1 gene and protein expression. HepG2 cells were exposed to 100 µM of maslinic acid for 1, 3, 6 and 12 h and analyzed for NQO1 (A) mRNA expression by RT-PCR [Values represent mean ± SD of three separate experiments, each performed in triplicate. Asterisk (*) represents $p< 0.05$ when compared to the untreated control (0 h)] and (B) protein expression by Western blotting [The NQO1 protein expression were normalized to beta actin followed by analysis of the relative intensity. The values shown are representative of fold change compared to untreated control (0 h)].

(A)

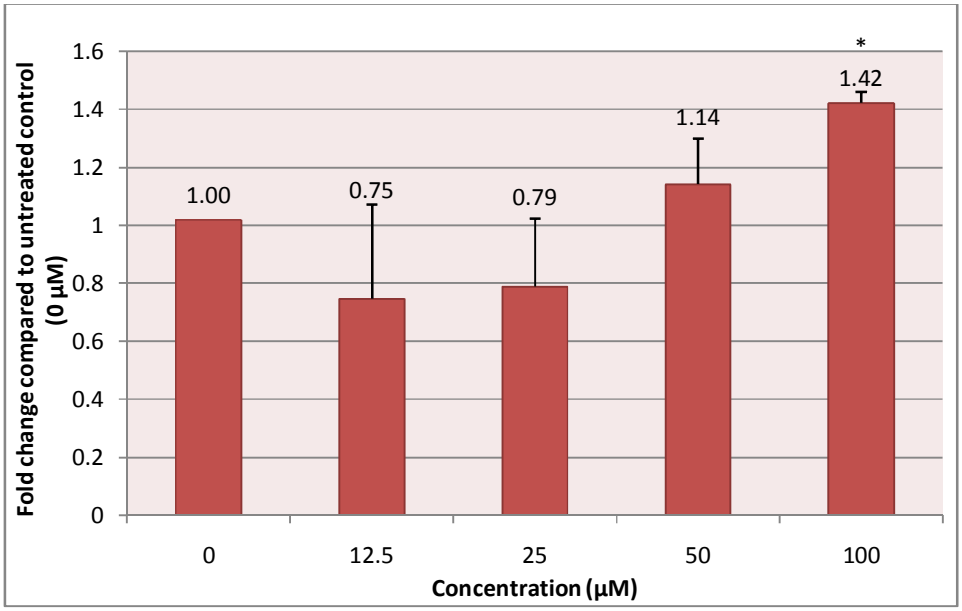

(B)

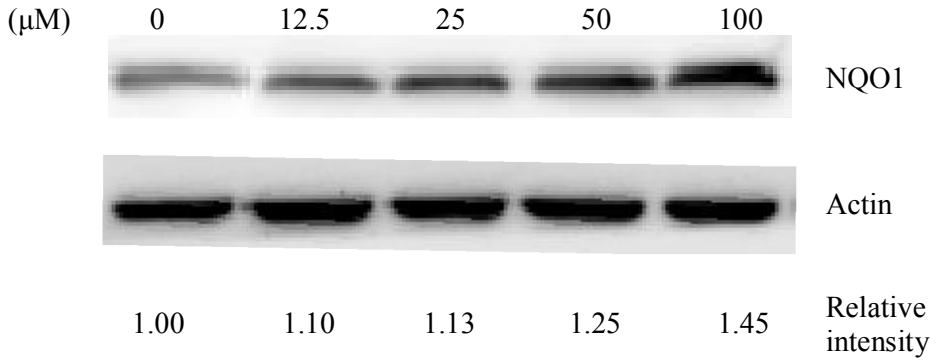

Figure 4.30: Concentration-dependent effects of oleanolic acid on detoxifying enzyme NQO1 gene and protein expression. HepG2 cells were exposed to 12.5, 25, 50, and 100 µM of oleanolic acid for 12 h and analyzed for NQO1 (A) mRNA expression by RT-PCR [Values represent mean ± SD of three separate experiments, each performed in triplicate. Asterisk (*) represents $p<$ 0.05 when compared to the untreated control (0 µM)] and (B) protein expression by Western blotting [The NQO1 protein expression were normalized to beta actin followed by analysis of the relative intensity. The values shown are representative of fold change compared to untreated control (0 µM)].

(A)

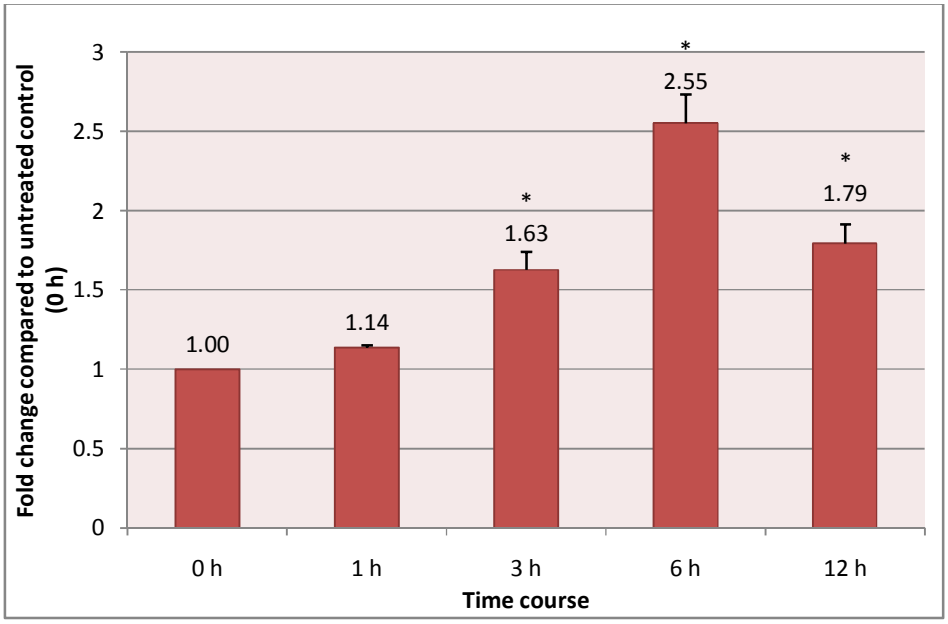

(B)

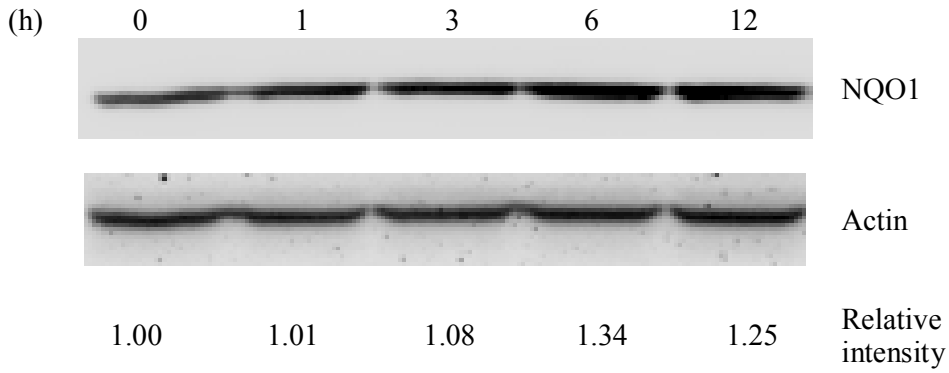

Figure 4.31: Time course effects of oleanolic acid on detoxifying enzyme NQO1 gene and protein expression. HepG2 cells were exposed to 100 µM of oleanolic acid for 1, 3, 6 and 12 h and analyzed for NQO1 (A) mRNA expression by RT-PCR [Values represent mean ± SD of three separate experiments, each performed in triplicate. Asterisk (*) represents $p< 0.05$ when compared to the untreated control (0 h)] and (B) protein expression by Western blotting [The NQO1 protein expression were normalized to beta actin followed by analysis of the relative intensity. The values shown are representative of fold change compared to untreated control (0 h)].

4.6.3 Anti-oxidant response element (ARE) binding activity

Most of the genes encoding phase II detoxifying and antioxidant enzymes have an ARE sequence in their promoter region. Whether maslinic acid could activate the ARE binding activity in association with the up-regulation of detoxifying and/or anti-oxidant enzymes was assessed by EMSA using an oligonucleotide harboring a consensus Nrf2-ARE binding element. Maslinic acid induced Nrf2-ARE binding activity in a concentration- and time-dependent manner. Increased Nrf2-ARE binding was observed at 25 μM, 50 μM, and 100 μM maslinic acid (Figure 4.32A). The Nrf2-ARE binding activity was observed after 3 h and remained elevated until 12 h (Figure 4.32B). The maximal Nrf2-ARE binding at 6 h coincided with the time course of HO-1 and NQO1 mRNA and protein accumulation.

The ARE binding is specific in which presence of 10-fold molar excess non-specific competitor (unlabeled NF-κB probe) did not affect binding but the binding was significantly reduced in presence of 10-fold excess of specific competitor (unlabeled ARE probe). As shown in Figure 4.33, no binding was observed in the first and second lanes which contained only the ARE probe and ARE probe with untreated cell lysates, respectively. In the third lane, significant binding was observed in the reaction of maslinic acid-treated cell lysates together with ARE probe, indicating that ARE binding was induced upon maslinic acid treatment but not in untreated cells. In order to determine whether the ARE binding induced is specific, a 10-fold molar excess of non-specific competitor (unlabeled NF-κB probe) and specific competitor (unlabeled ARE probe) were added. The unlabeled NF-κB probe which was

used as the non-specific competitor did not affect the maslinic acid-induced ARE binding (forth lane). By contrast, addition of specific competitor (unlabeled ARE probe) which has the same sequence as the ARE probe but lack of biotin labels competes for protein binding, therefore reducing the binding in the fifth lane.

Oleanolic acid also induced the ARE binding in a concentration- and time-dependent manner. However, the binding activity induced by oleanolic acid occurred later compared to maslinic acid, from 6 to 12 h (Figure 4.34). The observed binding activity was consistent with the time of oleanolic acid-induced HO-1 and NQO1 expression.

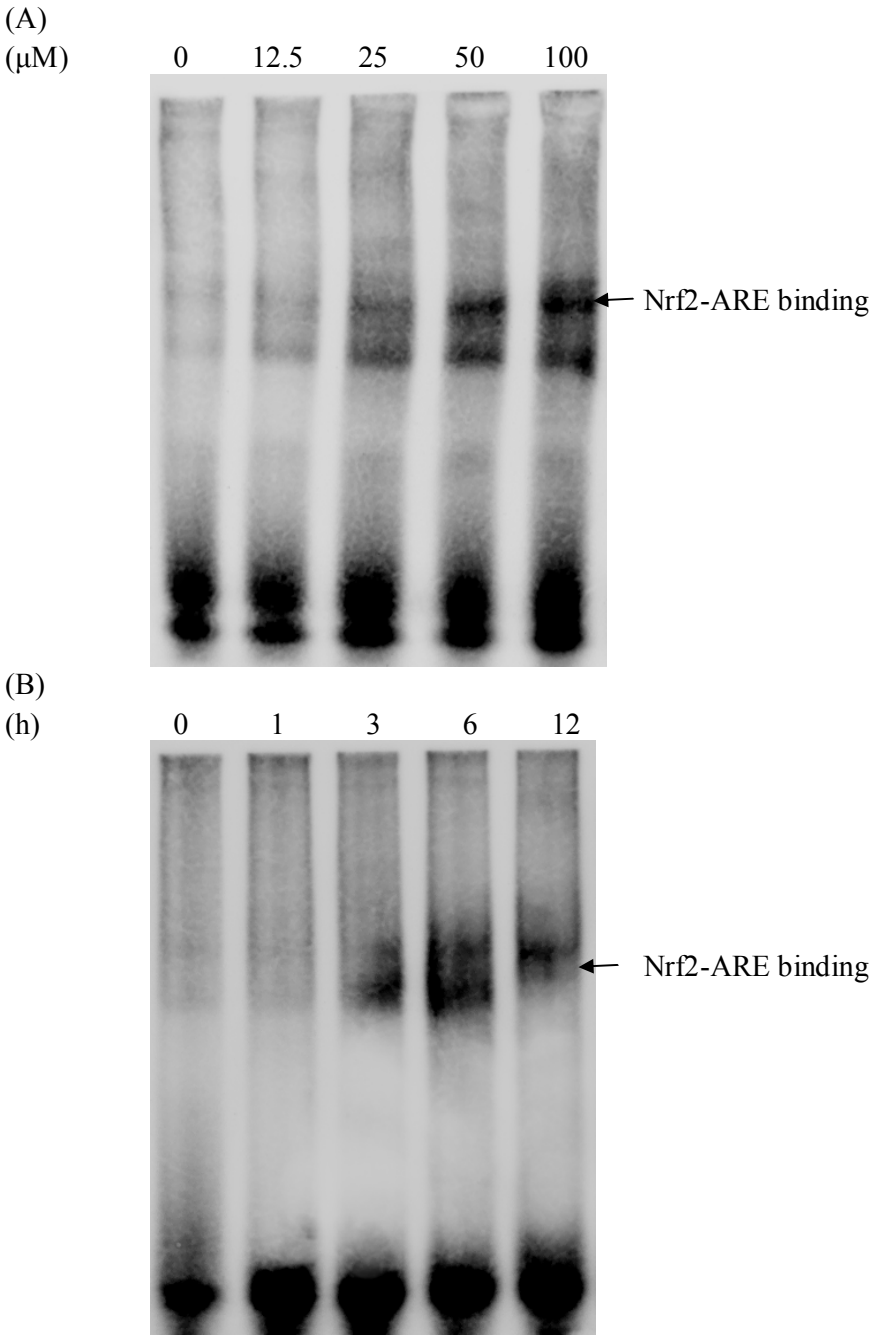

Figure 4.32: Effects of maslinic acid on the Nrf2-ARE-binding activity in HepG2 cells. HepG2 cells were treated with (A) increasing concentrations (12.5, 25, 50, and 100 μM) of maslinic acid for 12 h and at 100 μM for 1, 3, 6, and 12 h in the time course study. The nuclear extracts were prepared and analyzed for ARE binding activity using LightShift Chemiluminescent EMSA assay. Data presented are representative of three independent experiments showing similar trends.

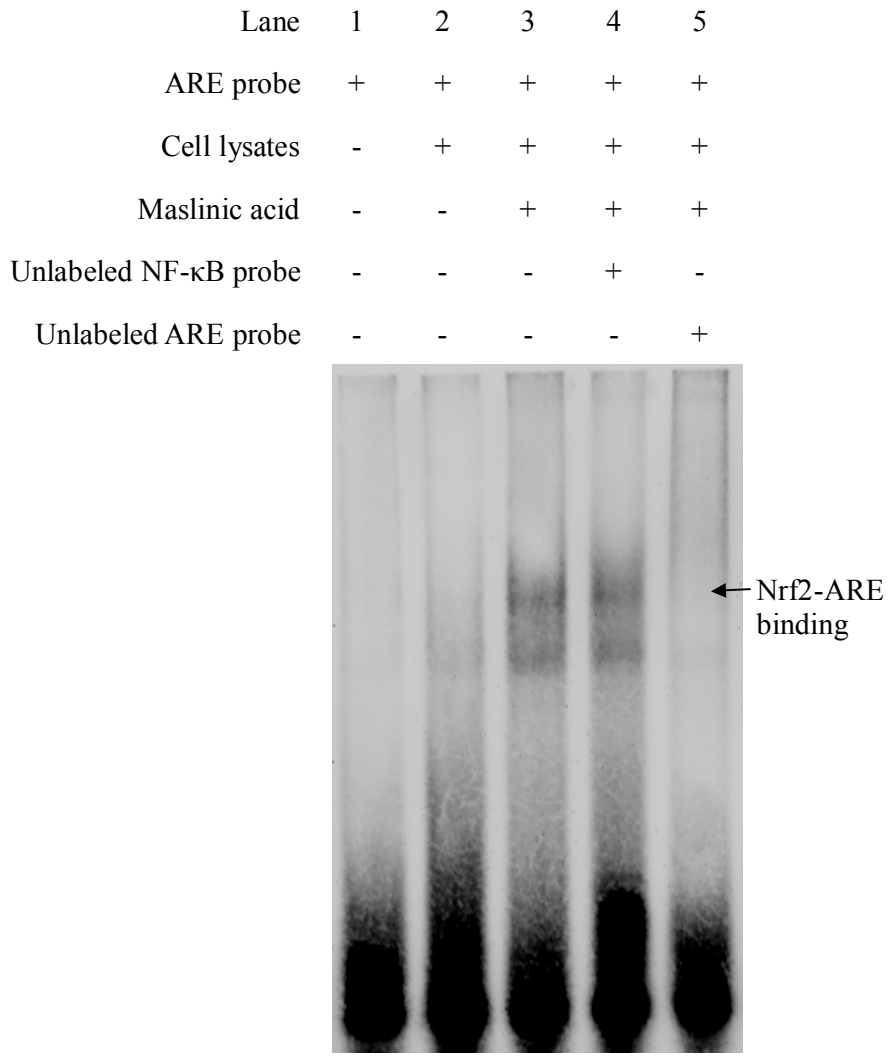

Figure 4.33: Specificity of Nrf2-ARE binding activity in HepG2 cells. ARE binding was induced by treatment with 100 μM of maslinic acid. Ten fold molar excess of unlabeled NF-κB probe and unlabeled ARE probe were added in the competition reactions to establish the specificity of ARE binding. The data presented is representative of three independent experiments showing similar trends.

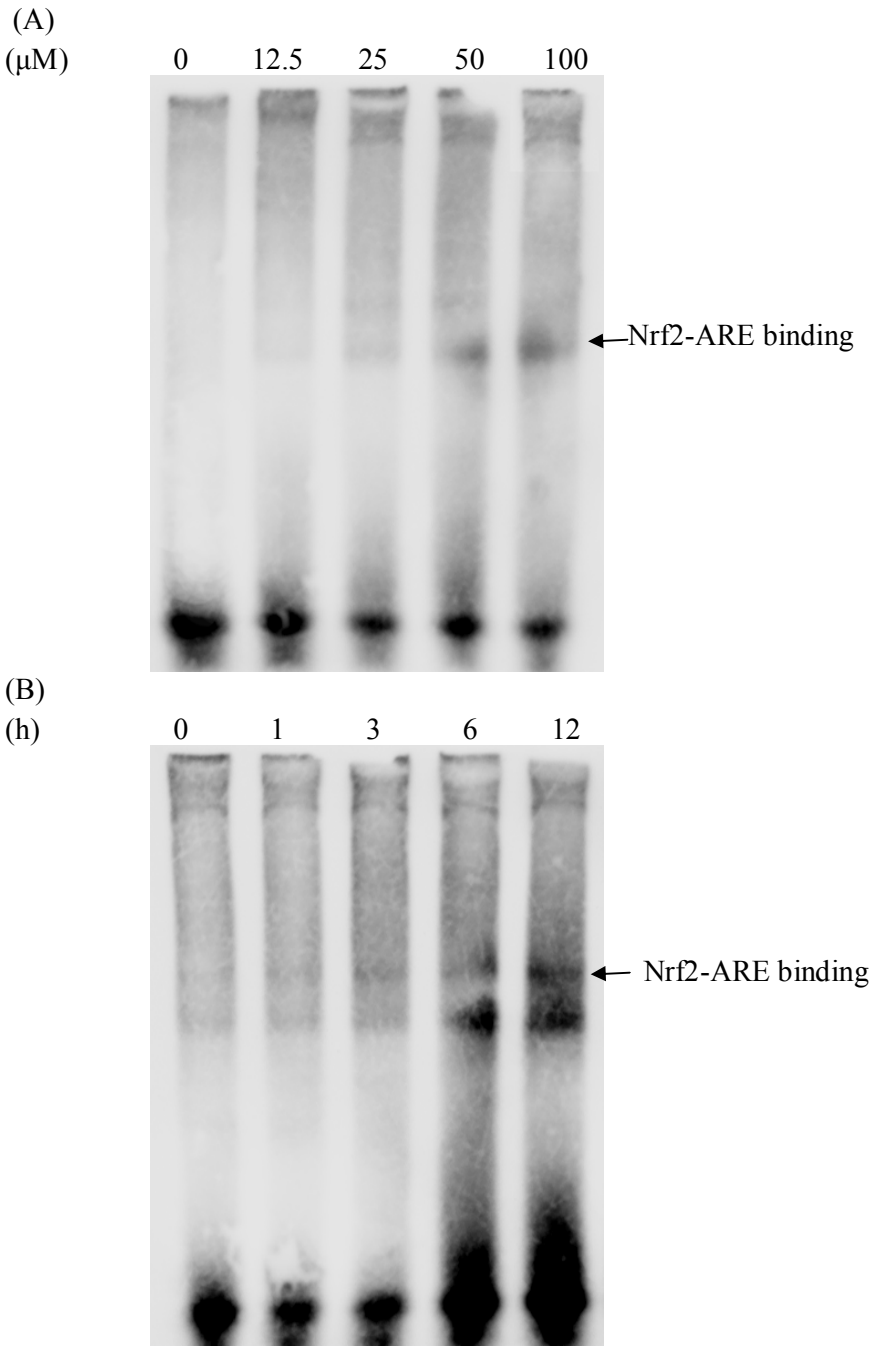

Figure 4.34: Effects of oleanolic acid on the Nrf2-ARE-binding activity in HepG2 cells. HepG2 cells were treated with (A) increasing concentrations (12.5, 25, 50, and 100 μM) of oleanolic acid for 12 h and at 100 μM for 1, 3, 6, and 12 h in the time course study. The nuclear extracts were prepared and analyzed for ARE binding activity using LightShift Chemiluminescent EMSA assay. The data presented are representative of three independent experiments showing similar trends.

4.6.4 Steady state levels of Nrf2 and Keap1 in the nucleus and cytoplasm

Maslinic acid-induced Nrf2-ARE binding may be linked to the regulation of Nrf2-Keap1 levels. The effect of maslinic acid on the steady-state level of endogenous Nrf2 and Keap1 were analyzed. The results showed that maslinic acid significantly enhanced nuclear Nrf2 accumulation at 100 μM (Figure 4.35) and this effect started as early as 3 h treatment (Figure 4.36B). The nuclear Nrf2 accumulation at 3 h might be caused by an increased pool of stabilized cytoplasmic Nrf2 at the same time point. Cytoplasmic Nrf2 protein increased significantly (76 %) after 3 h treatment (Figure 4.36A) and this expression was enhanced up to 12 h. The stabilized cytoplasmic Nrf2 might enter the nucleus, which account for the maximal nuclear Nrf2 expression (172 %) observed at 3 h treatment (Figure 4.36B). Keap1 expression was reduced by 30 % at 3 h when Nrf2 was enhanced but its expression was restored at 6 and 12 h.

Oleanolic acid-induced nuclear translocation of Nrf2 occurred in a similar manner but more slowly. Accumulation of nuclear Nrf2 was most significant (139 %) after treatment with 100 μM oleanolic acid (Figure 4.37). The cytoplasmic Nrf2 increased in a time-dependent manner and its expression was enhanced up to 124 % at 12 h (Figure 4.38A), which might contribute to the highest induction of nuclear Nrf2 at the same time point (Figure 4.38B). The Keap1 levels were not significantly altered.

There were two discrete Nrf2 protein bands in the cytoplasm which differs from the single Nrf2 band observed in the nucleus. A control experiment was

performed by separating the total, cytoplasmic and nuclear HepG2 lysates in the same SDS-PAGE gel (Figure 4.39). The upper Nrf2 band from the total and cytoplasmic cell lysates were in line with the nuclear Nrf2 protein and that both cytoplasmic and nuclear Nrf2 significantly increased with time after treatment with maslinic acid. The upper band may be the Nrf2 protein while the lower one is a non-specific band. Similar observations of single and double Nrf2 bands in the cytoplasm and nucleus were reported in other studies using the same source of goat polyclonal Nrf2 antibodies from Santa Cruz Biotechnology (Chen *et al*., 2004; Haridas *et al*., 2004; Li *et al*., 2005; Tanigawa *et al*., 2007; Chia *et al*., 2010). This may be a result of the nature of polyclonal antibodies which cause low level of cross-reactivity or the proteolysis of the target protein.

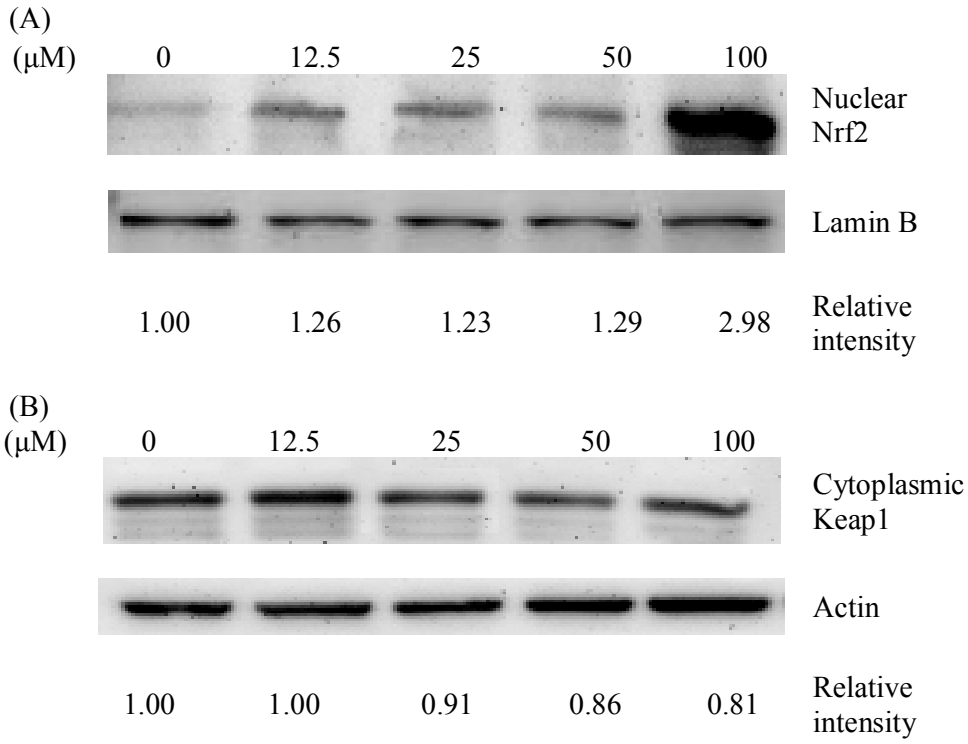

Figure 4.35: Concentration-dependent effects of maslinic acid on the steady-state levels of Nrf2 and Keap1. HepG2 cells were treated with 12.5, 25, 50, and 100 μM of maslinic acid for 12 h. The cell lysates obtained were fractionated into cytoplasmic and nuclear fractions. Each fraction was subjected to SDS-PAGE separation and Western blotting analysis. The (A) nuclear Nrf2 and lamin B levels as well as the (B) cytoplasmic Keap1 and beta actin expressions were detected with their respective antibodies. The nuclear Nrf2 expression was normalized to lamin b while the cytoplasmic Keap1 levels are normalized to beta actin. The values shown were representative of fold change compared to untreated control (0 μM).

The percentage change in protein expression is calculated by the following equation: (Relative intensity of treated sample – 1.00) x 100 %

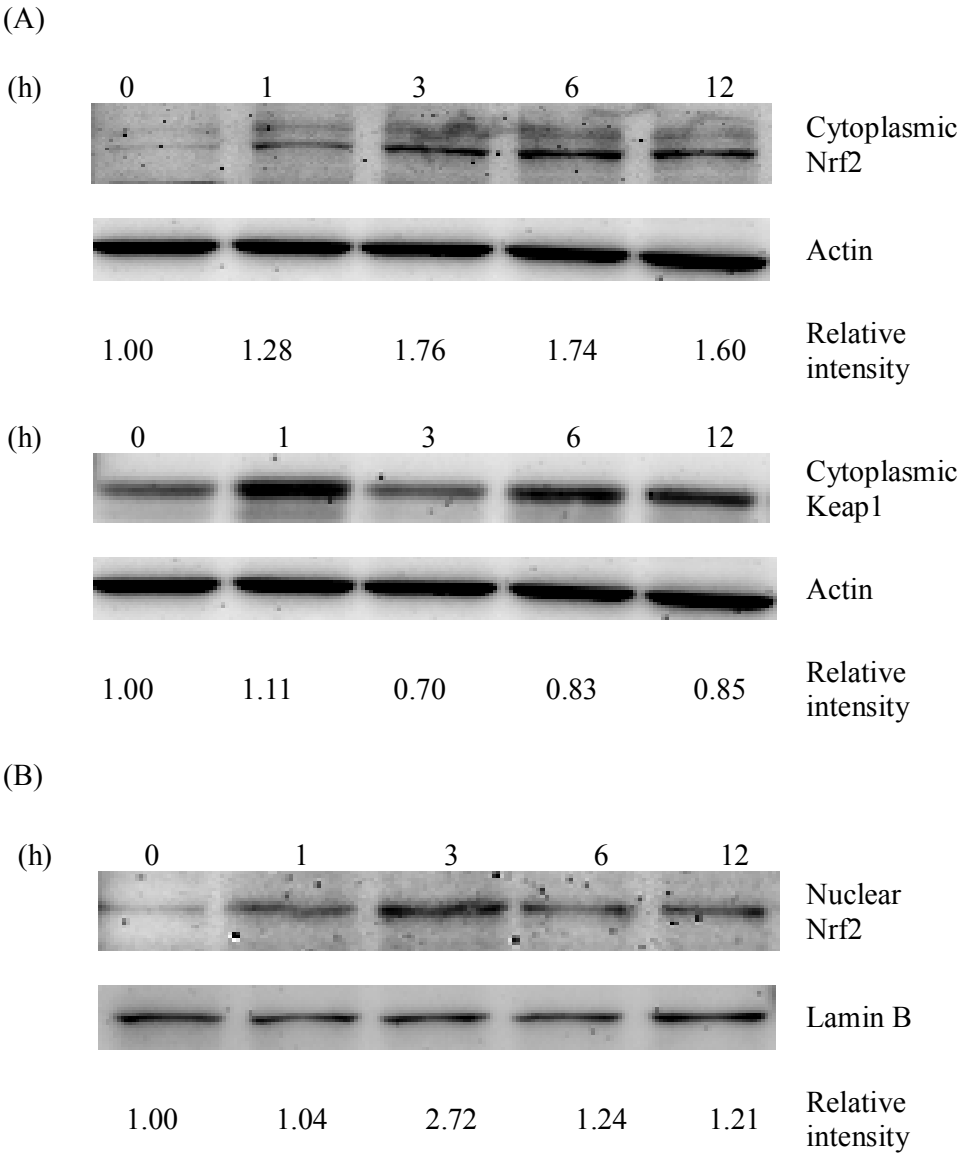

Figure 4.36: Time course effects of maslinic acid on the steady-state levels of Nrf2 and Keap1. HepG2 cells were treated with 100 μM of maslinic acid for 1, 3, 6, and 12 h. The cell lysates obtained were fractionated into cytoplasmic and nuclear fractions. Each fraction was subjected to SDS-PAGE separation and Western blotting analysis. The (A) cytoplasmic Nrf2, Keap1, and beta actin expressions as well as the (B) nuclear Nrf2 and lamin B levels were detected with their respective antibodies. The nuclear Nrf2 was normalized to lamin b while the cytoplasmic Nrf2 and Keap1 were normalized to beta actin. The values shown are representative of fold change compared to untreated control (0 h).

The percentage change in protein expression is calculated by the following equation: (Relative intensity of treated sample – 1.00) x 100 %

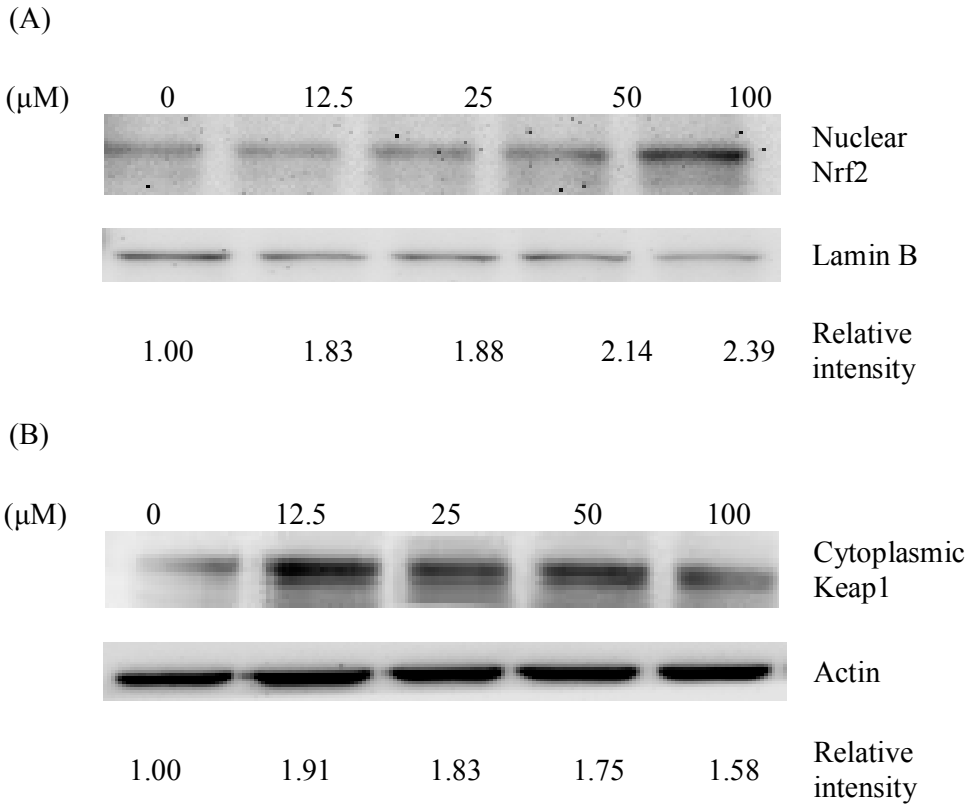

Figure 4.37: Concentration-dependent effects of oleanolic acid on the steady-state levels of Nrf2 and Keap1. HepG2 cells were treated with 12.5, 25, 50, and 100 μM of oleanolic acid for 12 h. The cell lysates obtained were fractionated into cytoplasmic and nuclear fractions. Each fraction was subjected to SDS-PAGE separation and Western blotting analysis. The (A) nuclear Nrf2 and lamin B levels as well as the (B) cytoplasmic Keap1 and beta actin expressions were detected with their respective antibodies. The nuclear Nrf2 expression was normalized to lamin b while the cytoplasmic Keap1 levels were normalized to beta actin. The values shown are representative of fold change compared to untreated control (0 μM).

The percentage change in protein expression is calculated by the following equation: (Relative intensity of treated sample – 1.00) x 100 %

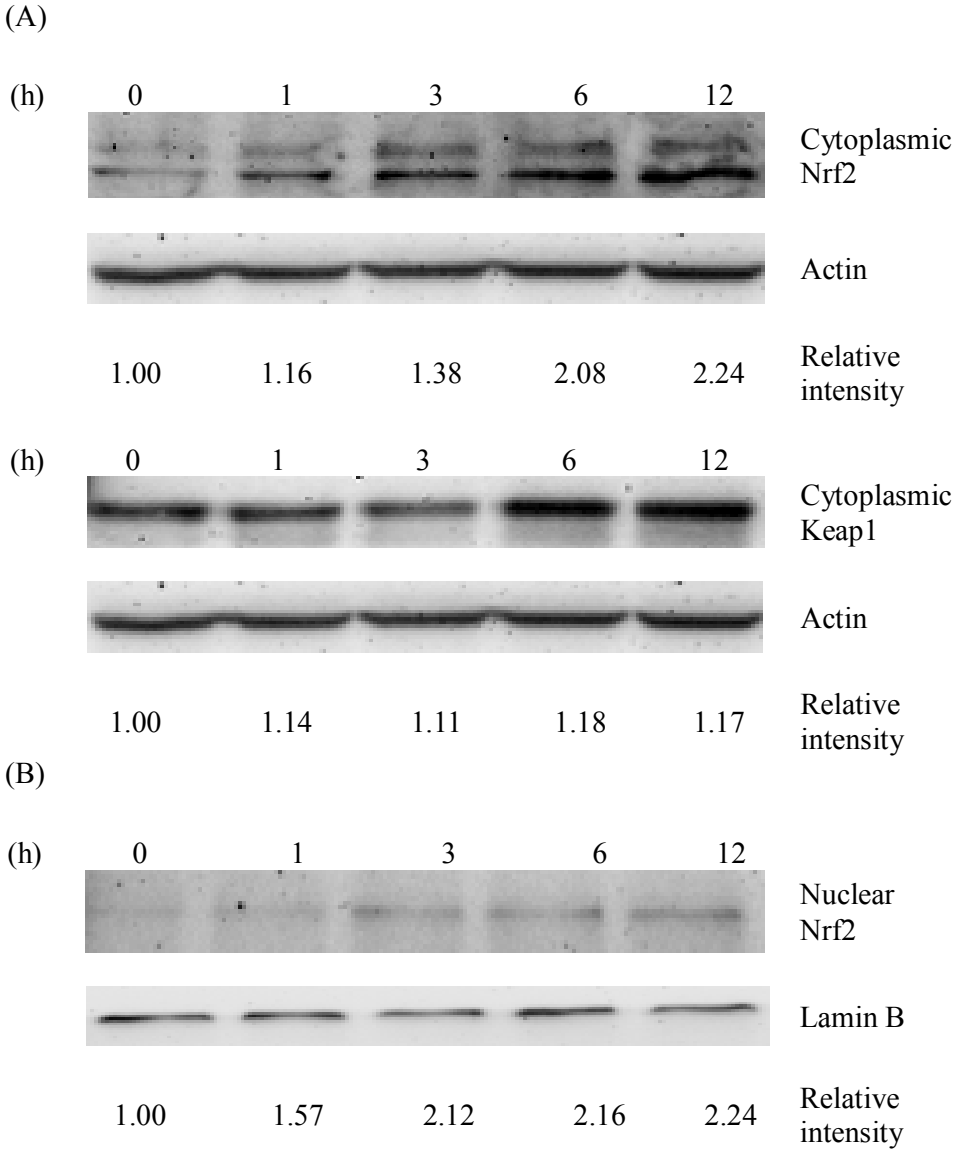

Figure 4.38: Time course effects of oleanolic acid on the steady-state levels of Nrf2 and Keap1. HepG2 cells were treated with 100 μM of oleanolic acid for 1, 3, 6, and 12 h. The cell lysates obtained were fractionated into cytoplasmic and nuclear fractions. Each fraction was subjected to SDS-PAGE separation and Western blotting analysis. The (A) cytoplasmic Nrf2, Keap1, and beta actin expressions as well as the (B) nuclear Nrf2 and lamin B levels were detected with their respective antibodies. The nuclear Nrf2 was normalized to lamin b while the cytoplasmic Nrf2 and Keap1 levels were normalized to beta actin. The values shown are representative of fold change compared to untreated control (0 h).

The percentage change in protein expression is calculated by the following equation: (Relative intensity of treated sample – 1.00) x 100 %

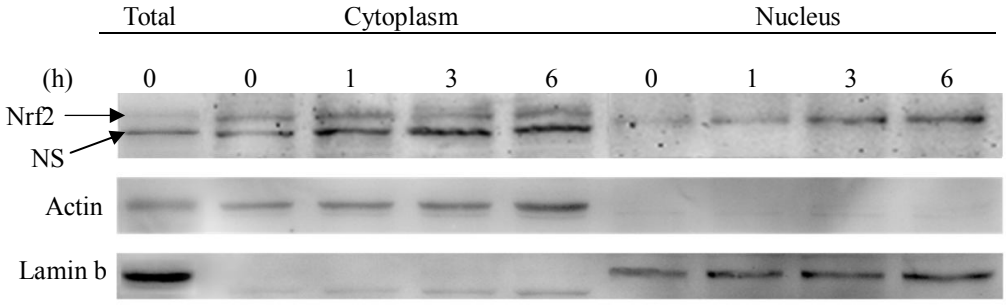

Figure 4.39: Nrf2 expression from total, cytoplasmic and nuclear lysates of HepG2 cells in response to treatment with maslinic acid for 1, 3, and 6 h. Nrf2, beta actin and lamin b expression levels were detected by Western blotting analysis with their respective antibodies.

4.6.5 Requirement of Nrf2 for the induction of HO-1 and NQO1 expression

The role of Nrf2 in maslinic acid-induced HO-1 and NQO1 expression was determined through siRNA silencing studies. A preliminary experiment was first carried out to determine the Nrf2 knockdown efficiency of Nrf2-siRNA. Four Nrf2-siRNAs including Nrf2-siRNA-1, Nrf2-siRNA-2, Nrf2-siRNA-3, and Nrf2-siRNA-4 were tested for their efficiency at knocking down Nrf2 expression. Among the four tested Nrf2-siRNAs, Nrf2-siRNA-1 significantly reduced Nrf2 expression (Figure 4.40) and was selected for further studies.

The Nrf2 mRNA and protein expression in cells transfected with a non-silencing control siRNA (Con-siRNA) is approximately twice that of non-transfected cells (Figure 4.40). This might be explained by the fact that Nrf2 is constitutively ubiquitinated and degraded under non-stimulated conditions such that its overall concentration is maintained at a low level (Nguyen *et al*., 2003). Upon introduction of Con-siRNA, exposure of cells to transfection reagent and siRNA might induce stress response and resulted in the increased Nrf2 expression. In fact, Nrf2 is a stress responsive protein. Transient transfection of cells with the four Nrf2-siRNA reduced Nrf2 mRNA by 66, 58, 57, and 56 %, respectively compared to cells transfected with Con-siRNA. Among the four tested Nrf2-siRNAs, Nrf2-siRNA-1 induced marked reduction of Nrf2 mRNA by 66 % and inhibited protein expression by 77 % relative to cells transfected with Con-siRNA and was therefore selected for further studies.

After 48 h, the non-transfected cells, cells transfected with Con-siRNA as well as cells transfected with Nrf2-siRNA-1 were treated with 100 μM maslinic acid for additional 8 h before the expression of Nrf2, NQO1 and HO-1 were determined. The results showed that maslinic acid significantly induced Nrf2, NQO1, and HO-1 expression in non-transfected HepG2 cells and cells transfected with Con-siRNA, but this effect was abrogated in cells transfected with Nrf2-siRNA (Nrf2 knockdown cells). As shown in Figure 4.41A, maslinic acid significantly increased Nrf2, NQO1 and HO-1 mRNA by 85, 66, and 47 %, respectively, in non-transfected cells. Similarly, the Nrf2, NQO1 and HO-1 mRNA levels were enhanced by 79, 61, and 61 %, respectively, upon maslinic acid treatment in Con-siRNA cells. The up-regulation of Nrf2, NQO1 and HO-1 mRNA levels by maslinic acid in non-transfected cells and Con-siRNA transfected cells were accompanied by a concomitant increase in protein expression (Figure 4.41B), indicating that maslinic acid induces transcription of these genes.

Upon transfection with Nrf2-siRNA-1, the mRNA expression of Nrf2, NQO1, and HO-1 were only increased by 4, 14, and 13 %, respectively. Similarly, induction of Nrf2, NQO1, and HO-1 protein expression by maslinic acid was abrogated in cells transfected with Nrf2-siRNA-1. This supports the hypothesis that maslinic acid-induced expression of NQO1 and HO-1 were mediated by activation of Nrf2.

(A)

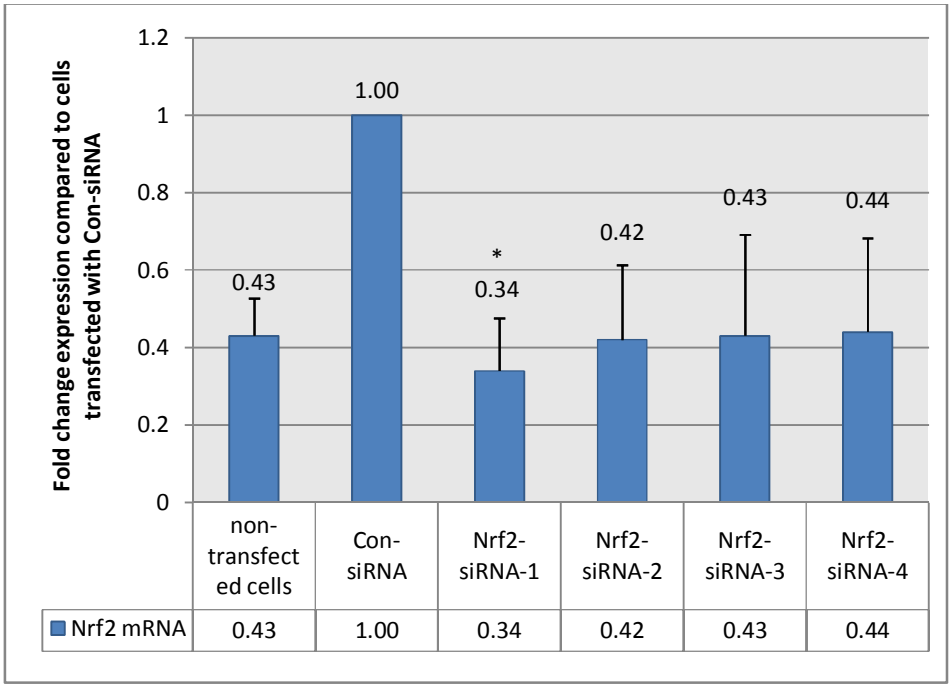

(B)

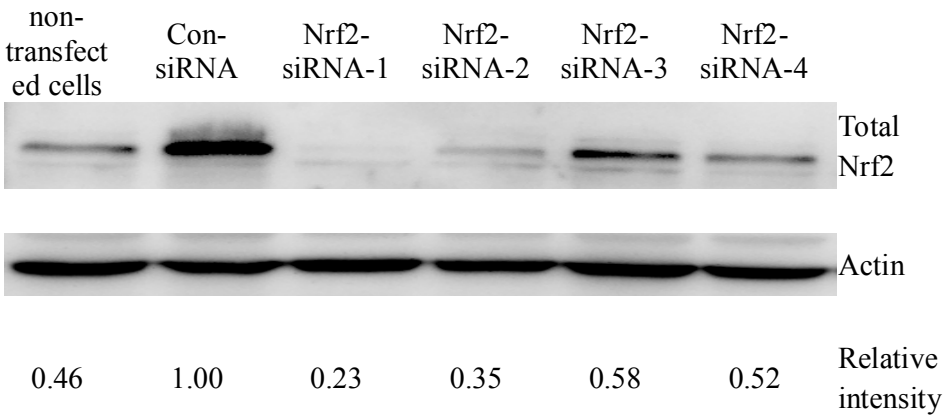

Figure 4.40: Effects of Nrf2-siRNAs on Nrf2 gene and protein expression in HepG2 cells. The Nrf2 expression of non-transfected HepG2 cells, cells transfected with Con-siRNA as well as cells transfected with each of the four different siRNAs targeting Nrf2 were investigated at the (A) mRNA and (B) protein level using real time RT-PCR and Western blotting method. Asterisk (*) represents $p< 0.05$ when compared to the cells transfected with non-silencing siRNA (Con-siRNA). Total Nrf2 protein levels were normalized to actin and the values shown were representative of fold change compared to cells transfected with Con-siRNA.

The percentage change in mRNA and protein expression is calculated by the following equation: (Relative intensity of treated sample – 1.00) x 100 %

(A)

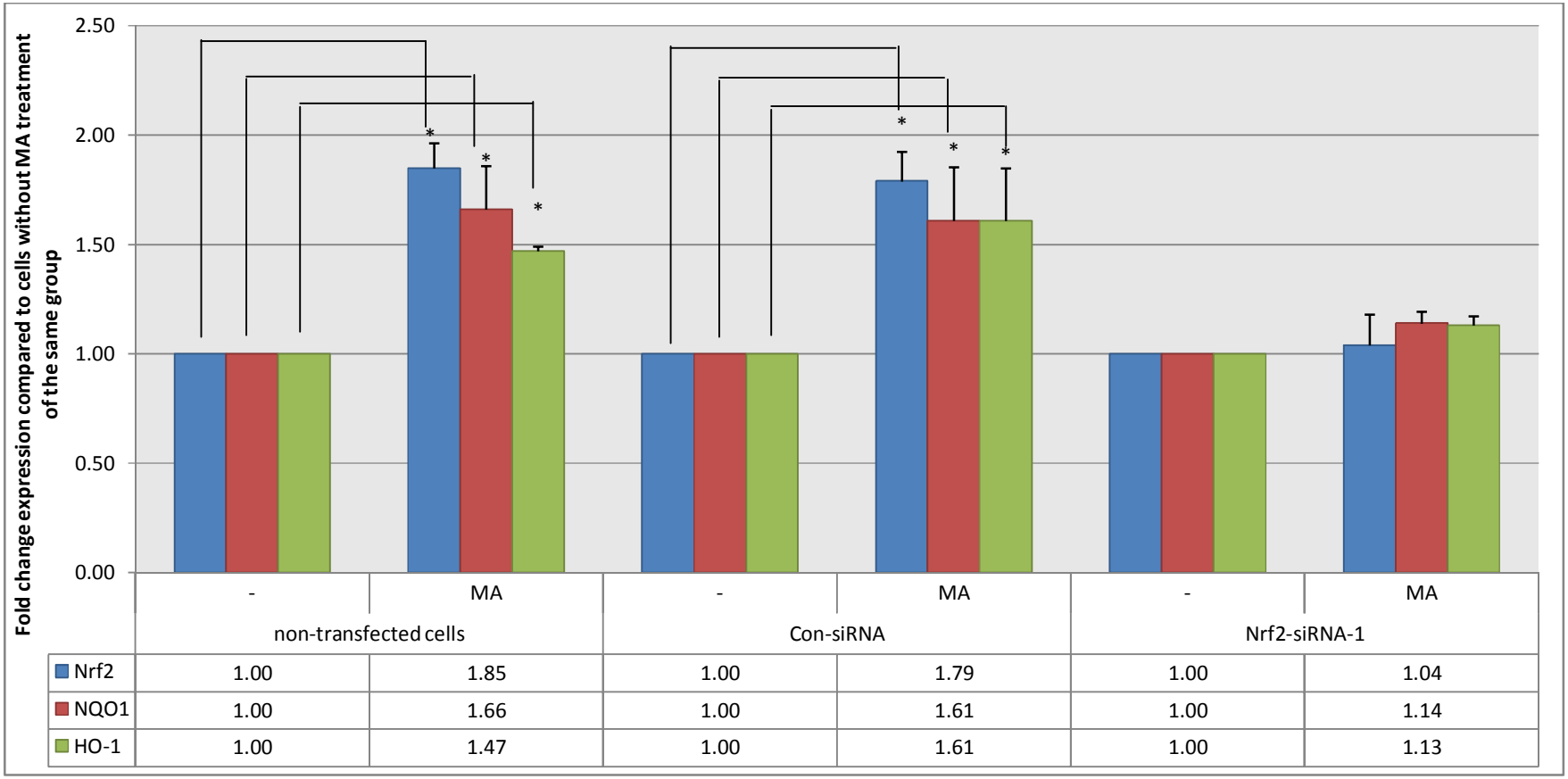

	non-transfected cells		Con-siRNA		Nrf2-siRNA-1	
	-	MA	-	MA	-	MA
Nrf2	1.00	1.85	1.00	1.79	1.00	1.04
NQO1	1.00	1.66	1.00	1.61	1.00	1.14
HO-1	1.00	1.47	1.00	1.61	1.00	1.13

(B)

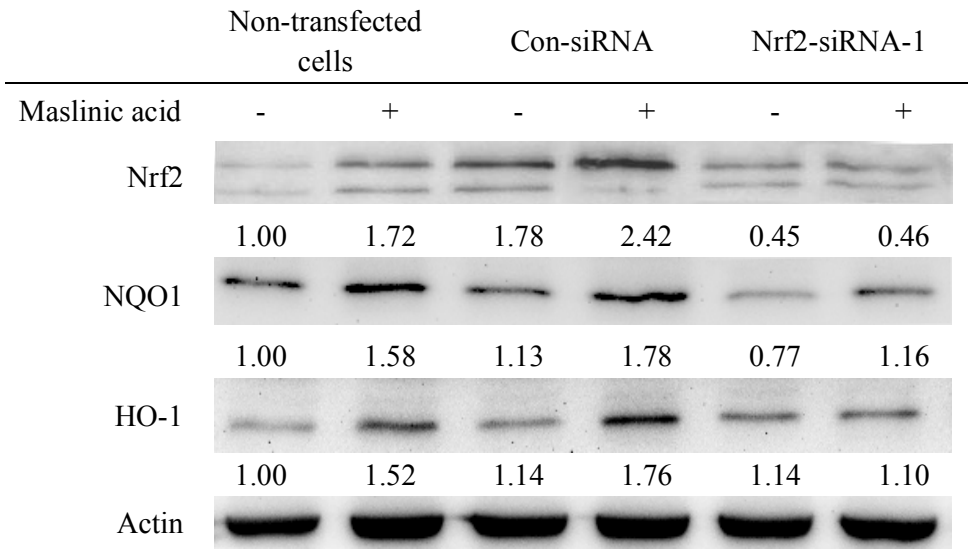

Figure 4.41: Effects of maslinic acid treatment at inducing Nrf2, NQO1 and HO-1 expression in non-transfected cells, cells transfected with control siRNA (Con-siRNA) and cells transfected with Nrf2-siRNA (Nrf2-siRNA-1). After 48 h transfection, HepG2 cells were treated with 100 µM maslinic acid (MA) for additional 8 h before the expression of Nrf2, HO-1 and NQO1 were determined at the (A) mRNA and (B) protein level by real time RT-PCR and Western blotting method. The mRNA expression levels were normalized against cells without maslinic acid treatment of the same group. Asterisk (*) represents $p< 0.05$ when compared to cells without maslinic acid treatment of the same group. Total Nrf2, NQO1, and HO-1 protein levels were normalized to actin and the values shown were representative of fold change compared to non-transfected control without treatment.

The percentage change in mRNA and protein expression is calculated by the following equation: (Relative intensity of treated sample – 1.00) x 100 %

4.7 Proteomic analysis of Raji cells in response to maslinic acid treatment

4.7.1 Differential proteomic changes in maslinic acid-treated and untreated Raji cells

The protein expression profile of Raji cells in response to maslinic acid treatment at a sub-cytotoxic level (50 μM) for 4, 8, 16, and 24 h was investigated. Figure 4.42 shows silver-stained 2D gels. About 1000 spots were detected and around 40 spots showed ≥ 2-fold changes in spot intensity compared to the untreated control. The images of the protein spots depicting differential changes in response to maslinic acid treatment are shown in Table 4.9. Tryptic digests from 17 spots were analyzed by MALDI TOF-TOF MS. Table 4.10 lists the proteins that were identified by the database. The functions of the differentially regulated proteins were obtained using their protein accession numbers from the NCBI protein function summary (http://www.ncbi.nlm.nih.gov/protein). In response to maslinic acid treatment, 17 proteins identified in the study were assigned to several functional groups, namely cell proliferation, cell cycle, cytoskeleton organization, energy metabolism, cell signaling, and apoptosis.

DUTPase and inorganic pyrophosphatase which are involved in cell proliferation were down-regulated after treatment with maslinic acid. Proteins participating in energy metabolism, e.g. isocitrate dehydrogenase and enoyl-coA hydratase were highly expressed in maslinic acid-treated Raji cells. Voltage-dependent anion-selective channel protein 1 (VDAC1) which participates in the formation of the permeability transition pore complex

(PTPC) responsible for releasing mitochondrial products that trigger apoptosis was up-regulated while prohibitin which regulates mitochondrial respiration and aging was down-regulated. VDAC1 and prohibitin have been implicated in apoptosis. The expression of transgelin-2 and tumour protein D52, which are involved in tumourigenesis, was decreased.

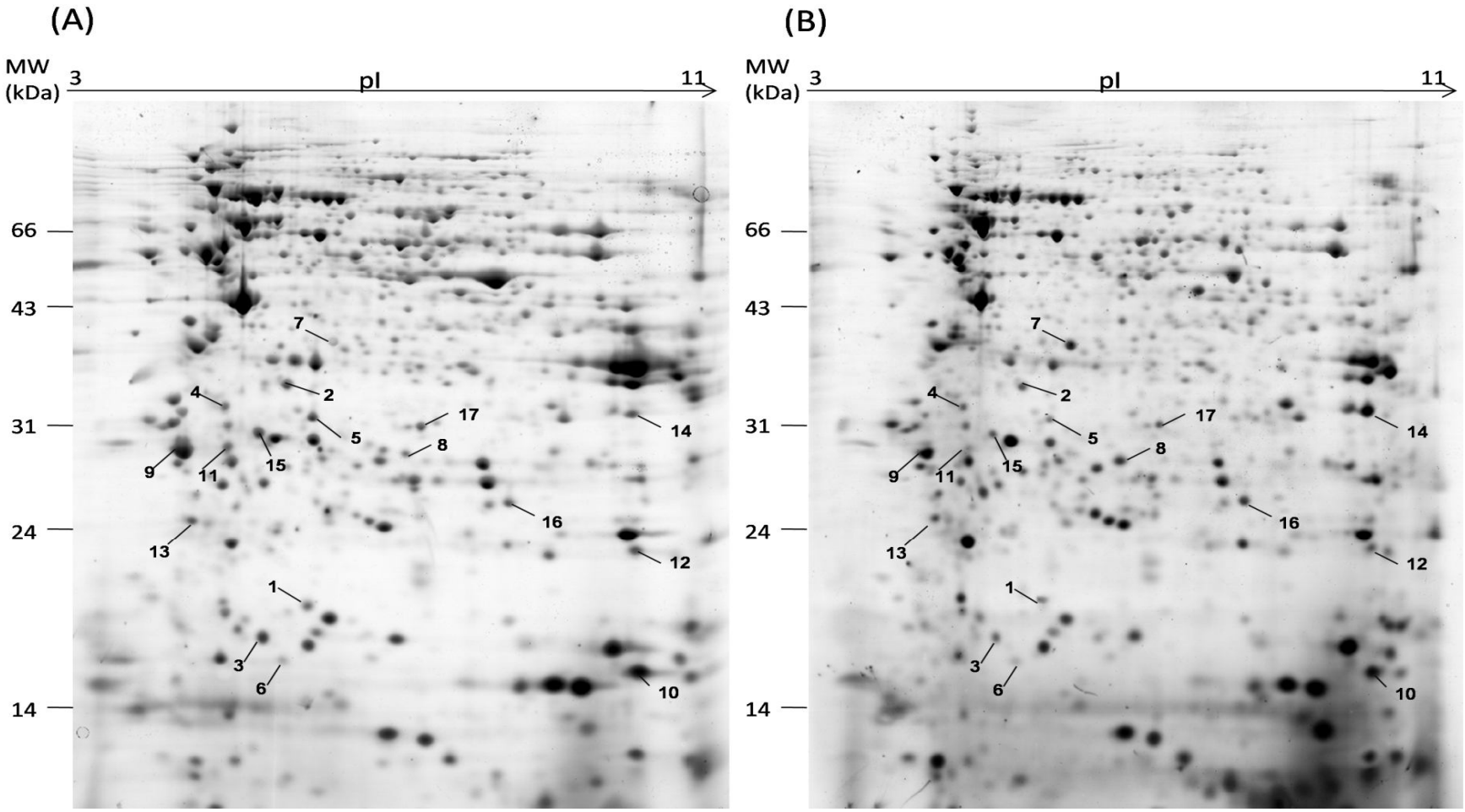
(A)
MW
(kDa)
3
pI
11
66
43
31
24
14
7
2
4
17
5
14
8
9
11
15
16
13
12
1
3
6
10
(B)
MW
(kDa)
3
pI
11
66
43
31
24
14
7
2
4
17
5
14
8
9
11
15
16
13
12
1
3
6
10

Figure 4.42: Proteomic profiling of Raji cells in response to treatment with 50 μM maslinic acid. Protein lysates from untreated and maslinic acid-treated Raji cells were separated using pH 3–11NL IPG strips for the first dimension and 12.5% SDS-polyacrylamide gel for the second dimension of separation. Silver stained-gels loaded with proteins from (A) untreated cells and (B) cells treated with 50 μM maslinic acid for 24 h. The protein spots numbered were excised, subjected to tryptic digestion and identified using MALDI TOF-TOF MS analysis.

Table 4.9: Closed up images of the spots showing differential expression of Raji cells proteins in response to 50 µM maslinic acid treatment for 4, 8, 16, and 24 h. Relative intensities of the protein spots were shown below each image.

Protein spot number	50 µM Maslinic acid treatment				
	0 h	4 h	8 h	16 h	24 h
1	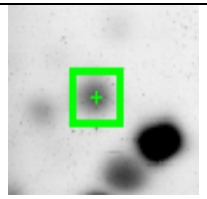 0.21	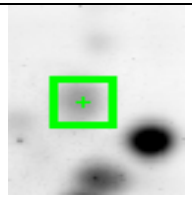 0.15	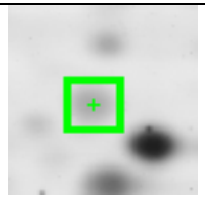 0.11	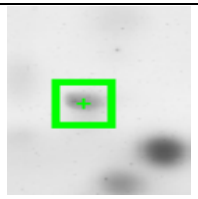 0.04	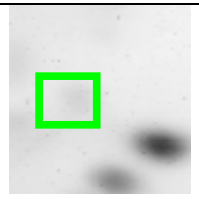 0.04
2	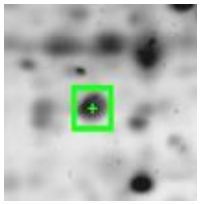 0.30	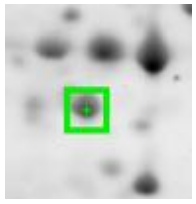 0.18	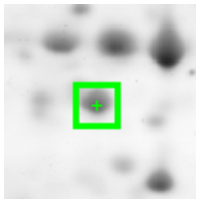 0.17	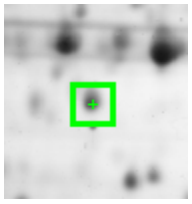 0.16	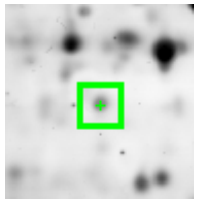 0.15
3	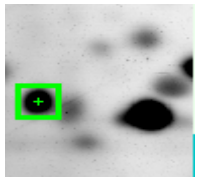 0.40	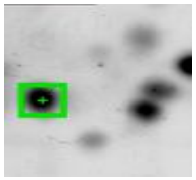 0.36	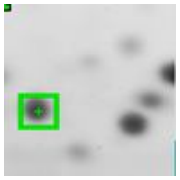 0.22	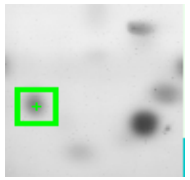 0.08	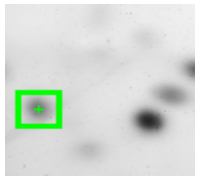 0.08

Table 4.9 (cont)

4	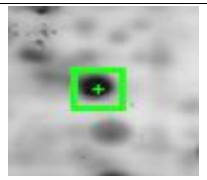	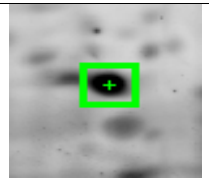	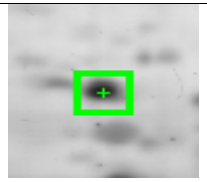	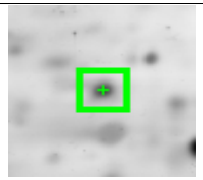	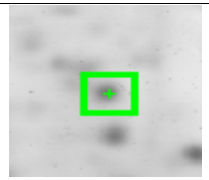
	0.29	0.22	0.15	0.12	0.11
5	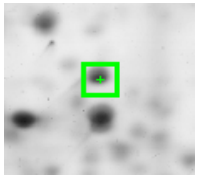	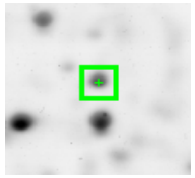	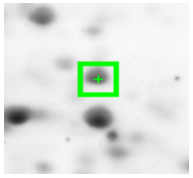	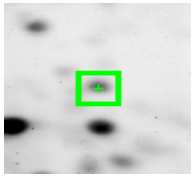	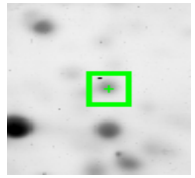
	0.27	0.19	0.18	0.16	0.13
6	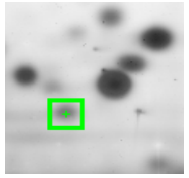	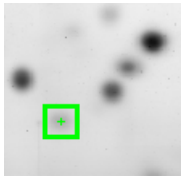	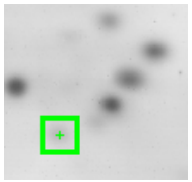	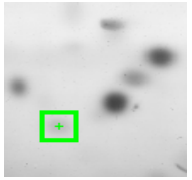	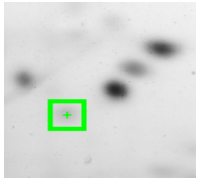
	0.18	0.09	0.08	0.05	0.05
7	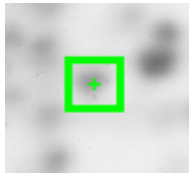	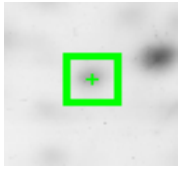	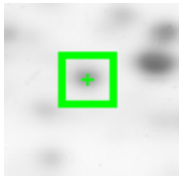	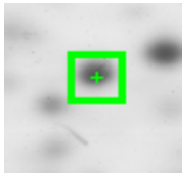	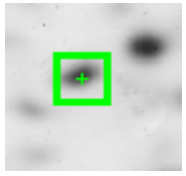
	0.08	0.12	0.14	0.14	0.31

Table 4.9 (cont)

8	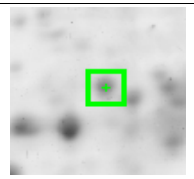	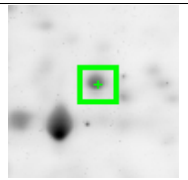	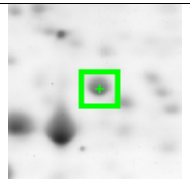	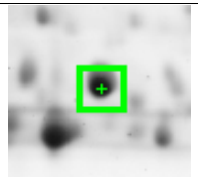	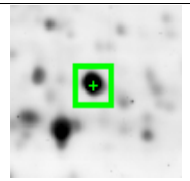
	0.12	0.19	0.19	0.27	0.32
9	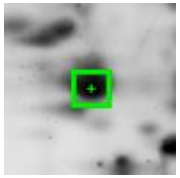	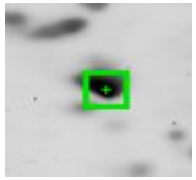	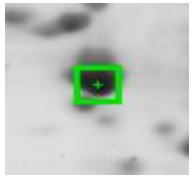	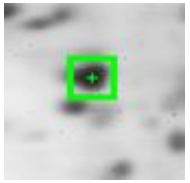	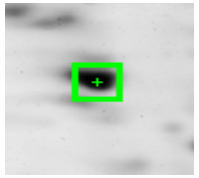
	1.59	0.66	0.65	0.49	0.49
10	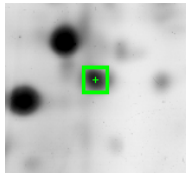	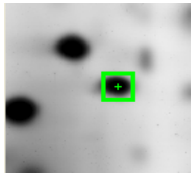	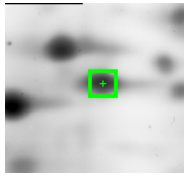	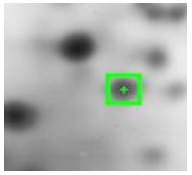	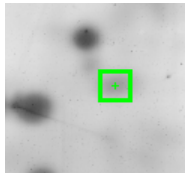
	1.05	0.94	0.71	0.46	0.39
11	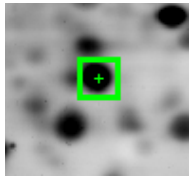	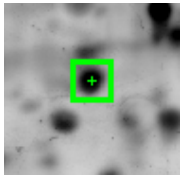	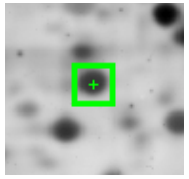	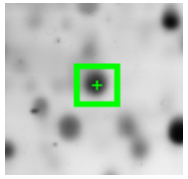	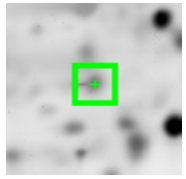
	0.58	0.34	0.29	0.21	0.11

Table 4.9 (cont)

12	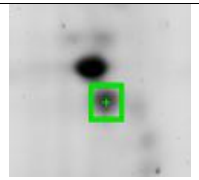	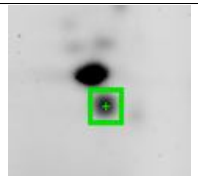	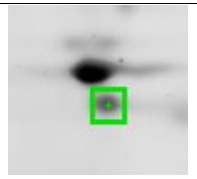	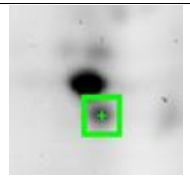	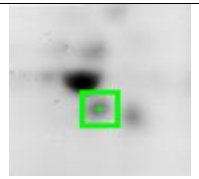
	0.57	0.52	0.43	0.20	0.16
13	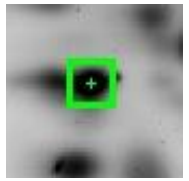	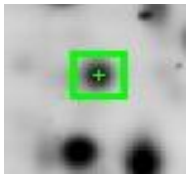	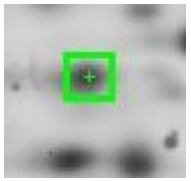	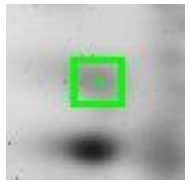	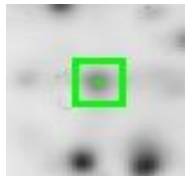
	0.29	0.20	0.18	0.07	0.04
14	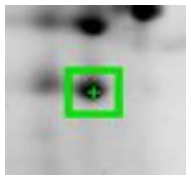	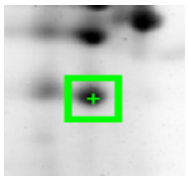	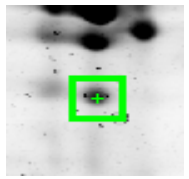	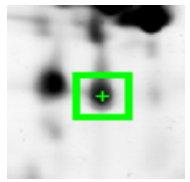	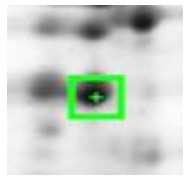
	0.21	0.18	0.20	0.71	0.54
15	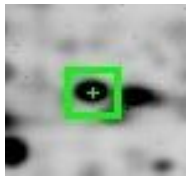	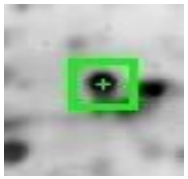	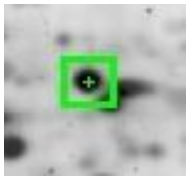	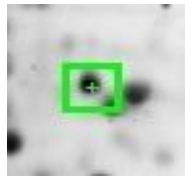	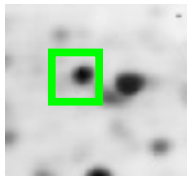
	0.44	0.42	0.39	0.23	0.22

Table 4.9 (cont)

16	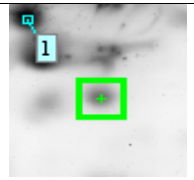	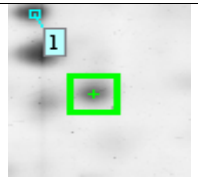		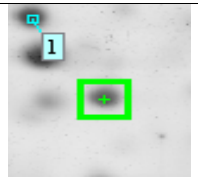	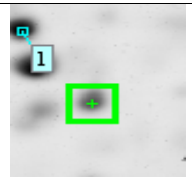
	0.12	0.15	0.19	0.23	0.29
17	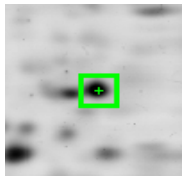	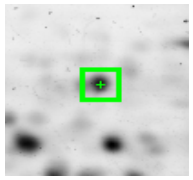	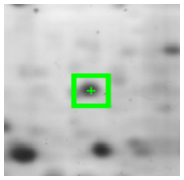	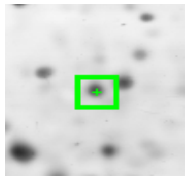	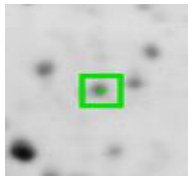
	0.25	0.15	0.14	0.13	0.06

Table 4.10: Differentially expressed proteins after treatment with 50 μM maslinic acid in Raji cells.

Spot number	Protein identity	Swiss-Prot database entries	MW/pI	Sequence coverage	Mowse score	Fold change	Biological function
1	dUTPase	P33316	17908/6.15	62%	553	-5.3	Cell proliferation
2	Inorganic pyrophosphatase	Q15181	33095/5.54	33%	369	-1.8	
3	Stathmin 1 isoform a	P16949	17292/6.02	43%	407	-5.2	Cell cycle
4	Microtubule associated protein RP/EB family member 1	Q15691	30151/5.02	46%	452	-2.7	
5	F-actin capping protein subunit beta	P47756	30852/5.52	21%	348	-2.1	Cytoskeleton
6	Actin related protein 2/3 complex subunit 5	O15511	16367/5.47	58%	447	-3.4	
7	Isocitrate dehydrogenase [NAD] subunit alpha, mitochondrial	P50213	34967/6.02	39%	356	+3.7	Energy Metabolism
8	Enoyl-coA hydratase mitochondrial	P30084	31361/6.09	53%	542	+2.6	
9	14-3-3 zeta/delta	P63104	29413/4.97	53%	391	-3.2	Cell signaling
10	Nucleoside diphosphate kinase B	P22392	17270/8.55	33%	260	-2.7	
11	Ran-specific GTPase-activating protein RANBP1	P43487	23610/5.21	21%	82	-5.3	
12	Transgelin-2	P37802	24609/8.41	86%	709	-3.5	
13	Tumour protein D52	P55327	24369/4.79	30%	336	-7.3	
14	Voltage-dependent anion-selective channel protein 1 (VDAC1)	P21796	30737/8.63	57%	414	+2.6	Apoptosis
15	Prohibitin	P35232	29859/5.57	73%	726	-1.9	
16	ES1 protein homolog, mitochondrial	P30042	24999/8.29	16%	202	+2.4	Others
17	Purine nucleoside phosphorylase	P00491	32382/7.09	73%	354	-4.2	

4.7.2 Validation of time-dependent differential expression of stathmin, EB1, and RanBP1

Based on the protein expression profile, maslinic acid appeared to regulate proteins that are involved in cell growth, proliferation and survival in Raji cells. Microtubule filament assembly and nucleocytoplasmic trafficking are important processes in the cell division cycle. Proteins such as stathmin, EB1 and RanBP1 which are involved in microtubule dynamics and nucleocytoplasmic transport were validated by immunoblot analysis to confirm differential expression. As shown in Figure 4.43, maslinic acid significantly reduced the expression of stathmin, EB1, and RanBP1 in a time-dependent manner. Maslinic acid inhibited more than 50 % stathmin protein expression after 16 h of treatment. Expression of EB1 was inhibited by 21, 25, 87, and 93 % after 4, 8, 16, and 24 h treatment with maslinic acid. RanBP1 expression was almost undetectable after 16 and 24 h of treatment.

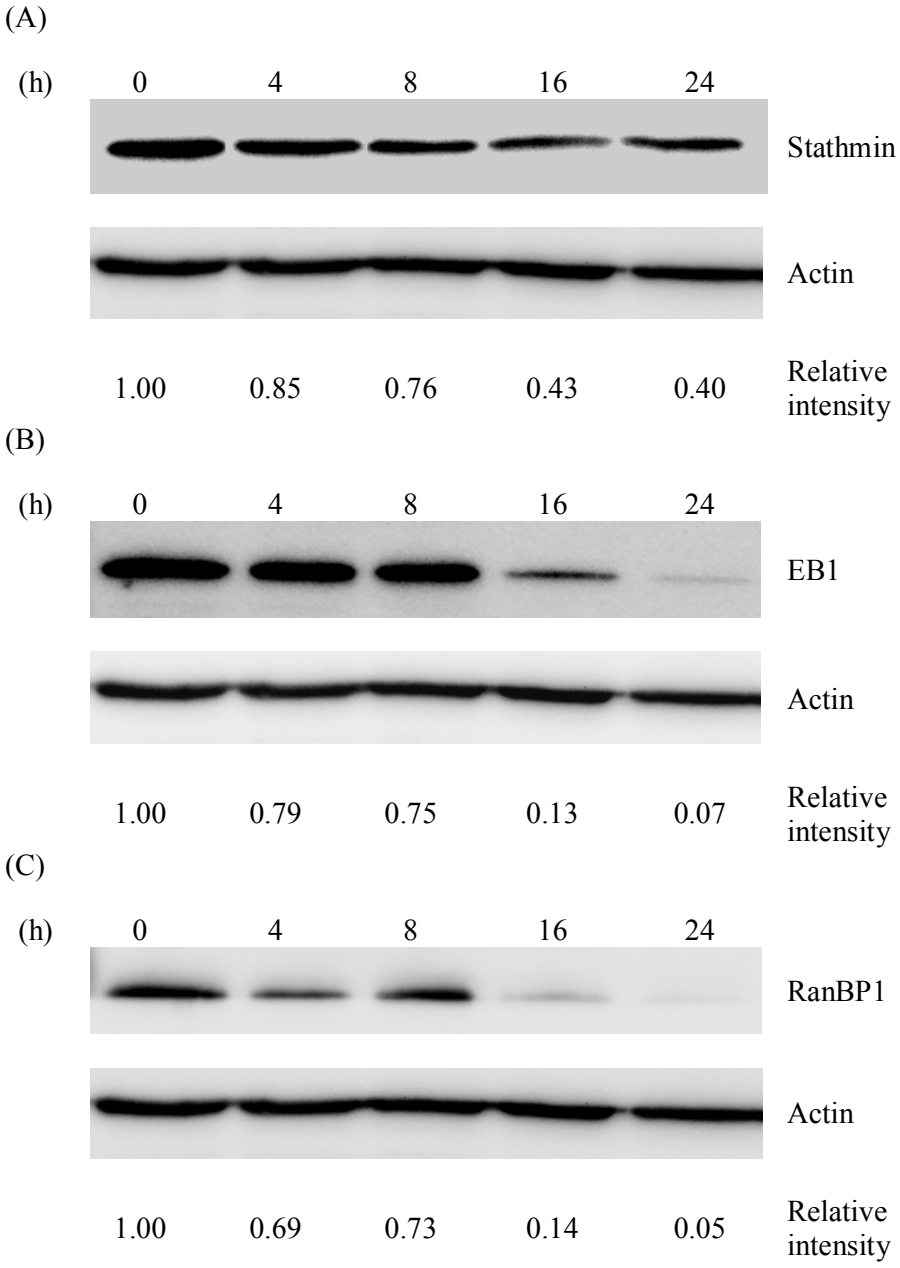

Figure 4.43: Validation of maslinic acid-regulated proteins in Raji cells by Western blotting. Cells were treated with 50 μM maslinic acid for 4, 8, 16, and 24 h. Cells were collected, total cell lysates prepared and subjected to SDS-PAGE followed by Western blotting. Membranes were probed with indicated antibodies and visualized by ECL detection system. The stathmin, EB1 and RanBP1 expression were normalized to actin and the values shown are representative of fold change compared to untreated control (0 h).

The percentage change in protein expression is calculated by the following equation: (Relative intensity of treated sample – 1.00) x 100 %

4.7.3 Induction of G1 cell cycle arrest

In order to confirm the role of maslinic acid in regulating the cell division cycle, cell cycle analysis was performed. Flow cytometry study of maslinic acid-treated Raji cells showed that maslinic acid induced G1 cell cycle arrest (Figure 4.44). Cells in the G1 phase increased sharply from 47 % (0 h) to 70 % after 16 h treatment and remained at 65 % up to 24 h. The increase in G1 cell population was accompanied by a decrease in the number of cells in both S and G2 phases. Treatment of cells with maslinic acid decreased the proportion of S phase cells from 25 % (0 h) to 11 % (24 h). The percentage of cells in the G2 phase decreased from 23 % (0 h) to 12 % at 24 h upon treatment.

4.7.4 Effects of maslinic acid on cell cycle regulatory molecules cyclin D1 and p21 expression

Based on the observation that maslinic acid induced G1 arrest in Raji cells, the effect of maslinic acid on cell cycle regulatory molecules of the G1–S phase transition were assessed by Western blotting analysis (Figure 4.45). Cyclin D1 was down-regulated by maslinic acid in a time-dependent manner. The cyclin D1 expression was reduced by 30 % after 8 h treatment and their levels were almost undetectable after 16 and 24 h of maslinic acid treatment. The CDK inhibitor p21 protein expression was, however, transiently up-regulated by maslinic acid. These effects were observed as early as 4 h of treatment (76 %) and reached a maximum expression at 8 h (154 %).

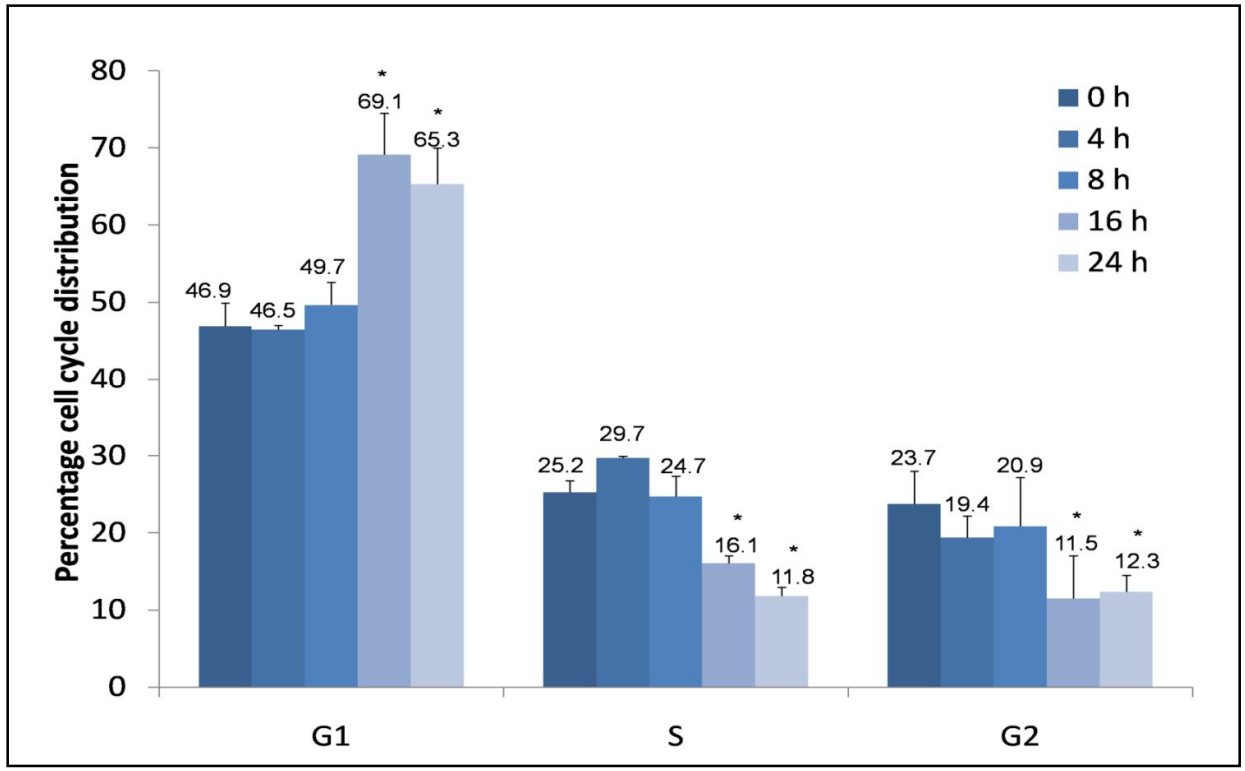

Figure 4.44: Raji cell cycle percentage distribution in response to treatment with 50 µM maslinic acid for 4, 8, 16, and 24 h. Cells were stained with propidium iodide (PI) and analyzed by flow cytometry. PI flow was detected on FL2 and data displayed as a histogram showing DNA content of cells in the G0/G1, S, and G2 phases of cell cycle. Ten thousand cells were analyzed for each data point. The values are expressed as mean ± S.D. of three experiments. Asterisk (*) denotes significant difference from the control at $p<0.05$.

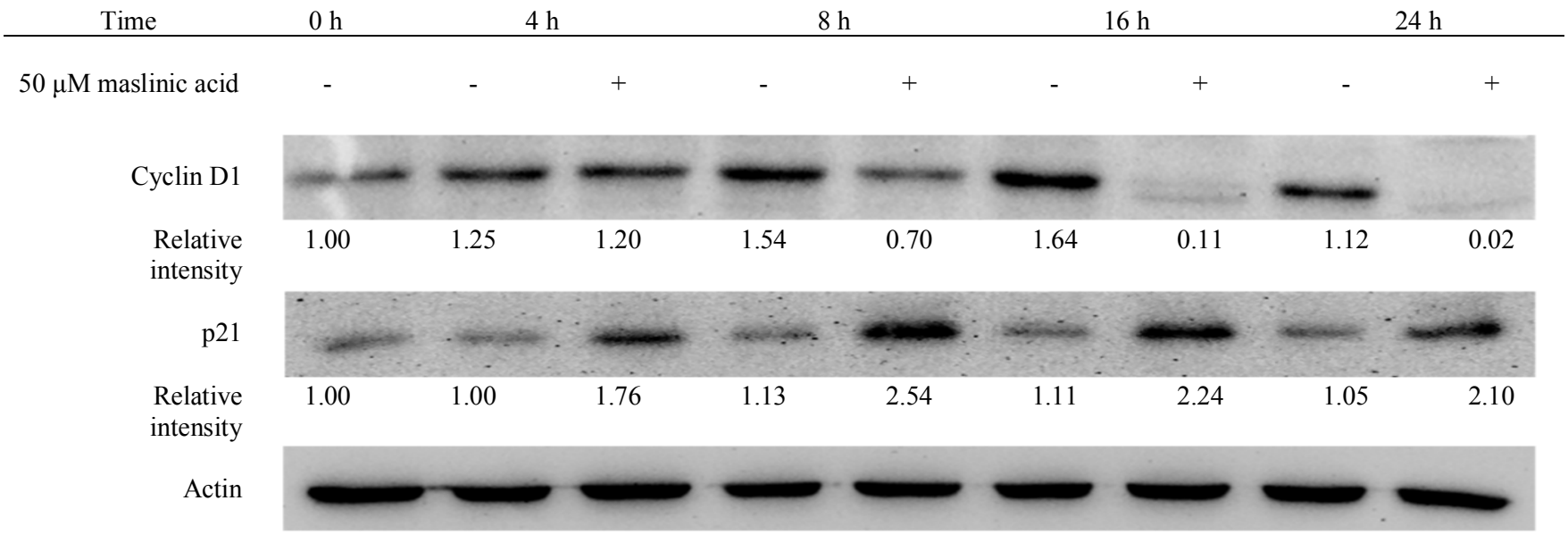

Figure 4.45: Time course effects of maslinic acid on the expression of G1 cell cycle components cyclin D1 and CDK inhibitor p21. Raji cells were treated with 50 μM maslinic acid for 4, 8, 16 and 24 h before harvested for Western blot analysis. The cyclin D1 and p21 expression were normalized to actin and the values shown are representative of fold change compared to the untreated control (0 h).

The percentage change in protein expression is calculated by the following equation: (Relative intensity of treated sample – 1.00) x 100 %

CHAPTER 5

DISCUSSION

Maslinic acid is a naturally occurring pentacyclic triterpene that has been shown to induce cell cycle arrest and to exert apoptotic effect in several cancer cell lines. There may be several mechanisms that are responsible for the anti-carcinogenic properties of maslinic acid. In this study, the anti-tumour-promoting effect of maslinic acid was confirmed using the EBV-EA activation assay. Down-regulation of COX-2 expression together with inhibition of NF-κB and AP-1 activation by maslinic acid is likely to contribute to the anti-tumour and anti-inflammatory effects of maslinic acid (Hsum *et al*., 2011). Maslinic acid also induced the expression of anti-oxidant and detoxifying enzymes via activation of the Nrf2 cytoprotective system. At the proteomic level, maslinic acid was shown to affect the expression of proteins involved in nucleotide metabolism, microtubule filament assembly, cytoskeleton organization, and adaptor proteins in the signal transduction pathway (Yap *et al*., 2012).

5.1 Inhibition of EBV-EA expression

In recent years, the progressive search for more effective and safer agents that target the promotion stage of carcinogenesis indicated in the Berenblum's multi-stage theory has received much attention. One of the screening methods

employed is a convenient primary *in vitro* assay for the inhibitory effect on EBV-EA activation induced by a well known tumour promoter, 12-*O*-tetradecanoylphorbol-13- acetate (TPA) or Phorbol 12-myristate 13-acetate (PMA) (Ito *et al*., 1981). The EBV-EA activation assay is an effective indicator for the evaluation of anti-tumour-promoting activity. Many compounds that exhibited positive results in the *in vitro* assay have been shown to inhibit tumour promotion in the *in vivo* two-stage carcinogenesis test (Konoshima *et al*., 1994).

Early studies on the isolation and characterization of triterpenes from some medicinal plant extracts revealed that maslinic acid has cytotoxic, anti-tumour and anti-inflammatory activities (Kim *et al*, 2000; Banno *et al*., 2005). In this study, maslinic acid isolated from the chloroform extract of *Coleus tuberosus* tubers was tested for its inhibitory effect on Epstein Barr virus early antigen activation induced by PMA and SnB. Maslinic acid inhibited 50 % early antigen activation (IC_{50}=25 μM) while maintaining high percentage cell viability (80 %). The inhibitory effect of PMA-induced EBV activation by maslinic acid is compared to other widely-studied anti-tumour agents such as the natural triterpenoid oleanolic acid (Ohigashi *et al*., 1986) and the isoflavone genistein (Wei *et al*., 1998). The inhibitory effect of maslinic acid is comparable to that of oleanolic acid (IC_{50}=35 μM) and genistein (IC_{50}=22 μM). All three compounds exhibit strong anti-tumour-promoting activity with more than 70 % inhibitory effect at 100 μM.

The Raji cell line (virus non-producer type) is an EBV-genome-carrying human lymphoblastoid cell line. At present, the mechanism of PMA and SnB induced EBV-EA activation in Raji cells is still poorly understood. The PMA/SnB combination represents a cooperative induction pathway which is related to the induction of viral enzymes during EBV activation (Nutter *et al*., 1987). In the latent forms of EBV infection, which occur primarily in B cells, only a small portion of the viral genome is expressed, and replication of the virus is mediated by an alternate origin of replication (oriP), the host cell DNA polymerase, and the viral Epstein Barr virus Nuclear Antigen-1 (EBNA-1) protein (Westphal *et al*., 2000). Tumour promoting phorbol esters PMA (Hausen *et al*., 1979) and SnB (Luka *et al*., 1979) can induce Raji cells to enter an abortive viral replication cycle and to synthesize EBV early antigen (EA). SnB is used as the EBV-EA co-inducer (Ohmori *et al*., 1998; Mentzer *et al*., 1998; Perrine *et al*., 1989).

The tumour-promoting phorbol ester PMA stimulates a wide variety of biochemical changes in cells, including stimulation of sugar transport, DNA synthesis and cell proliferation, alteration of cell morphology as well as enhancing cell transformation (Ruddon, 2007). Ohmori *et al* (1998) showed that EBV-EA induction by PMA was reduced to 65 % after treatment with 5 μg/mL palmitoyl-dl-carnitine (PC) which is a known phospholipid-sensitive Ca^{2+}-dependent protein kinase C inhibitor (Ohmori *et al*., 1998). This finding shows that tumour promoter induced EBV-EA expression is related to the activation of PKC. PMA substitute its binding to PKC by increasing the

affinity of PKC to Ca^{2+} and phosphatidylserine, thereby causing the translocation of PKC from cytosol to plasma membrane and causing its activation (Sharkey *et al*., 1984; Nishizuka, 1984).

Blocking the PMA from intercalating into the membrane to activate PKC may inhibit the EBV-EA expression. Pentacyclic triterpenes are structurally similar to sterols and interaction with the cell membrane is thought to be the molecular mechanism underlying their biological effects. It has been suggested that maslinic acid binds to transmembrane domains and competes with cholesterol (Cho) for the hydrogen-bonded ester carbonyl groups, thereby disturbing the localization and the physiological function of membrane-related proteins (Prades *et al*., 2011). Further investigation on the binding interaction between PKC and maslinic acid should be carried out to study its mechanism of action on cell membranes.

5.2 Inhibition of the NF-κB, AP-1 and COX-2 pro-inflammatory signaling

Several reports have indicated the intrinsic link between cancer and inflammation (Dorai and Aggarwal, 2004; Murakami and Ohigashi, 2007; Kundu and Surh, 2008). The tumour inflammatory microenvironment is characterized by the presence of tumour-associated macrophages and tumour-infiltrating lymphocytes which produce a range of pro-inflammatory cytokines (Kundu and Surh, 2008). Other inflammatory mediators including prostaglandins and nitric oxide which are produced by COX-2 and iNOS enzymes could further enhance the inflammatory response. Both cytokines and

inducible enzymes are induced by stimulation of transcription factors such as NF-κB and AP-1. Maslinic acid had been studied for its immunosuppressive activities through reduction of pro-inflammatory cytokines production in stimulated murine macrophages (Martin *et al*., 2006). Hence, the effect of maslinic acid in the inflammatory signaling was investigated through evaluation on the NF-κB and AP-1 binding activities and COX-2 expression.

5.2.1 Inhibition of NF-κB binding activity

NF-κB activation is critical for cancer development and progression. NF-κB activation occurs in premalignant cells and in microenvironment cells (Inoue *et al*., 2007). NF-κB activation in microenvironment cells leads to secretion of pro-inflammatory cytokines such as TNF, IL-1, and others, which in turn activate NF-κB in premalignant cells or tumour cells. This NF-κB activation leads to the induction of genes involved in proliferation, survival, angiogenesis and metastasis (Aggarwal and Shishodia, 2006). Blocking NF-κB can cause tumour cells to cease proliferation or become more sensitive to the action of chemotherapeutic agents (Naugler and Karin, 2008).

This study showed that maslinic acid inhibits the constitutive NF-κB activity in a concentration- and time-dependent manner in Raji cells. Modulation of the NF-κB activity may be a key mechanism for the anti-tumour and anti-inflammatory properties of maslinic acid. Other studies, however, indicate that maslinic acid inhibits growth and induces apoptosis in astrocytoma cells without regulating NF-κB activity (Martin *et al*., 2007). However, maslinic acid was recently reported to potentiate the anti-tumour activity of TNF-α by

inhibiting NF-κB signaling pathway and this was mediated by blocking IκBα degradation, p65 nuclear translocation and phosphorylation in Panc 28 pancreatic cancer cells (Li *et al*., 2010). The mechanism of maslinic acid differs from that of selective NF-κB inhibitor BAY 11-7085. The inhibition response of BAY occurred more rapidly (within 1-2 hours) compared to natural triterpenoids (maslinic acid and ursolic acid). BAY is a propenenitrile that was reported to directly inhibit TNF-α-induced IκBα phosphorylation, leading to suppression of nuclear translocation and transcriptional activity of NF-κB (Berger *et al*., 2007).

One of the possible molecular mechanisms for the inhibition of NF-κB signaling by maslinic acid might be attributed to its anti-oxidant activity. NF-κB and the signaling kinases upstream are regulated by redox state in the cells. Constitutive production of tolerable amounts of oxidative stress in cancer cells activate the MAPK signaling pathway, resulting in constant activation of redox-sensitive transcription factors including NF-κB and AP-1 (Figure 5.1). Maslinic acid is the 2-hydroxyderivative of oleanolic acid. Based on this structural characteristic, maslinic acid is predicted to have potent anti-oxidant properties compared to oleanolic acid, thereby more effective in suppressing NF-κB activity. Indeed, this study showed that maslinic acid is a stronger NF-κB inhibitor compared to oleanolic acid. Meanwhile, triterpenoids are also effective inducers of metallothionein, a small cysteine rich protein acting like glutathione in the body's defense system against toxic stress. The induction of metallothionein could be one of the important mechanisms for the anti-oxidant effects of maslinic acid (Cipak *et al*., 2006).

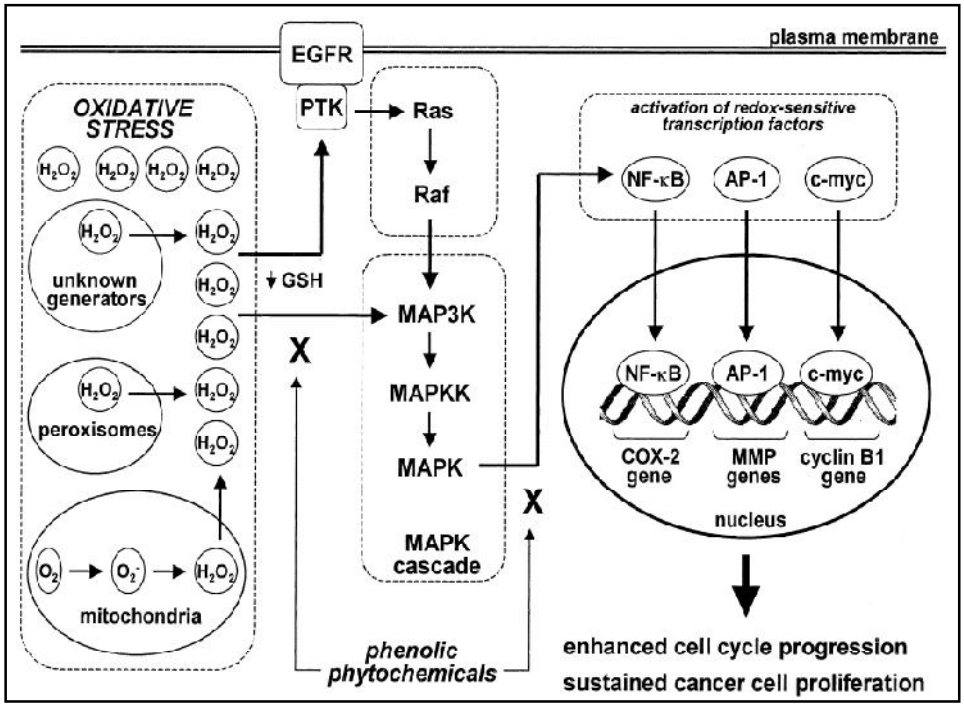

Adapted from Loo, 2003

Figure 5.1: Role of ROS in the proliferation of cancer cells and potential impact of chemopreventive phytochemicals. High amounts of H_2O_2 in cancer cells activate the MAPK pathway and induce redox-sensitive transcription factors and downstream genes that promote cancer cell viability. Chemopreventive phytochemicals may scavenge ROS or inhibit MAPK activation, thereby disrupting the course of events that lead to cell cycle progression and cancer cell proliferation.

Plant-derived terpenoids inhibit NF-κB by modulating targets upstream in the signaling cascade, for instance at the receptor level (Salminen *et al*., 2008). Lupeol, a lupane-type triterpenoid has been found to significantly reduce the expression of Ras oncoprotein and modulate the protein expression of various signaling molecules involved in protein kinase C alpha (PKCα)/ODC, PI3K/Akt and MAPKs pathways along with a significant reduction in the activation of IKKα, and degradation of IκBα, thereby inhibiting NF-κB activity (Chaturvedi *et al*., 2008). It has been reported that LMP1 strongly

activates NF-κB and stress activated protein kinases (e.g. JNK) to affect transcription (Eliopoulos *et al*., 2002). Some triterpenoids like ginsenosides and saikosaponins which suppress NF-κB activation also inhibit activation of JNK signaling (Salminen *et al*., 2008). Focusing on the distinct targets of maslinic acid upstream of IKK and NF-κB may help to further elucidate its molecular mechanism in this pathway.

5.2.2 Inhibition of AP-1 binding activity

Besides NF-κB, AP-1 also regulates the transcription of a variety of genes, some which are involved in neoplastic transformation and tumour promotion. AP-1 is a complex of oncogene protein of c-Fos and c-Jun families (Shaulian and Karin, 2002). C-jun and c-fos are induced by plethora of external stimuli including UV, TPA, growth factors and transforming oncogenes (Aggarwal and Shishodia, 2006). AP-1 participates in fundamental cellular processes, such as proliferation, differentiation, oncogenic transformation, apoptosis and metastasis (Tulchinsky, 2000). Chemopreventive agents specifically targeting AP-1 could be promising agents for the cancer treatment and prevention (Matthews *et al*., 2007).

The results showed that ursolic acid, maslinic acid and oleanolic acid inhibit PMA and SnB-induced AP-1 DNA binding activity in a concentration- and time-dependent manner. The AP-1 binding activity was significantly reduced during the first 4 h of treatment with maslinic acid. The inhibition effect of maslinic acid at early time points might be mediated by suppressing phosphorylation of a pool of constitutive AP-1 components induced by PMA

and SnB (Hsiang *et al*., 2005) or by inhibiting the transcriptional activity of SnB.

AP-1 is one of the redox-sensitive transcription factors whose activity appears to be regulated either directly or indirectly through reversible oxidation-reduction mechanism (Surh *et al*., 2005; Liu *et al*., 2005). AP-1 members such as c-Jun and c-Fos have single conserved cysteine residue in their DNA-binding domains that undergo reversible redox reactions and alter their DNA-binding properties (Abate *et al*., 1990). Dietary chemopreventive phytochemicals like curcumin, which is also a potent NF-κB inhibitor, have been reported to inhibit activation of TPA- induced AP-1 in HL-60 cells and Raji cells (Han *et al*., 2002; Hergenhahn *et al*., 2002). Analysis of the mechanism of curcumin and its analogs however showed that their function as AP-1 inhibitors is independent of their anti-oxidant activity or reactivity as a Michael acceptor (Park *et al*., 2005; Weber *et al*., 2006).

AP-1 inhibitors may inhibit other targets upstream of the signaling cascade. PMA activates PKC, and subsequently induces AP-1 responsive gene expression (Park *et al*., 2000). The activation of PKC results in rapid, site-specific dephosphorylation of c-Jun at one or more sites near the carboxyl terminal led to the increased AP-1 binding activity (Boyle *et al*., 1991). These phosphorylations are regulated by JNK for c-Jun and c-Fos regulating kinase (FRK) for Fos. Maslinic acid may target inhibition of PKC activation (as suggested in the EBV-EA inhibition in Section 5.1) and the downstream MAPK signaling, thereby inhibiting the AP-1 DNA binding activity. Lupeol

for example regulate activity of NF-κB, AP-1, p53, and Akt via the MAPK signaling pathway which transmits signals initiated by growth-inducing tumor promoters, including TPA, epidermal growth factor (EGF), and platelet-derived growth factor (PDGF) (Chaturvedi *et al*., 2008).

5.2.3 Inhibition of COX-2 expression

NF-κB and AP-1 are crucial transcription factors known to initiate transcription of the *hCOX-2* gene (Kosaka *et al*., 1994; Subbaramaiah and Dannenberg, 2003). Many dietary agents that suppress these transcription factors have the potential of inhibiting COX-2 expression (Aggarwal and Shishodia, 2006). COX-2 is the key enzyme in the biosynthesis of the prostaglandins mediating inflammation and other important physiological processes. Since maslinic acid suppresses NF-κB and AP-1 binding activities, its ability to inhibit COX-2 expression was studied.

Maslinic acid, ursolic acid (Subbaramaiah *et al*., 2000) and oleanolic acid (Janakiram *et al*., 2008) inhibit COX-2 expression in a concentration- and time-dependent manner. Although maslinic acid suppresses NF-κB and AP-1 binding activities, whether suppression of COX-2 is mediated via these two transcription factors in Raji cells is still unknown. In pancreatic cancer cells Panc28, maslinic acid was shown to suppress TNF-α-induced NF-κB binding to the COX-2 promoter (Li *et al*., 2010). Ursolic acid suppresses COX-2 protein via inhibition of PKC, ERK1/2, JNK and p38 MAPKs activation in PMA-treated human mammary epithelial cells (Subbaramaiah *et al*., 2000).

Curcumin was shown to suppress COX-2 activity through the suppression of NF-κB-inducing kinase (NIK) and IKK enzymes (Plummer *et al.*, 1999). Other chemopreventive agents, such as genistein and catechins function through down-regulation of EGFR and HER-2/neu activity, resulting in reduced expression of COX-2 (Aggarwal and Shishodia, 2006).

Most phytochemicals have the ability to affect COX-2 enzyme functions via transcriptional control of COX-2 gene expression. The inhibition of the NF-κB pathway or the perturbation of such kinase-dependent signaling events, such as those mediated by JNK, p38 or ERK, has been widely identified as the main mechanism (Surh *et al.*, 2001). COX-2 transcription might be mediated via the NF-κB pathway since both NF-κB and COX-2 have constitutive expression in Raji cells. The oncogenic property of EBV LMP1 which results in constitutive NF-κB activation appears to be responsible for the up-regulation of COX-2 (Murono *et al.*, 2001). In order to define the region of the *COX-2* promoter that responds to maslinic acid, transient transfections can be perform with a series of *COX-2* promoter deletion constructs using a luciferase reporter assay system. Silencing studies using siRNA targeting on components of the NF-κB and AP-1 pathways might help to elucidate the requirement of NF-κB and AP-1 for COX-2 expression in Raji cells.

5.3 Induction of the Nf2-Keap1-ARE pathway

There is a growing body of evidence that the Nrf2 signaling pathway is associated with inflammation. The induction of pro-inflammatory mediators such as IL-1α, IL-6, TNF-α, iNOS and COX-2 were observed in Nrf2

knockdown mice (Khor *et al*., 2006). It is postulated that induction of anti-oxidative and detoxifying enzymes via the Nrf2 pathway could reinforce the body's defense system against inflammation. A recent study showed that maslinic acid-containing olive oil regulates gene expression associated with inflammation in mouse liver (Guillen *et al*., 2009). Apart from suppressing the pro-inflammatory pathway as have been discussed in the previous section, whether maslinic acid can induce cytoprotective proteins through the Nrf2 pathway was investigated.

Under basal resting conditions, Nrf2 is sequestered in the cytoplasm by the cytoskeleton-associated protein Keap1. Keap1 functions as a negative regulator of Nrf2 by promoting ubiquitination and proteasomal degradation of Nrf2. In the presence of oxidative and electrophilic stress, Nrf2 is liberated from its repressor Keap1, translocates into the nucleus, and forms a heterodimer with a small Maf protein. The Nrf2-Maf dimer then binds to ARE, a *cis*-acting DNA regulatory element with a core nucleotide sequence of 5-GTGACNNNGCN-3, localized in the promoter region of cytoprotective genes, including NQO1, GST, HO-1, glutathione peroxidase (GPx), and peroxiredoxin I (Prx I) (Prestera and Talalay, 1995).

This study shows that maslinic acid induces nuclear Nrf2 accumulation, binding on the ARE, and up-regulation of anti-oxidant enzyme HO-1 and detoxifying enzyme NQO1 expression. More importantly, Nrf2 was shown to be essential for maslinic acid-induced expression of HO-1 and NQO1 expression. The results of this study demonstrated that cytoplasmic Nrf2

expression increased in a time-dependent manner and nuclear Nrf2 accumulation was observed after 3 h treatment. The nuclear Nrf2 accumulation might stimulate binding on the ARE as observed from 3 – 12 h. The significant Nrf2-ARE binding activity at 6 h could result in the maximal up-regulation of HO-1 and NQO1 expression observed at the same time point. Similarly, we also showed that oleanolic acid induces the Nrf2-ARE activation but at a slower pace compared to maslinic acid.

Nrf2 has a relatively short-half life of 10-30 min in the absence of cellular stress (Itoh *et al.*, 2003). Maslinic acid enhances cytoplasmic Nrf2 expression in a time-dependent manner and significantly increased nuclear Nrf2 accumulation after 3 h. The results suggest that maslinic acid stabilizes Nrf2 protein in the cytoplasm, before translocating into the nucleus and transcriptionally activate downstream genes by binding to the ARE. There are studies reporting that increasing Nrf2 stability is a mechanism that enhances Nrf2-mediated transcriptional activation of the ARE (Nguyen *et al.*, 2003; Kobayashi *et al.*, 2006). The steady-state level of Nrf2 appears to be maintained by a precise balance between the rates of synthesis and degradation by the proteasome (Furukawa and Xiong, 2005). In response to maslinic acid treatment, Nrf2 may continue to be synthesized at a normal rate, but the rate of its degradation decreases such that the balance would now tip toward accumulation of the protein, ultimately leading to an enhanced transcriptional activity.

The effect of maslinic acid-induced nuclear Nrf2 accumulation might be explained by the 'hinge and latch' model (Figure 5.2). The Nrf2-Keap1 interaction (hinge and latch) model suggests that Nrf2 has two Keap1-binding sites in the Neh2 domain (McMahon *et al*., 2006). Binding via the high affinity ETGE motif provides the 'hinge' while concomitant binding via the low-affinity DLG motif provides the 'latch'. Under conditions of chemical/oxidative stress, however, Nrf2 ubiquitination is perturbed, possibly via loss of binding through the DLG latch. Due to the consequent improper spatial positioning, Nrf2 is no longer directed for degradation, but remains associated with Keap1, most probably via the ETGE hinge. This leads to the saturation of Keap1, such that any newly synthesized Nrf2 can evade repression and accumulate within the nucleus, leading to the transactivation of ARE-regulated target genes (Tong *et al*., 2006).

In addition to enhancing cytoplasmic and nuclear Nrf2, maslinic acid also decreases Keap1 levels. Keap1 functions as a substrate adaptor for a Cullin-dependent E3 ubiquitin ligase complex and constitutively targets Nrf2 for ubiquitination and proteasomal degradation. Reduced Keap1 expression at 3 h coincided with significant nuclear Nrf2 expression and ARE binding activity at the same time point, indicating that maslinic acid may trigger degradation of

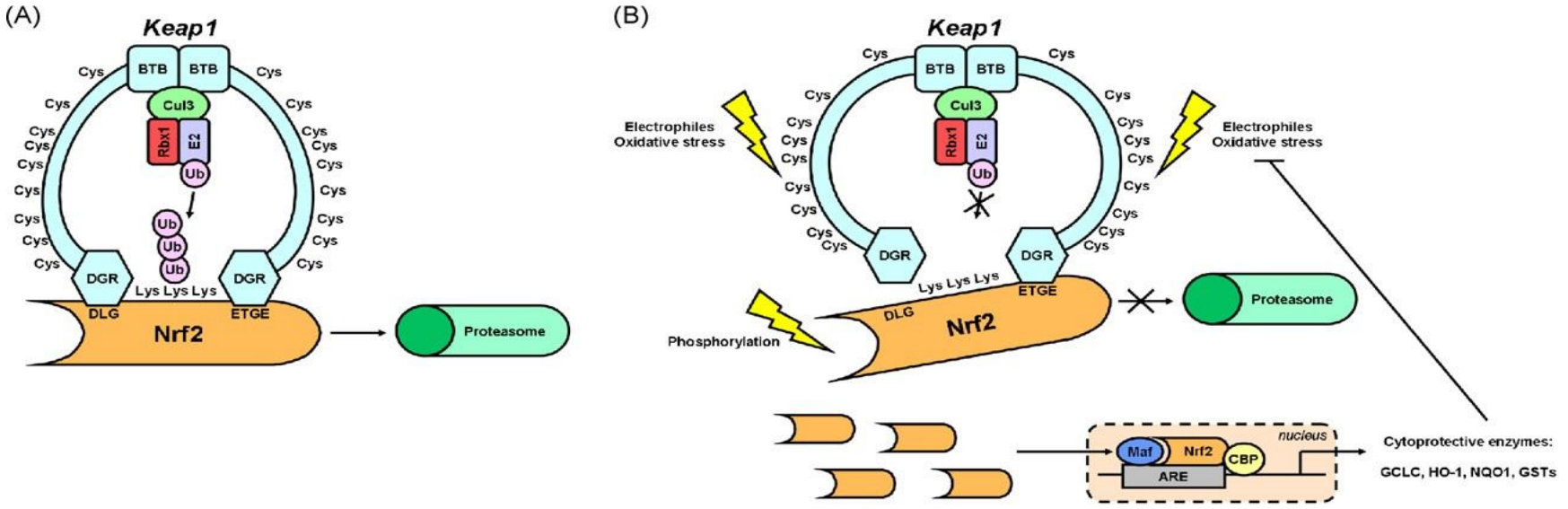

Adapted from Copple *et al.*, 2008

Figure 5.2: The Nrf2/Keap1 Hinge and Latch model. (A) In the absence of cellular stress, Nrf2 is bound by Keap1 homodimer. Binding of the double glycine repeat (DGR) domain in Keap1 with both the DLG and ETGE motifs on Nrf2, target Nrf2 for Cullin-dependent E3 ubiquitin ligase-mediated degradation. (B) Under chemical/oxidative stress, binding through the low-affinity DLG latch might be perturbed, probably by phosphorylation of Nrf2 or a conformational change in Keap1 through modification of cysteine residues. Nevertheless, binding through the high-affinity ETGE hinge is maintained, such that Nrf2 remains associated with Keap1. However, the transcription factor is no longer held in the correct position to facilitate ubiquitin transfer, and thus Nrf2 is not directed for proteasomal degradation. As a result, Keap1 becomes saturated, and any newly-synthesized Nrf2 is able to accumulate within the nucleus and transactivate cytoprotective genes.

Keap1, leading to Nrf2 nuclear accumulation and resulting in ARE gene induction. Studies show that different subset of Nrf2 inducers has very different effects on Keap1 ubiquitination and stability (Eggler *et al*., 2008). Some induced Keap1 ubiquitination and degradation by a proteasome-independent mechanism while others do not (Zhang *et al*., 2005). It has been suggested that normally Keap1 targets Nrf2 for ubiquitin-mediated degradation but electrophiles may trigger a switch of Cul3-dependent ubiquitination from Nrf2 to Keap1 (Lau *et al*., 2008). Eggler *et al*. (2005) demonstrated that modification of Keap1 Cys 151 residue leads to a change in the conformation of the BTB domain by means of perturbing the homodimerization site, disrupting Neh2 ubiquitination and causing ubiquitination of Keap1 (Eggler *et al*., 2005).

Keap1 expression was restored upon maslinic acid treatment at later time points (6 and 12 h). In fact, an autoregulatory loop exists within the Nrf2 pathway which regulates the nuclear Nrf2 levels and rapidly switches off the activation of Nrf2 downstream gene expression (Lee *et al*., 2007). An ARE was identified in the Keap1 promoter that facilitates Nrf2 binding, causing induction of the Keap1 gene (Kaspar *et al*., 2009). Some proposed that upon recovery of the redox balance, Keap1 travels into the nucleus, where it causes dissociation of Nrf2 from the ARE sequence and escorts it out for degradation (Lau *et al*., 2008). In some cases, it appears that Nrf2 inducers may stimulate a Src kinase, likely Fyn kinase, leading to the export of Nrf2 from the nucleus several hours after induction thereby shutting down the signaling response (Jain and Jaiswal, 2006).

Meanwhile, phosphorylation may be an important signaling event in both the activation and deactivation of Nrf2, through promotion of nuclear accumulation and export, respectively (Copple *et al*., 2008). Several protein kinases, including PKC, ERK, MAPK, p38, and PERK, are known to modify Nrf2 and activate its release from Keap1 (Bloom *et al*., 2003; Yu *et al*., 1999). Metabolism of antioxidants and xenobiotics generates ROS and electrophiles, which might act as second messengers, activating upstream MAPKs and subsequently induce ARE-mediated gene expression (Kaspar *et al*., 2009). Oleanolic acid has been shown to protect normal human liver cells against cytotoxicity through generation of glutathione and expression of Nrf2 as well as modulating activity of MAPKs, mainly JNK and ERK (Wang *et al*., 2010). In addition, oleanolic acid protects against acetaminophen hepatotoxicty in an Nrf2-dependent and Nrf2-independent cytoprotective mechanisms, which is due, in part, by the induction of metallothionein (Reisman *et al*., 2009). Hence, modulation of the upstream MAPKs and induction of metallothionein may have important roles in maslinic acid-induced Nrf2-ARE activation. Further studies are required to determine how maslinic acid modify Keap1, leading to changes in the ubiquitination of Nrf2 and possibly Keap1. Alteration of the Keap1-Cul3 interaction and the disruption of the Keap1-Nrf2 complex by Nrf2 phosphorylation are attractive mechanisms requiring further investigation.

5.4 Proteomic analysis of the molecular response to maslinic acid

The study of the effects of maslinic acid at the proteomics level may help to elucidate the complex interactions of the protein network. As revealed from

the proteome profile, the cytotoxic and pro-apoptotic effects of maslinic acid might be resulted from interference with DNA replication (down-regulation of dUTPase and inorganic pyrophosphatase), nucleo-cytoplasmic trafficking (down-regulation of RanBP1), and microtubule filament assembly (reduction of stathmin and EB1) as well as induction of apoptosis-related protein VDAC1. In the case of mitochondrial-regulated apoptosis, the process is ATP dependent and energy demanding (Mayer and Oberbauer, 2003). Down-regulation of VDAC1 expression by shRNA is associated with a decrease in energy production (Shoshan-Barmatz *et al*., 2008). Indeed, maslinic acid increases energy metabolism in cells by up-regulating mitochondria isocitrate dehydrogenase and enoyl-CoA hydratase. The data supports the suggestion by Reyes *et al*. (2008) that maslinic acid induces cell death via the mitochondrial apoptotic pathway (Reyes *et al*., 2008).

Maslinic acid also inhibited expression of adaptor proteins such as 14-3-3 zeta/delta and tumour protein D52 which regulate a large spectrum of both general and specialized signaling pathways. 14-3-3 zeta/delta is an important regulatory protein in intracellular signaling pathways and is known to interact with more than 100 cellular proteins, including oncogene and protooncogene products (Xing *et al*., 2000). It was speculated that 14-3-3 zeta/delta regulate inflammatory pathways in the tumour microenvironment (Kobayashi *et al*., 2009). Tumour protein D52 is a multi-functional adaptor protein that influences numerous cellular processes. Increased D52 expression may be an early event in cancer which contributes to subsequent tumour progression (Boutros *et al*., 2004). The expression of transgelin-2, a protein of the calponin

family found in high abundance in Raji cells (Gez *et al*., 2007) was down-regulated by maslinic acid. Elevated levels of transgelin were observed in tumourigenic cells and it significantly promotes cell migration and invasion (Lee *et al*., 2010).

Maslinic acid plays a critical role in the regulation of cell cycle progression. Down-regulation of proteins such as stathmin, EB1 and RanBP1 which are involved in microtubule dynamics and cell division were validated by Western blotting analysis. Elevated stathmin and RanBP1 expression have been reported in a variety of human malignancies (Antonucci *et al*., 2003) while EB1 expression was recently reported to be up-regulated in human breast cancer cell lines (Dong *et al*., 2010). The up-regulation of stathmin, EB1 and RanBP1 in neoplastic tissues may be part of the regulatory mechanism altered during tumorigenesis. Silencing or inhibition of stathmin, EB1 and RanBP1 causes aberrant mitotic spindle formation, inhibition of cancer cell proliferation, and apoptosis (Gez *et al*., 2007; Jeha *et al*., 1996). These observations, together with the findings of this study suggest that the inhibition of proteins regulating microtubule dynamics and cell division may suppress tumour cell growth and provide a valuable strategy for cancer treatment.

Reyes *et al*. (2006) reported that maslinic acid inhibit cell growth and induce G1 cell cycle arrest in Caco-2 colon cancer cells (Reyes *et al*., 2006). This study reports a similar effect of maslinic acid on the Raji cell cycle.

Interestingly, maslinic acid also down-regulated proteins associated with the cell cycle arrest at S and G2 phase. Inhibition of dUTPase induces early S (Tinkelenberg *et al*., 2002) or G2 (Marie *et al*., 2006) arrest due to stalled replication complexes caused by a lack of thymidine equivalents (dTTP or dUTP) available for DNA replication. Inhibition of stathmin expression leads to accumulation of cells in the G2 phase which is associated with severe mitotic spindle abnormalities and difficulty to exit from mitosis (Rubin and Atweh, 2004). By contrast, there are studies reporting that levels of stathmin phosphorylation were significantly lower in cells blocked during the G1/S phases of the cell cycle than in proliferating cells (Brattsand *et al*., 1994). Knockdown of Nm23-H1 (Dabernat *et al*., 2004), the target gene of nucleoside diphosphate kinase B (NDPKB) which was down-regulated by maslinic acid, has been shown to arrest cells in the G0/G1 phase of the cell cycle (Jin *et al*., 2009).

Progression through the cell division cycle is regulated by coordinated activities of cyclin/cyclin dependent kinases (CDK) complexes. Mitogenic signals that initiate DNA replication are first detected by expression of the D-type cyclins (D1, D2 and D3) that preferentially bind to, and activate, CDK4 and CDK6 during the G1 phase (Malumbres and Barbacid, 2001). Over-expression of cyclin D1 has been reported in several types of human cancers (Yu *et al*., 2001; Besson *et al*., 2008). Suppressing cyclin D1 over-expression may thus prevent oncogenic signaling. Another mechanism that prevents premature entry into the S phase relies on CDK inhibitors (CKIs) that bind onto cyclin-CDK complexes and disrupt their catalytic centre (Pavletich,

1999). The Cip/Kip family member of $p21^{Cip1/Waf1/Sdi1}$ is an important transcriptional target of p53 and mediates DNA-damage induced cell-cycle arrest (Besson *et al*., 2008). Suppressing cyclin D1 over-expression and inducing p21 levels by maslinic acid may thus prevent uncontrolled cell cycle progression.

Meanwhile, rearrangement of cytoskeleton organization is a general process in cells in response to apoptosis-inducing agents. Apart from providing structural support, microfilaments, microtubules, and intermediate filaments, exert important functions in cell motility, mitosis, and intracellular trafficking. Changes in the distribution and/or dynamics of these cytoskeletal proteins are in consistent with features of apoptosis (Ayscough and Gourlay, 2005). Although the mechanism is not well understood, the involvement of cytoskeletal actin in apoptosis has been suggested in some morphologic studies (Mashima *et al*., 1995). F-actin capping protein and actin-related protein 2/3 complex subunit 5 were reduced in maslinic acid-treated cells, suggesting that the proteolytic disassembly of the rigid cytoskeleton network may facilitate morphological manifestations of apoptosis.

The identification of proteins with altered expression profiles at multiple treatment time points may serve to elucidate the cellular mechanism involved in response to maslinic acid treatment. These results suggest that maslinic acid affects multiple signaling molecules and inhibits fundamental pathways regulating cell growth and survival in Raji cells (Figure 5.3).

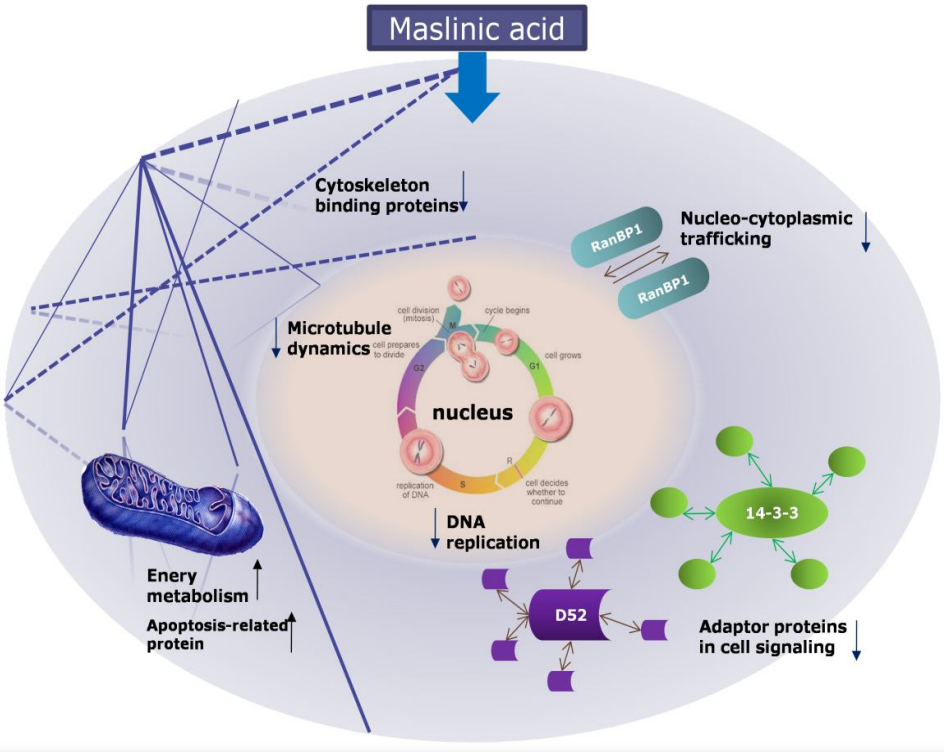

Figure 5.3: Schematic diagram of the molecular response of maslinic acid treatment in Raji cells. The effects of maslinic acid might be resulted from interference with DNA replication (down-regulation of dUTPase and inorganic pyrophosphatase), disturbance of nucleo-cytoplasmic trafficking system (down-regulation of Ran-specific GTPase-activating protein), microtubule filament system (reduction of stathmin and EB1), enhancing cell energy metabolism (up-regulation of isocitrate dehydrogenase and enoyl-coA hydratase) as well as induction of apoptosis related proteins (regulation of VDAC1 and prohibitin).

CHAPTER 6

CONCLUSION

From the traditional experimental carcinogenesis models which were used primarily to evaluate the efficacy of phytochemicals, there has been a gradual shift towards molecular chemoprevention where specific molecular targets are identified and signaling cascades for chemopreventive agents are examined. In continuation to the isolation of maslinic acid from *Coleus tuberosus* which has strong anti-tumour activity among selected Malaysian vegetables and fruits, maslinic acid has been shown to inhibit the NF-κB/AP-1/COX-2 pro-inflammatory signaling targets, induce Nrf2-regulated cytoprotective protein expression and modulate novel molecular targets associated with cell growth and survival at the proteomics level in this study.

Several studies have suggested the existence of a possible cross-talk between the Nrf2 and NF-κB signaling. Genetic disruption or pharmacologic inhibition of Nrf2 signaling increases the expression of pro-inflammatory mediators, such as COX-2, iNOS, TNF-α and IL-1β. These pro-inflammatory mediators are target genes of NF-κB. Since NF-κB has been recognized as an important molecular link between inflammation and cancer, it is possible that the anti-inflammatory and chemopreventive effects of maslinic acid be mediated through induction of Nrf2 gene products and down-regulation of NF-κB

signaling. The question of whether modulation of these pro-inflammatory mediators by Nrf2 is a direct transcriptional regulation or indirect through its transactivated target genes such as HO-1 and NQO-1 requires further investigation.

At the proteomic level, maslinic acid was shown to affect the expression of proteins involved in DNA replication, microtubule filament assembly, nucleo-cytoplasmic trafficking, apoptosis, energy metabolism, and cytoskeleton organization. Proteins such as stathmin, EB1 and RanBP1 which are associated with cell division and microtubule dynamics suggest that maslinic acid might have a role in regulating the cell cycle. Subsequent analysis showed that maslinic acid induces G1 cell cycle arrest and modulated G1-associated cell cycle regulatory proteins, i.e. cyclin D1 and p21. This study supports that treatment with maslinic acid activates the mitochondrial apoptotic pathway and suggests that the growth inhibition properties of maslinic acid might be mediated via modulation of the cell cycle.

The study of the chemopreventive mechanism of maslinic acid helps in the development of maslinic acid as a potential chemopreventive agent. Maslinic acid may provide protective effects in healthy individuals, particularly for the high-risk populations exposed to environmental carcinogens, by inducing detoxifying and antioxidant enzyme system for efficient neutralization and elimination of endogenous or exogenous carcinogenic species. For cancer patients with solid or hematopoietic tumours, maslinic acid may be used to in

combination with chemotherapeutic agents for potential synergistic and additive effects by inhibiting the inflammatory signaling as well as inducing apoptosis and cell-cycle arrest in pre-carcinoma and carcinoma cells.

REFERENCES

Abate, C., Patel, L., Rauscher, F. J. and Curran, T. (1990). Redox regulation of fos and jun DNA-binding activity in vitro. *Science*, 249(4973), 1157–1161.

Aggarwal, B. B. and Shishodia, S. (2006). Molecular targets of dietary agents for prevention and therapy of cancer. *Biochem. Pharmacol.*, 71, 1397-1421.

Ahn, N. G., Shabb, J. B., Old, W. M. and Resing, K. A. (2007). Achieving In-Depth Proteomics Profiling by Mass Spectrometry. *ACS Chem. Biol.*, 2, 39-52.

Alam, M. S., Chopra, N., Ali, M. and Niwa, M. (1996). Leanen and Stigmasterol derivatives from *Ambroma Augusta*. *Phytochemistry*, 41(4), 1197-1200.

Antonucci, F., Chilosi, M., Parolini, C., Hamdan, M., Astner, H. and Righetti, P. G. (2003). Two-dimensional molecular profiling of mantle cell lymphoma. *Electrophoresis*, 24, 2376-2385.

Athar, M., Back, J. H., Tang, X., Kim, K. H., Kopelovich, L. and Bickers, D. R. (2007). Resveratrol: a review of preclinical studies for human cancer prevention. *Toxicol. Appl. Pharmacol.*, 224, 274–283.

Ayscough, K. R. and Gourlay, C. W. (2005). The actin cytoskeleton: a key regulator of apoptosis and ageing? *Nat. Rev. Mol. Cell. Biol.*, 6, 583-589.

Bajaj, Y. P. (1994). Medicinal and Aromatic Plants. New York: Springer.

Banno, N., Akihisa, T., Tokuda, H., Yasukawa, K., Taguchi, Y., Akazawa, H., Ukiya, M., Kimura, Y., Suzuki, T. and Nishino, H. (2005). Anti-inflammatory and Antitumor-Promoting Effects of the Triterpene Acids from the Leaves of Eriobotrya japonica. *Biol. Pharm. Bull.*, 28(10), 1995-1999.

Begleiter, A., Sivananthan, K., Curphey, T. J. and Bird, R. P. (2003). Induction of NAD(P)H quinone: oxidoreductase1 inhibits carcinogen-induced aberrant crypt foci in colons of Sprague-Dawley rats. *Cancer Epidemiol. Biomarkers Prev.*, 12, 566–572.

Bellavita, V., Schiaffella, F. and Mezzetti, T. (1974). Triterpenoids of *Centaurium erythraea*. *Phytochemistry*, 13(1), 289-290.

Berger, N., Bassat, H. B., Klein, B. Y. and Laskov, R. (2007). Cytotoxicity of NF-κB inhibitors Bay 11-7085 and caffeic acid phenethyl ester to Ramos and other human B-lymphoma cell lines. *Exp. Hematol.*, 35,

1495–1509.

Besson, A., Dowdy, S. F. and Roberts, J. M. (2008). CDK Inhibitors: Cell Cycle Regulators and Beyond. *Dev. Cell.*, 14(2), 159-169.

Bloom, D. A. and Jaiswal, A. K. (2003). Phosphorylation of Nrf2 at Ser(40) by protein kinase C in response to antioxidants leads to the release of Nrf2 from INrf2, but is not required for Nrf2 stabilization/accumulation in the nucleus and transcriptional activation of antioxidant response element-mediated NAD(P)H:quinone oxidoreductase-1 gene expression. *J. Biol. Chem.*, 278, 44675-44682.

Bode, A. M. and Dong, Z. (2009). Cancer prevention research – then and now. *Nat. Rev. Cancer,* 9, 508-516.

Boutros, R., Fanayan, S., Shehata, M. and Byrne, J. A. (2004). The tumor protein D52 family: many pieces, many puzzles. *Biochem. Biophys. Res. Commun.*, 325, 1115-1121.

Boyle, W. J., Smeal, T., Defize, L. H., Angel, P., Woodgett, J. R., Karin, M. and Hunter, T. (1991). Activation of protein kinase C decreases phosphorylation of c-Jun at sites that negatively regulate its DNA-binding activity. *Cell*, 64, 573-584.

Brattsand, G., Marklund, U., Nylander, K., Roos, G. and Gullberg, M. (1994). Cell-cycle-regulated phosphorylation of oncoprotein 18 on Ser16, Ser25, and Ser38. *Eur. J. Biochem.*, 320, 359–368.

Calzado, M. A., Bacher, S. and Schmitz, M. L. (2007). NF-κB Inhibitors for the treatment of inflammatory disease and cancer. *Curr. Med. Chem.*, 14, 367-376.

Capone, M. L., Tacconelli, S., Francesco, L. I., Sacchetti, A., Sciulli, M. G. and Patrigani, P. (2007). Pharmacodynamic of cyclooxygenase inhibitors in humans. *Prostaglandins Other Lipid Mediat.,* 82, 85-94.

Cerella, C., Sobolewski, C., Dicato, M. and Diederich, M. (2010). Targeting COX-2 expression by natural compounds: A promising alternative strategy to synthetic COX-2 inhibitors for cancer chemoprevention and therapy. *Biochem. Pharmacol.*, 80(12), 1801-1815.

Chaturvedi, P. K., Bhui, K. and Shukla, Y. (2008). Lupeol: Connotations for chemoprevention. *Cancer Lett.*, 263, 1-13.

Chen, C., Pung, D., Leong, V., Hebbar, V., Shen, G., Nair, S., Li, W. and Kong, A.-N. T. (2004). Induction of detoxifying enzymes by garlic organosulfur compounds through transcription factor Nrf2: Effect of chemical structure and stress signals. *Free Radic. Biol. Med.*, 37(10), 1578–1590.

Chen, C. and Kong, A. N. T. (2005). Dietary cancer-chemopreventive compounds: from signaling and gene expression to pharmacological effects. *Trends Pharmacol. Sci.*, 26, 318-326.

Chia, A. J. L., Goldring, C. E., Kitteringham, N. R., Wong, S. Q., Morgan, P., and Park, B. K. (2010). Differential effect of covalent protein modification and glutathione depletion on the transcriptional response of Nrf2 and NF-κB. *Biochem. Pharmacol.*, 80, 410–421.

Chun, K. S. and Surh, Y. J. (2004). Signal transduction pathways regulating cyclooxygenase-2 expression: potential molecular targets for chemoprevention. *Biochem. Pharmacol.,* 68, 1089-1100.

Cipak, L., Lubica, G., Miadokova, E., Novotny, L. and Rauko, P. (2006). Dual activity of triterpenoids: apoptotic versus antidifferentiation affects. *Arch. Toxicol.*, 80, 429-435.

Copple, I. M., Goldring, C. E., Kitteringham, N. R. and Park B. K. (2008). The Nrf2Keap1 defence pathway: Role in protection against drug-induced toxicity. *Toxicology*, 246, 24-33.

Cseke, L. J., Kirakosyan, A., Kaufman, P. B., Warber, S. L., Duke, J. A. and Brielmann, H. L. (2006). Natural Products from Plants. United States of America: CRC Press.

Cullinan, S. B., Gordan, J. D., Jin, J., Harper, J. W. and Diehl, J. A. (2004). The Keap1-BTB protein is an adaptor that bridges Nrf2 to a Cul3-based E3 ligase: oxidative stress sensing by a Cul3-Keap1 ligase. *Mol. Cell Biol.*, 24, 8477–8486.

Dabernat, S. A., Masse, K., Smani, M., Peuchant, E., Landry, M., Bourbon, P. M., le Floch, R., Daniel, J. Y. and Larou, M. (2004). Nm23-M2/NDP kinase B induces endogenous c-myc and nm23-M1/NDP kinase A overexpression in BAF3 cells. Both NDP kinases protect the cells from oxidative stress-induced death. *Exp. Cell Res*., 301, 293-304.

Danaei, G., Vander Hoorn, S., Lopez, A. D., Murray, C. J. and Ezzati, M. (2005). Causes of cancer in the world: comparative risk assessment of nine behavioural and environmental risk factors. *Lancet*, 366, 1784-1793.

Dannenberg, A. J. and Subbaramaiah, K. (2003). Targeting cyclooxygenase-2 in human neoplasia: Rationale and promise. *Cancer Cell*, 4, 341-436.

Delgado, G., Hernandez, J. and Pereda-Miranda, R. (1989). Triterpenoid acids from *Cunila Lythrifolia*. *Phytochemistry*, 28(5), 1483-1485.

Dhakshinamoorthy, S. and Jaiswal, A. K. (2001). Functional characterization and role of INrf2 in antioxidant response element-mediated expression and antioxidant induction of NAD(P)H:quinone oxidoreductase 1 gene.

Oncogene, 20, 3906–3917.

Dong, X., Liu, F., Sun, L., Liu, M., Li, D., Su, D., Zhu, Z., Dong, J. T., Fu, L. and Zhou, J. (2010). Oncogenic function of microtubule end-binding protein 1 in breast cancer. *J. Pathol.*, 220(3), 361-369.

Dorai, T. and Aggarwal, B. B. (2004). Role of chemopreventive agents in cancer therapy. *Cancer Lett.*, 215, 129-140.

Dzubak, P., Hajduch, M., Vydra, D., Hustova, A., Kvasnica, M. and Biedermann, D. (2006). Pharmacological activities of natural triterpenoids and their therapeutic implications. *Nat. Prod. Rep.*, 23, 394-411.

Eferl, R. and Wagner, E. F. (2003). AP-1: a double-edged sword in tumourigenesis. *Nat. Rev. Cancer*, 3, 859–868.

Eggler, A. L., Liu, G., Pezzuto, J. M., van Breemen, R. B. and Mesecar, A. D. (2005). Modifying specific cysteines of the electrophile-sensing human Keap1 protein is insufficient to disrupt binding to the Nrf2 domain Neh2. *Proc. Natl. Acad. Sci.*, 102, 10070–10075.

Eggler, A. L., Gay, K. A. and Mesecar, A. D. (2008). Molecular mechanisms of natural products in chemoprevention: Induction of cytoprotective enzymes by Nrf2. *Mol. Nutr. Food Res.*, 52, 84-94.

Eliopoulos, A. G., Davies, C., Blake, S. S. M., Murray, P., Najafipour, S., Tsichlis, P. N. and Young, L. S. (2002). The Oncogenic Protein Kinase Tpl-2/Cot Contributes to Epstein-Barr Virus-Encoded Latent Infection Membrane Protein 1-Induced NF-κB Signaling Downstream of TRAF2. *J. Virol.*, 76(9), 4567–4579.

Farrell, P. J., Rowe, D. T., Rooney, C. M. and Kouzarides, T. (1989). Epstein-Barr virus BZLF1 trans-activator specifically binds to a consensus AP-1 site and is related to c-Fos. *EMBO J.*, 8, 127–132.

Flora, S. D. and Ferguson, L. R. (2005). Overview of mechanisms of cancer chemopreventive agents. *Mutat. Res.*, 591, 8-15.

Furukawa, M. and Xiong, Y. (2005). BTB protein Keap1 targets antioxidant transcription factor Nrf2 for ubiquitination by the Cullin 3-Roc1 ligase. *Mol. Cell Biol.*, 25, 162-171.

Gez, S., Crossett, B. and Christopherson, R. I. (2007). Differentially expressed cytosolic proteins in human leukemia and lymphoma cell lines correlate with lineages and functions. *Biochim. Biophys. Acta.*, 1774, 1173-1183.

Ghosh, S. (2007). Handbook of transcription factor NF-kappa B. United States of America: CRC Press.

Ghosh, S. and Hayden, M. S. (2008). New regulators of NF-κB in inflammation. *Nat. Rev.*, 8, 837-848.

Graf, B. A., Nazarenko, D. A., Borrello, M. A., Roberts, L. J., Morrow, J. D. and Palis, J. (1999). Biophenotypic B/macrophage cells express COX-1 and up-regulate COX-2 expression and prostaglandin E (2) production in response to pro-inflammatory signals. *Eur. J. Immunol.*, 29, 3793-3803.

Grunstein, M. (1997). Histone acetylation in chromatin structure and transcription. *Nature*, 389, 349–352.

Guillen, N., Acin, S., Surra, J.C., Arnal, C., Godino, J., García-Granados, A., Muniesa, P., Ruiz-Gutiérrez, V. and Osada, J. (2009). Apolipoprotein E determines the hepatic transcriptional profile of dietary maslinic acid in mice. *J. Nutr. Biochem.*, 20, 882-893.

Han, S. S., Keum, Y. S., Seo, H. J. and Surh, Y-J. (2002). Curcumin suppresses activation of NF-kappaB and AP-1 induced by phorbol ester in cultured human promyelocytic leukemia cells. *J. Biochem. Mol. Biol.*, 35(3), 337–342.

Haridas, V., Hanausek, M., Nishimura, G., Soehnge, H., Gaikwad, A., Narog, M., Spears, E., Zoltaszek, R., Walaszek, Z. and Gutterman, J. U. (2004). Triterpenoid electrophiles (avicins) activate the innate stress response by redox regulation of a gene battery. *J. Clin. Invest.*, 113, 65–73.

Hartsfield, C. L., Alam, J., Choi, A. M.K. 1998. Transcriptional regulation of the heme oxygenase 1 gene by pyrrolidine dithiocarbamate. *FASEB J.*, 17, 1675-1682.

Hausen, H., Bomkamm, G. W., Schmidt, R. and Hecker, E. (1979). Tumor initiators and promoters in the induction of Epstein-Barr virus. *Proc. Natl. Acad. Sci.*, 76, 782-785.

He, Z. M., Xin, B. Z., Yang, X. H., Chan, C. P. and Cao, L. (2000). Nuclear factor-kappa B activation is involved in LMP1-mediated transformation and tumorigenesis of Rat-1 fibroblasts. *Cancer Res.*, 60, 1845–1848.

Hebbes, T. R., Thorne, A. W. and Crane-Robinson, C. (1988). A direct link between core histone acetylation and transcriptionally active chromatin. *EMBO J.*, 7, 1395–1402.

Hergenhahn, M., Soto, U., Weninger, A., Polack, A., Hsu, C. H. and Cheng, A. L. (2002). The chemopreventive compound curcumin is an efficient inhibitor of Epstein–Barr virus BZLF1 transcription in Raji DR-LUC cells. *Mol. Carcinog.*, 33(3), 137–145.

Hoelzl, C., Lorenz, O., Haudek, V., Gundacker, N., Knasmüller, S. and Gerner, C. (2008). Proteome alterations induced in human white blood cells by consumption of Brussels sprouts: Results of a pilot intervention study. *Proteomics*, 2(1), 108-117.

Hong, G. K., Delecluse, H-J., Gruffat, H., Morrison, T. E., Feng, W-H., Sergeant, A. and Kenney, S. C. (2004). The BRRF1 Early Gene of Epstein-Barr Virus Encodes a Transcription Factor That Enhances Induction of Lytic Infection by BRLF1. *J. Virol.*, 78 (10), 4983–4992.

Hsiang, C. Y., Wu, S. L. and Ho, T. Y. (2005). Morin inhibits 12-O-tetradecanoylphorbol-13-acetate-induced hepatocellular transformation via activator protein 1 signaling pathway and cell cycle progression. *Biochem. Pharmacol*., 69(11), 1603-1611.

Hsum, Y. W., Yew, W. T., Lim, P. V. H., Soo, K. K., Hoon, L. S., Chieng, Y. C., Mooi, L. Y. (2011). Cancer chemopreventive activity of maslinic acid: suppression of COX-2 expression and inhibition of NF-κB and AP-1 activation in Raji cells. *Planta Med*., 77, 152-157.

Huang, H. C., Nguyen, T. and Pickett, C. B. (2002). Phosphorylation of Nrf2 at Ser-40 by protein kinase C regulates antioxidant response element-mediated transcription. *J. Biol. Chem.*, 277, 42769–42774.

Hyde, C. A. C. and Missailidis, S. (2009). Inhibition of arachidonic acid metabolism and its implication on cell proliferation and tumour-angiogenesis. *Int. Immunopharmacol.*, 9, 701–715.

Inoue, J., Gohda, J., Akiyama, T. and Semba, K. (2007). NF-kappa B activation in development and progression of cancer. *Cancer Sci*., 98(3), 268-274.

Issa, A. Y., Volate, S. R. and Wargovich, M. J. (2006). The role of phytochemicals in inhibition of cancer and inflammation: New directions and perspectives. *J. Food Compost. Anal.,* 19, 405-419.

Ito, Y., Kawanishi, M., Harayama, T. and Takabayashi, S. (1981). Combined effect of the extracts from Croton tiglium, Euphorbia lathyris or Euphorbia tirucalli and n-butyrate on Epstein-Barr virus expression in human lymphoblastoid P3HR-1 and Raji cells. *Cancer Lett.*, 175-180.

Itoh, K., Chiba, T., Takahashi, S., Ishii, T., Igarashi, K., Katoh, Y., Oyake, T., Hayashi, N., Satoh, K., Hatayama, I., Yamamoto, M. and Nabeshima, Y. (1997). An Nrf2/small Maf heterodimer mediates the induction of phase II detoxifying enzyme genes through antioxidant response elements. *Biochem. Biophys. Res. Commun*., 236, 313–322.

Itoh, K., Wakabayashi, N., Katoh, Y., Ishii, T., Igarashi, K., Engel, J. D. and Yamamoto, M. (1999). Keap1 represses nuclear activation of

antioxidant responsive elements by Nrf2 through binding to the amino-terminal Neh2 domain. *Genes Dev.*, 13, 76–86.

Itoh, K., Wakabayashi, N., Katoh, Y., Ishii, T., OConnor, T. and Yamamoto, M., (2003). Keap1 regulates both cytoplasmic-nuclear shuttling and degradation of Nrf2 in response to electrophiles. *Genes Cells*, 8, 379-391.

Jain, A. K., Bloom, D. A. and Jaiswal, A. K. (2005). Nuclear import and export signals in control of Nrf2. *J. Biol. Chem.*, 280, 29158–29168.

Jain, A. K. and Jaiswal, A. K. (2006). Phosphorylation of tyrosine 568 controls nuclear export of Nrf2. *J. Biol. Chem.*, 281, 12132-12142.

Jaiswal, A. K. (2004). Nrf2 signaling in coordinated activation of antioxidant gene expression. *Free Radic. Biol. Med.*, 36, 1199–1207.

Janakiram, N. B., Indranie, C., Malisetty, S. V., Jagan, P., Steele, V. E. and Rao, C. V. (2008). Chemoprevention of Colon Carcinogenesis by Oleanolic Acid and Its Analog in Male F344 Rats and Modulation of COX-2 and Apoptosis in Human Colon HT-29 Cancer Cells. *Pharm. Res.*, 25, 2151-2157.

Jeha, S., Luo, X. N., Beran, M., Kantarjian, H. and Atweh, G. F. (1996). Antisense RNA inhibition of phosphoprotein p18 expression abrogates the transformed phenotype of leukemic cells. *Cancer Res.*, 56, 1445–1450.

Jemal, A., Bray, F., Center, M. M., Ferlay, J., Ward, E. and Forman, D. (2011). Global cancer statistics. *CA Cancer J. Clin*., 61(2), 69-90.

Jiang, Z. Q., Chen, C., Yang, B., Hebbar, V. and Kong, A. N. (2003). Differential responses from seven mammalian cell lines to the treatments of detoxifying enzyme inducers. *Life Sci*., 72, 2243-2253.

Jin, J. L., Lee, Y. Y., Heo, J. E., Lee, S., Kim, J. M. and Choi, H. S. Y. (2004). Anti-Platelet Pentacyclic Triterpenoids from Leaves of *Campsis grandiflora*. *Arch. Pharm. Res.* 27(4), 376-380.

Jin, L., Liu, G., Zhang, C., Lu, C., Xiong, S., Zhang, M., Ge, F., He, Q., Kitazato, K., Kobayashi, N., Wang, Y. and Liu, Q. (2009). Nm23-H1 regulates the proliferation and differentiation of the human chronic myeloid leukemia K562 cell line: A functional proteomics study. *Life Sci*., 84, 458-467.

Jones, S., Zhang, X., Parsons, D. W., Lin, J. C., Leary, R. J., Angenendt, P., Mankoo, P., Carter, H., Kamiyama, H., Jimeno, A., Hong, S. M., Fu, B., Lin, M. T., Calhoun, E. S., Kamiyama, M., Walter, K., Nikolskaya, T., Nikolsky, Y., Hartigan, J., Smith, D. R., Hidalgo, M., Leach, S. D., Klein, A. P., Jaffee, E. M., Goggins, M., Maitra, A., Iacobuzio-

Donahue, C., Eshleman, J. R., Kern, S. E., Hruban, R. H., Karchin, R., Papadopoulos, N., Parmigiani, G., Vogelstein, B., Velculescu, V. E. and Kinzler, K. W. (2008). Core signaling pathways in human pancreatic cancers revealed by global genomic analyses. *Science*, 321(5897), 1801–1806.

Joy, P., Thomas, J., Mathew, D. and Skaria, B. (2001). Medicinal Plants. Calcutta: Tropical Horticulture, Naya Prokas.

Kaspar, J. W., Niture, S. K. and Jaiswal, A. K. (2009). Nrf2:INrf2 (Keap1) signaling in oxidative stress. *Free Radic. Biol. Med.*, 47, 1304-1309.

Kassie, F., Sundermann, V. M., Edenharder, R., Platt, K. L., Darroudi, F., Lhoste, E., Humbolt, C., Muckel, E., Uhl, M., Kundi, M. and Knasmuller, S. (2003). Development and application of test methods for the detection of dietary constituents which protect against heterocyclic aromatic amines. *Mutat. Res*., 523-524, 183-192.

Kaul, R., Verma, S. C., Murakami, M., Lan, K., Choudhuri, T. and Robertson, E. S. (2006). Epstein-Barr Virus Protein Can Upregulate Cyclo-Oxygenase-2 Expression through Association with the Suppressor of Metastasis Nm23-H1. *J. Virol.*, 80(3), 1321–1331.

Khor, T. O., Huang, M. T., Kwon, K. H., Chan, J. Y., Reddy, B. S., and Kong, A. N. (2006). Nrf2-deficient mice have an increased susceptibility to dextran sulfate sodiuminduced colitis. *Cancer Res*., 66, 11580-11584.

Kim, Y. K., Yoon, S. K. and Ryu, S. Y. (2000). Cytotoxic triterpenes from stem bark of *Physocarpus intermedius*. *Planta Med*., 66, 485-486.

Knowles, M. and Selby, P. (2006). Introduction to the cellular and molecular biology of cancer. Great Britain: Oxford University Press.

Kobayashi, M. and Yamamoto, M. (2006). Nrf2–Keap1 regulation of cellular defense mechanisms against electrophiles and reactive oxygen species *Advan. Enzyme Regul.*, 46, 113–140.

Kobayashi, A., Kang, M. I., Watai, Y., Tong, K. I., Shibata, T., Uchida, K. and Yamamoto, M. (2006). Oxidative and electrophilic stresses activate Nrf2 through inhibition of ubiquitination activity of Keap1. *Mol. Cell Biol.*, 26, 221–229.

Kobayashi, R., Deavers, M., Patenia, R., Rice-Stitt, T., Halbe, J., Gallardo, S. and Freedman, R. S. (2009). 14-3-3 zeta protein secreted by tumor associated monocytes/ macrophages from ascites of epithelial ovarian cancer patients. *Cancer Immunol. Immunother.*, 58, 247-258.

Kojima, H. and Ogura, H. (1986). Triterpenoids from *Prunella vulgaris*. *Phytochemistry*, 25, 729-733.

Kojima, H. and Ogura, H. (1989). Configuration studies on hydroxyl groups at C-2, 3 and 23 or 24 of oleanene and ursene-type triterpenes by NMR spectroscopy. *Phytochemistry*, 28, 1703-1710.

Konoshima, T., Takasaki, M., Tatsumoto, T., Kozuka, M. and Kasai, R. T. (1994). Inhibitory effects of cucurbitane triterpenoids on Epstein-Barr virus activation and two-stage carcinogenesis of skin tumours. *Biol. Pharm. Bull*., 17, 668-671.

Kosaka, T., Miyata, A., Ihara, H., Hara, S., Sugimoto, T. and Takeda, O. (1994). Characterization of the human gene (PTGS2) encoding prostaglandin- endoperoxide synthase 2. *Eur. J. Biochem.*, 221, 889–97.

Kundu, J. K. and Surh, Y-J. (2005). Breaking the relay in deregulated cellular signal transduction as a rationale for chemoprevention with anti-inflammatory phytochemicals. *Mutat. Res.*, 591, 123-146.

Kundu, J. K. and Surh, Y-J. (2008). Inflammation: Gearing the journey to cancer. *Mutat. Res.*, 659, 15-30.

Kundu, J. K. and Surh, Y-J. (2010). Nrf2-Keap1 Signaling as a Potential Target for Chemoprevention of Inflammation-Associated Carcinogenesis. *Pharm. Res*., 27(6), 999-1013.

Lau, A., Villeneuve, N. F., Sun, Z., Wong, P. K. and Zhang, D. D. (2008). Dual roles of Nrf2 in cancer. *Pharm. Res.*, 58, 262-270.

Ledford, H. (2010). The cancer genome challenge. *Nature*, 464, 972-974.

Lee, D. Y., Hayes, J. J., Pruss, D. and Wolffe, A. P. (1993). A positive role for histone acetylation in transcription factor access to nucleosomal DNA. *Cell*, 72, 73–84.

Lee, J-M and Johnson, J. A. (2004). An Important Role of Nrf2-ARE Pathway in the Cellular Defense Mechanism. *J. Biochem. Mol. Biol.,* 37(2), 139-143.

Lee, O., Jain, A. K., Papusha, V. and Jaiswal, A. K. (2007). An auto-regulatory loop between stress sensors INrf2 and Nrf2 controls their cellular abundance. *J. Biol. Chem.*, 282, 36412-36420.

Lee, E-K, Han, G-Y, Park, H. W., Song, Y. J. and Kim, C. W. (2010). Transgelin Promotes Migration and Invasion of Cancer Stem Cells. *J. Proteome Res.*, 9(10), 5108–5117.

Li, J., Johnson, D., Calkins, M., Wright, L., Svendsen, C. and Johnson, J. (2005). Stabilization of Nrf2 by tBHQ Confers Protection against Oxidative Stress-Induced Cell Death in Human Neural Stem Cells. *Toxicol. Sci.*, 83, 313–328.

Li, C., Yang, Z., Zhai, C., Qiu, W., Li, D., Yi, Z., Wang, L., Qian, M., Luo, J., Liu, M. and Tang, J. (2010). Maslinic acid potentiates the anti-tumor activity of tumor necrosis factor α by inhibiting NF-kB signaling pathway. *Mol. Cancer*, 9, 73.

Liebold, B. W., Graack, H. R. and Pohl, T. (2006). Two-dimensional gel electrophoresis as tool for proteomics studies in combination with protein identification by mass spectrometry. *Proteomics*, 6, 4688-4703.

Lim, Y. M. (2002). *Anti-tumour Promoting Activity Of Selected Malaysian Vegetables And Fruits, And Identification Of Anti-tumour Promoting And Antioxidant Compounds From Coleus Tuberosus, Benth (ubi Kemili)*, Ph.D. Thesis, Universiti Putra Malaysia, Malaysia.

Liu, H., Colavitti, R., Rovira, I. I. and Finkel T. (2005). Redox-dependent transcriptional regulation. *Circ. Res.*, 97, 967–974.

Liu, J. (2005). Oleanolic acid and ursolic acid: Research prospectives. *J. Ethnopharmacol*, 100, 92-94.

Liu, J., Wu, Q., Lu, Y-F, and Pi, J. (2008). New insights into generalized hepatoprotective effects of oleanolic acid: Key roles of metallothionein and Nrf2 induction. *Biochem. pharmacol.*, 76, 922–928.

Livak, K. J. and Schmittgen, T. D. (2001). Analysis of Relative Gene Expression Data Using RealTime Quantitative PCR and the $2^{-\Delta\Delta CT}$ Method. *Methods*, 25, 402–408.

Lo, S. C., Li, X., Henzl, M. T., Beamer, L. J. and Hannink, M. (2006). Structure of the Keap1:Nrf2 interface provides mechanistic insight into Nrf2 signaling. *EMBO. J.*, 25, 3605–3617.

Long, D. J., Waikel, R. L., Wang, X. J., Perlaky, L., Roop, D. R. and Jaiswal, A. K. (2000). NAD(P)H:quinone oxidoreductase 1 deficiency increases susceptibility to benzo(a)pyrene-induced mouse skin carcinogenesis. *Cancer Res.*, 60, 5913–5915.

Loo, G. (2003). Redox-sensitive mechanisms of phytochemicals-mediated inhibition of cancer cell proliferation. *J. Nutr. Biochem.*, 14, 64–73.

Lopez, J. L. (2007). Two-dimensional electrophoresis in proteome expression analysis. *J. Chromatogr. B Analyt. Technol. Biomed. Life Sci.*, 849, 190-202.

Lu, Q., Yang, Y., Jin, J. S., Zhang, Z., Heber, D. and Li, F. L. (2009). Effects of green tea extract on lung cancer A549 cells: Proteomic identification of proteins associated with cell migration. *Proteomics*, 9, 757-767.

Luka, J., Kallin, B. and Klein, G. (1979). Induction of the Epstein-Barr virus (EBV) cycle in latently infected cells by n-butyrate. *Virology*, 94, 228-

231.

Malumbres, M. and Barbacid, M. (2001). To cycle or not to cycle: a critical decision in cancer. *Nat. Rev. Cancer*, 1, 222-231.

Marie, G., Kemp, P. A. and Boiteux, S. (2006). dUTPase activity is critical to maintain genetic stability in Saccharomyces cerevisiae. *Nucleic Acids Res*., 34(7), 2056–2066.

Marks, F., Muller-Decker, K. and Furstenberger, G. (2000). A causal relationship between unscheduled eicosanoid signaling and tumor development: cancer chemoprevention by inhibitors of arachidonic acid metabolism. *Toxicology*, 153, 11–26.

Martin, D. B. and Nelson, P. S. (2001). From genomics to proteomics: techniques and applications in cancer research. *Trends Cell Biol.*, 11, 60-65.

Martín, M. A., Vázquez, R., Arche, A. and Gutiérrez, A. (2006). Suppressive effect of maslinic acid from pomace olive oil on oxidative stress and cytokine production in stimulated murine macrophages. *Free Radic. Res*., 40, 295–302.

Martin, R., Carvalho, J., Ibeas, E., Hernandez, M., Ruiz-Gutierrez, V. and Nieto, M. L. (2007). Acidic Triterpenes Compromise Growth and Survival of Astrocytoma Cell Lines by Regulating Reactive Oxygen Species Accumulation. *Cancer Res*., 67(8), 3741-3751.

Mashima, T., Naito, M., Fujita, N., Noguchi, K. and Tsuruo, T. (1995). Identification of actin as a substrate of ICE and an ICElike protease and involvement of an ICE-like protease but not ICE in Vp-16-induced U937 apoptosis. *Biochem. Biophys. Res. Commun*., 217, 1185-1192.

Matthews, C. P., Colburn, N. H. and Young, M. R. (2007). AP-1 a target for cancer prevention. *Curr. Cancer Drug Targets*, 7, 317-324.

Mayer, B. and Oberbauer, R. (2003). Mitochondrial regulation of apoptosis. *News Physiol. Sci.*, 18, 89-94.

McFarland, E. D., Davidson, D. M., Schauer, S. L., Duong, J. and Kieff, E. (2000). NF-κB inhibition causes spontaneous apoptosis in Epstein-Barr virus-transformed lymphoblastoid cells. *Proc. Natl. Acad. Sci.*, 97, 6055-6060.

McMahon, M., Thomas, N., Itoh, K., Yamamoto, M. and Hayes, J. D. (2006). Dimerization of substrate adaptors can facilitate cullin-mediated ubiquitylation of proteins by a "tethering" mechanism: a two-site interaction model for the Nrf2–Keap1 complex. *J. Biol. Chem*., 281, 24756–24768.

Mead, J., Alfin-Slater, R., Howton, D. and Popjak, G. (1986). Prostaglandins, Thromboxanes, and Prostacyclin. New York: Plenum Press.

Mentzer, S. J., Fingeroth, J., Reilly, J. J., Perrine, S. P. and Faller, D. V. (1998). Arginine butyrate-induced susceptibility to ganciclovir in an Epstein-Barr virus-associated lymphoma. *Blood Cells Mol. Dis*., 24, 114–123.

Mohler, J., Mahaffey, J. W., Deutsch, E. and Vani, K. (1995). Control of Drosophila head segment identity by the bZIP homeotic gene CNC. *Development*, 121, 237–247.

Mollinedo, F., Gajate, C., Tugores, A., Flores, I and Naranjo, J. R. (1993). Differences in expression of transcription factor AP-1 in human promyelocytic HL-60 cells during differentiation towards macrophages versus granulocytes. *Biochem. J.*, 294, 137-144.

Montilla, M., Agil, A., Navarro, M., Jimenez, M. and Granados, A. Parra, A. (2003). Antioxidant Activity of Maslinic Acid, a Triterpene Derivative Obtained fron Olea europaea. *Planta Med*., 69, 472-474.

Motohashi, H., O'Connor, T., Katsuoka, F., Engel, J.D. and Yamamoto, M. (2002). Integration and diversity of the regulatory network composed of Maf and CNC families of transcription factors. *Gene*, 294, 1–12.

Murakami, A., Jiwajinda, S., Koshimiza, K. and Ohigashi, H. (1995). Screening for *in-vitro* anti-tumor promoting activities of edible plants from Thailand. *Cancer Lett.*, 95, 139-149.

Murakami, A. and Ohigashi, H. (2007). Targeting NOX, INOS and COX-2 in inflammatory cells: Chemoprevention using food phytochemicals. *Int. J. Cancer*, 121, 2357–2363.

Murono, S., Inoue, H., Tanabe, T., Joab, I., Yoshizaki, T., Furukawa, M. and Pagano, J. S. (2001). Induction of cyclooxygenase-2 by Epstein-Barr virus latent membrane protein 1 is involved in vascular endothelial growth factor production in nasopharyngeal carcinoma cells. *Proc. Natl. Acad. Sci.*, 98, 6905–6910.

Mussini, P., Fulvia, O., Francesca, P. (1975). Triterpenes in leaves of *Olea europaea*. *Phytochemistry*, 14(4), 1135.

Nakshatri, H., Bhat-Nakshatri, P., Martin, D. A., Goulet, R. J. and Sledge, G.W. (1997). Constitutive activation of NF-κB during progression of breast cancer to hormone-independent growth. *Mol. Cell Biol*., 17(7), 3629-3639.

Naugler, W. E. and Karin, M. (2008). NF-κB and cancer. *Curr. Opin. Genet. Dev.*, 18, 19-26.

Ngounou, F. N., Lontsi, D. and Sondengam, B. L. (1988). A pentacyclic

triterpene diacid from *Myrianthus Arboreus*. *Phytochemistry*, 27(7), 2287-2289.

Nguyen, T., Huang, H. C. and Pickett, C. B. (2000). Transcriptional regulation of the antioxidant response element: activation by Nrf2 and repression by MafK. *J. Biol. Chem*., 275, 15466–15473.

Nguyen, T., Sherratt, P. J., Huang, H.-C., Yang, C. S. and Pickett, C. B. (2003). Increased protein stability as a mechanism that enhances Nrf2-mediated transcriptional activation of the antioxidant response element. Degradation of Nrf2 by the 26 S proteasome. *J. Biol. Chem*., 278, 4536-4541.

Nioi, P., McMahon, M., Itoh, K., Yamamoto, M. and Hayes, J. D. (2003). Identification of a novel Nrf2-regulated antioxidant response element (ARE) in the mouse NAD(P)H:quinone oxidoreductase 1 gene: reassessment of the ARE consensus sequence. *Biochem. J.*, 374, 337-348.

Nishizuka, Y. (1984). The role of Protein Kinase C in cell surface signal transduction and tumour promotion. *Nature*, 308(5961), 693-698.

Nobili, S., Lippi, D., Witort, E., Donnini, E., Bausi, L., Mini, L. and Capaccioli, S. (2009). Natural compounds for cancer treatment and prevention. *Pharmacol. Res.,* 59, 365-378.

Nutter, L. M., Grill, S. P., Li, J., Tan, R. and Cheng, Y. (1987). Induction of virus enzymes by phorbol esters and n-butyrate in Epstein-Barr virus genome-carrying Raji cells. *Cancer Res*., 47, 4407-4412.

Ohigashi, H., Takamura, H., Koshimizu, K., Tokuda, H. and Ito, Y. (1986). Search for possible antitumor promoters by inhibition of 12-o-tetradecanoylphorbol-13-acetate-induced Epstein-Barr virus activation: ursolic acid and oleanolic acid from an anti-inflammatory Chinese medicinal plant, *Glechoma hederaceae L. Cancer Lett*., 30, 143-151.

Ohmori, K., Miyazaki, K. and Umeda, M. (1998). Detection of tumor promoters by early antigen expression of EB virus in Raji cells using a fluorescence microplate-reader. *Cancer Lett.*, 132, 51–59.

Ojinnaka, C. M., Okogun, J. I., Okorie, D. A. (1980). Triterpene acids from *Myrianthus arboreus*. *Phytochemistry*, 19(11), 2482-2483.

Park, S., Lee, D. K., Whang, Y. H. and Yang, C. H. (2000). Momordin I, a compound of ampelopsis radix, inhibits AP-1 activation induced by phorbol ester. *Cancer Lett*., 152, 1-8.

Park, C. H., Lee, J. H. and Yang, C. H. (2005). Curcumin derivatives inhibit the formation of Jun-Fos-DNA complex independently of their conserved cysteine residues. *J. Biochem. Mol. Biol.*, 38, 474–480.

Parsons, D. W., Jones, S., Zhang, X., Lin, J.C., Leary, R. J., Angenendt, Mankoo, P., Carter, H., Siu, I-M., Gallia, G. L., Olivi, A., McLendon, R., Rasheed, B. A., Keir, S., Nikolskaya, T., Nikolsky, Y., Busam, D. A., Tekleab, H., Diaz, L. A., Hartigan, J., Smith, D. R., Strausberg, R. L., Marie, S. K. N., Shinjo, S. K. O., Yan, H., Riggins, G. J., Bigner, D. D., Karchin, R., Papadopoulos, N., Parmigiani, G., Vogelstein, B., Velculescu, V. E. and Kinzler, K. W. (2008). An integrated genomic analysis of human glioblastoma multiforme. *Science*, 321, 1807–1812.

Pastwa, E., Somiari, S. B., Czyz, M. and Somiari, R. I. (2007). Proteomics in human cancer research. *Proteomics Clin. App.*, 1, 4-17.

Pavletich, N. P. (1999). Mechanisms of cyclin-dependent kinase regulation: structures of Cdks, their cyclin activators, and Cip and INK4 inhibitors. *J. Mol. Biol.*, *287*, 821-828.

Pereda-Miranda, R. and Gascbn-Figueroa, M. (1988). Chemistry of Hyptis Mutabilis: New pentacyclic triterpenoids. *J. Nat. Prod.*, 51, 996-998.

Perrine, S. P., Miller, B. A. and Faller, D. V. (1989). Sodium butyrate enhances fetal globin gene expression in erythroid progenitors of patients with Hb SS and b thalassemia. *Blood*, 74, 454–459.

Plummer, S. M., Holloway, K. A., Manson, M. M., Munks, R. J., Kaptein, A. and Farrow, S. (1999). Inhibition of cyclo-oxygenase 2 expression in colon cells by the chemopreventive agent curcumin involves inhibition of NF-kappaB activation via the NIK/IKK signalling complex. *Oncogene*, 18(44), 6013–6020.

Poss, K. D. and Tonegawa, S. (1997). Reduced stress defense in heme oxygenase 1-deficient cells. *Proc. Natl. Acad. Sci.*, 94, 10925–10930.

Prades, J., Vögler, O., Alemany, R., Gomez-Florit, M., Funari, S. S., Ruiz-Gutierrez, V. and Barcel, F. (2011). Plant pentacyclic triterpenic acids as modulators of lipid membrane physical properties. *Biochim. Biophys. Acta*, 1808, 752–760.

Prestera, T. and Talalay, P. (1995). Electrophile and antioxidant regulation of enzymes that detoxify carcinogens. *Proc. Natl. Acad. Sci.*, 92, 8965–8969.

Reisman, S. A., Aleksunes, L. M. and Klaassen, C. D. (2009). Oleanolic acid activates Nrf2 and protects from acetaminophen hepatotoxicity via Nrf2-dependent and Nrf2-independent processes. *Biochem. pharmacol.*, 77, 1273–1282.

Reyes, F. J., Centelles, J., Lupianez, J. A. and Cascante, M. (2006). (2a,3b)-2,3-Dihydroxyolean-12-en-28-oic acid, a new natural triterpene from Olea europea, induces caspase dependent apoptosis selectively in colon

adenocarcinoma cells. *FEBS Lett.*, 580, 6302-6310.

Reyes, F. Z., Palomares, E. R. and Lupiáñez, J. M. C. (2008). Maslinic acid, a natural triterpene from Olea europaea L., induces apoptosis in HT29 human colon-cancer cells via the mitochondrial pathway. *Cancer Lett*., 273, 44-54.

Rubin, C. L. and Atweh, G. F. (2004). The Role of Stathmin in the Regulation of the Cell Cycle. *J. Cell. Biochem*., 93, 242-250.

Ruddon, R.W. (2007). Cancer Biology. New York: Oxford University Press

Rushmore, T. H., Morton, M. R. and Pickett, C. B. (1991). The antioxidant responsive element: activation by oxidative stress and identification of the DNA consensus sequence required for functional activity. *J. Biol. Chem.*, 266, 11632–11639.

Rushworth, S. A., MacEwan, D. J., O'Connell, M. A. (2008). Lipopolysaccharideinduced expression of NAD(P)H:quinone oxidoreductase 1 and heme oxygenase-1 protects against excessive inflammatory responses in human monocytes. *J. Immunol.*, 181, 6730–6737.

Russo, G. L. (2007). Ins and outs of dietary phytocehmicals in cancer chemoprevention. *Biochem. Pharmacol*., 74, 533-544.

Saimaru, H. Orihara, Y., Tansakul, P., Kang, Y-H., Shibuya, M. and Ebizuka, Y. (2007). Production of Triterpene Acids by Cell Suspension Cultures of Olea europaea. *Chem. Pharm. Bull.*, 55(5), 784—788.

Salminen, A., Lehtonen, M., Suuronen, T., Kaarniranta, K. and Huuskonen, J. (2008). Terpenoids: natural inhibitors of NF-kappaB signaling with anti-inflammatory and anticancer potential. *Cell Mol. Life Sci.*, 65(19), 2979-2999.

Sarkar, F. H. and Li, W. (2004). Cell signaling pathways altered by natural chemopreventive agents. *Mutat. Res.*, 555, 53-64.

Sealy, L. and Chalky, R. (1978). The effect of sodium butyrate on histone modification. *Cell*, 14, 115-121.

Sharkey, N. A., Leach, K. L. and Blumberg, P. M. (1984). Competitive inhibition by diacylglycerol of specific phorbol ester binding. *Proc. Natl. Acad. Sci.*, 81, 607–610.

Shaulian, E. and Karin, M. (2002). AP-1 as a regulator of cell life and death. *Nat. Cell Biol.*, 4, 131-136.

Shoshan-Barmatz, V., Keinan, N. and Zaid, H. (2008). Uncovering the role of VDAC in the regulation of cell life and death. *J. Bioenerg. Biomembr.*,

40(3), 183-191.

Smirnov, A. S., Ruzov, A. S., Budanov, A. V., Prokhortchouk, A. V., Ivanov, A. V. and Prokhortchouk, E. B. (2001). High constitutive level of NF-κB is crucial for viability of adenocarcinoma cells. *Cell Death Diff.*, 8, 621–630.

Sporn, M. B., Dunlop, N. M., Newtonm D. L. and Smith, J. M. (1976). Prevention of chemical carcinogenesis by vitamin A and its synthetic analogs (retinoids). *Fed. Proc*., 35, 1332-1338.

Subbaramaiah, K., Michaluart, P., Sporn, M. B. and Dannenberg, A. J. (2000). Ursolic Acid Inhibits Cyclooxygenase Transcription in Human Mammary Epithelial Cells. *Cancer Res.*, 60, 2399–2404.

Subbaramaiah, K. and Dannenberg, A. J. (2003). Cyclooxygenase 2: a molecular target for cancer prevention and treatment. *Trends Pharmacol. Sci*., 24(2), 96–102.

Surh, Y-J., Chun, K. S., Cha, H. H., Han, S. S., Keum, Y. S. and Park, K. K. (2001). Molecular mechanisms underlying chemopreventive activities of anti-inflammatory phytochemicals: down-regulation of COX-2 and iNOS through suppression of NF-kappa B activation. *Mutat. Res.*, 480-481, 243-268.

Surh, Y-J. (2003). Cancer chemoprevention with dietary phytochemicals. *Nat. Rev. Cancer*, 3, 768-780.

Surh, Y-J., Kundu, J. K., Na, H-K. and Lee, J-S. (2005). Redox-sensitive transcription factors as prime targets for chemoprevention with anti-inflammatory and antioxidative phytochemicals. *J. Nutr*., 135, 2993–3001.

Tanigawa, S., Fujii, M. and Hou, D-X. (2007). Action of Nrf2 and Keap1 in ARE-mediated NQO1 expression by quercetin. *Free Radic. Biol. Med.*, 42, 1690-1703.

Taniguchi, S., Imayoshi, Y., Kobayashi, E., Takamatsu, Y., Ito, H., Hatano, H., Sakagami, H., Tokuda, H., Nishino, H., Sugita, D., Shimura, S. and Yoshida, T. (2002). Production of bioactive triterpenes by *Eriobotrya japonica* calli. *Phytochemistry*, 59, 315-323.

Tinkelenberg, B. A., Hansbury, M. J. and Ladner, R. D. (2002). dUTPase and Uracil-DNA Glycosylase Are Central Modulators of Antifolate Toxicity in Saccharomyces cerevisiae. *Cancer Res.*, 62, 4909–4915.

Tong, K. I., Kobayashi, A., Katsuoka, F. and Yamamoto, M. (2006). Two-site substrate recognition model for the Keap1-Nrf2 system: a hinge and latch mechanism. *Biol. Chem.*, 387, 1311–1320.

Tsuen-Ih, R., Kakisawa, H., Chen, Y.P., Hsü, H.Y. (1976). Terpenoids from *Elaeagnus oldahmi*. *Phytochemistry*, 15(2), 335.

Tulchinsky, E. (2000). Fos family members: regulation, structure and role in oncogenic transformation. *Histol. Histopathol.*, 15, 921–928.

Urier, G., Buisson, M., Chambard, P. and Sergeant, A. (1989). The Epstein Barr virus early protein EB1 activates transcription from different responsive elements including AP-1 binding sites. *EMBO J.*, 8, 1447–1453.

Vogt, P. K. (2002). Fortuitous convergences: the beginnings of JUN. *Nat. Rev. Cancer*, 2, 465–469.

Wang, X., Chen, Y., Han, Q., Chan, C. Wang, H., Liu, Z., Cheng, C. H., Yew, D. T., Lin, M. C. M., He, M., Xu, H., Sung, J. J. Y. and Kung, H. (2009). Proteomic identification of molecular targets of gambogic acid: Role of stathmin in hepatocellular carcinoma. *Proteomics*, 9, 242-253.

Wang, X., Ye, X., Liu, R., Chen, H-L., Bai, H., Liang, X., Zhang, X-D., Wang, Z., Li, W-L. and Hai, C. X. (2010). Antioxidant activities of oleanolic acid in vitro: Possible role of Nrf2 and MAP kinases. *Chem. Biol. Interact.,* 184, 328-337.

Weber, W. M., Hunsaker, L. A., Gonzales, A. M., Heynekamp, J. J., Orlando, R. A., Deck, L. M. and Vander Jagt, D L. (2006). TPA-induced up-regulation of activator protein-1 can be inhibited or enhanced by analogs of the natural product curcumin. *Biochem. pharmacol*., 72, 928-940.

Wei, H., Bowen, R., Zhang, X. and Lebwohl, M. (1998). Isoflavone genistein inhibits the initiation and promotion of two-stage skin carcinogenesis in mice. *Carcinogenesis*, 19, 1509–1514.

Weinberg, R.A. (2007). The biology of cancer. United States of America: Garland Science, Taylor and Francis Group.

Westerink, W. M. A. and Schoonen, W. G. E. J. (2007). Phase II enzyme levels in HepG2 cells and cryopreserved primary human hepatocytes and their induction in HepG2 cells. *Toxicol. In Vitro*, 21, 1592-1602.

Westphal, E. M., Blackstock, W., Feng, W., Israel, B. and Kenney, S. C. (2000). Activation of Lytic Epstein-Barr Virus (EBV) Infection by Radiation and Sodium Butyrate *in Vitro* and *in Vivo*: A Potential Method for Treating EBV-positive Malignancies. *Cancer Res.*, 60, 5781–5788.

William, W. N., Heymach, J. V., Kim, E. S. and Lippman, S. M. (2009). Molecular targets for cancer chemoprevention. *Nat. Rev. Drug Discov.*, 8, 213-225.

Willis, D., Moore, A. R., Frederick, R., Willoughby, D. A. (1996). Heme oxygenase: a novel target for the modulation of the inflammatory response. *Nat. Med.,* 2, 87-90.

Wun, T., McKnight, H. and Tuscano, J. (2004). Increased cyclooxygenase-2 (COX-2): a potential role in the pathogenesis of lymphoma. *Leuk. Res*., 28, 179-190.

Xing, H., Zhang, S., Weinheimer, C., Kovacs, A. and Muslin, A. J. (2000). 14-3-3 proteins block apoptosis and differentially regulate MAPK cascades. *EMBO J.*, 19, 349-358.

Yamagishi, T., Zhang, D. C., Changa, J-J., McPhailb, D. R., McPhaila, A. T., Lee, K-H. (1988). The cytotoxic principles of *Hyptis capitata* and the structures of the new triterpenes hyptatic acid-A and –B. *Phytochemistry*, 27(10), 3213-3216.

Yap, W. H., Khoo, K. S., Lim, S. H., Yeo, C. C. and Lim, Y. M. (2012). Proteomic analysis of the molecular response of Raji cells to maslinic acid treatment. *Phytomedicine*, 19, 183-191.

Yazaki, Y. (1977). Polyphenols and triterpenoids of *Eugenia gustavioides* wood. *Phytochemistry*, 16(1), 138-139.

Yu, S., Zhou, B. N., Lin, L., Cordell, G. A. (1995). Triterpene saponins from *Aster yunnanensis*. *Phytochemistry*, 38(6), 1487-1492.

Yu, R., Mandlekar, S., Weber, M. J., Der, C. J., Wu, J. and Tony-Kong, A. N. (1999). Role of mitogen-activated protein kinase pathway in the induction of phase II detoxifying enzymes by chemicals. *J. Biol. Chem.*, 274, 27545-27552.

Yu, Q., Geng, Y. and Sicinski, P. (2001). Specific protection against breast cancers by cyclin D1 ablation. *Nature,* 411, 1017-1021.

Yu, X. and Kensler, T. (2005). Nrf2 as a target for cancer chemoprevention. *Mutat. Res.*, 591, 93-102.

Yuspa, S. H. (1994). The pathogenesis of squamous cell cancer: lessons learned from studies of skin carcinogenesis. *Cancer Res*., 54, 1178-1189.

Zalani, S., Holley-Guthrie, E. and Kenney, S. (1996). Epstein-Barr viral latency is disrupted by the immediate-early BRLF1 protein through a cell specific mechanism. *Proc. Natl. Acad. Sci.*, 93, 9194–9199.

Zhang, D. D., Lo, S.-C., Sun, Z., Habib, G. M., Lieberman, M. W. and Hannink, M. (2005). Ubiquitination of Keap1, a BTB-Kelch substrate adaptor protein for Cul3, targets Keap1 for degradation by a proteasome-independent pathway. *J. Biol. Chem*., 280, 30091 –30099.

Zhu, M. and Fahl, W. E. (2001). Functional characterization of transcription regulators that interact with the electrophile response element. *Biochem. Biophys. Res. Commun.*, 289, 212–219.

Zou, P., Kawada, J., Pesnicak, L. and Cohen, J. I. (2007). Bortezomib Induces Apoptosis of Epstein-Barr Virus (EBV)-Transformed B Cells and Prolongs Survival of Mice Inoculated with EBV transformed B cells. *J. Virol*., 81(18), 10029–10036.

Appendix A

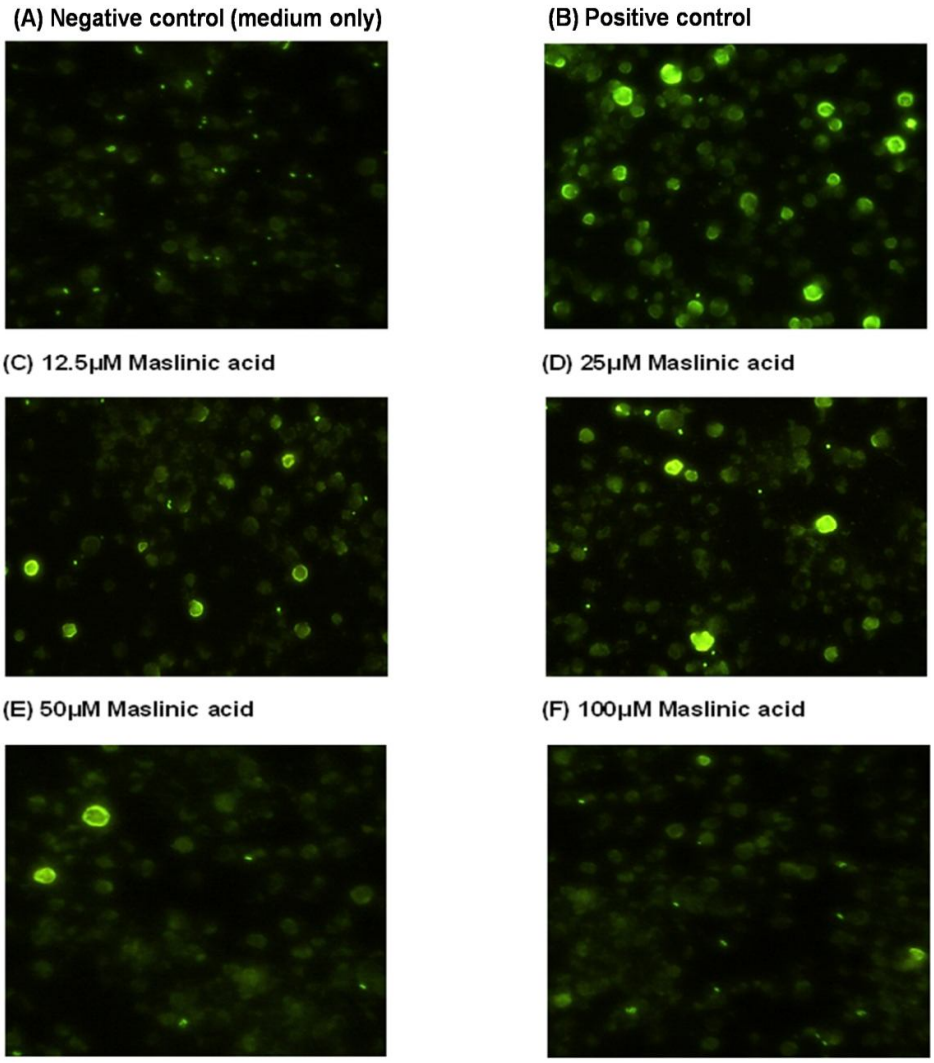

Figure 7.1: Immunofluorescent staining of (A) non-induced Raji cells as well as (B, C, D, E, and F) PMA and SnB-induced cells. (B) Positive control: cells induced with PMA and SnB only. Treatment of cells with (C) 12.5 µM, (D) 25 µM, (E) 50 µM, and (F) 100 µM maslinic acid along with PMA and SnB induction

Equation 1:

$$\text{Induction rate (IR)} = \frac{\text{Number of fluorescent cells}}{\text{Total number of cells}} \times 100\ \%$$

Equation 2:

$$\text{EBV-EA inhibition rate (anti-tumour promoting activity)} = \frac{\text{IR of positive control} - \text{IR of sample treatment}}{\text{IR of positive control}}$$

Equations 1 and 2: EBA-EA inhibition calculation for the anti-tumour promoting activities of samples

Table 7.1: Anti-tumour promoting activities of maslinic acid, tormentic acid, oleanolic acid and genistein

Compound	Concentrations (μM)	Percentage of EBV-EA inhibition	Percentage cell viability
Maslinic acid	100	(86 ± 5.6)%	(6 ± 4.7)%
	50	(77 ± 7.0)%	(34 ± 4.3)%
	25	(53 ± 4.3)%	(79 ± 9.4)%
	12.5	(19 ± 6.8)%	(84 ± 7.5)%
Tormentic acid	100	(56 ± 4.5)%	(95 ± 5.7)%
	50	(26 ± 6.5)%	(96 ± 4.8)%
	25	(15 ± 7.9)%	(96 ± 8.4)%
	12.5	(10 ± 4.6)%	(98 ± 3.4)%
Oleanolic acid	100	(80 ± 2.4)%	(10 ± 5.5)%
	50	(66 ± 6.5)%	(50 ± 7.5)%
	25	(33 ± 3.7)%	(80 ± 3.4)%
	12.5	(15 ± 3.2)%	(88 ± 9.8)%
Genistein	100	(89 ± 5.6)%	(11 ± 2.7)%
	50	(65 ± 4.3)%	(55 ± 8.1)%
	25	(54 ± 5.8)%	(80 ± 3.8)%
	12.5	(16 ± 5.5)%	(87 ± 8.6)%

Appendix B

Determination of PCR amplification efficiencies

A serial dilution of RNA template for four primer sets: genes of interest (NQO1, HO-1 and Nrf2) and reference gene (beta actin) were run by real time RT-PCR.

Analysis data for:

(A)

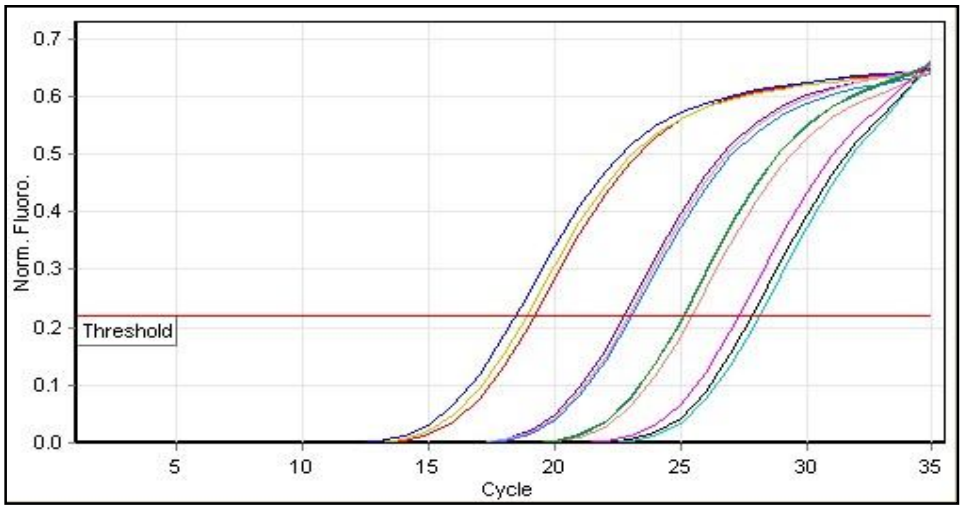

(B)

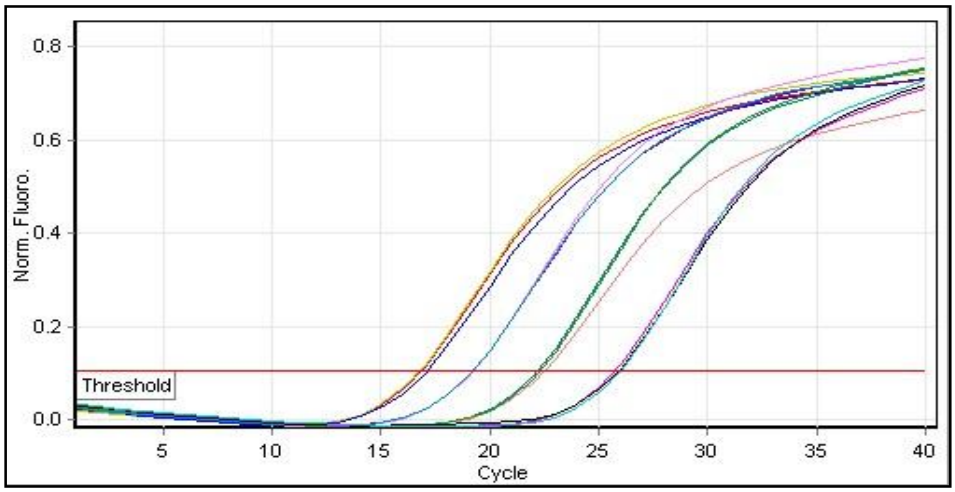

(C)

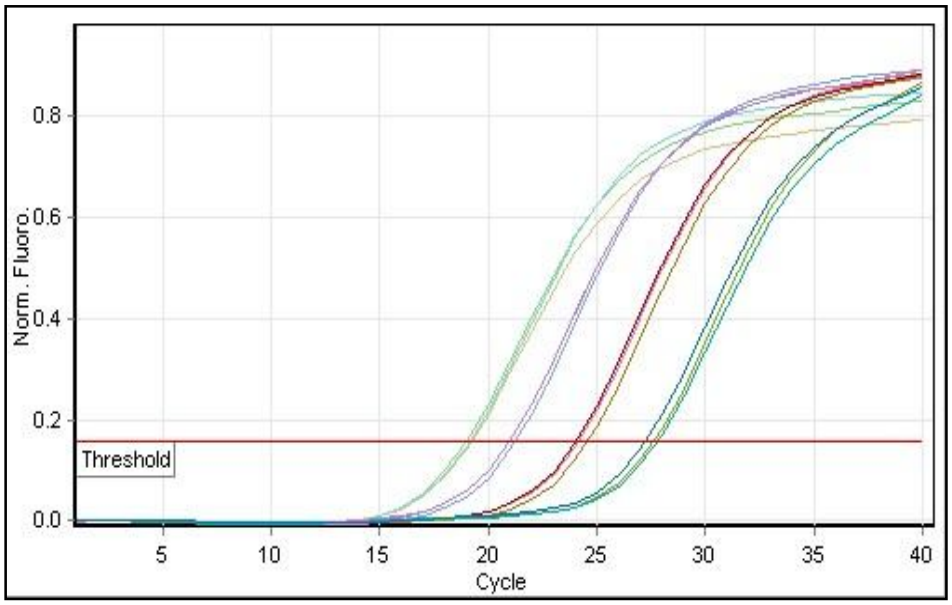

(D)

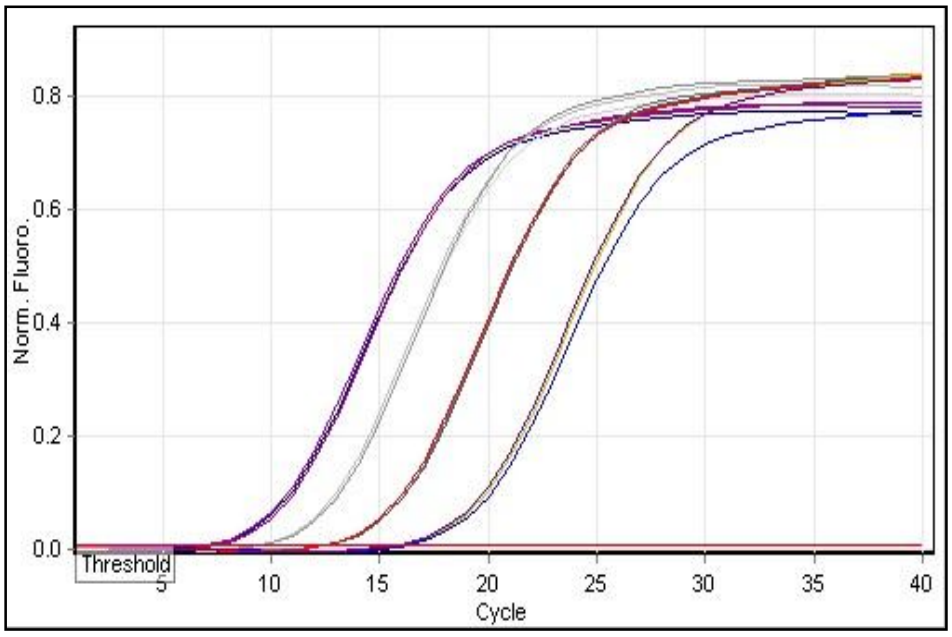

Figure 7.3: Real time RT-PCR profile of (A) Nrf2, (B) NQO1, (C) HO-1, and (D) beta actin gene. A serial dilution of RNA template was amplified using four different primer sets.

The C_T values of the reference gene (beta actin) are subtracted from the C_T values of the target genes (nqo1 and ho1). The differences in C_T values against the logarithm of amount of target were plotted. The amplification efficiencies are comparable if the slope of the graph from the resulting straight line is < 0.1. NQO1, HO-1 and Nrf2 have comparable amplification efficiencies (-0.001, 0.003, and -0.009) with reference gene beta actin.

		CT				ΔCT $=(CT_{GOI} - CT_{REF})$		
Standard	Conc (ng)	Gene of interest (GOI)			REF	NQO1	HO1	Nrf2
		NQO1	HO1	Nrf2	Beta actin			
1	100	16.94	19.12	18.84	7.44	9.5	11.68	11.4
2	10	19.27	21.08	22.93	9.71	9.56	11.37	13.22
3	1	22.37	24.25	25.52	12.8	9.57	11.45	12.43
4	0.1	25.91	27.55	27.79	16.2	9.71	11.35	11.59

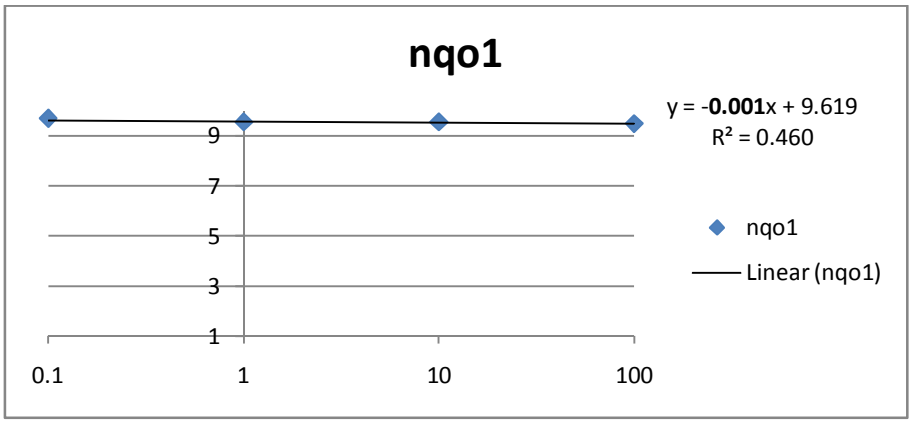

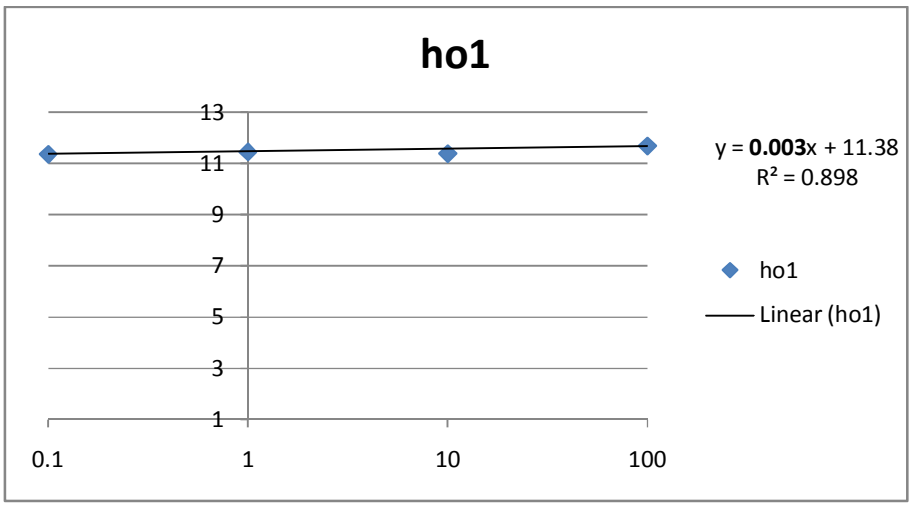

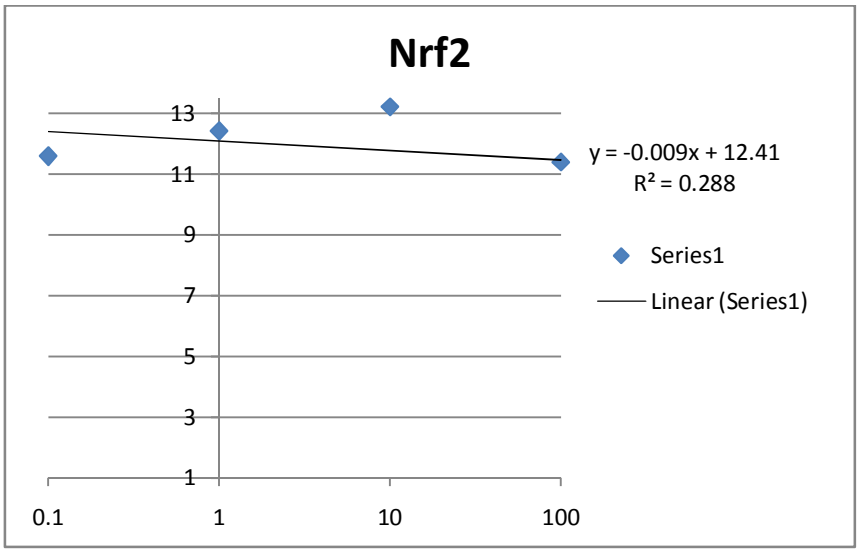
Nrf2
13
11
9
7
5
3
1
0.1
1
10
100
y = -0.009x + 12.41
R² = 0.288
Series1
Linear (Series1)

Cancer Chemopreventive Activity of Maslinic Acid: Suppression of COX-2 Expression and Inhibition of NF-κB and AP-1 Activation in Raji Cells

Authors Yap Wei Hsum[1], Wong Teck Yew[1], Paul Lim Vey Hong[2], Khoo Kong Soo[1], Lim Saw Hoon[3], Yeo Chew Chieng[4], Lim Yang Mooi[1]

Affiliations The affiliations are listed at the end of the article

Key words
- *Coleus tuberosus*
- Lamiaceae
- maslinic acid
- cyclooxygenase-2 (COX-2)
- nuclear factor-kappa B (NF-κB)
- activator protein-1 (AP-1)

Abstract

Chronic inflammation is one of the predisposing factors for neoplastic transformation. Targeting inflammation through suppression of the pro-inflammatory pathway by dietary phytochemicals provides an important strategy for cancer prevention. Maslinic acid is a novel natural triterpenoid known to inhibit proliferation and induce apoptosis in some tumor cell lines. Although maslinic acid has cytotoxic and pro-apoptotic effects on cancer cells, the underlying mechanisms of its effects on the inflammatory pathway have yet to be elucidated. It has been reported that abnormal expression of pro-inflammatory enzyme cyclooxygenase-2 (COX-2) causes promotion of cellular proliferation, suppression of apoptosis, enhancement of angiogenesis and invasiveness. In the present study, the suppressive effect of maslinic acid on COX-2 expression and the binding activity of upstream transcription factors NF-κB and AP-1, which are known to regulate COX-2 transcriptional activation, were assessed using Raji cells. The anti-inflammatory action of maslinic acid was benchmarked against oleanolic acid and other standard drugs. Western blot analysis and electrophoretic mobility shift assay (EMSA) were employed to analyze COX-2 expression as well as NF-κB and AP-1 binding activity. Our results showed that maslinic acid suppresses COX-2 expression in a concentration-dependent manner. Likewise, the constitutive nuclear NF-κB (p65) activity as well as phorbol 12-myristate 13-acetate (PMA)- and sodium *n*-butyrate (SnB)-induced AP-1 binding activity in Raji cells were significantly reduced following treatment with maslinic acid. Since maslinic acid suppresses COX-2 expression in Raji cells at concentrations that also lowered the NF-κB (p65) and AP-1 binding activity, it is possible that the suppression of COX-2 by this natural triterpenoid might be achieved, at least in part, via the NF-κB and AP-1 signaling pathways.

Supporting information available online at http://www.thieme-connect.de/ejournals/toc/plantamedica

received March 9, 2010
revised July 3, 2010
accepted July 6, 2010

Bibliography
DOI http://dx.doi.org/10.1055/s-0030-1250203
Published online July 28, 2010
Planta Med 2011; 77: 152–157

ISSN 0032-0943

Correspondence
Dr. Lim Yang Mooi
Faculty of Engineering and Science
Universiti Tunku Abdul Rahman
Kuala Lumpur Campus,
Jalan Genting Kelang
53300 Setapak
Kuala Lumpur
Malaysia
Phone: + 60 3 41 07 98 02 ext. 17 8
Fax: + 60 3 41 07 98 03
ymlim@utar.edu.my

Introduction

Numerous phytochemicals from edible plants have been reported to interfere with specific stages of carcinogenesis [1]. Much effort has been directed towards the progressive search for novel chemopreventive agents from edible plants. *Coleus tuberosus* Benth, also known as "ubi kemili" is an herbaceous plant which belongs to the family Lamiaceae. Its tubers are eaten as vegetables and pickles while the leaves of other *Coleus* species are used as spices [2]. *Coleus tuberosus* Benth has strong antitumor promoting properties [3].

One of the active antitumor promoting compounds in *Coleus tuberosus* tubers was identified as maslinic acid [4]. Maslinic acid (**Fig. 1**), a pentacyclic triterpene commonly present in medicinal herbs, has antioxidant and antitumor properties. Triterpenoids, which are synthesized in many plants by the cyclization of squalene, are widely used in Asian medicine [5]. They act at various stages of tumor development to inhibit tumor initiation and promotion as well as to induce differentiation and apoptosis [6].

Prostaglandins are oxygenated-lipid signaling molecules formed from arachidonate and some other highly unsaturated fatty acids; they regulate a wide variety of physiological processes, including blood clotting, wound healing, immune responses, bone metabolism, nerve growth and development, and inflammation [7]. The synthesis of prostaglandins is catalyzed by the cyclooxygenase (COX) enzymes. COX-2, in particular, is the inducible form of COX, and COX-2 expression re-

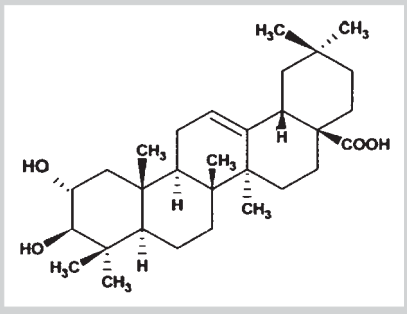

Fig. 1 Structure of maslinic acid.

sults in the upregulation of prostaglandins synthesis which in turn causes promotion of cellular proliferation, suppression of apoptosis, and enhancement of angiogenesis and invasiveness [8].

NF-κB and AP-1 are crucial transcription factors known to initiate transcription of the *hCOX-2* gene [9]. Both are evolutionarily conserved transcription factors which act independently or coordinately to regulate expression of target genes involved in various physiological processes [10]. Improper activation of NF-κB and/or AP-1 contributes to tumorigenesis either by transactivating several target genes that have inflammatory, anti-apoptotic, and cell cycle regulatory functions or by downregulating apoptosis-inducing genes [7].

Considering that these molecular targets are implicated in the carcinogenic process, testing of novel phytochemicals that act on these specific cellular targets followed by validation in animal carcinogenesis model and clinical trials will help to streamline chemoprevention research. This study is designed to investigate the mechanism of action of maslinic acid through evaluation of its suppressive effect on pro-inflammatory enzyme COX-2 expression and upstream transcription factors NF-κB and AP-1 binding activity.

Materials and Methods

Chemicals

Biotinylated AP-1 consensus sequence was purchased from Eurogentec AIT. NoShift Transcription Factor Assay kit, NoShift NF-κB (p65) reagents, and BAY 11-7085 were obtained from Calbiochem, Merck. NE-PER extraction kit and LightShift Chemiluminescent EMSA kit were obtained from PIERCE. COX-2 and β-actin antibodies were purchased from Cell Signaling Technology. Phorbol 12-myristate 13-acetate (PMA), sodium *n*-butyrate (SnB), oleanolic acid (≥ 97% pure as determined by HPLC), and ursolic acid (≥ 90.0% pure as determined by HPLC) were purchased from Sigma Chemical Co. Maslinic acid is obtained from the tubers of *Coleus tuberosus* Benth (Lamiaceae) [11]. The compound used is a chemically pure white powder (> 95% pure as determined by HPLC) and is stable when stored at 4 °C. A stock solution of 10 mg/mL was stored at − 20 °C. This solution was diluted in cell culture medium for use in tests.

Cell culture and sample treatment

The Raji B lymphoma cell line was obtained from the RIKEN Cell Bank. Cells were grown at 37 °C in RPMI medium supplemented with 10% FBS in a humidified atmosphere of 5% CO_2. Cells were incubated with increasing concentrations of maslinic acid (12.5, 25, 50, and 100 µM) or standard drugs for concentration-dependent studies. The viability of Raji cells was determined before and after treatment by the Trypan Blue staining method.

Western blot analysis

Raji cells were plated in 24-well plates in the presence of maslinic acid, oleanolic acid, and ursolic acid at various concentrations for 8 h. In order to prepare whole-cell lysis extracts, cells were harvested, washed twice with ice-cold PBS and lysed with modified RIPA buffer (50 mM Tris-Cl, 1% v/v NP-40, 0.35% w/v sodium-deoxycholate, 150 mM NaCl, 1 mM EDTA, 1 mM EGTA, pH 7.4, 1 mM phenylmethylsulfonyl fluoride [PMSF], 1 mM NaF, 1 mM Na_3VO_4, 10 µg/mL each of aprotinin, leupeptin, and pepstatin A) for 15 min at 4 °C. After centrifugation at 12 000 × *g* for 10 min at 4 °C, the supernatant was collected. The protein concentration was determined using Bio-Rad DC protein quantification assay. Samples containing 50 µg of protein were fractionated by SDS-PAGE in % T = 12 gels which were then electroblotted onto PVDF membranes (0.45 µm, PIERCE). Immunodetections of COX-2 and β-actin proteins were carried out using respective primary antibodies (1 : 1000 in 3% BSA in PBST buffer) and horseradish peroxidase (HRP) conjugated secondary antibodies (1 : 10 000 in 3% BSA in PBST buffer). Labeled protein bands were visualized and quantified using an Alpha Innotech system gel imager. The relative image densities were quantified by normalizing the values of COX-2 to the corresponding β-actin levels.

Electrophoretic mobility shift assay (EMSA)

Raji cells were plated in 24-well plates incubated with 0.05 µM PMA and 3 mM SnB along with various concentrations of maslinic acid and oleanolic acid for 4 h. EMSA was performed as described [12]. Briefly, nuclear extracts were prepared using the NE-PER nuclear extraction reagent, and AP-1 DNA binding activity was performed with the LightShift Chemiluminescent EMSA kit. The binding reactions contained 10 µg of nuclear protein extract, buffer, 50 ng of poly (dI-dC), and 20 fmol biotin-labeled AP-1 DNA (5′ CGCTTGATGA CTCAGCCGGAA 3′). The reactions were incubated for 20 min at room temperature in a final volume of 20 µL. The reaction mixture was electrophoretically separated on a 5% native polyacrylamide gel in 0.5 × Tris-borate EDTA buffer and transferred to a nylon membrane. The biotin-labeled DNA was detected by chemiluminescence. Specific and nonspecific competition reactions were performed by adding 10-fold excess of unlabeled AP-1 DNA as well as 10-fold excess of unlabeled NF-κB DNA to the reaction mix to validate the specificity of AP-1 binding.

In order to assess NF-κB binding activity, Raji cells were plated in 24-well plates and treated with maslinic acid, oleanolic acid, and NF-κB inhibitor BAY 11-7085 at various concentrations for 8 h. Following treatment, nuclear extracts were prepared with NE-PER extraction reagent, and the NF-κB DNA binding reactions were carried out using NoShift Transcription Factor Assay kit and NoShift NF-κB (p65) reagents. The nuclear extract was mixed with the biotinylated double-stranded NF-κB oligonucleotides along with NoShift Bind Buffer, poly (dI.dC), and salmon sperm DNA to a final volume of 20 µL and incubated for 30 min on ice. The reaction mixture was then transferred to a streptavidin coated plate where the protein-DNA complex was captured. The bound transcription factor (NF-κB) was then detected with specific antibody (p65), followed by secondary antibody HRP conjugate and chromogenic reactions with tetramethylbenzidine (TMB) substrate. The absorbance was then read at 450 nm.

Several controls were included for the experiments to establish the specificity of NF-κB binding activity. They include reactions performed in the absence of DNA binding protein extract (blank), reactions with nonspecific competitor mutant DNA, as well as reactions with specific competitor DNA. The amount of specific and nonspecific competitor DNA is a 10-fold molar excess over wild type DNA for each competition analysis.

Statistical analysis

Statistical analyses were performed using SPSS 15.0 software. Treatment effects were analyzed using one-way ANOVA. $P < 0.05$ was used to indicate significance.

Supporting information

Basal and PMA-induced COX-2 expression (**Fig. 1S**) and NF-κB (p65) activity (**Fig. 2S**) in Raji cells, as well as the percentage cell viability before and after treatment with maslinic acid (**Fig. 3S**) are available as Supporting Information.

Results

We found that Raji cells expressed COX-2, and that the level of PMA-induced COX-2 expression increase was not significantly different (**Fig. 1S**). The constitutive COX-2 expression in Raji cells is in agreement with other studies which confirmed that B lymphoma cells are capable of expressing COX-2 as compared to primary B cells [13]. Findings by Wun et al. suggested that COX-2 protein expression is part of the process whereby B cells become malignant, and that certain B cell malignancies require COX-2 for survival [14]. COX-2 expression in Raji cells treated with maslinic acid was inhibited by 3%, 15%, 33%, and 51% at 12.5, 25, 50, and 100 µM, respectively, as seen in **Fig. 2A**. Similarly, oleanolic acid (**Fig. 2B**) suppressed COX-2 expression, with maximum inhibition (> 50%) at the highest concentration tested (100 µM) [15]. Ursolic acid, a natural COX-2 inhibitor on the other hand, abolished COX-2 expression at 50 µM (**Fig. 2C**) [16].

To further investigate the molecular mechanisms involved in maslinic acid-mediated suppression of COX-2 protein expression, we focused on the NF-κB signaling pathway, which is known to be responsible for COX-2 transactivation [17]. The NF-κB binding activity in untreated Raji cells was comparable to the one in PMA-induced cells, indicating that it had constitutive nuclear NF-κB activity (**Fig. 2S**). From the data shown in **Fig. 3A**, the NF-κB (p65) binding activity in Raji cells was specific; the presence of a nonspecific competitor (mutant DNA) did not affect the NF-κB binding activity in Raji cells but it was significantly reduced in the presence of specific competitor DNA. Transformation of B cells by the Epstein-Barr virus induces NF-κB activity, and this activity is necessary for the survival of these cells *in vitro* [18].

We then evaluated the inhibitory effect of maslinic acid, oleanolic acid, and the NF-κB inhibitor BAY 11-7085 on the constitutive NF-κB (p65) activity in Raji cells. As shown in **Fig. 3B**, NF-κB inhibitor BAY 11-7085 exhibited a potent suppressive effect, with more than an 80% inhibitory effect at 5 µM [19]. Treatment with maslinic acid resulted in substantial NF-κB DNA binding activity inhibition, reaching 70% inhibition at 100 µM with an IC_{50} value of approximately 25 µM (**Fig. 3C**). By comparison, oleanolic acid treatment only inhibited 53% NF-κB DNA binding activity at 100 µM (**Fig. 3C**). The suppressive effect of maslinic acid on COX-2 and NF-κB were independent of its cytotoxic activity as the cell viability scored 80% after treatment at 8 h (**Fig. 3S**). The

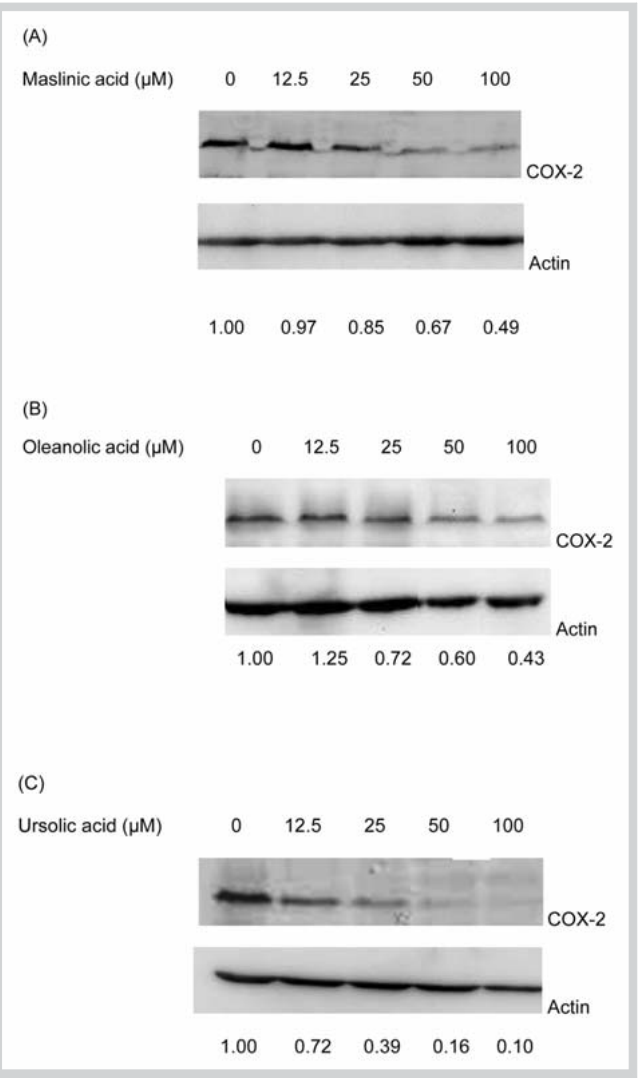

Fig. 2 Western blot analysis of COX-2 protein expression in Raji cells. Effects of maslinic acid (**A**), oleanolic acid (**B**), and ursolic acid (**C**) on COX-2 expression. Raji cells were treated with 12.5, 25, 50, and 100 µM of maslinic acid, oleanolic acid, and ursolic acid for 8 hours. Total cell lysates were analyzed for COX-2 expression by immunoblotting. The relative image densities were quantified by normalizing the values of COX-2 to the corresponding β-actin levels. The values shown represent the fold change relative to that of the control. Each data represents the average of three independent experiments.

NF-κB pathway may be only one pathway among several others regulated by maslinic acid. Thus, we further investigated other upstream targets that may be regulated by maslinic acid.

Apart from NF-κB, AP-1 is another ubiquitous eukaryotic transcription factor which has been attributed to the elevated expression of COX-2 in phorbol ester-induced tumorigenesis [20]. As shown in **Fig. 4A**, tumor promoter PMA- and enhancer SnB-induced AP-1 DNA binding activity could be detected after 4 h of treatment. The induced AP-1 DNA binding activity may be due to the histone deacetylase inhibitor activity of SnB, which results in facilitating transcription factor access to the promoter regions of certain genes, thereby enhancing transcription [21].

The specificity of AP-1 DNA binding induced by PMA/SnB (**Fig. 4A**) was determined by competition experiments. AP-1

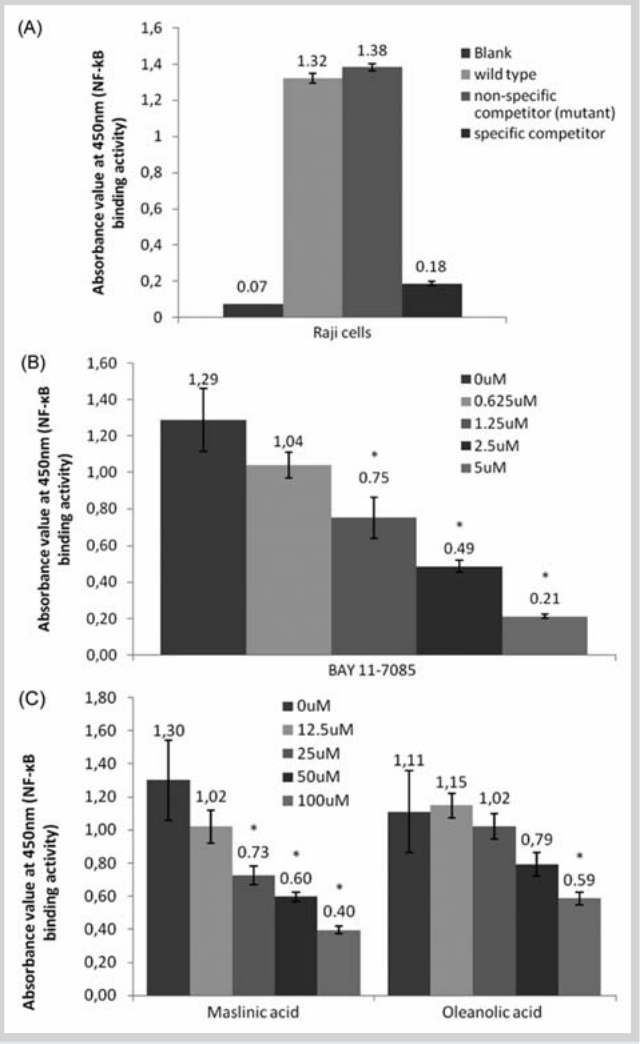

Fig. 3 NF-κB (p65) DNA binding activity in Raji cells. Basal NF-κB (p65) activity in Raji cells (**A**); effects of NF-κB inhibitor BAY 11-7085 (**B**), as well as maslinic and oleanolic acids (**C**) on NF-κB (p65) DNA binding activity. Raji cells were treated with various concentrations of BAY 11-7085, maslinic acid, and oleanolic acid for 8 hours. Nuclear extracts were prepared after treatment and quantified for NF-κB (p65) activity using a NoShift Transcription Factor Assay kit. Each data point represents the average ± SD of three independent experiments. An asterisk (*) denotes a significant difference from control at $p < 0.05$.

DNA binding was abolished in the presence of 10-fold molar excess unlabeled AP-1 DNA (specific competitor) but was not affected in the presence of unlabeled NF-κB DNA (nonspecific competitor). We next examined the effect of maslinic acid and oleanolic acid on AP-1 DNA binding activity induced by PMA and SnB. Gel shift assays (▶ **Fig. 4B** and **C**) showed that the combined treatment of PMA/SnB/maslinic acid and PMA/SnB/oleanolic acid significantly reduced AP-1 binding activity. The inhibitory effects of both maslinic and oleanolic acid are concentration-dependent, and both these compounds abolished AP-1 binding activity at 100 µM.

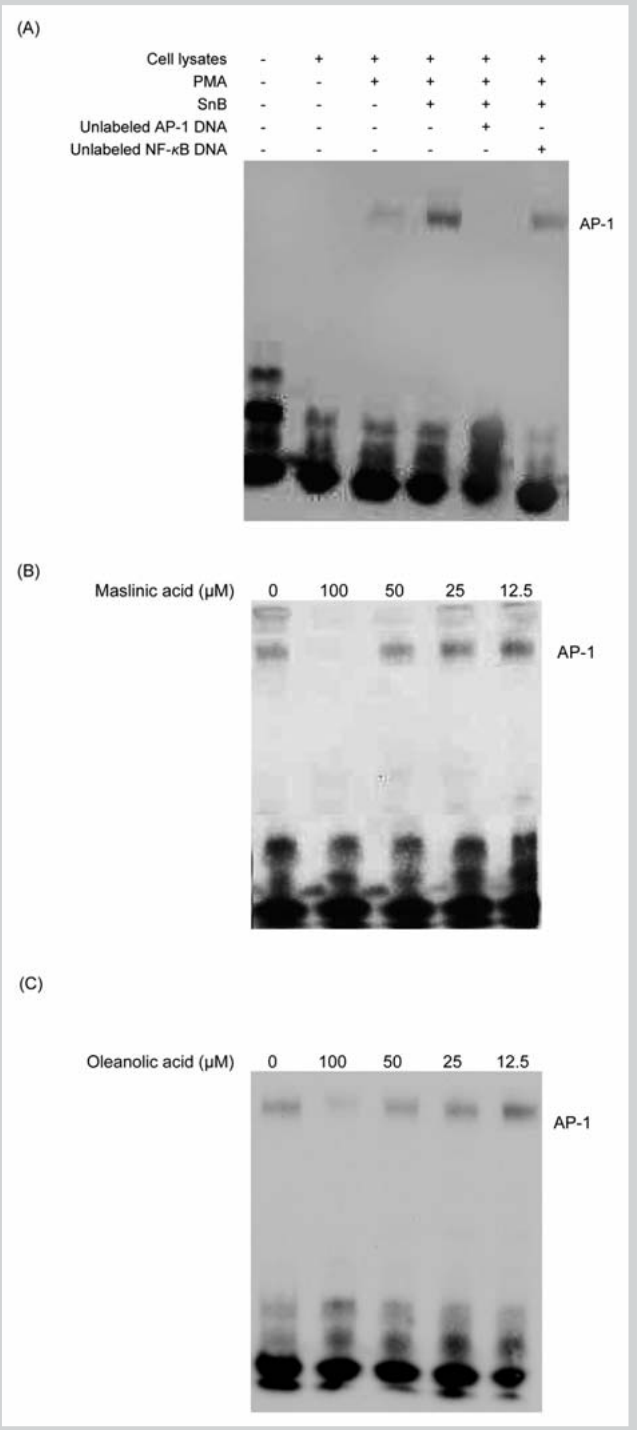

Fig. 4 AP-1 DNA binding activity in Raji cells. Basal, PMA-induced, and PMA/SnB-induced AP-1 DNA binding activity in Raji cells (**A**); effects of maslinic acid (**B**) and oleanolic acid (**C**) on PMA/SnB-induced AP-1 binding activity. Raji cells were treated with 0.05 µM PMA, 3 mM SnB, as well as maslinic and oleanolic acids at various concentrations (12.5, 25, 50, and 100 µM) for 4 hours. Nuclear extracts were prepared and analyzed for AP-1 binding activity using a LightShift Transcription Factor Assay kit. Data presented are representative of three independent experiments showing similar trends.

Discussion

Naturally-occurring dietary phytochemicals are a convenient source of chemopreventive agents. Maslinic acid has been shown to inhibit proliferation and induce apoptosis in tumor cell lines. A study by Reyes et al. showed that maslinic acid induced apoptosis in HT29 human colon cancer cells via the mitochondrial pathway [22]. In addition, an animal model study showed that endogenous plasma lipoperoxide levels and susceptibility to lipid peroxidation were decreased after treatment with maslinic acid in mice [23]. Our study investigates the anti-inflammatory effect of maslinic acid on COX-2 expression and DNA binding activities of NF-κB and AP-1 in Raji cells.

Our results showed that maslinic acid suppresses COX-2 expression after 8 hours of treatment, with 50% inhibition at 100 µM. Constitutive NF-κB (p65) DNA binding activity was inhibited by > 70% at 100 µM while PMA/SnB-induced AP-1 binding activity was also abolished at 100 µM. Similarly, other natural chemopreventive agents like ursolic acid from the ursane group of natural triterpenoids have been reported to lower the expression of COX-2 through inhibition of the protein kinase C (PKC) signaling pathway and AP-1 binding activity [6]. Downregulation of COX-2 expression together with inhibition of NF-κB and AP-1 activation by maslinic acid is likely to contribute to the antitumor promoting effects of maslinic acid in Raji cells. Our study is the first to show that B cell lymphoma cells may be sensitive to treatment with maslinic acid.

The pro-apoptotic and cytotoxic effects of maslinic acid on several tumor cell lines [24] may be partly mediated by the inhibition on NF-κB and AP-1 DNA binding activity as this activity is necessary for cell survival. Indeed, activation of NF-κB and/AP-1 are known to mediate the transcriptional upregulation of anti-apoptotic genes like *Bcl-2, Bcl-X_L, cIAP1*, and *cIAP2* as well as downregulation of apoptosis-inducing genes like *p21, p16, p19,* and *p53* [25]. Both NF-κB and AP-1 promote cell cycle progression through upregulation of cyclin D1 [26]. Transcriptional activation of these genes thus provides tumor cells with a survival advantage. Inhibition of the DNA-binding activity of NF- κB and AP-1 by maslinic acid may thus help to block tumor cell cycle progression and induce apoptosis.

Schreck et al. have proposed an interrelationship between redox status and the NF-κB activation process, focusing on the role of reactive oxygen species as a potential mediator of the NF-κB signaling cascade [27]. Since both NF-κB and AP-1 are redox sensitive transcription factors, their inhibition by maslinic acid might be attributable to its antioxidant activity. Indeed, triterpenoids have been reported to have beneficial effects on the cardiovascular system due to their antioxidant activities [28]. Natural triterpenoids such as ursolic acid and oleanolic acid are effective inducers of metallothionein (a cysteine-rich protein acting like glutathione in the body's defense system against toxic stress). The induction of metallothionein could be one of the important mechanisms for the anti-oxidative effects of maslinic acid [29]. Evaluation of the potential effects of maslinic acid at inducing phase II detoxifying/antioxidative enzymes through activation of the Nrf2 signaling pathway may serve to explain the anti-inflammatory and cytoprotective effects of maslinic acid [30].

In conclusion, maslinic acid was shown to inhibit COX-2 expression as well as the NF-κB and AP-1 binding activity, which may explain the anti-inflammatory and antitumor promoting activity of this compound.

Acknowledgements

The authors would like to express their deepest gratitude to the Universiti Tunku Abdul Rahman and the MOSTI e-science fund (00-02-11-SF0028) for financially supporting this project.

Affiliations

[1] Department of Science, Faculty of Engineering & Science, Universiti Tunku Abdul Rahman, Kuala Lumpur, Malaysia
[2] Tung Shin Hospital, Jalan Pudu, Kuala Lumpur, Malaysia
[3] School of Biological Sciences, Faculty of Science, Monash University, Victoria, Australia
[4] Faculty of Agriculture and Biotechnology, Universiti Darul Iman Malaysia, Jalan Sultan Mahmud, Kuala Terengganu, Malaysia

References

1 *Surh Y-J.* Cancer chemoprevention with dietary phytochemicals. Nat Rev Cancer 2003; 3: 768–780
2 *Bajaj YP.* Medicinal and aromatic plants. New York: Springer; 1994: 69
3 *Lim YM, Wahab NA, Lajis NH, Ali AM.* Chemopreventive property of phytosterols and maslinic acid in inhibiting the expression of EBV-early antigen in Raji cells. Chem Biodivers 2010; 7: 1267–1275
4 *Reyes FJ, Centelles J, Lupianez JA, Cascante M.* (2α,3β)-2,3-Dihydroxyolean-12-en-28-oic acid, a new natural triterpene from *Olea europea,* induces caspase dependent apoptosis selectively in colon adenocarcinoma cells. FEBS Lett 2006; 580: 6302–6310
5 *Liby KT, Yore MM, Sporn MB.* Triterpenoids and rexinoids as multifunctional agents for the prevention and treatment of cancer. Nat Rev Cancer 2007; 7: 357–368
6 *Dzubak P, Hajduch M, Vydra D, Hustova A, Kvasnica M, Biedermann D, Markova L, Urban M, Sarek J.* Pharmacological activities of natural triterpenoids and their therapeutic implications. Nat Prod Rep 2006; 23: 394–411
7 *Aggarwal BB, Shishodia S.* Molecular targets of dietary agents for prevention and therapy of cancer. Biochem Pharmacol 2006; 71: 1397–1421
8 *Dannenberg AJ, Subbaramaiah K.* Targeting cyclooxygenase-2 in human neoplasia: rationale and promise. Cancer Cell 2003; 4: 431–436
9 *Kosaka T, Miyata A, Ihara H, Hara S, Sugimoto T, Takeda O, Takahashi E, Tanabe T.* Characterization of the human gene (PTGS2) encoding prostaglandin-endoperoxidase synthase 2. Eur J Biochem 1994; 221: 889–897
10 *Dorai T, Aggarwal BB.* Role of chemopreventive agents in cancer therapy. Cancer Lett 2004; 215: 129–140
11 *Lim YM.* Anti-tumour promoting activity of selected malaysian vegetables and fruits, and identification of anti-tumour promoting and anti-oxidant compounds from *Coleus tuberosus*, Benth [dissertation]. Serdang: Universiti Putra Malaysia; 2002
12 *Chaturvedi MM, Mukhopadhyay A, Aggarwal BB.* Assay for redox sensitive transcription factor. Methods Enzymol 2000; 319: 585–602
13 *Graf BA, Nazarenko DA, Borrello MA, Roberts LJ, Morrow JD, Palis J, Phipps RP.* Biophenotypic B/macrophage cells express COX-1 and up-regulate COX-2 expression and prostaglandin E(2) production in response to pro-inflammatory signals. Eur J Immunol 1999; 29: 3793–3803
14 *Wun T, McKnight H, Tuscano J.* Increased cyclooxygenase-2 (COX-2): a potential role in the pathogenesis of lymphoma. Leuk Res 2004; 28: 179–190
15 *Janakiram NB, Indranie C, Malisetty SV, Jagan P, Steele VE, Rao CV.* Chemoprevention of colon carcinogenesis by oleanolic acid and its analog in male F344 rats and modulation of COX-2 and apoptosis in human colon HT-29 cancer cells. Pharm Res 2008; 25: 2151–2157
16 *Subbaramaiah K, Michaluart P, Sporn MB, Dannenberg AJ.* Ursolic acid inhibits cyclooxygenase-2 transcription in human mammary epithelial cells. Cancer Res 2000; 60: 2399–2404
17 *D'Acquisto F, Luvone T, Rombola L, Sautebin L, Di Rosa M, Carnuccio R.* Involvement of NF-kB in the regulation of cyclooxygenase-2 protein expression in LPS-stimulated J774 macrophages. FEBS Lett 1997; 418: 175–178
18 *McFarland ED, Davidson DM, Schauer SL, Duong J, Kieff E.* NF-κB inhibition causes spontaneous apoptosis in Epstein-Barr virus-transformed lymphoblastoid cells. Proc Natl Acad Sci 2000; 97: 6055–6060

19 *Bergera N, Bassatb HB, Kleinb BY, Laskov R.* Cytotoxicity of NF-kB inhibitors Bay 11-7085 and caffeic acid phenethyl ester to Ramos and other human B-lymphoma cell lines. Exp Hematol 2007; 35: 1495–1509
20 *Eferl R, Wagner EF.* AP-1: a double-edged sword in tumourigenesis. Nat Rev Cancer 2003; 3: 859–868
21 *Sealy L, Chalky R.* The effect of sodium butyrate on histone modification. Cell 1976; 14: 115–121
22 *Reyes FZ, Palomares ER, Lupiáñez JMC.* Maslinic acid, a natural triterpene from *Olea europaea* L., induces apoptosis in HT29 human colon-cancer cells via the mitochondrial pathway. Cancer Lett 2008; 273: 44–54
23 *Montilla M, Agil A, Navarro M, Jimenez M, Granados A, Parra A, Cabo MM.* Antioxidant activity of maslinic acid, a triterpene derivative obtained from *Olea europaea*. Planta Med 2003; 69: 472–474
24 *Kim YK, Yoon SK, Ryu SY.* Cytotoxic triterpenes from stem bark of *Physocarpus intermedius*. Planta Med 2000; 66: 485–486
25 *Shaulian E, Karin M.* AP-1 as a regulator of cell life and death. Nat Cell Biol 2002; 4: 131–136
26 *Kundu JK, Surh Y-J.* Molecular basis of chemoprevention by resveratrol: NF-κB and AP-1 as potential targets. Mutat Res 2004; 555: 65–80
27 *Schreck R, Rieber P, Baeurle PA.* Reactive oxygen intermediates as apparently widely used messengers in the activation of the NF-κB transcription factor and HIV-1. EMBO J 1991; 10: 2247–2258
28 *Liu J.* Oleanolic acid and ursolic acid: research prospectives. J Ethnopharmacol 2005; 100: 92–94
29 *Cipak L, Lubica G, Miadokova E, Novotny L, Rauko P.* Dual activity of triterpenoids: apoptotic versus antidifferentiation affects. Arch Toxicol 2006; 80: 429–435
30 *Yu X, Kensler T.* Nrf2 as a target for cancer chemoprevention. Mutat Res 2005; 591: 93–102

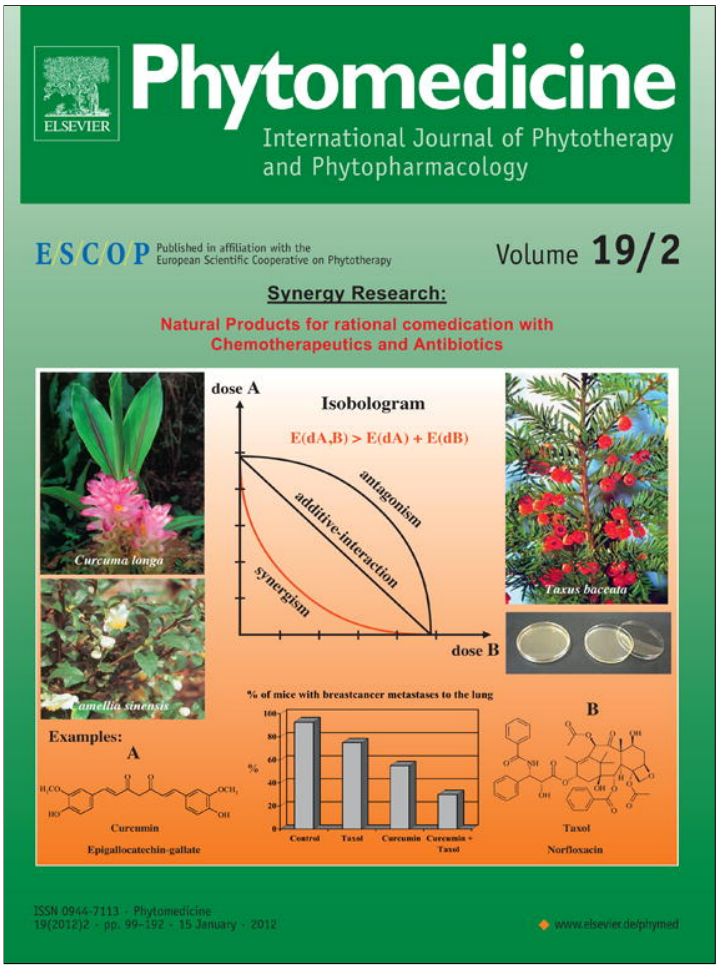

Phytomedicine 19 (2012) 183–191

Contents lists available at ScienceDirect

Phytomedicine

journal homepage: www.elsevier.de/phymed

Proteomic analysis of the molecular response of Raji cells to maslinic acid treatment

W.H. Yap[a], K.S. Khoo[a], S.H. Lim[b], C.C. Yeo[c], Y.M. Lim[d,*]

[a] Faculty of Science, Universiti Tunku Abdul Rahman, Bandar Barat, 31900 Kampar, Perak, Malaysia
[b] School of Biological Sciences, Faculty of Science, Monash University, Victoria 3800, Australia
[c] Faculty of Agriculture and Biotechnology, Universiti Darul Iman Malaysia, Jalan Sultan Mahmud, 20400 Kuala Terengganu, Malaysia
[d] Faculty of Medicine and Health Sciences, Universiti Tunku Abdul Rahman, Lot PT21144, Jalan Sungai Long, Bandar Sungai Long, 43000 Kajang, Malaysia

ARTICLE INFO

Keywords:
EB1
Maslinic acid
NF-κB
RanBP1
Stathmin

ABSTRACT

Maslinic acid, a natural pentacyclic triterpene has been shown to inhibit growth and induce apoptosis in some tumour cell lines. We studied the molecular response of Raji cells towards maslinic acid treatment. A proteomics approach was employed to identify the target proteins. Seventeen differentially expressed proteins including those involved in DNA replication, microtubule filament assembly, nucleocytoplasmic trafficking, cell signaling, energy metabolism and cytoskeletal organization were identified by MALDI TOF-TOF MS. The down-regulation of stathmin, Ran GTPase activating protein-1 (RanBP1), and microtubule associated protein RP/EB family member 1 (EB1) were confirmed by Western blotting. The study of the effect of maslinic acid on Raji cell cycle regulation showed that it induced a G1 cell cycle arrest. The differential proteomic changes in maslinic acid-treated Raji cells demonstrated that it also inhibited expression of dUTPase and stathmin which are known to induce early S and G2 cell cycle arrests. The mechanism of maslinic acid-induced cell cycle arrest may be mediated by inhibiting cyclin D1 expression and enhancing the levels of cell cycle-dependent kinase (CDK) inhibitor p21 protein. Maslinic acid suppressed nuclear factor-kappa B (NF-κB) activity which is known to stimulate expression of anti-apoptotic and cell cycle regulatory gene products. These results suggest that maslinic acid affects multiple signaling molecules and inhibits fundamental pathways regulating cell growth and survival in Raji cells.

Introduction

Triterpenoids, as major constituents of plants used in Asian traditional medicine, have been reported to have anti-inflammatory, hepatoprotective, analgesic, antimicrobial, antimycotic, virostatic, immunomodulatory and tonic effects (Dzubak et al. 2006). Their biosynthesis involves cascade cyclizations and rearrangements of the acyclic precursor squalene and 2,3-oxidosqualene (Abe 2007), leading to tetra and pentacyclic triterpene skeleta. Maslinic acid is a naturally occurring pentacyclic triterpene found in medicinal plants such as *Aster yunnanensis* (Yu et al. 1995), *Elaeagnus oldahmi* (Tsuen-Ih et al. 1976), *Eugenia gustavioides* (Yazaki 1977), *Centaurium erythraea* (Bellavita et al. 1974), *Coleus tuberosus* (Mooi et al. 2010) and *Olea europaea* (Mussini et al. 1975). Maslinic acid has antioxidant (Montilla et al. 2003), anti-inflammatory (Martín et al. 2006), anti-tumour (Reyes et al. 2006; Hsum et al. 2011), anti-diabetic (Chen et al. 2006) and anti-viral properties (Xu et al. 1996).

There are several mechanisms that are responsible for the anti-carcinogenic properties of chemopreventive compounds (Surh 2003). Some chemopreventive mechanisms are interconnected. Modulation of a given end-point may be the result of a specific mechanism or the consequences of upstream mechanisms (Flora and Ferguson 2005). Maslinic acid induces apoptosis in HT-29 human colon cancer cells by inhibiting expression of anti-apoptotic protein Bcl-2, increasing the ratio of pro-apoptotic protein Bax, releasing cytochrome c from the mitochondria and activating caspase-9 followed by caspase-3 (Reyes-Zurita et al. 2008). The pro-apoptotic and cytotoxic effects of maslinic acid on tumour cell lines may be mediated by the inhibition on NF-κB and AP-1 DNA binding activities (Hsum et al. 2011).

Proteomic techniques facilitate the qualitative and quantitative measurement of a broad-spectrum of proteins (Pastwa et al. 2007). Information derived from 2-DE and MALDI TOF-TOF MS allow the assessment of differentially expressed proteomes of cancer cells in response to chemopreventive drug treatment. This may serve as a model for cancer therapeutics, and is useful for the discovery

* Corresponding author. Tel.: +60 3 90194722x178; fax: +60 3 90194722.
E-mail address: ymlim@utar.edu.my (Y.M. Lim).

0944-7113/$ – see front matter © 2011 Elsevier GmbH. All rights reserved.
doi:10.1016/j.phymed.2011.08.058

of drug-specific biomarkers (Liebold et al. 2006). The study of the effects of maslinic acid at the proteomics level may help to elucidate the complex interactions of the protein network that relates signaling pathways.

Cell cycle deregulation is a common feature of human cancers. The cell cycle includes a gap period (G1 phase) which is controlled by positive (growth, survival and mitogenic) and negative (apoptotic and cytostatic) signals (Massague 2004). Another gap period (G2 phase) monitors replication errors before mitosis. Oncogenic transformation may result from the aberrancy in these G1 and G2 mechanisms. Deregulation of the cell cycle check points and overexpression of growth-promoting factors such as cyclin D1 and CDKs have been associated with tumourigenesis (Aggarwal and Shishodia 2006). Constitutive and deregulated CDK activation may contribute to unscheduled proliferation, genomic instability, and chromosomal instability (Malumbres and Barbacid 2009). Maslinic acid has been reported to induce G1 arrest in human colon cancer cells Caco-2 without affecting the cell cycle of non-tumoural intestine cell lines IEC-6 and IEC-1 (Reyes et al. 2006). However, its regulation of the human B lymphoma Raji cell cycle, cyclin and CDK inhibitor levels has not yet been investigated.

In this study, a proteomics approach was used to identify new molecular targets of maslinic acid in Raji cells. The growth inhibition effect of maslinic acid was measured using the 3-(4, 5-dimethylthiazol-2-yl)-2,5-diphenyltetrazolium bromide (MTT) assay. After determining the growth inhibition concentration, 2-DE and MALDI TOF-TOF MS were used to identify the target proteins. The expression of proteins which had been identified were evaluated by Western blotting to validate the variation in their levels in response to treatment. This study also determined a possible block in the cell cycle induced by maslinic acid in Raji cells and its effect on the G1 phase cell cycle regulatory molecules cyclin D1 and CDK inhibitor protein p21. A time course study on NF-κB DNA binding activity was undertaken to further investigate the molecular basis for the growth inhibition properties of maslinic acid.

Materials and methods

Chemical reagents and tissue culture

Maslinic acid (Fig. 1) was obtained from the tubers of *Coleus tuberosus Benth* following to the procedure of Mooi et al. (2010). The compound used was a chemically pure white powder (>95% pure as determined by HPLC). A stock solution of 10 mg/ml in dimethyl sulphoxide (DMSO) was stored at −20 °C. This solution was diluted in the cell culture medium for use in treatment.

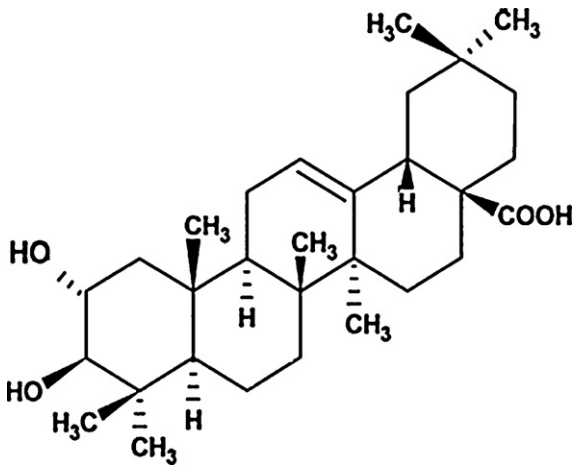

Fig. 1. Chemical structure of maslinic acid.

FBS, RPMI and trypsin-EDTA were purchased from Gibco (NY, USA). EB1, stathmin, p21 and cyclin D1 antibodies were obtained from Cell Signaling Technology (Beverly, MA). RanBP1 was purchased from Calbiochem, Merck (Germany). MTT was purchased from Sigma–Aldrich (Deutschland). Raji cells were grown in RPMI medium supplemented with 10% FBS in a 5% CO_2 humidified environment at 37 °C. Maslinic acid was applied to the cell cultures dissolved in DMSO to a final concentration of 0.5% (v/v) in all the experiments. Controls were treated with the same amount of DMSO.

Cell proliferation assessment with MTT assay

Raji cells were seeded at a density of 5×10^4 cells/well in a 96-well plate in complete medium (100 μl/well). The cells were treated with 12.5, 25, 50, 100, and 200 μM of maslinic acid and were incubated in a humidified environment with 5% CO_2 at 37 °C for 72 h. The cells were centrifuged at 1500 rpm for 5 min and the medium was removed. Twenty μl of 5 mg/ml MTT was added and the plates were incubated at 37 °C for 3 h. Hundred micolitres of DMSO was added to each well. The plate was then gently agitated for 5 min and the absorbance at 570 nm was determined. The experiments were performed in triplicates.

Two dimensional-polyacrylamide gel electrophoresis (2D-PAGE)

Protein extraction and sample preparation for 2D-PAGE

Raji cells (5×10^5 cells/ml) were seeded in 24-well plates and incubated with 50 μM of maslinic acid for 4, 8, 16, and 24 h. After incubation, the cells were lysed with lysis buffer (7 M urea, 2 M thiourea, 4% CHAPS, 40 mM DTT, 0.5% pH 3–11 NL IPG buffer, protease inhibitor mix). The cell lysate was centrifuged at 14,000 × *g* for 10 min at 4 °C. After centrifugation, pre-chilled acetone was added to the supernatant to remove contaminants. The samples were then incubated for 2 h at −20 °C, after which they were centrifuged at 13,000 × *g* for 10 min at 4 °C, and the supernatant was removed. The resulting protein pellets were dissolved in a rehydration buffer (7 M urea, 2 M thiourea, 4% CHAPS, 0.5% pH 3–11 NL IPG buffer, 20 mM DTT, 0.02% bromophenol blue). Biorad RCDC Protein Assay reagents (Biorad, Hercules, CA) were used to determine the protein concentration. The protein samples were then stored at −80 °C.

2D-PAGE conditions

Protein separation and protein profile analysis were carried out as described previously (Wang et al. 2009), with minor modifications. One hundred and fifty micrograms of proteins was loaded to the non-linear pH 3–11 IPG strips (13 cm; GE Healthcare) which were used for SDS-PAGE gels for silver staining while 1 mg of proteins was loaded to the IPG strips which were eventually used for SDS-PAGE gels for Coomassie staining. The IPG strips were rehydrated with protein samples for 12 h at room temperature. After rehydration, proteins on the strips were focused at 20,000 Vh at 20 °C using a Ettan™ IPGphore system (GE Healthcare). After focusing, the strips were reduced using 1% DTT and alkylated with 2% iodoacetamide (GE Healthcare) in equilibration buffer (6 M urea, 50 mM Tris–Cl, 30% glycerol, 2% SDS, 0.02% bromophenol blue) for 15 min at room temperature with gentle agitation. For the second dimension of electrophoresis, the equilibrated strips were loaded on 12.5% polyacrylamide gels. 0.5% agarose was used to fix the strip. Electrophoresis was carried out at 20 mA for 2.5 h.

Image analysis and spot selection

ProteoSilver™ Plus Silver Stain kit (Sigma, USA) was used for silver staining and colloidal blue staining kit (Invitrogen Life Technologies) for Coomassie-blue staining of SDS-PAGE gels. Gels were scanned to produce the proteome maps of the control Raji cells and

maslinic acid-treated Raji cells. Silver-stained gels (in triplicates) of untreated Raji cells and maslinic acid-treated cells were compared using Image-Master 2D Platium 7 software (GE Healthcare). Protein spots with ≥2-fold changes and $p < 0.05$ were selected for in-gel digestion.

In-gel digestion

Selected protein spots were excised from Colloidal Blue-stained gels. These spots were destained for 10 min, thrice, with 25 mM ammonium bicarbonate. The destained gel spots were washed thrice with 10% acetic acid/50% methanol for 1 h each time and then washed twice with deionized water for 30 min each time. The gel pieces were immersed in 100% ACN until they turned opaque and were dried in a vacuum centrifuge. The dried gel particles were rehydrated with 10 ng/nl trypsin in 50 mM ammonium bicarbonate (pH 8.0) and were incubated at 37 °C for 4 h. The digests were dried by vacuum centrifugation for about 15 min and subjected to MALDI TOF-TOF MS analysis.

Database searching and protein identification

The digested peptide samples were analyzed by MALDI TOF-TOF MS using a 4800 Proteomics Analyzer (TOF/TOF) (Applied Biosystems, USA). The instrument was operated in a positive ion reflection mode of 20 kV accelerating voltage. Combined MS–MS/MS searches were conducted with Data Processing Software GPS Explorer™ software v 3.6 (Applied Biosystems). The spectra were processed and analyzed with the MASCOT v 2.1 software (Matrix Science Ltd., London, UK) to search for the peptide mass fingerprints and MS/MS data in the NCBInr database using the parent ion mass. The error tolerance was 100 ppm and the MS/MS fragment mass tolerance was 0.2 Da. Carbamidomethylation of cysteine (fixed modification) and methionine oxidation (variable modification) were taken into consideration. A protein score greater than 82 was considered to be significant ($p < 0.05$).

Cell cycle analysis

Raji cells (5×10^5 cells/ml) were seeded in 24-well plates and incubated with 50 μM of maslinic acid for 4, 8, 16, and 24 h. The cells were then fixed in 70% (v/v) ethanol and stored overnight at −20 °C. The ethanol-suspended cells were centrifuged for 5 min at 200 × *g*. The ethanol was discarded. The cell pellet was rinsed with PBS and centrifuged. The supernatant was removed and the pellet was resuspended in 500 μl PBS together with 4 μl of propidium iodide (PI) staining solution (2.5 mg/ml) and 1 μl RNase (10 mg/ml). Cells in the PI-containing solution were incubated for 10 min at 37 °C after which they were analyzed by flow cytometry. The flow cytometer was equipped with a 488 nm laser and PI flow emission was detected on the FL2 channel. Ten thousand cells were recorded for each data point and the results analyzed on CellQuest® software. Boundary markers were manually positioned on the histogram plots to determine the percentage of cell population at different stages of the cell cycle.

Nuclear protein extraction and electrophoretic mobility shift assay (EMSA)

Raji cells were plated in 24-well plates and treated with 50 μM maslinic acid for 1, 2, 4, and 8 h, respectively. Nuclear extracts were prepared with NE-PER Nuclear and Cytoplasmic Extraction Reagents (PIERCE, Rockford). NF-κB DNA binding reactions were carried out using NoShift Transcription Factor Assay kit and NoShift NF-κB (p65) reagents (Merck, Germany). The nuclear extract was mixed with the biotinylated double stranded NF-κB oligonucleotides (wild type sequence), NoShift Bind Buffer, poly(*dI*/*dC*) and salmon sperm DNA to a final volume of 20 μl and incubated on ice for 30 min. The reaction mixture was then transferred to a streptavidin-coated plate where the protein–DNA complexes were bound to the plate. The bound transcription factor (NF-κB) was then detected with a specific primary antibody (p65) followed by the secondary HRP-conjugated antibody. After reaction with the tetramethylbenzidine (TMB) substrate, the absorbance was read at 450 nm. Several controls were included in the experiments to establish the specificity of NF-κB binding activity. These include reactions performed in the absence of DNA-binding protein extract (blank), reactions with non-specific competitor DNA and reactions with specific competitor DNA. A 10-fold molar excess of specific and non-specific competitor DNA were added for each competition analysis.

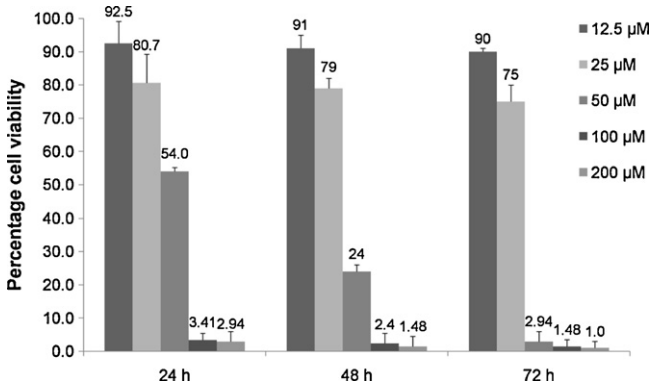

Fig. 2. Inhibition of Raji cells proliferation by maslinic acid. Raji cells were treated with 12.5, 25, 50, 100, and 200 μM of maslinic acid for 24, 48, and 72 h. Cell viability was determined by MTT assay and percentage cell viability was expressed as percentage compared to untreated control. Each data point represents the mean ± standard deviations from 3 experiments. Experiments were performed in triplicates.

Western blotting

Raji cells (5×10^5 cells/ml) were seeded in 24-well plates and incubated with 50 μM of maslinic acid for 4, 8, 16, and 24 h. The protein expression of EB1, stathmin, RanBP1, cyclin D1, and p21 were determined by Western blotting. SDS-PAGE and Western blotting were done as previously described (Hsum et al. 2011). Total protein was extracted using M-PER Mammalian Protein Extraction Reagent from PIERCE (Rockford, USA). Protein concentration was determined using Bio-Rad DC protein assay. Samples containing 50 μg of protein were fractionated by SDS-PAGE in 12% gels with constant current of 20 mA for about 2 h. The gel was then carefully removed and electroblotted to a 0.45 μm PVDF membrane (PIERCE, Rockford, USA) using a standard tank transfer apparatus for mini gels. Immunodetection was carried out using respective primary antibodies (1:1000 in 3% BSA in PBST buffer) and HRP-conjugated secondary antibodies (1:10,000 in 3% BSA in PBST buffer).

Statistical analysis

Statistical analyses were performed using SPSS 15.0 software. Treatment effects were analyzed using one-way ANOVA. $p < 0.05$ was used to indicate significance.

Results

Inhibition of Raji cell growth

In order to analyze the anti-proliferative effect of maslinic acid, Raji cells were treated with 12.5, 25, 50, 100 and 200 μM of maslinic acid for 24, 48, and 72 h. As shown in Fig. 2, maslinic acid inhibited

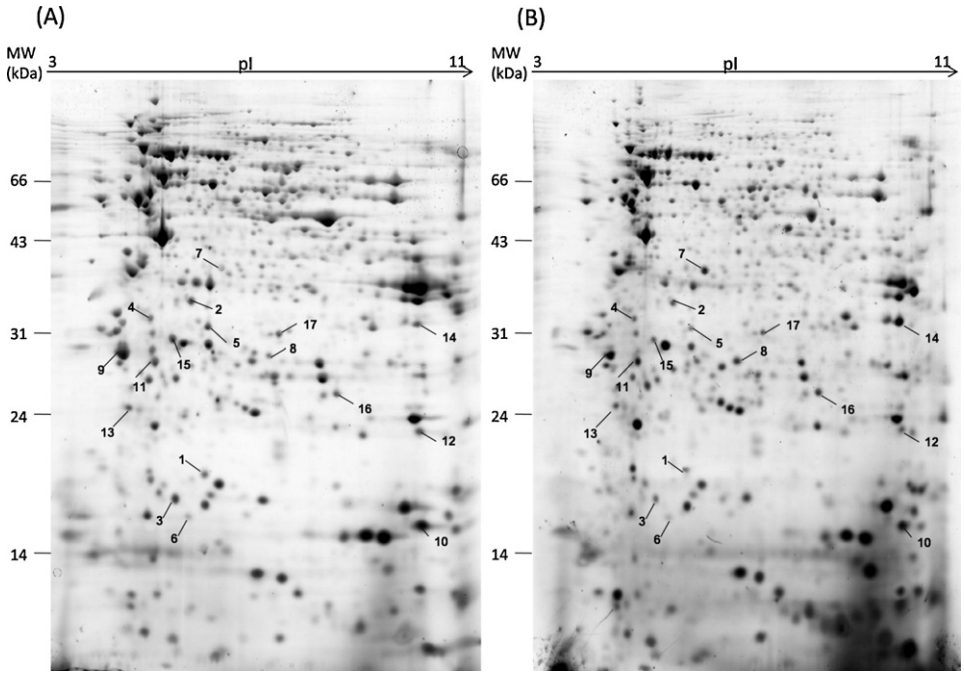

Fig. 3. Proteomic profiling of Raji cells in response to treatment with 50 μM maslinic acid. Protein lysates from untreated and maslinic acid-treated Raji cells were separated using pH 3–11 NL IPG strips for the first dimension and 12.5% SDS-polyacrylamide gel for the second dimension of separation. Silver stained-gels had been loaded with proteins from (A) untreated cells and (B) cells treated with 50 μM maslinic acid for 24 h. The proteins spots numbered were excised, subjected to tryptic digestion and identified using MALDI TOF-TOF MS analysis.

cell proliferation in a concentration- and time-dependent manner. Treatment with 50 μM maslinic acid resulted in 46% inhibition of cell proliferation at 24 h, 76% inhibition at 48 h, and 97% inhibition at 72 h. The percentage of cell viability was less than 5% when treated with 100 and 200 μM of maslinic acid for 24, 48, and 72 h.

Differential proteomic changes in maslinic acid-treated and untreated Raji cells

The protein expression profile of Raji cells in response to maslinic acid treatment at a sub-cytotoxic level (50 μM) for 4, 8, 16, and 24 h was investigated. Fig. 3 show silver-stained 2D gels. About 1000 spots were detected and around 40 spots showed ≥2-fold changes in spot intensity compared to the untreated control. Tryptic digests from 17 spots were analyzed by MALDI TOF-TOF MS. Table 1 lists the proteins that were identified by the database. The functions of the differentially regulated proteins were obtained using their protein accession numbers from the NCBI protein function summary (http://www.ncbi.nlm.nih.gov/protein). The 17 proteins identified in this study were assigned into several functional groups, namely cell proliferation, cell cycle, cytoskeleton organization, energy metabolism, cell signaling, and apoptosis. Among the proteins that were down-regulated after treatment with maslinic acid, dUTPase and inorganic pyrophosphatase are involved in cell proliferation. Proteins participating in energy metabolism, e.g. isocitrate dehydrogenase and enoyl-coA hydratase were highly expressed in maslinic acid-treated Raji cells. Voltage-dependent anion-selective channel protein 1 (VDAC1) which participates in the formation of the permeability transition pore complex (PTPC) responsible for releasing mitochondrial products that trigger apoptosis was up-regulated while prohibitin which regulates mitochondrial respiration and aging was down-regulated. VDAC1 and prohibitin have been implicated in apoptosis. Expression of transgelin-2 and tumour protein D52, which are involved in tumourigenesis were decreased.

Validation of time-dependent differential expression of stathmin, EB1, and RanBP1

Validation of the proteomics findings by immunoblot analysis was performed to confirm the differential expression of specific proteins. The expression of 3 proteins, i.e. stathmin, EB1 and RanBP1 are shown in Fig. 4. Raji cells were treated with 50 μM maslinic acid for up to 24 h. Cells treated for 4, 8, 16, and 24 h, together with the controls, were harvested and their total proteins were extracted. Maslinic acid significantly reduced the expression of stathmin (Fig. 4A and B), EB1 (Fig. 4C and D), and RanBP1 (Fig. 4E and F) within 24 h of treatment. EB1 and RanBP1 expression were almost undetectable after 24 h of treatment.

Induction of G1 cell cycle arrest

Based on the protein expression profile, maslinic acid appeared to regulate proteins that are involved in cell growth, proliferation and survival in Raji cells. Flow cytometry analysis of maslinic acid-treated Raji cells showed that it induced G1 cell cycle arrest. Cells in the G1 phase increased sharply from 47% (0 h) to 70% after 16 h treatment and remained at 65% up to 24 h (Fig. 5). The increase in G1 cell population was accompanied by a decrease in the number of cells in both S and G2 phase. Treatment of cells with maslinic acid decreased the proportion of S phase cells from 25% (0 h) to 11% (24 h). The percentage of cells in the G2 phase decreased from 23% (0 h) to 12% at 24 h upon treatment.

Effects on cell cycle regulatory molecules

Based on the observation that maslinic acid induced G1 arrest in Raji cells, the effect of maslinic acid on cell cycle regulatory molecules of the G1–S phase transition were assessed by Western blot analysis. Cyclin D1 was down-regulated by maslinic acid in a time-dependent manner (Fig. 6). After 16 and 24 h of maslinic acid treatment, cyclin D1 levels was undetectable. The CDK inhibitor

Table 1
Proteins differentially expressed by Raji cells after treatment with 50 μM maslinic acid.

Spot number	Protein identity	Swiss-prot database entries	MW/pl	Sequence coverage (%)	Mowse score	Fold change	Biological function
1	dUTPase	P33316	17,908/6.15	62	553	−5.3	Cell proliferation
2	Inorganic pyrophosphatase	Q15181	33,095/5.54	33	369	−1.8	
3	Stathmm 1 isoform a	P16949	17,292/6.02	43	407	−5.2	Cell cycle
4	Micratubule associated protein RP/EB family member 1	Q15691	30,151/5.02	46	452	−2.7	
5	F-actin capping protein subunitbeta	P47756	30,852/5.52	21	348	−2.1	Cytoskeleton
6	Actin related protein 2/3 complex subunit 5	O15511	16,367/5.47	58	447	−3.4	
7	Isocitrate dehydrogenase [NAD] subunit alpha, mitochondrial	P50213	34,967/6.02	39	356	+3.7	Energy Metabolism
8	Enoyl-coA hydratase mitochondrial	P30084	31,361/6.09	53	542	+2.6	
9	14-3-3 zeta/delta	P63104	29,413/4.97	53	391	−3.2	Cell signaling
10	Nucleoside diphosphate kinase B	P22392	17,270/8.55	33	260	−2.7	
11	Ran GTPase-activating protein RANBP1	P434B7	23,310/5.21	21	82	−5.3	
12	Transgelin-2	P378D2	24,609/8.41	86	709	−3.5	
13	Tumour protein D52	P55327	24,369/4.79	30	336	−7.3	
14	Voltage-dependent anion-selective channel protein 1 (VDAC1)	P21796	30,737/8.63	57	414	+2.6	Apoptosis
15	Prohibitin	P35232	29,859/5.57	73	726	−1.9	
16	ES1 protein homo log, mitochondrial	P30042	24,999/8.29	16	202	+2.4	Others
17	Purine nucleoside phosphorylase	P00491	32,382/7.09	73	354	−4.2	

p21 protein expression was, however, transiently up-regulated by maslinic acid. These effects were observed as early as 4 h of treatment and reached a maximum expression at 8 h.

Inhibition of NF-κB (p65) activity

The effect of maslinic acid on NF-κB activity was studied. Raji cells were treated with 50 μM of maslinic acid at early time points (1, 2, 4, and 8 h). As shown in Fig. 7A, the NF-κB (p65) binding activity in Raji cells was specific; presence of non-specific competitor (mutant DNA) did not affect the NF-κB binding activity in Raji cells but was significantly reduced in the presence of specific competitor DNA. Maslinic acid suppressed NF-κB (p65) binding activity in a time-dependent manner, with 8.3%, 42.9%, 63% and 70% inhibition observed at 1, 2, 4, and 8 h treatment (Fig. 7B).

Discussion

Previous studies suggest that the growth inhibition response of maslinic acid is mediated via activation of the mitochondrial apoptotic pathway as apoptotic proteins such as Bax, caspase 3 and caspase 9 were activated upon maslinic acid treatment (Reyes-Zurita et al. 2008). However, the effect of maslinic acid at the proteomic level has not been investigated. In this study, a comprehensive proteome profiling which deduced the target genes of maslinic acid as well as its effect on the cell cycle are reported. Maslinic acid was shown to affect the expression of proteins involved in nucleotide metabolism, microtubule filament assembly, cytoskeleton organization, and adaptor proteins in the signal transduction pathway. The results suggest that maslinic acid induces G1 cell cycle arrest with induction of G1 phase cell cycle regulatory proteins p21 and the degradation of cyclin D1, and inhibits nuclear NF-κB (p65) activity.

Maslinic acid inhibited Raji cell growth in a concentration- and time-dependent manner. This confirms the anti-proliferative activity of maslinic acid as similar observations were also reported in other tumour cell lines (Kim et al. 2000). As revealed from the proteome profile, the cytotoxic and pro-apoptotic effects of maslinic acid might be resulted from interference with DNA replication (down-regulation of dUTPase and inorganic pyrophosphatase), nucleo-cytoplasmic trafficking (down-regulation of RanBP1), and microtubule filament assembly (reduction of stathmin and EB1) as well as induction of apoptosis related protein VDAC1. In the case of mitochondrial-regulated apoptosis, the process is ATP dependent and energy demanding (Mayer and Oberbauer 2003). Down-regulation of VDAC1 expression by shRNA is associated with a decrease in energy production (Shoshan-Barmatz et al. 2008). Indeed, maslinic acid increases energy metabolism in cells by up-regulating mitochondria isocitrate dehydrogenase and enoyl-CoA hydratase. This supported the suggestion by Reyes et al. that maslinic acid induces cell death via the mitochondrial apoptotic pathway (Reyes-Zurita et al. 2008).

Maslinic acid also inhibited adaptor proteins such as 14-3-3 zeta/delta and tumour protein D52 which regulate a large spectrum of both general and specialized signaling pathways. 14-3-3 zeta/delta is an important regulatory protein in intracellular signaling pathways and is known to interact with more than 100 cellular proteins, including oncogene and protooncogene products (Xing et al. 2000). 14-3-3 zeta/delta may regulate inflammatory pathways in the tumour microenvironment (Kobayashi et al. 2009). Tumour protein D52 is a multi-functional adaptor protein that influences numerous cellular processes. Increased D52 expression may be an early event in cancer which contributes to subsequent tumour progression (Boutros et al. 2004). The expression of transgelin-2, a protein of the calponin family found in high abundance in Raji cells (Gez et al. 2007) was down-regulated by maslinic acid. Elevated levels of transgelin were observed in tumourigenic cells and it significantly promotes cell migration and invasion (Lee et al. 2010).

Maslinic acid plays a critical role in the regulation of cell cycle progression. Proteins such as stathmin, EB1 and RanBP1 which are involved in microtubule dynamics and cell division were down-regulated. Elevated stathmin and RanBP1 expression had been

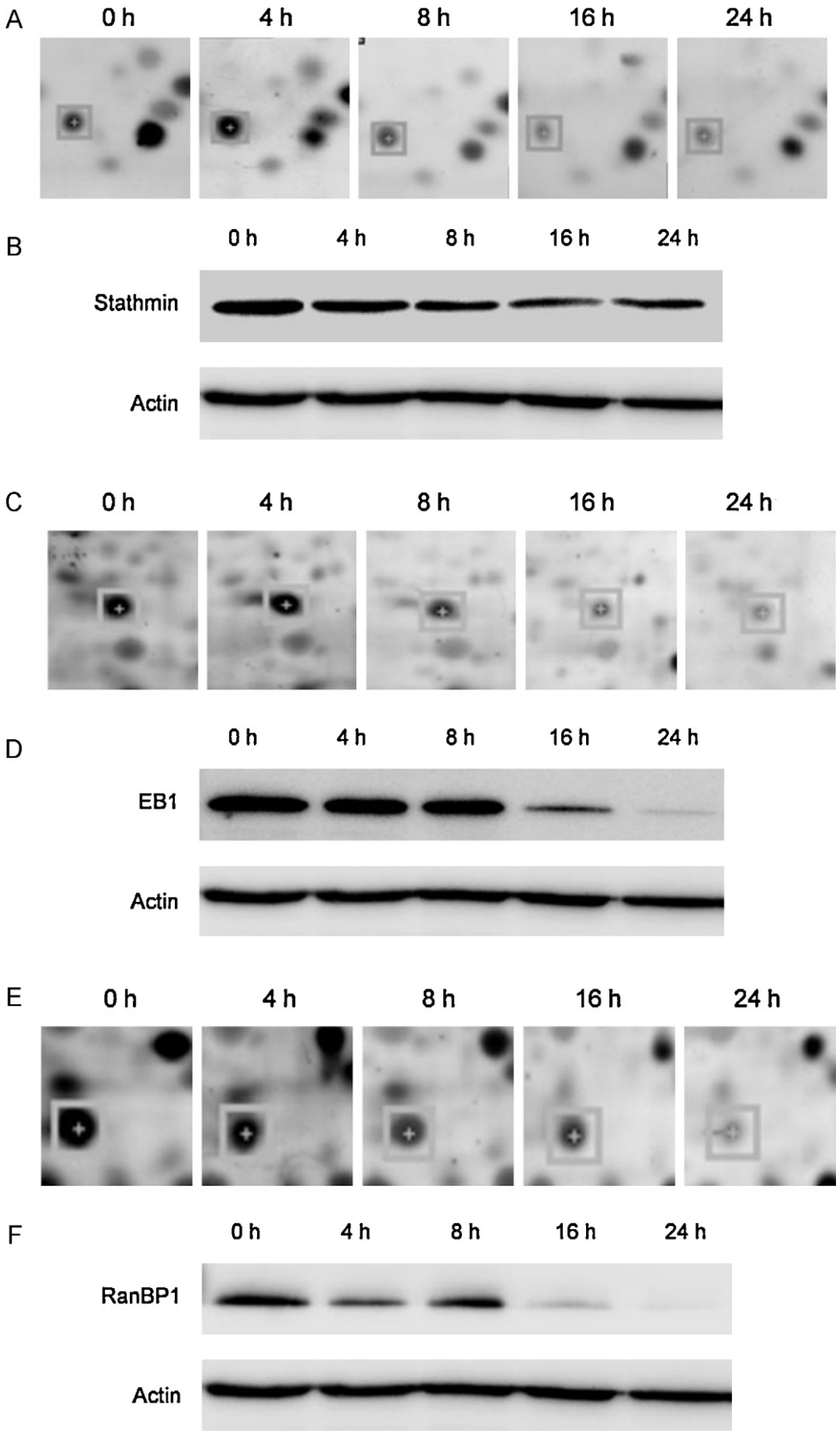

Fig. 4. Validation of maslinic acid-regulated proteins in Raji cells by Western blotting. The upper rows (A, C, and E) show the 2-DE images and the lower panels (B, D, and F) show the Western blots. Cells were treated with 50 μM maslinic acid for the periods indicated. Cells were collected, total cell lysates prepared and subjected to SDS-PAGE followed by Western blotting. Membranes were probed with indicated antibodies and visualized by ECL detection system. Beta actin was used as the internal control.

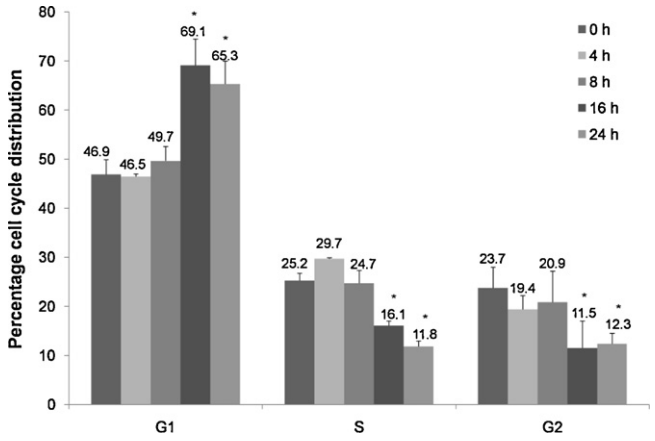

Fig. 5. Raji cell cycle percentage distribution in response to treatment with 50 μM maslinic acid for 4, 8, 16, and 24 h. Cells were stained with propidium iodide (PI) and analyzed by flow cytometry. PI flow was detected on FL2 and data displayed as a histogram showing DNA content of cells in the G0/G1, S, and G2 phases of cell cycle. Ten thousand cells were analyzed for each data point. Values were expressed as mean ± standard deviations. Asterisk (*) denotes significant difference from the control at $p < 0.05$.

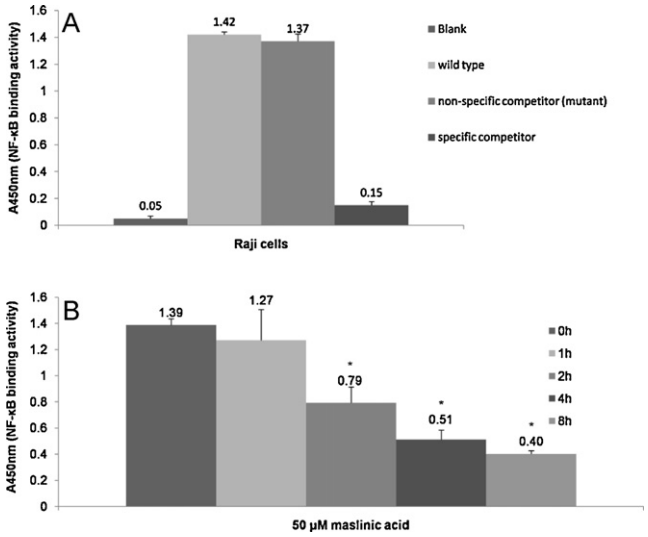

Fig. 7. Effect of maslinic acid on the NF-κB (p65) binding activity in Raji cells. (A) Specificity of the NF-κB (p65) binding activity; and (B) time course study of maslinic acid on NF-κB (p65) binding activity in Raji cells. Cells were treated with 50 μM maslinic acid for 1, 2, 4 and 8 h. Nuclear extracts were prepared after treatment and quantified for NF-κB (p65) activity using NoShift Transcription Factor Assay kit. Each data point represents average ± standard deviations of three independent experiments. Asterisk (*) denotes significant difference from the control at $p < 0.05$.

reported in a variety of human malignancies (Antonucci et al. 2003) while EB1 expression was recently reported to be up-regulated in human breast cancer cell lines (Dong et al. 2010). The up-regulation of stathmin, EB1 and RanBP1 in neoplastic tissues may be part of the regulatory mechanism altered during tumourigenesis. Silencing or inhibition of stathmin, EB1 and RanBP1 causes aberrant mitotic spindle formation, inhibition of cancer cell proliferation, and apoptosis (Jeha et al. 1996; Gez et al. 2007). These observations, together with the findings of this study suggest that the inhibition of proteins regulating microtubule dynamics and cell division may suppress tumour cell growth.

Reyes et al. reported that maslinic acid inhibits cell growth and induces G1 cell cycle arrest in Caco-2 colon cancer cells (Reyes et al. 2006). This study reports a similar effect of maslinic acid on the Raji cell cycle. Maslinic acid also down-regulated proteins associated with the cell cycle arrest at S and G2 phase. Inhibition of dUTPase induces early S (Tinkelenberg et al. 2002) or G2 (Marie et al. 2006) arrest due possibly to stalled replication complexes caused by a lack of thymidine equivalents (dTTP or dUTP) available for DNA replication. Inhibition of stathmin expression leads to accumulation of cells in the G2 phase which is associated with severe mitotic spindle abnormalities and difficulty to exit from mitosis (Rubin and Atweh 2004). In contrast, there are studies reporting that levels of stathmin phosphorylation were significantly lower in cells blocked during the G1/S phases of the cell cycle than in proliferating cells (Brattsand et al. 1994). Knockdown of Nm23-H1 (Dabernat et al. 2004), the target gene of nucleoside diphosphate kinase B (NDPKB) which was down-regulated by maslinic acid, has been shown to arrest cells in the G0/G1 phase of the cell cycle (Jin et al. 2009).

Progression through the cell division cycle is regulated by coordinated activities of cyclin/cyclin dependent kinases (CDK) complexes. Mitogenic signals that initiate DNA replication are first detected by expression of the D-type cyclins (D1, D2 and D3) that preferentially bind to, and activate, CDK4 and CDK6 during the G1 phase (Malumbres and Barbacid 2001). Over-expression of cyclin D1 has been reported in several types of human cancers (Yu et al. 2001; Besson et al. 2008). Suppressing cyclin D1 over-expression may thus prevent oncogenic signaling. Another mechanism that prevents premature entry into the S phase relies on CDK inhibitors (CKIs) that bind onto cyclin-CDK complexes and disrupt their catalytic centre (Pavletich 1999). The Cip/Kip family member of $p21^{Cip1/Waf1/Sdi1}$ is an important transcriptional target of p53 and mediates DNA-damage induced cell-cycle arrest (Besson et al. 2008). Suppressing cyclin D1 over-expression and inducing p21 levels by maslinic acid may thus prevent uncontrolled cell cycle progression.

Cyclin D1 is a transcriptional target of NF-κB (Hinz et al. 1999) and NF-κB activation is essential for growth and survival of

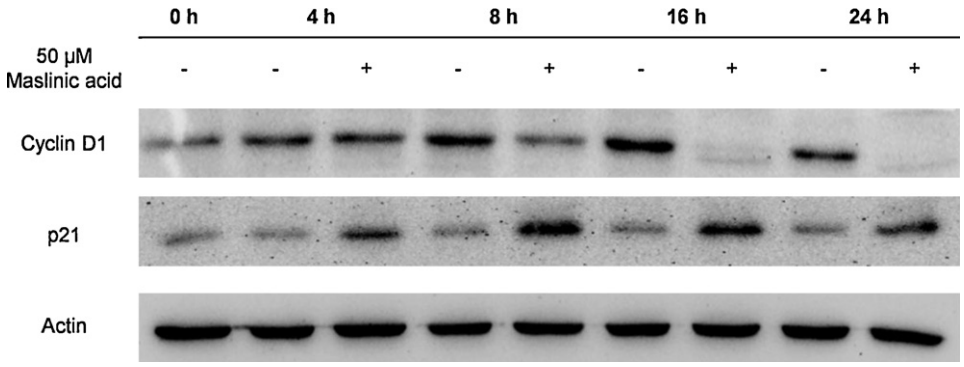

Fig. 6. Time course effect of maslinic acid on the expression of G1 cell cycle components cyclin D1 and CDK inhibitor p21. Raji cells were treated with 50 μM maslinic acid or the DMSO vehicle control for 4, 8, 16 and 24 h followed by Western blot analysis for cyclin D1 and p21 protein. Beta actin was used as the internal control.

Epstein-Barr virus (EBV)-transformed B lymphoma Raji cells (McFarland et al. 2000; McFarland and Kieff 2002). NF-κB also regulates target genes that are activated in the early and late stages of aggressive cancers, including apoptosis suppressor proteins such as Bcl-2 and Bcl X_L and those required for metastasis and angiogenesis, such as matrix metalloproteases (MMP) and vascular endothelial growth factor (VEGF) (Aggarwal and Shishodia 2006). The results of this study showed that maslinic acid significantly reduced nuclear NF-κB activity in a time-dependent manner. A similar effect was also observed in pancreatic cancer cells Panc-28 where maslinic acid inhibits cell proliferation by suppressing tumour necrosis factor-alpha (TNFα) -induced NF-κB activation (Li et al. 2010). The induction of G1 cell cycle arrest, modulation of G1 phase cell cycle components and suppression of NF-κB activity by maslinic acid may contribute to its growth inhibitory effect.

Conclusion

The identification of proteins with altered expression profiles at multiple treatment time points may serve to elucidate the cellular mechanism involved in response to maslinic acid treatment in Raji cells. Proteins such as stathmin, EB1 and RanBP1 which are associated with cell division and microtubule dynamics suggest that maslinic acid might have a role in regulating the cell cycle. Maslinic acid induced a G1 cell cycle arrest and modulated G1 associated cell cycle regulatory proteins, i.e. cyclin D1 and p21. Transcriptional activation of NF-κB which is known to promote cell cycle progression through up-regulation of cyclin D1 expression and essential for Raji cells growth and survival was inhibited in response to treatment. This study supports that treatment with maslinic acid activates the mitochondrial apoptotic pathway as has been reported by Reyes-Zurita et al. (2008), and suggests that the growth inhibition properties of maslinic acid might be mediated by modulation of the cell cycle.

Conflict of interest

The authors have declared no conflicts of interest.

Acknowledgement

The authors would like to express their deepest gratitude to Universiti Tunku Abdul Rahman and MOSTI e-science fund (00-02-11-SF0028) for supporting this project.

References

Abe, I., 2007. Enzymatic synthesis of cyclic triterpenes. Nat. Prod. Rep. 24, 1311–1331.
Aggarwal, B.B., Shishodia, S., 2006. Molecular targets of dietary agents for prevention and therapy of cancer. Biochem. Pharmacol. 71, 1397–1421.
Antonucci, F., Chilosi, M., Parolini, C., Hamdan, M., Astner, H., Righetti, P.G., 2003. Two-dimensional molecular profiling of mantle cell lymphoma. Electrophoresis 24, 2376–2385.
Bellavita, V., Schiaffella, F., Mezzetti, T., 1974. Triterpenoids of *Centaurium erythraea*. Phytochemistry 13 (1), 289–290.
Besson, A., Dowdy, S.F., Roberts, J.M., 2008. CDK inhibitors: cell cycle regulators and beyond. Dev. Cell 14, 159–169.
Boutros, R., Fanayan, S., Shehata, M., Byrne, J.A., 2004. The tumor protein D52 family: many pieces, many puzzles. Biochem. Biophys. Res. Commun. 325, 1115–1121.
Brattsand, G., Marklund, U., Nylander, K., Roos, G., Gullberg, M., 1994. Cell-cycle-regulated phosphorylation of oncoprotein 18 on Ser16, Ser25, and Ser38. Eur. J. Biochem. 320, 359–368.
Chen, J., Liu, J., Zhang, L.Y., Wu, G., Hua, W., Wu, X., Sun, H., 2006. Pentacyclic triterpenes. Part 3: synthesis and biological evaluation of oleanolic acid derivatives as novel inhibitors of glycogen phosphorylase. Bioorg. Med. Chem. Lett. 16, 2915–2919.
Dabernat, S.A., Masse, K., Smani, M., Peuchant, E., Landry, M., Bourbon, P.M., le Floch, R., Daniel, J.Y., Larou, M., 2004. Nm23-M2/NDP kinase B induces endogenous c-myc and nm23-M1/NDP kinase A overexpression in BAF3 cells. Both NDP kinases protect the cells from oxidative stress-induced death. Exp. Cell Res. 301, 293–304.
Dong, X., Liu, F., Sun, L., Liu, M., Li, D., Su, D., Zhu, Z., Dong, J.T., Fu, L., Zhou, J., 2010. Oncogenic function of microtubule end-binding protein 1 in breast cancer. J. Pathol. 220 (3), 361–369.
Dzubak, P., Hajduch, M., Vydra, D., Hustova, A., Kvasnica, M., Biedermann, D., Markova, L., Urban, M., Sarek, J., 2006. Pharmacological activities of natural triterpenoids and their therapeutic implications. Nat. Prod. Rep. 23, 394–411.
Flora, S.D., Ferguson, L.R., 2005. Overview of mechanisms of cancer chemopreventive agents. Mutat. Res. 591, 8–15.
Gez, S., Crossett, B., Christopherson, R.I., 2007. Differentially expressed cytosolic proteins in human leukemia and lymphoma cell lines correlate with lineages and functions. Biochim. Biophys. Acta 1774, 1173–1183.
Hinz, M., Krappmann, D., Eichten, A., Heder, A., Scheidereit, C., Strauss, M., 1999. NF-kappaB function in growth control: regulation of cyclin D1 expression and G0/G1-to-S-phase transition. Mol. Cell. Biol. 19 (4), 2690–2698.
Hsum, Y.W., Yew, W.T., Lim, P.V.H., Soo, K.K., Hoon, L.S., Chieng, Y.C., Mooi, L.Y., 2011. Cancer chemopreventive activity of maslinic acid: suppression of COX-2 expression and inhibition of NF-κB and AP-1 activation in Raji cells. Planta Med. 77, 152–157.
Jeha, S., Luo, X.N., Beran, M., Kantarjian, H., Atweh, G.F., 1996. Antisense RNA inhibition of phosphoprotein p18 expression abrogates the transformed phenotype of leukemic cells. Cancer Res. 56, 1445–1450.
Jin, L., Liu, G., Zhang, C., Lu, C., Xiong, S., Zhang, M., Ge, F., He, Q., Kitazato, K., Kobayashi, N., Wang, Y., Liu, Q., 2009. Nm23-H1 regulates the proliferation and differentiation of the human chronic myeloid leukemia K562 cell line: a functional proteomics study. Life Sci. 84, 458–467.
Kim, Y.K., Yoon, S.K., Ryu, S.Y., 2000. Cytotoxic triterpenes from stem bark of *Physocarpus intermedius*. Planta Med. 66, 485–486.
Kobayashi, R., Deavers, M., Patenia, R., Rice-Stitt, T., Halbe, J., Gallardo, S., Freedman, R.S., 2009. 14-3-3 zeta protein secreted by tumor associated monocytes/macrophages from ascites of epithelial ovarian cancer patients. Cancer Immunol. Immunother. 58, 247–258.
Lee, E.-K., Han, G.-Y., Park, H.W., Song, Y.J., Kim, C.W., 2010. Transgelin promotes migration and invasion of cancer stem cells. J. Proteome Res. 9 (10), 5108–5117.
Li, C., Yang, Z., Zhai, C., Qiu, W., Li, D., Yi, Z., Wang, L., Qian, M., Luo, J., Liu, M., Tang, J., 2010. Maslinic acid potentiates the anti-tumor activity of tumor necrosis factor α by inhibiting NF-κB signaling pathway. Mol. Cancer 9, 73.
Liebold, B.W., Graack, H.R., Pohl, T., 2006. Two-dimensional gel electrophoresis as tool for proteomics studies in combination with protein identification by mass spectrometry. Proteomics 6, 4688–4703.
Malumbres, M., Barbacid, M., 2001. To cycle or not to cycle: a critical decision in cancer. Nat. Rev. Cancer 1, 222–231.
Malumbres, M., Barbacid, M., 2009. Cell cycle, CDKs and cancer: a changing paradigm. Nat. Rev. Cancer 9, 153–166.
Marie, G., Kemp, P.A., Boiteux, S., 2006. dUTPase activity is critical to maintain genetic stability in *Saccharomyces cerevisiae*. Nucleic Acids Res. 34 (7), 2056–2066.
Martín, M.A., Vázquez, R., Arche, A., Gutiérrez, A., 2006. Suppressive effect of maslinic acid from pomace olive oil on oxidative stress and cytokine production in stimulated murine macrophages. Free Radic. Res. 40, 295–302.
Massague, J., 2004. G1 cell-cycle control and cancer. Nature 432, 298–306.
Mayer, B., Oberbauer, R., 2003. Mitochondrial regulation of apoptosis. News Physiol. Sci. 18, 89–94.
McFarland, C., Davidson, D.M., Schauer, S.L., Duong, J., Kieff, E., 2000. NF-κB inhibition causes spontaneous apoptosis in Epstein-Barr virus-transformed lymphoblastoid cells. Proc. Natl. Acad. Sci. 97, 6055–6060.
McFarland, C., Kieff, E., 2002. NF-kappa B inhibition in EBV-transformed lymphoblastoid cell lines. Cancer Res. 159, 44–48.
Montilla, M., Agil, A., Navarro, M., Jimenez, M., Granados, A., Parra, A., Cabo, M.M., 2003. Antioxidant activity of maslinic acid, a triterpene derivative obtained fron *Olea europaea*. Planta Med. 69, 472–474.
Mooi, L.Y., Wahab, N.A., Lajis, N.H., Ali, A.M., 2010. Chemopreventive property of phytosterols and maslinic acid in inhibiting the expression of EBV-early antigen in Raji cells. Chem. Biodivers. 7 (5), 1267–1275.
Mussini, P., Fulvia, O., Francesca, P., 1995. Triterpenes in leaves of *Olea europaea*. Phytochemistry 14 (4), 1135.
Pastwa, E., Somiari, S.B., Czyz, M., Somiari, R.I., 2007. Proteomics in human cancer research. Proteomics Clin. Appl. 1, 4–17.
Pavletich, N.P., 1999. Mechanisms of cyclin-dependent kinase regulation: structures of Cdks, their cyclin activators, and Cip and INK4 inhibitors. J. Mol. Biol. 287, 821–828.
Reyes, F.J., Centelles, J., Lupianez, J.A., Cascante, M., 2006. (2α,3β)-2,3-Dihydroxyolean-12-en-28-oic acid, a new natural triterpene from *Olea europea*, induces caspase dependent apoptosis selectively in colon adenocarcinoma cells. FEBS Lett. 580, 6302–6310.
Reyes-Zurita, F.J., Rufino-Palomares, E.E., Lupiáñez, J.A., Cascante, M., 2008. Maslinic acid, a natural triterpene from *Olea europaea* L., induces apoptosis in HT29 human colon-cancer cells via the mitochondrial pathway. Cancer Lett. 273, 44–54.
Rubin, C.L., Atweh, G.F., 2004. The role of stathmin in the regulation of the cell cycle. J. Cell. Biochem. 93, 242–250.
Shoshan-Barmatz, V., Keinan, N., Zaid, H., 2008. Uncovering the role of VDAC in the regulation of cell life and death. J. Bioenerg. Biomembr. 40 (3), 183–191.

Surh, Y.-J., 2003. Cancer chemoprevention with dietary phytochemicals. Nat. Rev. Cancer 3, 768–780.

Tinkelenberg, B.A., Hansbury, M.J., Ladner, R.D., 2002. dUTPase and uracil-DNA glycosylase are central modulators of antifolate toxicity in *Saccharomyces cerevisiae*. Cancer Res. 62, 4909–4915.

Tsuen-Ih, R., Kakisawa, H., Chen, Y.P., Hsü, H.Y., 1996. Terpenoids from *Elaeagnus oldahmi*. Phytochemistry 15 (2), 335.

Wang, X., Chen, Y., Han, Q., Chan, C., Wang, H., Cheng, C.H., Yew, D.T., Lin, M.C.M., He, M., Xu, H., Sung, J.J.Y., Kung, H., 2009. Proteomic identification of molecular targets of gambogic acid: role of stathmin in hepatocellular carcinoma. Proteomics 9, 242–253.

Xing, H., Zhang, S., Weinheimer, C., Kovacs, A., Muslin, A.J., 2000. 14-3-3 proteins block apoptosis and differentially regulate MAPK cascades. EMBO J. 19, 349–358.

Xu, H.X., Zeng, F.Q., Wan, M., Sim, K.Y., 1996. Anti-HIV triterpene acids from *Geum japonicum*. J. Nat. Prod. 59, 643–645.

Yazaki, Y., 1977. Polyphenols and triterpenoids of *Eugenia gustavioides* wood. Phytochemistry 16 (1), 138–139.

Yu, Q., Geng, Y., Sicinski, P., 2001. Specific protection against breast cancers by cyclin D1 ablation. Nature 411, 1017–1021.

Yu, S., Zhou, B.N., Lin, L., Cordell, G.A., 1995. Triterpene saponins from *Aster yunnanensis*. Phytochemistry 38 (6), 1487–1492.